REFERENCE ONLY

UNIVERSITY OF LONDON THESIS

Degree PhD Year 2006 Name of Author Sperle, G

ATTEMPTS TO GENERATE ATHEROPROTECTIVE LECITHIN:CHOLESTEROL ACYLTRANSFERASE (LCAT) PHENOTYPES BY CHIMERAPLASTY

By

Galia Sperber

A thesis submitted in partial fulfilment of the requirements for the degree of

Doctor of Philosophy

Royal Free Hospital
School of Medicine
University College London

2006

ProQuest LLC
789 East Eisenhower Parkway
P.O. Box 1346
Ann Arbor, MI 48106-1346

Abstract

ATTEMPTS TO GENERATE ATHEROPROTECTIVE LECITHIN:CHOLESTEROL ACYLTRANSFERASE (LCAT) PHENOTYPES BY CHIMERAPLASTY

Lecithin-cholesterol acyltransferase (LCAT) is a high-density lipoprotein (HDL)-associated enzyme, which is secreted mainly by the liver. By esterifying cholesterol in the surface of immature HDL, LCAT drives reverse cholesterol transport, an important process in preventing atherosclerosis. Specific point mutations in the *LCAT* gene, producing serine to alanine amino acid substitutions at positions 208 or 216, are reported to increase enzymatic activity up to 14 times. Here, I attempt to create these mutations using a new technology, termed chimeraplasty — targeted gene repair *in situ* using synthetic RNA-DNA oligonucleotides (chimeraplasts).

First, I demonstrated that the Ser208Ala and Ser216Ala mutations do increase LCAT specific activity by comparing recombinant Chinese hamster ovary (CHO) cells secreting wild-type LCAT (CHO-LCAT), $LCAT_{Ser216Ala}$, or $LCAT_{Ser208Ala+Ser216Ala}$. I then targeted CHO-LCAT cells, and a human hepatoma cell line (HepG2), *in vitro* with chimeraplasts directed at the Ser208 and Ser216 sites. However, I was unable to create the required thymidine to guanine nucleotide substitution required using standard procedures, even by varying transfection conditions, repeat targeting, or altering chimeraplast design. I studied, therefore, chimeraplast uptake into the nucleus with various polyethylenimine (PEI)-based transfection reagents by using fluorescently-labelled oligonucleotides and a validated chimeraplast, able to mutate the apolipoprotein E (*APOE)* gene. I found that melittin-PEI, transferrin-PEI and galactose4-PEI were superior to linear PEI, but targeting the *LCAT* gene with these optimal reagents failed to produce either Ser208Ala or Ser216Ala mutations. Moreover, co-targeting cells simultaneously with LCAT and apoE chimeraplasts mutated the *APOE* gene, but not the *LCAT* gene.

Finally, to investigate possible gene position or sequence effects I produced recombinant CHO cells expressing both LCAT and apoE targeting regions adjacent to each other. When these cells were co-targeted the Ser216Ala mutation was successful. I conclude that chimeraplast-directed gene mutation/repair is a promising technique but further investigation is required to explain inconsistent results when targeting different cell lines.

TABLE OF CONTENTS

LIST OF FIGURES

CHAPTER 5

CHAPTER 6

LIST OF TABLES

To my little angel, Nina, for kicking from within to encourage me to start writing and then pulling from without to persuade me to finally finish it.

ACKNOWLEDGEMENTS

I would like to first thank Prof. Jim Owen for his guidance, support and understanding during the years that I was his PhD student. I am also extremely appreciative for the critical reviewing and proof reading of this manuscript provided by Prof. Owen, Prof. Mia Sperber, and Dr. Eldad Avital.

Special thanks go to Dr. Silke Schepelmann and Dr. Anita Stannard for teaching a clinician how to get started in the world of laboratory research. I would also like to thank my friends in the group, Drs. Zahra Mohri, Jane Mulcahy, Anna Manzano, Aris Tagalakis and Mr. Shani Thilakawardhana for making my PhD not only interesting and stimulating, but also fun. Furthermore, this work would not have been possible without the financial support of the British Heart Foundation.

Finally, I would like to thank my family. My parents, Mia and Charles Sperber, first encouraged me in my pursuit of this degree and I am eternally grateful to them for their help in innumerable ways. My darling husband, Eldad Avital, has been my foremost adviser in all things academic and I thank him with all my heart for his patience, understanding, and constant support. I would not have been able to complete this thesis without your confidence in me.

Galia Sperber, May 2005

ABBREVIATIONS

AAV..... adeno-associated virus

ABCA1..... ATP-binding-cassette transporter class A1

Ad..... adenovirus

apoA-I..... apolipoprotein A-I

apoA-II.....apolipoprotein A-II

apoC-II..... apolipoprotein C-II

apoE.....apolipoprotein E

AU.....arbitrary unit

BCA..... bicinchoninic acid

B-PEI.....branched polyethylenimine

BSA..... bovine serum albumin

CE..... cholesteryl ester

CETP..... cholesteryl ester transfer protein

CFTR..... cystic fibrosis conductance regulator

CHD.....coronary heart disease

CHO..... Chinese hamster ovary

CIAP..... calf intestinal alkaline phosphatase

dCTP.....deoxycytidine triphosphate

DEAE.....diethylaminoethyl

DEPC..... diethylpyrocarbonate

DFP.....di-isopropyl fluorophosphate

DHEA.....dihydroepiandrosterone

DHFR.....dihydrofolate reductase

DMEM..... Dulbecco's modified eagle medium

dNTP..... deoxynucleotide triphosphate

DOPE.....1,2-dioleoyl phosphatidylethanolamine

DOTAP.....N-[-1-(2,3-dioleoyloxy)propyl]-N,N,N-trimethylammonium

dpm..... disintegrations per minute

ECL..... enhanced chemiluminescence

EDTA..... ethylenediaminetetra-acetate

ELISA..... enzyme-linked immunosorbent assay

eNOS..... endothelial nitric oxide synthase

FACS.....fluorescence activated cell sorter

FBS..... foetal bovine serum

FC..... free cholesterol

Gal4-PEI.....galactose4-polyethylenimine

GFP..... green fluorescent protein

HBS.....HEPES buffered saline

HDL.....high density lipoprotein

HEPES..... 2-hydroxyethyl-1-piperazine ethanesulphonic acid

HIV..... human immunodeficiency virus

HRP..... horseradish peroxidase

HSV..... herpes simplex virus

HT.....hypoxanthine and thymidine

IDL..... intermediate density lipoprotein

Ig..... immunoglobulin

IL-1.....interleukin-1

IP-10.....interferon-inducible protein 10

IRES..... internal ribosome entry site

I-TAC.....interferon-inducible T-cell alpha chemoattractant

ITR..... inverted terminal repeat

lac-PEI..... lactosylated polyethylenimine

LB.....Luria-Bertani

LCAT..... lecithin:cholesterol acyltransferase

LDL.....light density lipoprotein

LDL-R.....low density lipoprotein receptor

LOX-1..... lectin-like oxidized LDL receptor-1

L-PEI.....linear polyethylenimine

LRP..... low density lipoprotein receptor-related protein

LTR..... long terminal repeat

MCP-1..... macrophage chemoattractant protein-1

Mel-PEI.....melittin-polyethylenimine

MIG.....monokine induced by interferon-γ

Mo-MLV..... Moloney murine leukaemia virus

NEAA.....non-essential amino acids

NF-κB..... nuclear factor-kappaB

NO..... nitric oxide

OD.....optical density

OTC..... ornithine transcarbamylase

oxLDL.....oxidized low density lipoprotein

PA..... phosphatidic acid

PAF..... platelet activating factor

PAGE..... polyacrylamide gel electrophoresis

PBS..... phosphate buffered saline

PC..... phosphatidylcholine

PCR..... polymerase chain reaction

PE..... phosphatidyl ethanolamine

PEG..... polyethylene glycol

PEI.....polyethylenimine

PG..... phosphatidyl glycerol

PL..... phospholipid

PS..... phosphatidylserine

RCT.....reverse cholesterol transport

RFLP..... restriction fragment length polymorphism

rHDL..... reconstituted high density lipoprotein

SDS..... sodium dodecyl sulphate

SFHR..... short fragment homologous replacement

siRNA..... small interfering RNA

SNP.....single nucleotide polymorphism

SR-B1..... scavenger receptor B1

SR-PSOX..... scavenger receptor for phosphatidylserine and oxidized lipoprotein

SSON..... single-stranded oligonucleotide

TFO..... triplex-forming oligonucleotide

Tf-PEI..... transferrin-polyethylenimine

TG..... triglyceride

TLC..... thin layer chromatography

TNF-α..... tumour necrosis factor-α

UC.....unesterified cholesterol

UV.....ultraviolet

VCAM-1.....vascular cell adhesion molecule-1

VLDL..... very light density lipoprotein

VSMC..... vascular smooth muscle cells

VSV..... vesicular stomatitis virus

WT..... wild-type

X-SCID..... X-linked severe combined immunodeficiency

Chapter 1 –

Introduction

1.1 ATHEROSCLEROSIS AND LIPOPROTEIN METABOLISM

Cardiovascular disease ranks as the top cause of death in the UK, with about 238,000 mortalities a year [1]. To illustrate the size of the problem, approximately 2 million people suffer from angina, the most common symptom of coronary heart disease (CHD), and the disease causes the premature death of 22% of men in this country. Economically, CHD costs the country a total of about £7,000 million a year, for the healthcare system and as work days lost because of the disease. Atherosclerosis, the cause of coronary heart disease and strokes, is the subject of much investigation, as researchers attempt to come to as much understanding as possible of this multifactorial process, in the hopes of finding targets that can be used to prevent or reverse its occurrence.

1.1.1 ATHEROGENESIS

Atherogenesis is the process by which an atheroma is formed: a build-up of lipids, cholesterol, calcium and cellular debris, associated with endothelial dysfunction and vascular inflammation, within the intima of a blood vessel wall. The exact course of events in the formation of such a lesion is still incompletely understood, but we do know that early lesions are the fatty streaks seen even in children's arteries: sites of inflammation made up solely of monocyte-derived macrophages and T lymphocytes. Progression to a more advanced form of lesion is currently explained by the "response-to-injury" hypothesis, which holds that the resulting endothelial dysfunction is caused by injury [2]. This injury can be in the form of oxidized low-density lipoproteins (LDL), free radicals created by cigarette smoking, hypertension, diabetes mellitus, an infectious agent, a toxin, or homocystinaemia.

Whatever the stimulus, lesion progression begins with the entry of mononuclear leucocytes and platelets to the intima. The signal received by these leucocytes, calling them to the vascular endothelium, is mediated by a host of factors. Adhesion molecules such as the selectins and vascular cell adhesion molecule-1 (VCAM-1) are secreted as a result of the presence of oxidatively modified

lipoproteins, local shear stress, and the presence of interleukin-1 (IL-1) and tumour necrosis factor-α (TNF-α), leading to the aggregation of lymphocytes and monocytes [3].

After the leucocytes adhere to the endothelium they begin to enter the artery wall. It is currently believed that this process is directed by certain chemokines. For example, atherogenesis appears to be reduced in mice lacking the macrophage chemoattractant protein-1 (MCP-1) molecule [4]. Other chemokines, such as those produced by vascular cells: interferon-inducible protein 10 (IP-10), monokine induced by interferon-γ (MIG), and interferon-inducible T-cell alpha chemoattractant (I-TAC) have also been associated with atheromatous lesions. Literature produced over the past few years increasingly demonstrates that modified lipoproteins can cause the expression of adhesion molecules and cytokines associated with the early stages of atherogenesis, as they carry oxidized phospholipids [5,6]. As soon as macrophages collect in the intima, they begin to accumulate LDL, forming foam cells, the trademark of the early atheroma. The resulting fatty streak may be reversible, but further accumulation of macrophages in the arterial intima leads to progression of the atheroma.

The result of these changes is increased adhesiveness of the endothelium, increased procoagulant properties instead of the normal anticoagulant properties of the endothelium, and the formation of vasoactive molecules, including cytokines and growth factors. The lesion at this stage can follow one of two directions: the offending agents can be destroyed and removed from the site of inflammation, or the inflammation can proceed indefinitely, with migration and proliferation of smooth muscle cells, forming the intermediate lesion. At this point arterial remodelling will occur, including dilatation of the arterial wall to accommodate its thickening [7]. Meanwhile, cell numbers will increase at the lesion site, with more macrophages and lymphocytes appearing as they multiply *in situ* and become activated, releasing hydrolytic enzymes, cytokines, chemokines and growth factors.

The accumulation of smooth muscle cells and their secretion of matrix macromolecules lead to the formation of a more fibrous plaque and the creation of an advanced, complicated lesion. The extracellular connective tissue matrix forms a cap over the foam cells, extracellular lipids and necrotic cellular debris which form the core of the plaque [8]. At this point rupture of the fibrous cap may result in luminal exposure to platelet-derived growth factor, insulin-like growth factor, transforming

growth factors alpha and beta, thrombin and angiotensin II: molecules that are produced by activated platelets and macrophages and aid in taking the plaque to a more dangerous level [9]. Plaque rupture can result in the formation of thrombus, with partial or complete occlusion of the artery.

For the purposes of this thesis, the most important element to understand in the atherogenic process is that a high circulating level of LDL leads to the presence of oxidized LDL (oxLDL). This is due to the fact that the antioxidant properties of the healthy endothelium are overwhelmed in the presence of elevated serum levels of LDL. LDL can be oxidized by a variety of substances, such as superoxide anion radicals [10], myeloperoxidase [11], lipoxygenases [12], or transition metals [13]. Both lipid [14] and protein [15] components of LDL can be oxidized. Though quantification of LDL oxidation is difficult, one study found that patients who had suffered an acute myocardial infarction had approximately 5% circulating oxLDL, compared to 0.01% in normal patients [16]. The resulting oxLDL is preferentially taken up by macrophages [17], leading to the formation of foam cells.

The recent discovery of lectin-like oxidized LDL receptor-1 (LOX-1) has allowed valuable new insights into the mechanisms by which oxLDL is atherogenic. LOX-1 is the major oxLDL receptor on endothelial cells, but also has inducible expression in macrophages and smooth muscle cells. Association of oxLDL with the receptor leads to endothelial changes, namely by stimulation of nuclear factor-kappaB (NF-κB), which leads to induction of adhesion molecules and endothelial apoptosis [18]. Another receptor, scavenger receptor for phosphatidylserine and oxidized lipoprotein (SR-PSOX), was found on macrophages and was shown to be upregulated in these cells present in human atherosclerotic lesions, but not in normal aorta [19]. Oxidized LDL also competes with oxidatively damaged and apoptotic cells for CD36 and scavenger receptor type B1 (SR-B1) on macrophages [20,21].

Oxidized LDL was also found to contain platelet activating factor (PAF)-like fragments that activate the PAF receptor. The effect of this activation was demonstrated by injecting PAF-like oxLDL into the mouse pleural cavity [22]. This resulted in inflammatory infiltration, recruitment of monocytes, neutrophils and eosinophils because of induction of 5-lipoxygenase expression in leucocytes and expression of MCP-1 and leukotriene B_4. Therefore, we can see that oxLDL can act via several receptors.

The elements that make up LDL also play an important part in whether the molecule will act in an atherogenic manner. One study looked at oxLDL inhibition of nitric oxide (NO) activity in macrophages, an important anti-atherogenic factor. The protein segment of LDL appeared to have no inhibitory effect, linoleic acid and phosphatidylcholine oxidized separately also had no effect, but linoleic acid and cholesterol oxidized together showed a strong inhibitory effect on NO production, antagonising its vasodilatative effect [23]. NO is known for its anti-atherogenic properties, as it inhibits monocyte aggregation and the secretion of certain molecules (e.g. TNF-α) that stimulate VCAM-1 expression, and thus here we find another path through which oxLDL is pro-atherogenic.

Oxidized LDL has a variety of toxic effects, leading to impaired endothelium-dependent dilatation and paradoxical vasoconstriction [24], elements associated with atherosclerosis. In conclusion, we see that an important aim in the prevention of atheromatous development should be control of the circulating level of LDL. Reverse cholesterol transport is an essential process in LDL management and is discussed in *Section 1.1.3.* In order to study cholesterol transport, it is necessary to understand the molecules that carry cholesterol, namely the lipoproteins.

1.1.2 LIPOPROTEINS AND THEIR NORMAL METABOLISM

Cholesterol and triglycerides are transported in the body by lipoproteins, macromolecules made up of lipids and proteins. These complexes consist of a core of hydrophobic lipids covered by a layer of polar lipids, phospholipids and proteins [25], forming a globular structure. There are five major types of lipoproteins and they vary by their lipid and protein composition (**Table 1-1**), as well as by their function. The five types of lipoproteins are classified according to their density, which is determined by the ratio of proteins to lipids in the complex: the higher the protein content, the denser the lipoprotein. Despite this classification, physiological events that involve the lipoproteins alter them incessantly so that they cannot be considered fixed structures.

The protein components of lipoproteins are known as apolipoproteins (apo). They have important functions in lipid transport and metabolism and interact with cell receptors or have regulatory functions towards specific enzymes involved in lipid

modification. The structure of apolipoproteins always includes amphipathic α-helices with hydrophobic side chains that can interact with the lipid interior of lipoproteins and hydrophilic residues that interact with the surface phospholipids or with plasma elements [26].

Lipoprotein	Density (g/ml)	Apolipoproteins	Lipids (Major components)
Chylomicrons	< 0.94	A-I, B-48, C-I, C-II, C-III, E	TG>>>PL,FC,CE
Very-low-density lipoproteins (VLDL)	0.950-1.006	B-100, C-II, C-III, E	TG >>PL, FC, CE
Intermediate-density-lipoproteins (IDL)	1.006-1.019	B-100, C-III, E	TG > PL, CE > FC
Low-density lipoproteins (LDL)	1.019-1.063	B-100	CE > PL > FC, TG
High-density lipoproteins (HDL)	1.063-1.125 (HDL_2) 1.125-1.21 (HDL_3)	A-I, A-II, C-III	PL>CE>FC,TG

Table 1-1: Properties of the lipoproteins.

Density and components of the different lipoprotein complexes [27]. ***TG****: triglycerides,* ***PL****: phospholipids,* ***CE****: cholesteryl esters,* ***FC****: free cholesterol.*

When transport processes function optimally, lipids in the blood are kept at levels that meet the requirements of target organs, with just enough to be stored away for situations when increased energy is necessary. If an excess of lipids is found in plasma, this can lead to the development atheromas, as was discussed in *Section 1.1.1.*

Dietary fats are carried into the circulation by chylomicrons, which are assembled in the intestinal mucosa. These large lipoproteins are made up of triglycerides, phospholipids, and cholesteryl esters, as well as the protein, apoB-48. Chylomicrons are transported to the blood through the lymphatic system. On its travels, chylomicrons acquire C apolipoproteins from high-density lipoproteins (HDL). Once they reach muscle and adipose tissue, apolipoprotein C-II (apoC-II) in the lipoprotein surface activates the enzyme lipoprotein lipase (LPL) expressed on the surface of vascular endothelial cells [28]. The enzyme catalyses the reaction that breaks down triglycerides to fatty acids and glycerol, which is taken up and re-esterified in adipose tissue and muscle. The chylomicrons become progressively smaller as they lose their triglycerides and eventually become chylomicron remnants. On the way to becoming remnants they also transfer their cholesterol, phospholipids and apoC to HDL in exchange for apolipoprotein E (apoE). Recognition of apoE by the LDL receptor (LDL-R) and the LDL receptor-related protein (LRP) in the liver results in the chylomicron remnants being taken up for degradation [29].

Lipoproteins other than chylomicrons are responsible for the transport of endogenous lipids. Here, circulation of lipids involves shuttling of lipoproteins between the liver and peripheral tissues. Fatty acids and cholesterol are carried away from the liver by triglyceride-rich very-low-density liporoteins (VLDL). ApoC-II is present on the particles and therefore these lipoproteins can also interact with LPL and provide fatty acids to muscle and adipose tissue [30]. In the process of losing their fats, the lipoprotein progressively becomes smaller and is now termed an intermediate-density lipoprotein (IDL).

IDL can also give up more fatty acids to become LDL particles, or can be taken up by the liver via the LDL receptor. Additionally, all the while that VLDL and IDL are in plasma, they can transfer phospholipids to HDL using phospholipid transfer protein (PLTP), and also exchange triglycerides for HDL's cholesteryl esters with the help of cholesteryl ester transfer protein (CETP) [31].

LDL delivers cholesterol to peripheral tissues. This lipoprotein carries most of the cholesterol in blood and has only apolipoprotein B-100 (apoB-100) as its protein component. Most of the cholesterol ends up in the liver, but the rest is taken to any other tissues that express LDL-R. The LDL-R is found on the exterior surface of cells in clathrin-coated pits. The receptor binds apoB-100 and apoE of LDL or other lipoproteins. The lipoprotein is taken into the cell by endocytosis of the coated pit to form a coated vesicle. The clathrin is then released to go back to the plasma membrane, while the vesicle fuses with an acidic endosome. The acidic environment results in the separation of LDL from the receptor. The receptor buds off and is recycled, while the endosome containing the LDL fuses with a lysosome. The LDL is then degraded, the apoB-100 digested by proteases, and the cholesterol used in membranes or stored away as cholesteryl esters [32].

The cell acquires cholesterol from LDL via the LDL-R and also by endogenous synthesis. For excess cholesterol to leave the cell, HDL comes into the picture, and functions as a means to transport cholesterol to the liver for degradation. This pathway is necessary because the sterol nucleus of cholesterol cannot be degraded by cells (only modified to allow excretion [33]) and therefore needs to be removed when in excess. Reverse cholesterol transport (RCT) is this pathway of cholesterol transport from extrahepatic tissues back to the liver.

1.1.3 HDL AND REVERSE CHOLESTEROL TRANSPORT

Tangier disease is characterised by lipid-laden tonsils and abnormally low serum HDL levels [34]. This rare condition was found to be associated with mutations in the ATP-binding-cassette transporter class A1 (ABCA1) gene [35]. Reverse cholesterol transport begins with release of cholesterol from cells via ABCA1, a membrane-spanning transporter containing a highly hydrophobic segment at its centre. The export of cholesterol is accomplished by a "flippase" action of the transporter, where binding and hydrolysis of ATP results in a flipping of cholesterol and phospholipids to the outer half of the lipid bilayer at this hydrophobic region [36]. The externalised cholesterol is then taken up by lipid-poor apolipoprotein A-I (apoA-I) to form nascent HDL. This primordial form of HDL is discoidal and contains mainly apoA-I and phospholipids. On its travels in plasma, nascent HDL sequesters cholesterol from peripheral cells, and therefore RCT flows following a

gradient of cholesterol from peripheral tissues to the liver. The cholesterol at the surface of HDL particles can act as a substrate for the enzyme lecithin:cholesterol acyltransferase (LCAT), resulting in the esterification of cholesterol, which moves to the core of the HDL particle and forms spherical HDL (HDL_3) [37].

Once the mature, CE-laden HDL (HDL_2) reaches the liver, it is taken up by hepatocytes via SR-BI. This receptor is present in caveolae in the cell membrane: invaginations containing glycosphingolipids, cholesterol and caveolins (proteins that can bind cholesterol) [38]. The mechanism by which selective uptake of HDL-cholesterol occurs at this receptor remains unclear, but it is thought that after endocytosis of HDL, the cholesteryl esters are hydrolysed by neutral esterases. Cholesterol is then released to the endosomal membrane, while the CE-depleted HDL (HDL_3) is recycled back to the cell surface.

The inverse relationship between plasma levels of HDL and coronary heart disease has been established by a variety of studies [39-42], and RCT is implicated here. However, RCT being a key function of atheroprotection, it is not the only process, since HDL has anti-atherogenic functions beyond that of carrying cholesterol away from peripheral tissues back to the liver. In recent years it has been shown that HDL has the ability to counteract detrimental effects of LDL. OxLDL leads to vasodilatation, but this can be reversed by HDL [43]. More specifically, lysophosphatidylcholine, a product of LDL oxidation, inhibits vasodilatation but is antagonised by HDL [44]. OxLDL causes a displacement of endothelial nitric oxide synthase (eNOS) from caveolae, causing impaired production of NO. A proposed mechanism for HDL's protective effect is through prevention of this blockade of NO synthesis [45]. HDL also has a mitogenic effect on vascular smooth muscle cells (VSMC). In an environment such as that of an atheromatous plaque, where there is no endothelial barrier, VSMC are exposed to high concentrations of HDL, leading to endothelial proliferation which aids in revitalising cells in the fibrous cap and offsetting VSMC apoptosis, ultimately leading to plaque stability [46].

Another effect of HDL is in preventing endothelial adhesiveness, by inhibiting cytokine-induced expression of adhesion molecules such as VCAM-1. This was shown to be true both using isolated plasma HDL and using artificially reconstituted HDL [47]. Platelet activation in the atheroma leads to a more complex lesion. HDL has the ability to inhibit platelet activation through the presence of apoE in the HDL particle. Our laboratory has shown that apoE can interact with the LRP8 receptor on

the platelet surface, setting off a cascade that results in the production of NO, which contributes to inhibition of platelet activation [48,49]. Other binding sites for HDL on the platelet surface have also been proposed, but the exact identity of these receptors is not yet clear. Nevertheless, binding of HDL here appears to lead to stimulation of diacylglycerol production and activation of protein kinase C. This leads to inhibition of phosphatidylinositol-specific phospholipase C activation, as well as to increased Na^+/H^+ exchange, both leading to inhibition of platelet activation [50,51].

Finally, HDL also has a potentially anti-atherogenic role to play by its function as an anti-oxidant. It can reduce the oxidative modification of LDL by transition metal ions and 12-lipooxygenase. HDL also mops up some of the products of LDL oxidation, for example lysophosphatidylcholine, and transports them to the liver for degradation [52,53]. ApoA-I and paraoxonase are components of the HDL particle that are believed to contribute to its anti-oxidative properties [54]. Paraoxonase catalyses the degradation of oxidized phospholipids in LDL and also decreases the lipid peroxide content of coronary and carotid atheromas [55].

In conclusion, HDL has multiple anti-atherogenic functions: sequenstration of cholesterol for transport to the liver, endothelial cell proliferation leading to plaque stability, inhibition of endothelial adhesion and leukocyte activation, inhibition of platelet activation, and anti-oxidant properties, to name a few. It thus becomes clear that there are a vast number of reasons for promoting good HDL physiological function. The next section will look at a protein that has an essential role in the formation of mature HDL particles and the subject of this thesis: LCAT.

1.2 LECITHIN:CHOLESTEROL ACYLTRANSFERASE (LCAT)

1.2.1 STRUCTURE AND FUNCTION

LCAT plays an important role in lipoprotein metabolism, as it is responsible for the synthesis of most of the cholesteryl esters in plasma. The enzyme was first identified by Glomset in 1962 [56]. Since then it has been elucidated that LCAT is a glycoprotein of about 63-kDa, made up of a single polypeptide chain of 416 amino acid residues. Primary and secondary features of the enzyme were found to be similar to those of members of the lipase family, based on the presence of an α/β hydrolase fold [57]. The 3-dimensional structure of human LCAT is not yet complete, but the proposed model is based on that of pancreatic lipase and consists of a central sheet of seven parallel β-strands connected by four α-helices (***Fig. 1.1***). This model also predicts the amino acids that make up the catalytic triad, the closely apposed Ser_{181}, Asp_{345} and His_{377} [58].

The polypeptide contains six cysteine residues, four of which make two disulphide bridges: Cys_{50}-Cys_{74} and Cys_{313}-Cys_{356}. The first is essential for the protein's ability to bind to lipoprotein surfaces and resembles the 'lid' seen in lipases [59,60]. The lid partially covers the active site of the enzyme in solution, then opens up when bound to lipid surfaces, helping provide hydrophobic contacts with surfaces and protein cofactors, and is also involved in the selection and binding of lipid molecules at the active site [61]. The LCAT sequence also contains four N-glycosylation sites that are used for glycan chain attachment, although their role is not clearly understood. Nevertheless, it has been shown that removing certain chains affects enzymatic activity, although it does not change folding or secretion of the protein [62,63].

The main reaction catalysed by LCAT is the conversion of cholesterol and phosphatidylcholine (PC) to cholesteryl ester (CE) and lysophosphatidylcholine (lysoPC) (see ***Fig. 1.1***). This reaction occurs on the surface of HDL and involves binding of the enzyme to the lipid surface, activation of the enzyme by apoA-I, PC binding, acyl enzyme formation (transfer of an acyl chain from the PC to Ser_{181}), release of lysoPC, cholesterol binding, transfer of the acyl chain to the 3-β hydroxyl group of cholesterol, and release of cholesteryl ester and enzyme [64]. Although the

forward reaction in favoured, a reverse reaction can occur on the surface of LDL, where lysoPC levels are more elevated. The rate limiting step is the binding of PC to the active site, based on studies conducted that looked at activation energies and rates of product formation [65]. Besides Ser_{181}, it has recently been suggested that amino acids 149 and 294 also participate in binding PC at the active site and affect fatty acyl specificity [66].

LCAT can act on the surface of both HDL and LDL, and recent studies have investigated binding affinities to these particles. Using the surface plasmon resonance biosensor method, Jin *et al.*[67] found that LCAT has the same association constant when binding to all lipoproteins, but that the dissociation constant depends on the presence of apoA-I and on the surface lipids. For example, replacing apoA-I with apoA-II in reconstituted HDL (rHDL) increases the dissociation constant by four times, indicating that there is a specific interaction with apoA-I that does not occur with apoA-II. The same authors also found that LCAT dissociates from HDL after only one catalytic cycle, which is different from dissociation patterns of other lipases as they tend to remain bound to the lipid surface until they exhaust their substrates [68].

Fielding *et al.* were the first to show that LCAT is activated by apoA-I [69]. Other apolipoproteins, such as apoE, apoA-IV and apoC-I, also activate the enzyme, but to a lesser extent. It is the α-helix between residues 143 and 165 of the apoA-I protein which is involved in this essential interaction with LCAT, and requires a specific sequence. This has been verified by the fact that certain amino acid substitutions within the region decrease LCAT activity [70], and more recently, three key arginine residues (149, 153, and 160) in this region have been identified as crucial to the interaction with LCAT [71]. On the LCAT side, interaction with apoA-I has not been narrowed down to an exact region, but is thought to involve residues P_{10} and T_{123}, and possibly the helix between amino acids 151-174 [37,72]. If general lipase patterns apply it would involve the lid area, so that apoA-I would stabilise the open lid once binding to the lipid interface occurred.

Studies into binding of LCAT's substrates at the active site show that the orientation of PC does not have to be the same each time it binds, although *sn*-2 and *sn*-1 ester bonds need to be very close to the catalytic triad for the reaction to take place. This fact was elucidated as it became apparent that although transfer of *sn*-2 acyl groups from PC to cholesterol is preferable, the *sn*-1 acyl chain can be used

instead [73]. The binding site for cholesterol is not known, but there must be two distinct sites for PC and cholesterol because PC and CE can be bound to LCAT simultaneously [74]. The mechanism of the reaction is probably similar to that of lipases, where there is a nucleophilic attack by the Ser-OH that cleaves the *sn*-2 or *sn*-1 ester bond of the PC, leading to acylation of the enzyme. The acyl-enzyme intermediate then transfers the acyl chain to cholesterol [73].

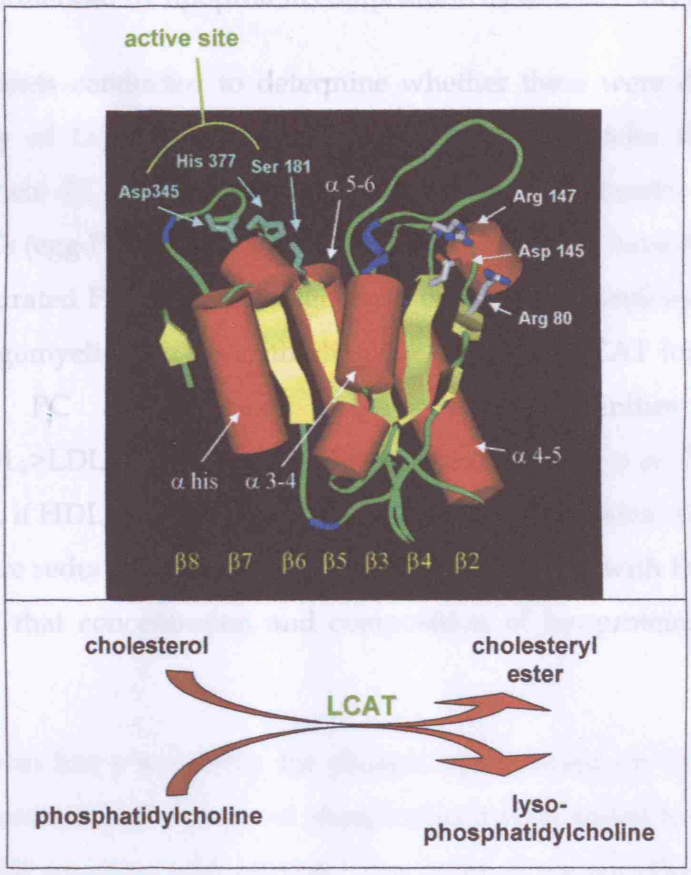

Fig. 1.1: The structure and reaction of LCAT.

The proposed 3-dimensional model of the human LCAT protein (upper box) is based on pancreatic lipase. The 63-kDa glycoprotein consists of seven parallel β-strands (yellow) connected by four a-helices (red). The reaction catalysed by LCAT (lower box) is believed to take place at the active site made up of the catalytic triad Ser181, Asp345 and His377. Ser208 is predicted to be present at the third position of β-strand 6, while Ser216 resides within the long loop (amino acids 211-332) that separates the N- from the C-terminal region. [Protein model adapted from Peelman, F. et al. (2001) J. Lipid Res. **42**, *471-479.]*

1.2.2 REGULATION OF LCAT ACTIVITY

The concentrations of LCAT in plasma were investigated by Albers and colleagues [75]. They found that there is little variation in values obtained in different age groups and between men and women. Even in smokers and with steroid hormone use, the LCAT concentrations appeared to remain stable. The only deviation was found in LCAT deficient patients, where levels were severely reduced. Measurement of LCAT activity is complex because of levels being dependent on substrate and influenced by lipoprotein composition as well as concentration.

Experiments conducted to determine whether there were differences in the binding affinity of LCAT to a variety of lipoprotein particles showed that this depends on their PC components, not on protein components. For example, unsaturated PCs (egg-PC or palmitoyl oleoyl-PC) appeared to have higher affinity for LCAT than saturated PC. Also, the higher the content of phosphatidylethanolamine (PE) and sphingomyelin, the lower the binding affinity of LCAT for rHDL particles. In terms of PC concentration, the order of affinities is rHDL(egg-PC)≥HDL_3>HDL_2>LDL [76]. Based on these findings, Kosek *et al.* [77] deduced that physiologically, if HDL_3 is abundant, most of the LCAT in plasma will be bound to it. If HDL levels are reduced, more LCAT will be free, fitting in with the above findings that concluded that concentration and composition of lipoproteins regulate LCAT activity.

LCAT also has a selectivity for phospholipids based on their structure, not only their concentration. A variety of phospholipids were tested for LCAT reactivity in identical rHDL particles with apoA-I. The order of phospholipid selectivity was found to be PE≥PC>PG>PA>PS, and chain length preference was in the order 12:0<14:0≥16:0>>18:0 (symmetrical saturated PCs). Branched or long polyunsaturated (20:4) chains showed very low activity [78,79]. This means that the active site recognises the phosphate group but has no specific preference for the head groups of the phospholipids. It also will not accommodate chains longer or bulkier than 16:0 or 18:1.

Lipoproteins are important in controlling the LCAT reaction, but another crucial regulatory factor is apoA-I. This apolipoprotein is involved in LCAT's reaction in several ways: 1) mediation of the binding of LCAT to lipid surfaces; 2)

stabilization of the activated form of LCAT; 3) concentration of lipid substrates around LCAT; 4) binding and presentation of lipid substrates to LCAT in an optimal conformation; 5) help in product removal; and 6) help in dissociating LCAT from lipid surfaces [76]. These supportive functions to the enzyme's activity are evident in patients with mutations in the *APOAI* gene in the region believed to be involved in interactions with LCAT, as they show impaired LCAT activation [80] and abnormal HDL maturation [81,82]. ApoA-II has an additional regulatory effect, as apoA-II added to rHDL discs containing apoA-I has been shown to alter apoA-I conformation to make it less effective in activating LCAT [83]. This is another example of how important lipoprotein content is to the regulation of LCAT activity.

It is also interesting to note that the acyl chain removed from phospholipids in the LCAT reaction can be accepted by a variety of other plasma components beside cholesterol. Other sterols have been shown to be acyl acceptors with a preference order of pregnenolone>cholesterol>dihydroepiandrosterone (DHEA)>>oestradiol = corticosterone [84,85]. Nevertheless, cholesterol is much more abundant in plasma compared to other sterols, which makes it preferential in the LCAT reaction. Other acyl acceptors include lysoPC, water, long chain alcohols and diacylglycerol in vitro [86]. Therefore, there is some competition for cholesterol with other acyl acceptors at this stage of the reaction.

To summarize, LCAT activity is regulated by the composition of the lipoproteins with which it interacts, by the phospholipids that serve as its substrates, by apolipoproteins either activating or inhibiting the enzyme's activity, and by the presence of acyl acceptors in plasma.

1.2.3 ROLE IN REVERSE CHOLESTEROL TRANSPORT

LCAT has the essential role in lipid metabolism of creating a gradient for cholesterol flux from peripheral cells through interstitial fluid and plasma into the liver, by the esterification of cholesterol in HDL (***Fig. 1.2***). Along with hepatic lipase (HL), ABCA1, and CETP, the four proteins are essential in RCT and contribute towards atheroprotection. LCAT also maintains the shape and structure of HDL acceptor particles [87]. Both these functions explain how LCAT plays a part in

protecting against atherosclerosis. Nevertheless, RCT may not be as simple as esterification of cholesterol in HDL and transport directly to the liver.

Chung and colleagues examined the flow of UC in plasma under different conditions [88]. In a postprandial state, efflux of cholesterol from red blood cells increased and was mainly accepted by chylomicrons and VLDL. Despite low levels of HDL, cellular cholesterol efflux was not inhibited, and after 18 hours most of the cholesterol was in ester form. Under fasting conditions, LDL was the only source of UC. Based on these and other supportive findings [89-91] Dobiasova and Frohlich proposed a new concept for LCAT's role in RCT [92]. They believe that UC is transferred from cells via pre-β-HDL or chylomicrons to LDL. UC is then taken from these lipoproteins to HDL for esterification by LCAT. Part of this new CE is incorporated in large HDL particles, while some is transferred by CETP to VLDL and LDL. The CE remaining in HDL can then be delivered to SR-BI receptors in liver or steroidogenic tissues. In this scheme, LCAT function depends on plasma LDL content and LDL/HDL ratio, so that in a dyslipidaemic scenario (where the LDL/HDL ratio is high) excess LDL would prevent cellular UC efflux and only UC already on LDL would be esterified in HDL. The lack of larger HDL particles would force more CE transfer via CETP to VLDL and LDL, leading to atherogenesis.

An earlier study by Francone and colleagues [93] found that cell-derived cholesterol gets transferred to α-migrating HDL after esterification, but is present in preβ$_3$-HDL before esterification. LCAT distribution was examined by two-dimensional electophoresis and immunoblotting, and cholesterol esterification was followed by incubating fibroblasts with [^{3}H]-cholesterol. These preβ$_3$-HDL particles were found to contain a large proportion (30%) of LCAT and LCAT-derived CE (30%). Also, the strong presence of CETP in these lipoproteins could explain the quick turnover of the CEs, which were then found in α-HDL.

The same laboratory later used transgenic mice expressing human LCAT to study the importance of the enzyme on RCT [94]. Using plasma from these mice to efflux cholesterol from fibroblasts, they found that their HDL was 44% more efficient than control mouse HDL. A proposed explanation for this result is that the capacity to promote cholesterol efflux is due to LCAT-mediated changes in the HDL particle's lipid composition. Esterification of cell-derived cholesterol was also significantly increased using LCAT transgenic mouse plasma, as was the flux of CE to the liver compared to control mouse plasma.

Another possible role for LCAT is beginning to come to light, with evidence appearing that it is able to reverse oxidation of LDL. Goyal and colleagues [95] inhibited LCAT activity in plasma with di-isopropyl fluorophosphate (DFP) and found that oxidized polar PCs accumulated. This suggested that LCAT detoxified polar PCs created during LDL oxidation. This finding was verified by other groups [96,97]. At the same time, it has been shown that lipid oxidation has an inhibitory effect on LCAT activity [98], but while the enzyme loses its ability to esterify, it can still hydrolyse water soluble substrates. Wang and Subbaiah [99,100] studied the protein to gain understanding of the mechanisms involved in the interaction of LCAT with oxidized LDL. Using site-directed mutagenesis they found that the primary locations of influence by oxidation products are the SH groups of the enzyme, as modification of these groups led to protection of LCAT against oxidative inactivation. They also noticed that the interfacial binding domain of LCAT is involved in oxidative interaction, but is independent of esterification activity. Based on these findings, they concluded that LCAT can still detoxify oxLDL even when it has lost its ability to esterify cholesterol.

The above studies clearly demonstrate that LCAT has an important role to play in reducing the risk of atherosclerosis. This is achieved by maintaining the free cholesterol gradient towards the liver while producing CE-HDL, as well as by limiting the damage that can be caused by products of oxidation.

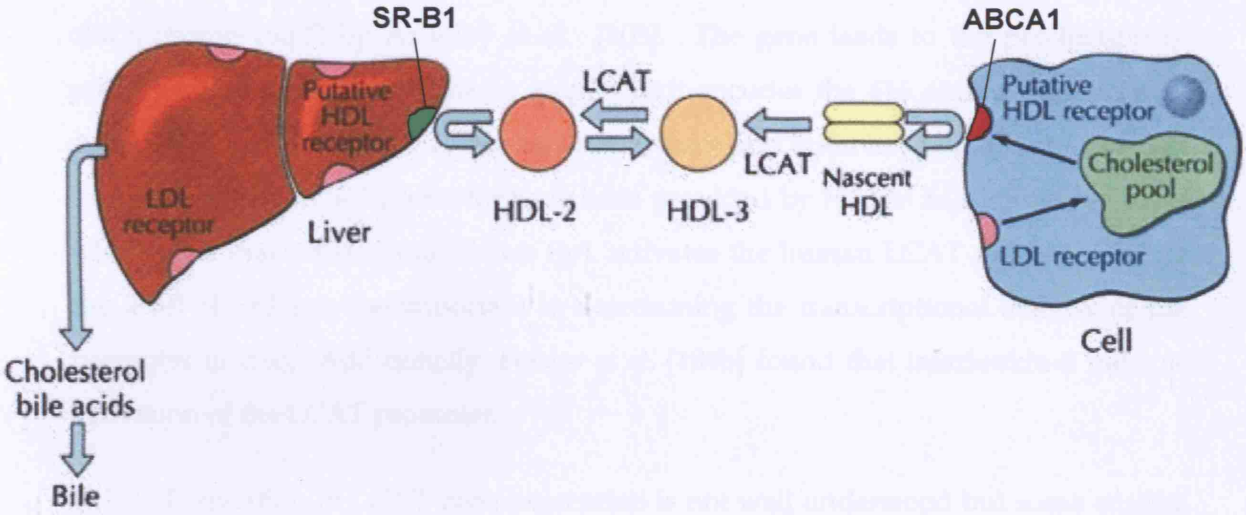

Fig. 1.2: The role of LCAT in reverse cholesterol transport.

Cholesterol is taken up by lipid-poor apoA-I from peripheral cells via ABCA1 (red) and forms nascent, discoidal HDL. As cholesterol continues to be sequestered, LCAT esterifies it at the surface of the particle. The CEs then move to the core to form mature, spherical HDL. Upon reaching the liver, HDL is taken up via SR-BI (green) in the hepatocyte cell membrane.

[Adapted from the website of the Medical University of South Carolina, http://www.musc.edu/bmt737/spring2001/Andrea]

1.2.4 THE LCAT GENE

McLean and colleagues were the first to clone and sequence the *LCAT* gene in 1986 [101,102]. They found that the gene contains 6 exons separated by 5 introns and spans about 4.2 kilobases (accession number XO4981). A year later it was mapped to chromosome 16q22 by Azoulay *et al.* [103]. The gene leads to the production of mRNA approximately 1550 bases long, which encodes the 416 amino acid protein, expressed mainly in the liver, but also in the testis and brain in small quantities [104]. Insights into the LCAT promoter have been provided by Hoppe and Francone [104a] who found that transcription factor Sp1 activates the human LCAT promoter, while the level of Sp3 may be important in determining the transcriptional activity of the promoter *in vivo*. Additionally, Feister *et al.* [104b] found that interleukin-6 induces activation of the LCAT promoter.

Regulation of LCAT gene expression is not well understood but some studies show that changes in LCAT mRNA levels are detectable with varying conditions. For example, Staels *et al.* [105] examined the effect of hormones and hypolipidaemic drugs on rat hepatic LCAT expression, factors that are known to affect lipoprotein metabolism. They found that hepatic LCAT mRNA levels fell after treatment with fenofibrate and that regulation appeared to be at a transcriptional level, while no change was seen in the testis or brain. This demonstrates regulation which is also tissue-specific. Ethinyloestradiol, L-thyroxine, hydrocortisone, probucol, simvastatin and nicotinic acid had no apparent effect on mRNA levels. Later studies showed that TGF-β and TNF downregulate LCAT expression, suggesting a role for cytokines in the regulation of LCAT levels in plasma during acute physiological states [106,107].

The greatest amount of literature concerning the *LCAT* gene describe clinical states of LCAT deficiency. Mutations in the *LCAT* gene present in two main forms: familial LCAT deficiency (FLD) and fish-eye disease (FED), both rare diseases (only about 60 patients with FLD and 20 patients with FED have been identified worldwide), and both transmitted in an autosomal recessive manner [108]. FLD was first reported in 1967 in a Norwegian family [109] and manifests itself clinically with corneal opacities, anaemia, proteinuria and renal disease. Blood profiles of these patients reveal low or undetectable LCAT levels, markedly decreased cholesteryl esters in lipoproteins, abnormal lipoprotein patterns and abnormal erythrocytes. A recent 25 year follow-up of a Canadian family with FLD showed that there were no

significant vascular changes in the two homozygote family members, but abnormal lipid profiles and atherosclerotic vascular changes in 9 heterozygotes [110]. The authors try to explain these findings by postulating that the presence of some LCAT results in reduced cholesterol efflux but increased levels of esterified cholesterol, including in LDL, while no LCAT leads to a decrease in RCT but also no accumulation of cholesteryl esters.

FED was first encountered in two Swedish families [111] and these patients show no major clinical signs other than corneal opacities. Their LCAT activity is reduced with HDL substrates, but LDL esterification is unaffected. The genetic cause for these two diseases is a variety of mutations. Approximately 40 of these have so far been described and are dispersed over the entire gene (see ***Table 1-2***), making it difficult to predict the associated biochemical or clinical phenotype [76].

The LCAT deficiency syndromes result in plasma containing mainly nascent HDL particles due to lack of cholesterol esterification. Nevertheless, very few patients presenting with LCAT mutations have signs of premature atherosclerosis. The reason for this is still under investigation, but not enough patients exist with the same biochemical profile to make any definitive conclusions.

The features of LCAT deficiency have successfully been reproduced in animal models. Sakai and colleagues [112] produced LCAT knockout mice that showed great similarity to the picture seen in FLD. They found that their homozygous mice showed a negligible cholesterol esterification rate, low levels of total cholesterol, cholesteryl esters, HDL-cholesterol and apoA-I, and increased levels of triglyceride. VLDL was the lipoprotein particle most in abundance in these animals, and the apoA-I-containing lipoproteins were cholesterol-poor and mainly of the pre-β variety. On feeding these mice a high-fat high-cholesterol diet, there was no increase in CE, non-HDL cholesterol or apoB. This demonstrates that LCAT modulates a diet-induced lipid response, as shown by the fact that apoB-containing lipoproteins increased in a dose-dependent manner with increased LCAT activity.

The same team also overexpressed *LCAT* in transgenic rabbits [113]. Nine LCAT transgenic and 10 control male rabbits of 5-6 months age were compared. After 17 weeks on a high-cholesterol diet, LCAT activity was 3-fold higher in transgenics compared to controls, HDL levels were 5-fold higher, and while the total cholesterol/HDL cholesterol ratio was 12 times increased in controls, transgenic

rabbits barely had a 2-fold increase. Aortic dissection and staining for lipids revealed that in controls 35% of the surface was covered in plaque, while only 5% of surface was affected in LCAT overexpressors. Also interesting is the fact that there was a dose-response effect in both sets of animals: the higher the LCAT activity, the lower the extent of atherosclerotic changes. The authors explain these results by the reduced levels of apoB lipoproteins and increased levels of HDL lipoproteins. The low apoB lipoprotein levels may in turn be responsible for the reduced endothelial damage and cellular proliferation. Therefore LCAT overexpression could be an option for treatment of atherosclerosis in man.

More recently, the human LCAT gene was introduced into Watanabe heritable hyperlipidaemic rabbits (deficient in the LDL receptor) to investigate the effect of LCAT overexpression in a model of familial hypercholesterolaemia [114]. Lipoprotein levels and metabolic studies showed that LCAT appears to modulate LDL metabolism via the LDL-R pathway and importantly, that LCAT only requires a single functional LDL-R allele to exert an antiatherogenic effect.

Unlike the work described above in rabbits, overexpression of LCAT in mice may not provide accurate information that can be equated to a similar situation in humans. Berard and colleagues [115] found that LCAT overexpression in mice resulted in the formation of abnormal HDL particles and increased atherosclerotic changes. The reason for their observations appears to be related to the fact that mice do not produce CETP, unlike rabbits or humans. The effect of the lack of CETP is that cholesteryl esters are not exchanged as easily into apoB-containing lipoproteins, therefore accumulating in HDL and resulting in larger particles with abnormal lipid and protein composition. This was confirmed in a later study by the same investigators [116], where LCAT transgenic mice were cross-bred with CETP transgenic mice with the result that atherogenic changes found in LCAT overexpressors were reduced, as were the unusual HDL particles. We learn from these experiments that when wanting to simulate physiological situations in order to understand human diseases, choice of animal is very important.

Treatment of LCAT deficiency has begun to appear in the form of gene therapy. Using adenoviral or retroviral vectors carrying LCAT cDNA [117-119], these techniques have the potential of reinstituting active LCAT into a setting where LCAT expression is low or completely absent, although this field is in its early preclinical stages and has not yet reached human trials.

MUTATIONS	Clinical phenotype		References
	FLD	FED	
Homozygous			
1. C-insertion (codons 9,10)	X		
2. P10L		X	
3. G30S	X		
4. Y83-stop	X		
5. A93T	X		
6. T123I		X	} 72
7. N131D		X	
8. R140H	X		
9. G141-insertion	X		
10. L209P	X		
11. N228K	X		
12. G230R	X		120
13. R244K	X		
14. M252K	X		
15. M293I	X		
16. L300-deletion	X		
17. T321M	X		} 72
18. G344S	X		
19. G344S	X		
20. G-deletion (codon 264)	X		
Heterozygous			
1. P10Q R135Q		X	
2. L32P T321M	X		
3. G33R 30 bp insertion (codon 4)	X		
4. T83-stop Y156N	X		
5. T123I Y144C		X	
6. T123I Intron 4 defect		X	
7. T123I T347M		X	
8. T123I Unknown		X	} 72
9. R135W A-insertion (codon 376)	X		
10. R147W Unknown	X		
11. G183S A-T subst/C-del (codon 120)	X		
12. M252K N391S		X	
13. P260-stop	X		121
14. T321M C-deletion (codon 168)	X		72
15. R399C C-insertion (codon 9,10)	X		72
Polymorphism S208T	–	–	127

Table 1-2: Naturally occurring mutations of the LCAT gene.

The mutations that have been identified to date usually present with the clinical features of either familial LCAT deficiency (FLD) or fish-eye disease (FED), but are rare, with frequencies of less than 1:10,000 [127]. Only one polymorphism has so far been described, with no associated pathology.

1.2.5 GAIN-OF-FUNCTION MUTATIONS

In 1991 Francone and Fielding published a study aimed at clarifying the roles of the serines at positions 181 and 216 of the LCAT protein [122]. Their interest in the two sites came after previous experiments showed that when blocking LCAT activity with [^{3}H]-DFP, label was recovered at residues 181 and 216 [123,124]. Using site-directed mutagenesis they modified the gene so that amino acid changes from serine to alanine, glycine or threonine would result, then expressed the mutated gene back into Chinese hamster ovary (CHO) cells and conducted a variety of tests to compare the mutated LCAT proteins to wild-type LCAT secreted by the cells. They found that an S→T or G change at position 181 resulted in complete elimination of LCAT catalytic activity, strongly supporting the idea that Ser_{181} forms part of the active site of LCAT. Interestingly, in the case of Ser_{216} all mutants retained LCAT activity, and substitution to alanine resulted in a 14-fold increase in maximal reaction velocity and significantly increased specific activity. (LCAT activity was determined by following the rate of production of CE from vesicles containing [^{3}H]-cholesterol, and LCAT mass was estimated by solid-phase immunoassay using ^{125}I-labelled antibodies.)

Support for these findings came a few years later when Qu *et al.* [125] studied these two and several other serine residues to determine whether they influenced enzyme activity. Again using site-directed mutagenesis, they produced seven serine-to-alanine mutants at different locations, expressed the *LCAT* gene in COS-6 cells and analysed the secreted protein by [^{3}H]-cholesterol activity assays and solid-phase radioimmunoassays. Of all the results obtained, the most interesting in this context were the Ser_{208}→Ala (S208A) and Ser_{216}→Ala (S216A) mutants. They showed increased catalytic activities (1.6 and 2 times that of wild-type LCAT, respectively), that were not seen with the other mutations assayed. An explanation for this increased activity has not yet been established, but the authors wondered whether the region in question is involved in phospholipid binding. They considered that alanine is less hydrophilic than serine, which means that the alanine mutation might facilitate substrate binding at this site.

To date, only one other mutant form of the *LCAT* gene has appeared in the literature that does not hinder the enzyme's activity (**Table 1-3**). In rats, amino acid 149 of LCAT is an alanine [128]. The E149A mutation (glutamic acid to alanine) in human LCAT results in an activation of the enzyme towards phospholipid substrates

containing arachidonic acid in the sn-2 position [129]. Furbee *et al.* [130] explain that an animal model carrying LCAT with this mutation would help understand the importance of CE fatty acyl composition in preventing atherosclerosis. They therefore created transgenic mice overexpressing human *LCAT* with the E149A mutation. On a chow diet these mice were found to have HDL containing CE enriched in long-chain polyunsaturated fatty acids. The authors have not yet published atherosclerosis studies on these mice. Similarly, the S208A and S216A mutations have not yet been shown to be atheroprotective *in vivo*, but increased LCAT activity could certainly be regarded as having the potential to be anti-atherogenic. For this reason, the two serine-to-alanine mutations were picked for this study, as gene therapy targets that could promote atheroprotection.

MUTATIONS	References	MUTATIONS	References
Eliminating LCAT activity		**Not alterating LCAT activity**	
1. K39A/K42A	|	1. S19A	125
2. R52A/K53A	|	2. R52A	126
3. E110Q	|	3. R53A	126
4. D113N	|	4. D136N	126
5. R135A	} 126	5. S181A	122
6. R140A	|	6. S383A	125
7. D145N	|		
8. R147W	|	**Increasing LCAT activity**	
9. R147A	|	1. S208A	122, 125
10. S181G	122, 125	2. S216A	122
11. S181T	122		
		Increasing reactivity of LCAT with *sn*-2 arachidonic acid	
Decreasing LCAT activity		E149A	125
1. K42A	126		
2. R80Q	126		
3. R99Q	126		
4. S216G	122		
5. S216T	122		
6. S19A + N20T	125		
7. S225A	125		
8. 238A/K240A	126		
9. R280A	126		
10. R351A	126		
11. S383A + N384T	125		

Table 1-3: Engineered mutations of the LCAT gene.

A varied range of mutations have been created in vitro. They are shown here in groups according to their effect on LCAT activity. Only two mutations are so far known to increase LCAT activity, the serine-to-alanine mutations at amino acids 208 and 216.

1.3 GENE THERAPY

The field of gene therapy aims at preventing or reversing the course of diseases by manipulating them at the DNA level. Theoretically, this should be possible, as it has become apparent that all disease processes originate from the expression of abnormal proteins or from the lack of normal protein expression. The ideal gene therapy technique would then be able to either insert a functional copy of the gene in question (gene addition) or correct the faulty gene *in situ* (gene repair) with minimal side effects.

Slightly outside the gene therapy realm is the field of gene silencing, which aims at controlling gene products rather than the gene *per se*. One of these techniques uses small interfering RNA (siRNA), which involves post-transcriptional gene silencing by either degrading or arresting the translation of RNA [131]. An example of development in this area is as a treatment for chronic myeloid leukaemia, by targeting a fusion gene that is the product of the Philadelphia chromosome [132]. Antisense technology involves inhibition of target RNA sequences using oligonucleotides and has already been used successfully *in vivo* for the suppression of apoB-100 mRNA in order to reverse hyperlipidaemia [133].

The development of gene therapy techniques has grown immensely in the last 15 years and has now spread into treatment goals in a variety of medical areas. Up to the end of 2004, almost 900 different clinical gene therapy trials had been instituted [134]. Of all the diseases targeted, cancers take the lead, followed by monogenic diseases such as X-linked severe combined immunodeficiency (X-SCID) and familial hypercholesterolaemia. Besides these, a whole host of other targets are being investigated that have not yet reached the clinical stage. The next sections with explore the various gene addition and gene repair techniques currently being used to develop disease therapies.

1.3.1 GENE ADDITION

The vectors used to deliver genes to target organs or cells can be broadly divided into two groups: viral and non-viral. Within each group are various delivery methods, each with their own advantages and disadvantages regarding transgene

size limit, expression ability, control ability, stability and safety. The main problem with viral vectors is the risk of infection or mutagenesis. This is not the case with non-viral vectors, which do not require the complex proteins of viruses and have the potential to be produced on a large scale.

1.3.1.1 Viral vectors

The idea to use viruses to introduce DNA into cells came from the fact that viruses have a natural predisposition to infect and transduce certain cell types. By replacing specific viral genes with a gene of interest, the virus can be used to accomplish a goal other than originally intended. In choosing a viral vector, ideally it should be able to deliver an adequate amount of therapeutic gene with the least toxicity. With regards to vector toxicity, many problems have to be overcome, both on the level of cellular immunity (response against the transduced cells) and humoral immunity (response against the therapeutic gene product). Additionally, there is the potential for insertional mutagenesis by the vectors that integrate into the genome and the possibility that there will be inadvertent transmission of vector sequences into germ cells, both factors that need to be taken into consideration, but are difficult to control at this stage of general knowledge of viral mechanisms. Practically, the choice of vector should depend on the size of the insert required, the cells intended to be targeted, the number of cells targeted ideally, and whether short-term or long-term expression is required. **Table 1-4** summarizes the features of some of these delivery methods.

The greatest proportion of viral gene therapy trials use retroviral vectors [134]. This is because the sequence arrangement makes it easy to design a retroviral vector and these vectors are good at integrating into host cell chromatin. Additionally, the technique of pseudotyping, involving the replacement of the env gene with that of another virus, allows interaction of retroviral particles with other receptors and thus expands the host range [135]. On the negative side, productive transduction depends on rapid target cell mitosis, which limits the use of retrovirus to haematopoietic progenitor cells or lymphocytes [136]. Retroviral vectors can also transform cells by integrating near a cellular proto-oncogene and causing inappropriate expression, or by disrupting a tumour suppresser gene. The most successful use of a retroviral vector has been in targeting mutations in the common gamma chain gene to treat the

X-linked form of severe combined immunodeficiency (X-SCID) in children [137]. To illustrate the risks associated with use of these vectors, in this case there was activation of the oncogene LMO2, associated with leukaemia [138], in three of the 11 treated patients [139] almost three years following treatment. Therefore, there are serious safety issues that need to be addressed in the use of viral vectors as gene therapy techniques.

	RETROVIRUS	LENTIVIRUS	ADENOVIRUS	AAV	HSV
Genetic components	7-11 kb ss RNA, 3 main genes	7-11 kb ss RNA, more complex genome than retrovirus	35 kb ds DNA	5 kb ss DNA	152 kb ds DNA
Integration	Target cell chromatin	Active transport by cell's nuclear import machinery	Replicates as episome	Random chrom. integration or episomal expression	Intranuclear episome
Insert space	~ 8 kb	~ 8 kb	~ 8 kb	4.5 kb	40-50 kb
Targetable cells	Dividing cells, most cell types	Dividing and non-dividing cells; neuronal, epithelial, hepatic, hematopoietic stem cells	Dividing and non-dividing cells; variety of cell types to different degrees	Dividing and non-dividing cells; variety of cell types	Neuronal cells
Advantages	Can add selectable markers, pseudotyping possible, efficient integration	Longer expression, transduction of non-proliferating cells	Transfection efficient in vitro and in vivo, can be produced at high titres, wide spectrum of target cells	Prolonged expression, non-immunogenic, non-pathogenic to humans	Very large insert capacity, can be produced at high titres
Dis-advantages	Can stimulate tumor growth, cannot carry more than 8 kb, prolonged expression difficult, expression affected by complement, IFNs, antibodies	Vectors derived from HIV - safety issues, obligatory RNA step, limited size of transgene cassette	Transient expression in vivo (inactivated by complement), helper-dependent vector system developed because cannot construct packaging cell line	Small insert capacity, relatively low yields	Lack of experience in vivo in humans, complex targeting, unknown effects of long-term expression
Examples of clinical applications	SCID-X1, melanoma	Successful animal trials only, promising for treatment of Parkinson's disease, type VII mucopolysaccharidosis, etc.	Cystic fibrosis , coronary artery disease	Haemophilia	
Notes and references	Most commonly used vector system in clinical trials	Subclass of retrovirus [140-144]	[145-152]	[153-159]	Persists in latent form after primary infection [160-163]

Table 1-4: Viral vectors.
Comparison of the main features of the most commonly used viral vectors in gene therapy research. AAV: adeno-associated virus; HSV: herpes simplex virus; ss: single-stranded; ds: double-stranded.

1.3.1.2 Non-viral vectors

Despite some successes with viral gene therapy and the continued ambition to cure diseases using this method, non-viral gene delivery is an attractive alternative because it circumvents many of the problems associated with the use of viruses. The advantages of using a non-viral system are low immunogenicity, infinite capacity, no infectious or mutagenic capability, and the possibility of large scale production.

Plasmids

The use of naked plasmids as a means of delivering genes is attractive because they are poorly immunogenic, relatively cheap to produce and to a high purity, and are expressed episomally, thus preventing insertional mutagenesis from occurring. Plasmids can be directly injected into muscle or attached to gold for particle bombardment into tissue. They can produce prolonged low levels of expression, as was demonstrated by injection of an apoE plasmid into apoE(-/-) mouse skeletal muscle [164] with resulting reduction in markers of atherosclerosis. Plasmid delivery is also being developed into vaccines, for example against HIV [165], as they have the advantage of being unaffected by pre-existing immunity.

Sleeping beauty transposons

DNA transposons are natural, nonviral elements that can move a specific DNA segment from one genetic location to another by a cut-and-paste mechanism. *Sleeping Beauty* (SB) is a transposon constructed from inactive transposon fossils found in fish genomes to use in vertebrates [166]. SB has the highest activity of all transposons that can be used in vertebrates. Its structure consists of a gene that codes for transposase flanked by terminal inverted repeats containing binding sites for the transposase. The transposase gene can be replaced by any DNA sequence up to approximately 10 kb. The therapeutic gene can be delivered alongside the transposase gene on the same plasmid, on a separate plasmid, or transposase can be delivered in protein form at the same time as the plasmid. SB transposons can be delivered by a viral method, but most of the work already done with this technique

has been by plasmid transfection or injection. This is a new gene therapy method, but several studies have found successful integration and long-term expression of the gene in question [167-169]. In order to avoid further transposition of an inserted gene, it will probably be important in future studies to deliver transposase as protein rather than DNA, as SB is only able to move when exogenous transposase is supplied. This technique may have a place in the future of gene therapy, but safety issues will have to be addressed, as gene integration in unwanted locations leading to dangerous activation/inactivation may occur just as with viral vectors.

1.3.2 GENE EDITING

Viral gene therapy works by introducing a gene into a cell, while most non-viral methods alter genes *in situ*, as we will see below. This means that the gene is left as it was in terms of interaction with regulatory elements. The studies conducted in this thesis were accomplished using RNA/DNA oligonucleotides (chimeraplasts) or modified single-stranded oligonucleotides (SSONs). These will be discussed in *Section 1.3.3*, but first two other gene modifying methods will be touched upon.

1.3.2.1 Small fragment homologous replacement (SFHR)

SFHR uses single-stranded or double-stranded DNA fragments homologous to a genomic or episomal target to mediate homologous exchange intracellularly [170]. The exact mechanisms that lead to this ability to induce nucleotide change are still unclear, but the method is flexible in that it can direct insertion, deletion or alteration of up to 4 bp at a time. The potential of SFHR has led to studies in cystic fibrosis research, where so far correction of the cystic fibrosis conductance regulator (*CFTR*) gene by insertion of 3 bp has been successful in up to 10% of treated human epithelial cells *in vitro* [171]. Two other diseases that have shown the benefit of using this technique are sickle cell anaemia (caused by a point mutation in the human β-globin gene) [172] and Duchenne's muscular dystrophy (caused by a point mutation in the *mdx* gene) [173], though in both cases correction frequencies were low. Although this method seems to have many positive points, a possible setback could

be if self-annealing of the single-stranded molecules occurred resulting in double-stranded DNA that randomly integrated into the genome [174].

1.3.2.2 *Triplex-forming oligonucleotides (TFOs)*

DNA triplexes are formed when a purine-rich DNA duplex binds with a single-stranded oligonucleotide through hydrogen bonds in the major groove of the DNA helix. When a third strand is present, DNA loses its flexibility along with its ability to recognise proteins. TFOs can therefore be used to direct nuclease cutting in specific locations [175] or induce mutations [176] in the genome. They are also able to inhibit mRNA synthesis, which could lead to their use in the treatment of cancers [177]. The problems associated with TFO use are low stability, their dependence on polypurine target sequences, and susceptibility to nucleases. At this point in time TFO technology is in the *in vitro* stage, but the future could see drug development based on the technique. Recent analysis of the human genome for TFO susceptibility has found that these sites are common and many contain single nucleotide polymorphisms (SNPs) [178], opening up many possibilities for controlling gene expression and correcting SNP-related diseases.

1.3.3 GENE EDITING WITH CHIMERAPLASTS AND SSONS

1.3.3.1 *Chimeraplasty background*

Chimeraplasts are oligonucleotides of roughly 50 to 90 nucleotides, though in most published studies a 68-mer length is used. They are mainly DNA, with short RNA segments, and are able to hybridize with a target gene location to mediate the correction of single-base mutations *in situ*. The technique of chimeraplasty first made its appearance in 1996, when it was shown to mediate correction in the human alkaline phosphatase gene [179]. Development of the chimeric RNA-DNA oligonucleotide originated from studies into homologous recombination by the same group. While looking at the optimal conditions required by the RecA protein to promote recombination, they came to the conclusion that 50 to 72 bases of sequence homology were necessary for RecA-mediated changes to occur. Then in order to try to reduce the number of bases required, the use of RNA was examined. Results

obtained pointed towards the ability to form stable joint molecules with only 15 bases of shared homology if a chimeric RNA/DNA hairpin was used. The RNA element in the oligonucleotide also proved to be more resistant to RNase H digestion than oligonucleotides made of DNA alone [180].

Whereas the first published success using chimeraplasts targeted an episomal gene transiently transfected into CHO cells, the publication that quickly followed targeted a gene in its natural position. This study used a chimeraplast to mutate the β-globin gene in lymphoblastoid cells of a patient with sickle cell anaemia. The *in vitro* experiment was analysed by RFLP and sequencing, and produced up to 50% base conversion from T to A [181].

A year later, hepatocytes were shown to be amenable to targeting by chimeraplasty when the human hepatoma cell line HuH-7 was used in order to mutate the alkaline phosphatase gene again. Confocal microscopy of cells transfected with fluorescently-labelled chimeraplast showed a clear migration of the oligonucleotides into the nucleus after 24 hours. Colony lift hybridization analysis showed an initial conversion of 37% when cells were transfected with 150 nM of chimeraplast, with an increase to 43% with 300 nM of chimeraplast, indicating a dose-dependent response. The authors also treated the same cells with a chimeraplast that targets the β-globin gene, to prove that a gene need not be transcriptionally active in order for chimeraplasty to work [182].

The first *in vivo* use of chimeraplasty appeared in 1998 to target the factor IX gene (associated with haemophilia) in rats. *In vitro* work showed that using lactosylated polyethylenimine (lac-PEI) as a delivery vehicle into primary hepatocytes can create a higher conversion rate at lower chimeraplast doses. Tail-vein injections of 350 μg chimeraplast showed a 40% conversion 5 days post-injection when delivered with lac-PEI. The conversion created here changed the wild-type gene to a mutated variant, which codes for a faulty factor IX with diminished coagulation properties. After *in vivo* chimeraplasty, coagulation activity decreased by at least 50% in the treated rats, demonstrating that the changes created by chimeraplasts are evident at the genotypic as well as phenotypic level [183].

A nice example of success in creating a clear phenotypic change using chimeraplasty is in a publication demonstrating targeting of the tyrosinase gene, responsible for the production of melanin, in albino melanocytes. Here the point

mutation to convert cells back to black pigmentation is immediately apparent, with further analysis serving as confirmation of the mutation at the genomic level. Treated cells were cloned and were able to keep the phenotypic change for over 3 months, and the genotypic change for 15 passages, showing that this was a stable and inheritable mutation [184].

The first doubts as to the true capabilities of chimeraplasty appeared with a publication by a Swedish group, who claimed to have targeted 6 different human genes and one canine gene with 42 chimeraplasts of varying size and composition, with no lasting success. On PCR analysis they report a 2-10% conversion with one of their targets after the first 3 days of treating cells, but a disappearance of the conversion after 14 days. Allele-specific PCR resulted in a 5% conversion, with inability to confirm this by cloning or sequencing. The group's worry was whether the unstable conversion they observed was actually a PCR artefact created by the chimeraplast's presence, possibly still near its target sequence even after DNA purification from cells [185].

Although this may well be a possibility, Kren *et al.* were careful to show that no PCR artefacts were responsible for their results by sequencing the start and end-points of their PCR product to show that they corresponded exactly to those of the primers and not of the nondegraded chimeraplasts. On the other hand, the stability of these chimeric oligonucleotides was demonstrated early on, in the first paper published on the subject [179]. The authors transfected cells with the chimeric oligonucleotides, then isolated them by lysing the cells with detergents and proceeding to a phenol/chloroform extraction, followed by separation on polyacrylamide gels. They managed to show that the chimeraplast is a very stable molecule and is still intact after being subjected to the above treatment. This would indicate that PCR reactions performed on DNA purified from chimeraplast-treated cells probably contain intact chimeraplast in the reaction mix. Our laboratory has shown that there is no evidence that chimeraplasts serve as PCR templates and thus are not able to lead to artefactual indications of gene correction [186].

Nevertheless, chimeraplasty work continued to appear, with possible uses in dermatology, against hyperbilirubinaemia, against Duchenne's muscular dystrophy and in agriculture targeting plant cells [187-190]. However, no studies have been reported in which chimeraplasty was used in the cardiovascular field, until the publication by our group of chimeraplasty to target the apolipoprotein E (apoE) gene.

The study showed that a SNP which had mutated the apoE3 genotype to apoE2 was sensitive to reversal by chimeraplast action, and produced both genotypic and phenotypic changes *in vitro*, confirmed by RFLP, sequencing, and isoelectric focusing. Preliminary results showed that the apoE2→E3 chimeraplast was also successful *in vivo* by intraperitoneal injection into mice [191]. ***Table 1-5*** summarises the main chimeraplasty work to date.

1.3.3.2 Structure and activity of chimeraplasts

Chimeraplast structure consists of an oligonucleotide with a 5′ end that is all-DNA and matches the sequence of the target, with the mismatch correction at its centre. This DNA segment is followed by four thymidines allowing the molecule to bend. Next is a 2′-O-methyl RNA segment which is the homologous targeting region, with at its centre 5 DNA nucleotides corresponding to the mutator site. Further downstream is a GC-rich clamp (to increase nuclease resistance) bridged by another four thymidines, followed by a nick which allows swivelling of the chimeraplast, allowing it to coil with its target double-stranded DNA. The design of the chimeraplast molecule allows it to become self-complimentary and fold into a double-hairpin ***(Figure 1.3A)***.

Mismatch repair is thought to occur in two stages. It is believed that the first step involves the alignment of the chimeraplast with its homologous DNA target by interaction with recombinase proteins. The cell's repair machinery would then notice an unusual structure when it reached the genomic target region, which would set off the sequence of events that would exchange nucleotides to repair the mismatch, possibly involving hMSH2, a protein involved in mismatch repair [192].

Gamper and colleagues [193] published the most comprehensive study into the relationship between chimeraplast structure and function, in order to try to understand why some targets are repaired at higher frequencies than others. By structurally modifying an oligonucleotide created to mutate the neomycin phosphotransferase gene, they came to some interesting realisations about the importance of certain features of these chimeric molecules. They found that initiation of the process probably involved heteroduplex formation between the DNA strand of the chimeraplast and the complementary strand of the target gene. The DNA strand then serves as a template for mismatch repair. They also found that some mismatches

are repaired more efficiently than others; for example, a G-G mismatch is repaired better than a C-C mismatch.

By modifying the RNA content of the chimeraplast, Gamper demonstrated that this modulates the frequency of gene correction. They showed that an all-DNA oligonucleotide had half the activity of one containing 2'-O-methyl RNA in the homologous targeting region. The RNA region is believed to provide stability for the whole structure when hybridized with the target DNA. The length of the homologous region was also examined, with the conclusion that detectable repair activity requires at least 16 bp of homology, but that increasing the length also increases activity.

Further insight into the mechanisms involved in gene repair mediated by chimeraplasts was gained by assaying gene conversion in *Saccharomyces cerevisiae* yeast strains deficient in members of the RAD52 epistasis group [194]. These genes are involved in homologous recombination and repair. The study showed that RAD1 and RAD59 are required for gene conversion whereas RAD52 actually suppresses gene correction. Investigations also revealed that RAD51 has a role in strand pairing, as reduction of this protein decreased strand pairing activity [195]. It is also believed that a double-displacement loop structure is formed when chimeraplasts interact with their target [196] and that RAD51 may stabilize this structure. The importance of this protein was confirmed in chimeraplasty studies that used cells overexpressing RAD51, where correction efficiencies were increased [197]. This fact could provide a useful addition to chimeraplasty protocols to improve gene correction activity.

Target gene	Publication	Target cells	Mutation	Analysis methods	Results
Human alkaline phosphatase	Yoon *et al.* [179]	Recombinant CHO cells	A→G (...AC<u>A</u>CC...)	Histochemical staining, Hirt DNA probing	30% conversion at 11 nM chimeraplast
	Kren *et al.* [182]	Huh-7 cells	As above	Colony lift hybridisation, sequencing	37% conversion at 150 nM
Human β-globin	Cole-Strauss *et al.* [181]	Lymphoblastoid cells	T→A (...TG<u>T</u>GG...)	PCR-RFLP, sequencing	50% conversion at 1.34 nM
Rat factor IX	Kren *et al.* [183]	Primary rat hepatocytes (*in vitro* + *in vivo*)	A→C (...AT<u>A</u>GT...)	Colony lift hybridisation, coagulation studies	19% conversion *in vitro* (270 nM) >50% decrease in coagulation *in vivo*
Mouse tyrosinase	Alexeev *et al.* [184]	Melan-c cells	C→G (...CT<u>C</u>TA...)	Microscopy for colour change, PCR-RFLP, sequencing, Western blotting	15% conversion at 440 nM
Plant acetolactate synthase	Beetham *et al.* [190]	Tobacco plant cells	C→A/T(...GC<u>C</u>AC ...)	Cell selection, sequencing	Positive on sequencing
Kanamycin	Cole-Strauss *et al.* [192]	Plasmids in E. coli	G→C (...TA<u>G</u>GA...)	Colony counts on plates, PCR-RFLP	Maximum ~0.1% conversion
Tetracyclin	As above	As above	A→T (...CT<u>A</u>GG...)	As above	As above
Plant acetohydroxyacid synthase	Zhu *et al.* (1999) *Proc. Natl. Acad. Sci. USA* **96**, 8768-8773	Maize cells *in vivo*	G→A (...AA<u>G</u>TC...) C→G (.....<u>C</u>CG....)	PCR-RFLP	Mutation frequency 10^{-4}
Rat UDP-glucuronosyltransferase	Kren *et al.* [188]	Rat hepatocytes	A→G (...TG<u>A</u>AA...)	Filter lift hybridisation, sequencing	Conversion 15.3%
Dog dystrophin	Bartlett *et al.* [189]	Dog skeletal muscle *in vivo*	G→A (...TC<u>G</u>GG...)	RT-PCR, Western blotting	Repair positive for 48 weeks
Human apoE	Tagalakis *et al.* [171]	Recombinant CHO cells and rat *in vivo*	T→C (...AG<u>T</u>GC...)	PCR-RFLP, sequencing	37% conversion at 400 nM

Table 1-5: Genes successfully targeted by chimeraplaty.

1.3.3.3 Gene repair with single-stranded oligonucleotides

The observations of Gamper and colleagues [198] that the all-DNA strand of the chimeraplast directs the repair event led them to consider whether a solitary DNA strand might function efficiently without the remaining sequences. Using cell-free extracts to correct a mutation in the gene conferring kanamycin resistance, the group tested various short (25 nt) molecules and found that an all-DNA construct was one fifth as active as the traditional chimeraplast. When phosphorothioate linkages were added to the 3′ and 5′ ends of the molecule to increase resistance to nucleases, correction activity was up to 3.7 times higher than for the chimeraplast. The same study also showed that these single-stranded oligonucleotides (SSONs) can repair deletion mutations successfully, and this was confirmed in a later study [199]. Additionally, optimisation of SSON length found 74 nt and 6 phosphorothioate linkages to result in the most active molecules (***Figure 1.3B***).

Another interesting development into SSON function is that they have strand bias. When comparing modified SSONs that are designed to hybridise with the transcribed strand or the non-transcribed strand of a target sequence, repair of the non-transcribed strand is up to 50 times greater. This is believed to reflect the fact that RNA polymerase is more active on the transcribed strand of DNA. Therefore the SSON targeting the transcribed strand gets displaced by the polymerase more readily than the SSON targeting the non-transcribed strand [200]. This hypothesis was supported by showing strand bias when targeting a transcriptionally active gene.

Work continues into the mechanisms involved in gene repair, and with the prospects of developing efficient gene therapy tools, methods to improve SSON activity are the most interesting. Several gene repair enhancers have been suggested: camptothecin, an anticancer drug that promotes DNA breakage at replication forks [201]; 2′,3′-dideoxycytidine to elongate the S phase [202]; or overexpression of Rad51 [203]. All these have been shown to increase correction frequencies.

The potential of SSONs as a gene therapy modality is obvious, but to date it has only been shown to correct a mutation in the gene responsible for Huntington's disease [204], and the β-globin and γ-globin genes to treat sickle cell disease [205], both in an *in vitro* setting. It will be interesting to see in the future whether this technology is exploited to its fullest potential and reaches clinical applications.

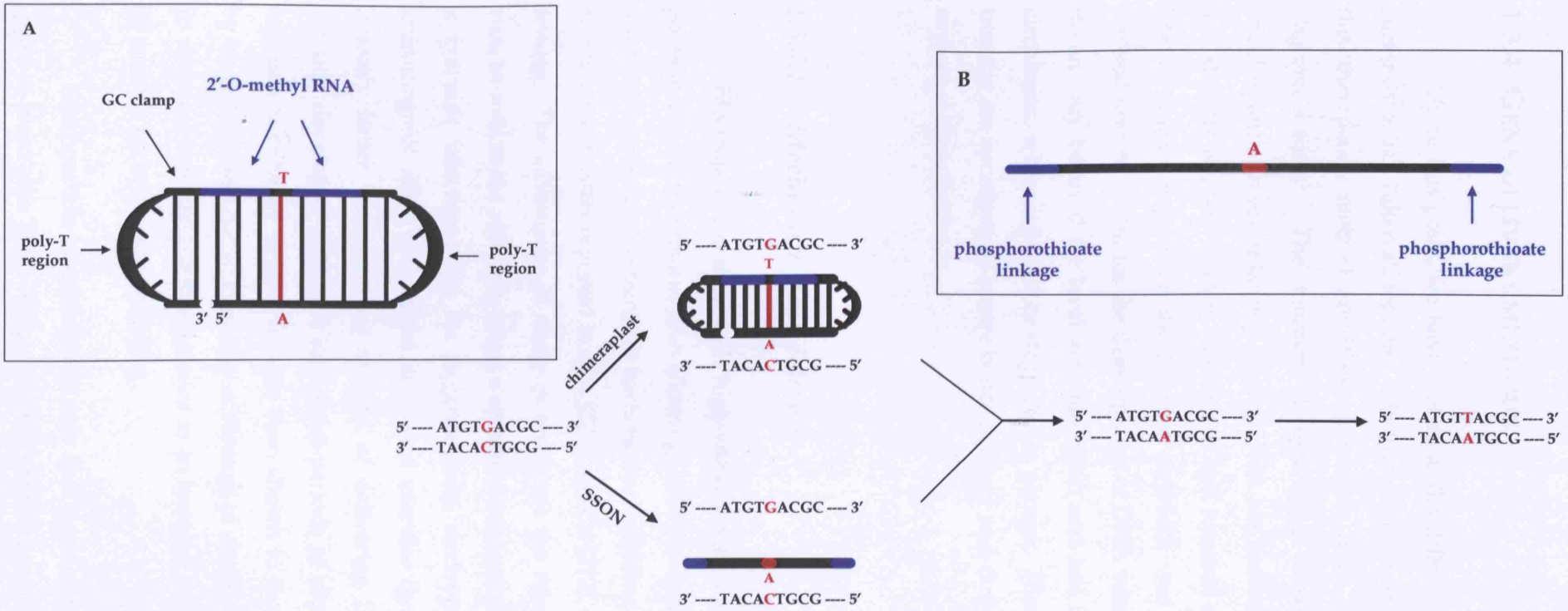

Figure 1.3: Structure and function of chimeraplasts and single-stranded oligonucleotides.

***A**: A typical chimeraplast consists of a targeting DNA segment, two poly-T regions, a 2′-O-methyl-RNA segment (blue) with DNA centre mutator region and a GC clamp. **B**: A modified single-stranded oligonucleotide (SSON) is all DNA with the mutation site at its centre (red) and phosphorothioate linkages at both ends (blue). The bottom diagram illustrates that both chimeraplasts and SSONs have a similar proposed mechanism of action. After hybridizing with its target sequence, the chimeraplast/SSON directs correction of one strand (here C→A) followed by a second mismatch repair event to correct the complementary strand (here G→T).*

1.3.4 GENE DELIVERY METHODS

Up to this point, we have looked at the different gene therapy strategies that currently exist. Taken all together, whether viral or non-viral, the objects that mediate this therapeutic method are DNA molecules, from large plasmids to very short oligonucleotides. The manner of delivering these molecules to their target cells/organs also varies largely. Naked DNA has been used to inject into muscle [206] and directly applied to liver, epidermal, and tumoral cells [207-209], and results in low level gene expression the purpose of which was immunisation. This simple method may be useful for the development of DNA vaccines, but its limitation is that it can only be used for local administration and not for injection into the general circulation, where it would be degraded in plasma. Therefore, other methods of gene transfer are necessary to assure better delivery and target specific organs. Below are several of these methods.

1.3.4.1 Mechanical gene delivery

Electroporation uses short high-voltage pulses to create transient hydrophilic pores in the cell membrane, thus allowing DNA molecules to enter the cell [210]. It is most commonly used to transfect bacteria, but is finding a place in gene therapy, with *in vivo* gene transfer reported in skin [211], muscle [212], and liver [213] amongst other tissues. The advantages of electroporation are the relative low cost and low safety risk, as well as the ability to target a specific treatment site, which is not possible with a systemic injection. On the negative side, electroporation appears to have an immunogenic effect and causes decreased vascular flow to the targeted area [200]. Possibly better would be the method of delivering DNA using ultrasound. This recently developed technique uses short periods of ultrasound exposure after DNA injection to enhance uptake, and has been shown to increase expression of transgene by up to 10 times [214] *in vitro*. The advantage of ultrasound is its safely, confirmed by its wide use over the last few decades as an imaging modality, and it would therefore be suitable for *in vivo* gene delivery.

Microparticle bombardment was first developed in 1987 in order to deliver genes to plant cells [215]. Originally the particle propellant was gunpowder, but the

current method is to use DNA-coated gold particles in what is known as the "gene gun." The particles are small enough to pass through the cell membrane. Once inside the cell, the DNA disassociates from the gold particles and can make its way to the nucleus. An example of recent use of this method for gene transfer is to introduce dystrophin cDNA into skeletal muscle of mice with muscular dystrophy. Although *in vitro* expression was sustained for 60 days [216], only transient transfection was found when the same technique was used *in vivo*. Some positive points to using the gene gun are the ability to deliver DNA of variable size, cell-receptor independent delivery, and the possibility to repeat administration. Nevertheless, unless the technique is used directly on skin, cells would have to be transfected *ex vivo* from any other internal site, complicating matters.

Microinjection is another method that does not allow *in vivo* applications other than into embryos, but the great advantage here is that DNA can be introduced directly into the cell nucleus. This eliminates the problems associated with reactions of the organism to a systemically introduced vector and degradation of the vector in plasma or inside the cell. This technique is widely used for delivering genetic material to many types of cells [217-219], including embryonic stem cells, where it will in the long run probably be of most use as a gene therapy delivery tool.

1.3.4.2 Chemical facilitation of gene transfer

One of the most common methods for transfecting cells with DNA is using calcium phosphate precipitation. DNA forms complexes with calcium phosphate, allowing endocytosis while protecting the DNA from degradation before its entry into the cell. The problem with this technique is that investigation into its action showed that over 50% of internalised DNA gets degraded in the cytoplasm before even reaching the nucleus, where less than 10% was found [220]. It is therefore not ideal as a gene delivery agent on its own. Nonetheless, Hasan and colleagues [221] showed that transfections combining calcium phosphate with pre-treatment of cells with chloroquine can increase transfection efficiencies by up to 20 times. This is because chloroquine is believed to neutralise lysosomal enzymes by raising the pH and therefore protects internalised DNA from degradation. Nevertheless, though it does improve gene delivery, this study showed a best efficiency of only 0.2%.

Cationic lipids such as (N-[1-92,3-diolyloxy)propyl]-N,N,N-trimethylammonium chloride, 1,2-dioleoyl phosphatidylethanolamine (DOPE) or N-[-1-(2,3-dioleoyloxy)propyl]-N,N,N-trimethylammonium methyl sulphate (DOTAP) work as DNA carriers because of polar heads that are protonated at physiological pH. By forming vesicles they surround DNA molecules (making lipoplexes), their amine groups binding electrostatically to the phosphate groups of DNA. These reagents can be injected intravenously, but end up mainly in the lungs [222]. To circumvent this, the addition of polyethylene glycol (PEG) diverts the DNA-liposome complexes away from the lungs [223]. Although able to protect DNA on its travels to target organs, there have been reports of cell toxicity with these formulations [224].

Another class of delivery agents are the cationic polymers. Examples of these are diethylaminoethyl dextran (DEAE-dextran), poly-L-lysine, and PEI. These carriers can have a linear or branched backbone and vary in degree of protonation at physiological pH. The condensing ability of cationic polymers is independent of DNA length or molecular weight [225]. To some extent, the cell type that is transfected is a factor in choosing the most efficient polymer, possibly because of the different nature of the plasma membrane and endosomes of each cell line [226]. Though many polymer formulations exist, the most widely used of this class of reagents is PEI and this was the reagent of choice for the experiments performed in this thesis.

1.3.4.3 Polyethylenimine (PEI)

PEI has been used for many years outside the biomedical field, for example in the production of shampoos and paper. It exists in two forms: linear and branched, and in both the structure is such that every third atom is an amino nitrogen, which confers the protonability of the reagent. The usefulness of PEI, as with other cationic polymers, comes from its ability to condense DNA for gene delivery. Each amine can bind a DNA phosphate, and at physiological pH only some of them are protonated [227]. This feature makes PEI more efficient than other polymers as a gene delivery agent. PEI is described as being a "proton sponge," because when the pH of endosomes becomes acidic it captures protons causing osmotic swelling that leads to endosomal rupture and release of carried DNA into the cytosol [228].

Further evidence of the mechanisms of PEI's action as a delivery agent was provided by a study that tracked the course of fluorescently-labelled PEI and plasmid DNA after transfection by confocal microscopy [229]. The time course for uptake of PEI/DNA complexes into cytoplasmic vesicles appeared to be about 3 h. The complexes then either stay there or are dispersed in the cytoplasm following vesicular rupture. At 3.5 h fluorescence begins to appear in the nucleus, and interestingly the DNA at this point is still associated to PEI. A more recent study [230] tried to elucidate what happens to PEI/DNA complexes in the nucleus and showed that the presence of PEI attached to template DNA does not impair transcription.

PEI is able to transfect a variety of cell lines [231] both *in vitro* and *in vivo* [228,232]. The excess of positive charges present in PEI/DNA complexes is very useful for targeting cells *in vitro* because the positive charge allows binding to the anionic cell surface [233]. At the same time, this advantageous property leads to problems when the reagent is used *in vivo*. The complexes induce erythrocyte aggregation [234] and interact with albumin, fibrinogen and the complement. When injected intravenously, most of the complexes end up in the lungs [235], probably because complex aggregates get trapped in pulmonary capillaries. As mentioned in *Section 1.3.4.2*, in order to avoid the entrapment in the lungs, PEG can be used to coat polyplexes and mask the surface charge [236]. Although adding PEG does help to a certain extent, it also reduces PEI's ability to bind DNA and the interactions between PEI/DNA complexes and target cells are diminished, resulting overall in less efficient gene delivery [237]. To overcome this problem, cell-specific ligands can be used.

In order to target a specific organ or type of cell, knowledge of receptors on that cell can be exploited in order to use receptor-mediated endocytosis instead of the non-specific electrostatic interactions of regular PEI/DNA complexes. Various ligands have been found to target complexes specifically, in the form of sugar residues, peptides, proteins or antibodies. Galactose has been used to target the asialoglycoprotein receptor of hepatic cells [238], mannose the mannose receptor on macrophages [239], transferrin the transferrin receptor [240] and epidermal growth factor (EGF) the EGF receptor on tumour cells [241], amongst others.

One other interesting PEI conjugate which has recently appeared is melittin-PEI. Melittin is a peptide derived from bee sting venom with membrane lytic activity [242]. It was conjugated to PEI in order to enhance transfection efficiency. Most transfected PEI/DNA complexes get trapped in cytoplasmic endosomes, but the

presence of melittin releases the complexes so that more can reach the nucleus, as well as enhancing transport into the nucleus. Delivery efficiency *in vitro* was shown to increase from 10% to 40% in the presence of melittin-PEI rather than ordinary PEI. The use of PEI and its various conjugates continues, with promising advances [243-245] that will hopefully lead to successful gene transfer in human therapies.

1.4 AIMS OF THE THESIS

Gene therapy for atherosclerosis is still in its infancy. There are many possible targets, though few investigations have currently arrived to the clinical trial phase. Two main categories exist in treatment approach. The first aims to influence the coronary and peripheral vasculature by delivering anti-atherogenic genes locally. The other uses a systemic approach to modulate the expression of circulating proteins associated with atherosclerosis, such as LCAT. LCAT-related research has so far only used gene addition strategies for LCAT-deficient states and to illustrate the effects of overexpression in transgenic animals.

LCAT has important atheroprotective functions: it promotes cholesterol efflux from peripheral tissues into HDL, enhances uptake of CE by the liver, and functions as an antioxidant for LDL. *Section 1.2.5* discussed two point mutations in the LCAT gene that have been shown to increase the enzyme's activity, therefore possibly amplifying its anti-atherogenic properties. Then we saw in *Section 1.3.3* that a technique called chimeraplasty can introduce point mutations to genes *in situ*. Taken together, these two elements can be combined to create a form of gene therapy that promotes atheroprotection.

Building on the above, the aims of my thesis were:

Aim 1: To generate a recombinant cell line expressing LCAT with a double mutation - Ser208Ala and Ser216Ala, and to assess the relative activity of this LCAT variant compared to wild-type LCAT and LCAT with just the Ser216Ala mutation.

Aim 2: To optimise transfection efficiency for delivery of chimeraplasts by comparing PEI and its conjugates as delivery agents using a chimeraplast that mutates the *APOE* gene, a validated target for chimeraplasty. Delivery efficiency would be analysed by measuring uptake of chimerplast into the nucleus by FACS and gene correction by RFLP.

Aim 3: To transfect a hepatoma cell line, HepG2, with chimeraplasts and SSONs directed at the LCAT gene sites Ser208 and Ser216 in order to mutate these sites to alanines using optimal gene transfer conditions. If this is successful, to go on to clone the mutated cells and analyse the mutated LCAT for increased enzymatic activity.

Chapter 2 –

Materials and Methods

MATERIALS

Plasmid vectors containing the LCAT cDNA were kindly provided by Dr. D. Vinogradov (Royal Free & University College Medical School, London, UK). The vector from which the LCAT-IRES-apoE sequence was taken was generously provided by Dr. T. Athanasopoulos (Royal Holloway University of London, Egham, Surrey, UK). All oligonucleotide primers were made to order by Sigma Genosys (Cambridge, UK). *Pfu* Turbo DNA polymerase was purchased from Stratagene (Cambridge, UK). Calf intestinal alkaline phosphatase and T4 DNA ligase were obtained from Promega (Southampton, UK). Methanol, ethanol, diethyl ether, chloroform, hexane, and glacial acetic acid were bought from BDH Laboratory Supplies (Poole, UK). Ecoscint A scintillation fluid was bought from National Diagnostics (Leicestershire, UK). All other reagents, unless otherwise stated in the text, were obtained from Sigma-Aldrich Company Ltd. (Poole, UK).

EXPERIMENTAL METHODS

2.1 MOLECULAR BIOLOGY

2.1.1 GEL ELECTROPHORESIS

Gel electrophoresis is a simple, yet very useful method of visualising DNA molecules [246]. When DNA is placed in a matrix of agarose or polyacrylamide and a current is applied, the DNA migrates through the porous matrix towards the positive pole. The size of the pores in the gel determines the mobility of the DNA through it. By increasing the concentration of the agarose or polyacrylamide, the average pore size is decreased and larger DNA molecules will therefore stop moving earlier. This leads to separation of DNA fragments when a mixed sample is applied to the gel. Agarose is used for separating fragments of DNA ranging in size from a few hundred base pairs to about 20 kb, while polyacrylamide gels are more useful for separating smaller fragments. The bands of DNA in the gel are stained with

ethidium bromide, an intercalating dye, and can be seen as fluorescence when the gel is illuminated with ultraviolet (UV) light.

In this thesis, agarose gels were made up in Tris-borate ethylenediaminetetra-acetate (TBE) buffer [100 mM Tris, pH 8.4, 90 mM boric acid, 1 mM ethylenediaminetetra-acetate (EDTA); diluted from a 10x stock (Life Technologies, Paisley, UK)] as shown in **Table 2-1**, boiled in a microwave for about 2 minutes to dissolve the agarose, cooled to about 50°C, after which 0.1 µg/ml ethidium bromide was added before pouring into a cast. Once set, gels were placed in a minigel tank (Horizon, Life Technologies) and covered in TBE buffer. Samples were mixed 9:1 with 10x concentrated loading buffer [10 mM Tris-HCl, pH 7.5, containing 50 mM EDTA, 10% (w/v) Ficoll 400, 0.25% (w/v) bromophenol blue, 0.25% (w/v) xylene cyanol FF] and loaded into the wells. The samples were run in parallel with 1-2 µg of a 1 kb or 100 bp DNA ladder (Life Technologies) to help estimate DNA fragment size. A voltage of 150 V was applied to the gel until the bromophenol blue reached approximately 2 cm from the bottom of the gel. Gels were then viewed immediately and photographed on a UV light box.

% agarose	g agarose / 100 ml buffer	fragment size resolved
0.8	0.8	5 - 10 kb
1	1	1 - 6 kb
2	2	200 bp - 1 kb

Table 2-1: Agarose gel electrophoresis.

Commonly used concentrations and the DNA molecule sizes that can be visualised at that concentration. The buffer used was 1x TBE.

The polyacrylamide gels used in this thesis were precast Novex 20% TBE-polyacrylamide gels (Invitrogen, The Netherlands) that were run in a vertical tank (Mini-cell Xcell II gel tank; Invitrogen). Samples were mixed 4:1 with 5x concentrated Novex High-density TBE sample buffer (Invitrogen) [18 mM Tris base,

18 mM boric acid, 0.4 mM EDTA (free acid), 3% Ficoll 400, 0.02% (w/v) bromophenol blue, 0.02% (w/v) xylene cyanol FF] and a maximum of 35 µl sample loaded per well. The gel was immersed in 1x TBE buffer and a 200 V current was applied until the bromophenol blue reached the bottom of the gel. Gels were then stained in 1x TBE buffer containing 0.1 µg/ml ethidium bromide for 5 min before being visualised and photographed.

For resolving oligonucleotides, TBE-urea gels were used. These are similar to the ones described above, but are denaturing, therefore appropriate for the separation of single-stranded oligonucleotides or RNA. Precast gels were used (Novex TBE-urea gels; Invitrogen) to visualise chimeraplasts in order to have an indication of whether structures were intact. A single band of the correct size (68 or 80 nt) suggests that the chimeraplast molecules are not degraded, whereas degradation appears as a smear. The concentration of gel used was 15%, as this is optimal for visualising oligonucleotides as small as 20 nt. Electrophoresis was achieved by mixing 100 pmol of chimeraplast 1:1 with Novex TBE-urea 2x concentrated sample buffer [45 mM Tris base, 45 mM boric acid, 1 mM acid free EDTA, 6% (w/v) Ficoll 400, 3.5 M urea, 0.005% (w/v) bromophenol blue, 0.025% (w/v) xylene cyanol], then heating the sample to 96°C for 10 min before loading into the gel. The gel was then placed in a vertical tank, immersed in 1x TBE buffer and a current of 150 V was applied for 1 h. The gel was stained in 1x TBE buffer containing 0.1 µg/µl ethidium bromide for 5 min before visualising by UV.

2.1.2 EXTRACTION OF DNA FROM AGAROSE GELS

Following manipulation of DNA by PCR (*Section 2.1.3*) or restriction digestion (*Section 2.1.4*), the resulting fragments were frequently extracted from agarose after visualisation under UV light, in order to proceed to restriction digests or ligation into plasmids. The QIAquick Gel Extraction kit (Qiagen, Crawley, UK) was used to extract bands from agarose. DNA was cut out of the gel over UV light using a scalpel. The gel pieces were weighed and 3 volumes of the kit's QG solution were added to every volume of gel (i.e. 3 µl per mg gel). To solubilise the gel, sample and solution were heated at 50°C for 10 min, then vortexed. Once all the agarose had dissolved, one volume of 100% (v/v) isopropanol was added for every volume of gel to precipitate the DNA, then the sample was transferred to a QIAquick spin column and

spun at 24,000 g for 1 min to bind the DNA to the column. The flow-through was discarded and the column washed with 750 µl of the kit's PE buffer and centrifuged again for 1 min. The column was then transferred into a clean 1.5 ml microtube, 30 µl deionised water was added to the column, left for 1 min, and the DNA was eluted by centrifugation for 1 min.

DNA concentration was determined by measuring the absorbance at 260 nm (A_{260}) using a spectrophotometer (UVIKON 930, Kontron Instruments, Hertfordshire, UK) and the following equation:

DNA concentration (µg/ml) = A_{260} x dilution factor x 50 µg/ml

2.1.3 POLYMERASE CHAIN REACTION (PCR)

PCR is a process by which a specific sequence of DNA can quickly be amplified to great quantities [247]. The reaction uses two oligonucleotide primers flanking the DNA sequence to be amplified that hybridize to the opposite strand once the DNA had been denatured. DNA polymerase then proceeds to synthesize new DNA between the two primers, which can in turn hybridize with the primers to yield more copies of the target region. The reaction goes through repeated cycles of heat denaturation, primer hybridization, and extension, so that an exponential amount of DNA is quickly synthesized.

In the course of my work, two genes were examined by PCR: *LCAT* and *APOE*. For LCAT, the region that was amplified encoded the amino acid 208 and 216 sites targeted by chimeraplasty. Two sets of primers were designed based on sequences from database accession numbers X04981 and NM_000229, one to amplify the region from genomic DNA (primers "S208A genomic"), the other from cells containing LCAT cDNA (primers "S208A cDNA") The cDNA primers were necessary because one of the genomic primers hybridizes within an intron and would therefore not be of use for studying LCAT cDNA. ***Figs. 2.2*** and ***2.3*** show the amplification regions and RFLP patterns obtained. Optimization of annealing temperature was achieved by using a heating block that can run a gradient of temperatures (RoboCycler 40 Gradient Cycler, Stratagene). For each of the two primer pairs annealing temperatures of 58-62°C were tried. For apoE (accession number NM_000041), the primers used analysed the region that showed the genotypic

differerence between apoE2/apoE3 and apoE3/apoE4 (primers "TF, TR") (*Fig. 2.4*) and the cycling conditions had already been previously established [191].

The primer sequences are shown in *Fig. 2.1*. **Table 2-2** shows the optimal PCR conditions used for each primer pair. PCR reactions were set up in 0.5 ml tubes and volumes made up to 50 µl using DEPC water. All PCR analyses included a negative control (containing DEPC water instead of the DNA template) to ensure that no DNA contaminated the master mix.

S208A genomic primers:

Forward: 5' - AGGAGATGCACGCTGCCTA - 3'
Reverse: 5'- CCCAGGATCAGCTTGGTCT – 3'

S208A cDNA primers:

Forward: 5' – AGGAGATGCACGCTGCCTAT – 3'
Reverse: 5' – TCTTTCAGCTTGATGCTGGA – 3'

ApoE primers:

TF: 5' – TCCAAGGAGCTGCAGGCGGCGCA – 3'
TR: 5' – ACAGAATTCGCCCCGGCCTGGTACACTGCCA – 3'

Fig. 2.1: Sequences of the primers used in this thesis for RFLP analyses.

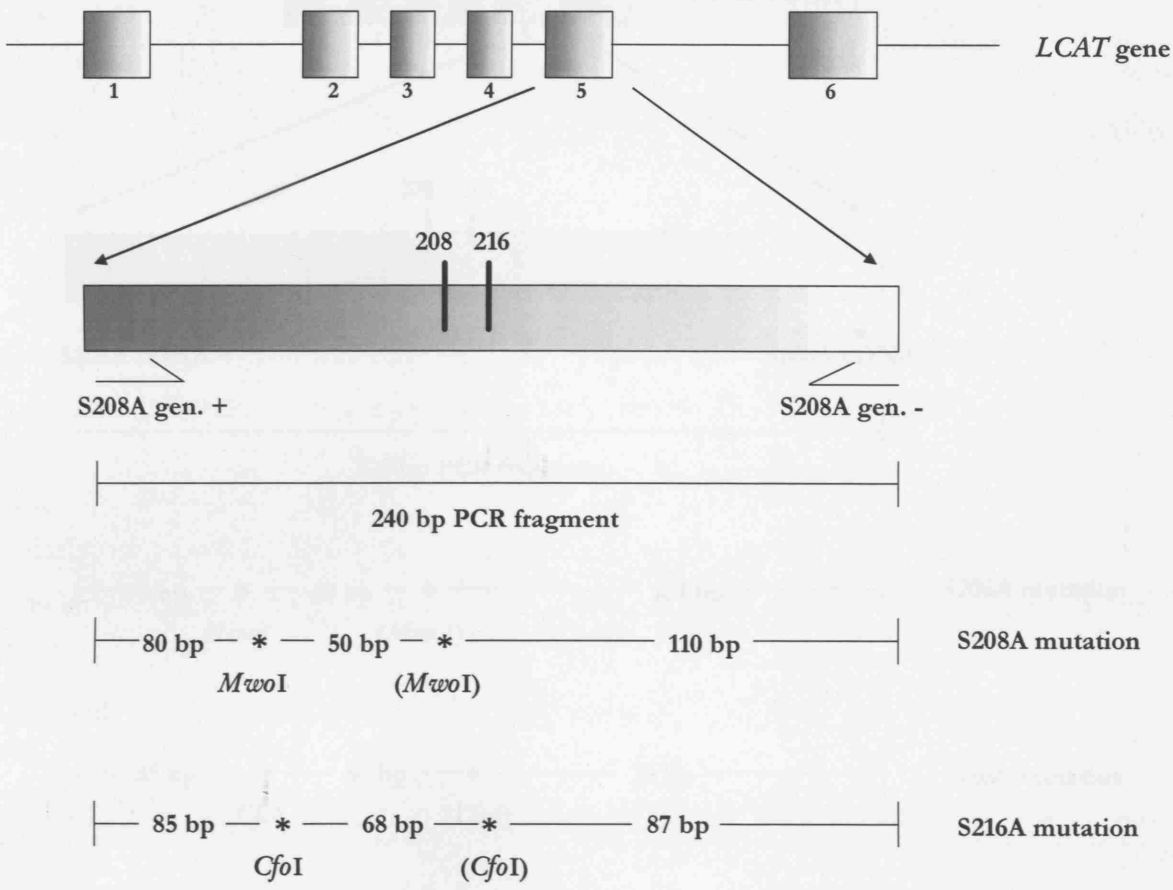

Fig. 2.2: PCR-RFLP for analysis of LCAT genomic DNA.

The LCAT gene (accession number X04981) is represented above with boxes for its six exons. The S208A genomic primers amplify a 240 bp fragment that encodes the 208 and 216 targeting areas. To look for a mutation at the 208 site, the PCR fragment is digested with MwoI. Wild-type LCAT DNA produces two restriction fragments, while with the S208A mutation an additional restriction site appears resulting in three digest fragments. Similarly, for analysis at the 216 site, digest with CfoI results in two fragments for wild-type LCAT and three fragments when the S216A mutation is present due to the appearance of a new digest site. Restriction sites are indicated by stars. The digest sites in parentheses refer to those present only if the mutations are present.

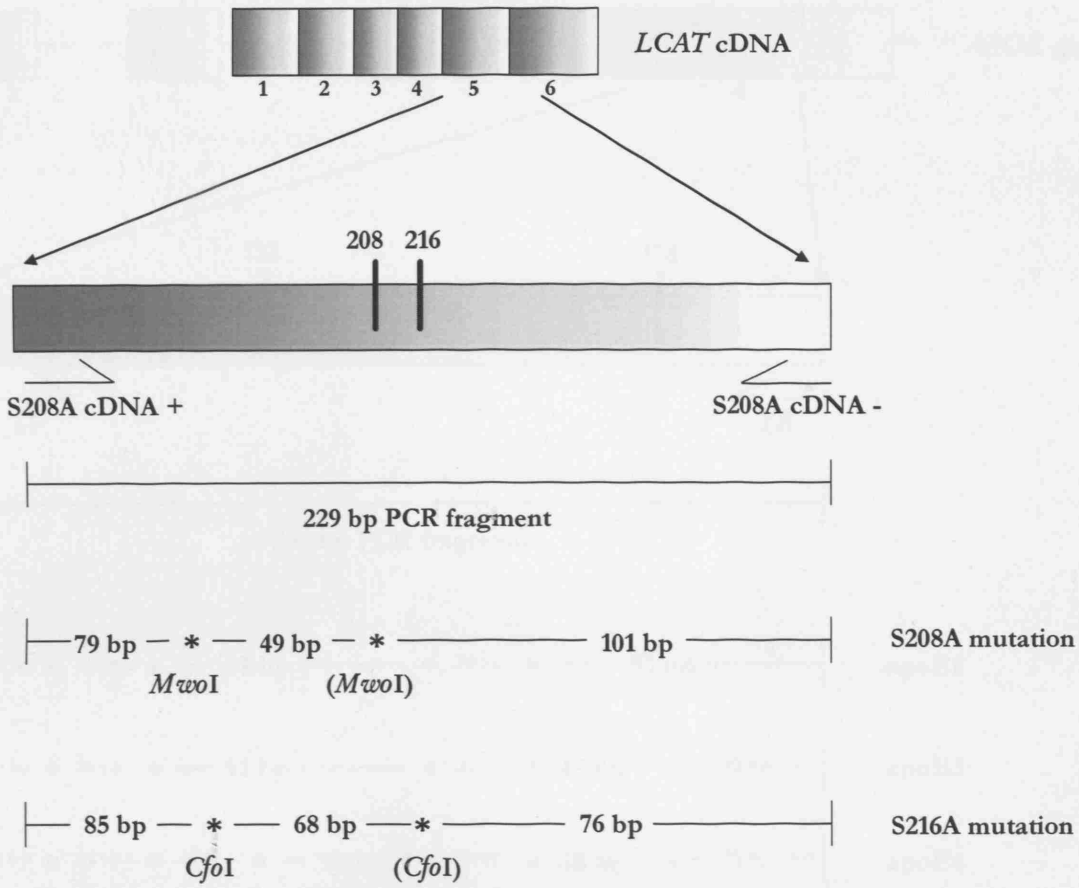

Fig. 2.3: PCR-RFLP for analysis of LCAT cDNA.

The S208A cDNA (accession number NM_000229) primers amplify a 229 bp PCR fragment contanining the 208 and 216 codons. The 208 site is analysed by digest of the PCR fragment with MwoI. Wild-type LCAT appears as two digest products, while the S208A mutation adds a second restriction site (in parentheses) resulting in three restriction fragments. For the 216 site, the pattern is similar after digest with CfoI, where the S216A mutation adds a second restriction site. Digest sites are indicated by stars.

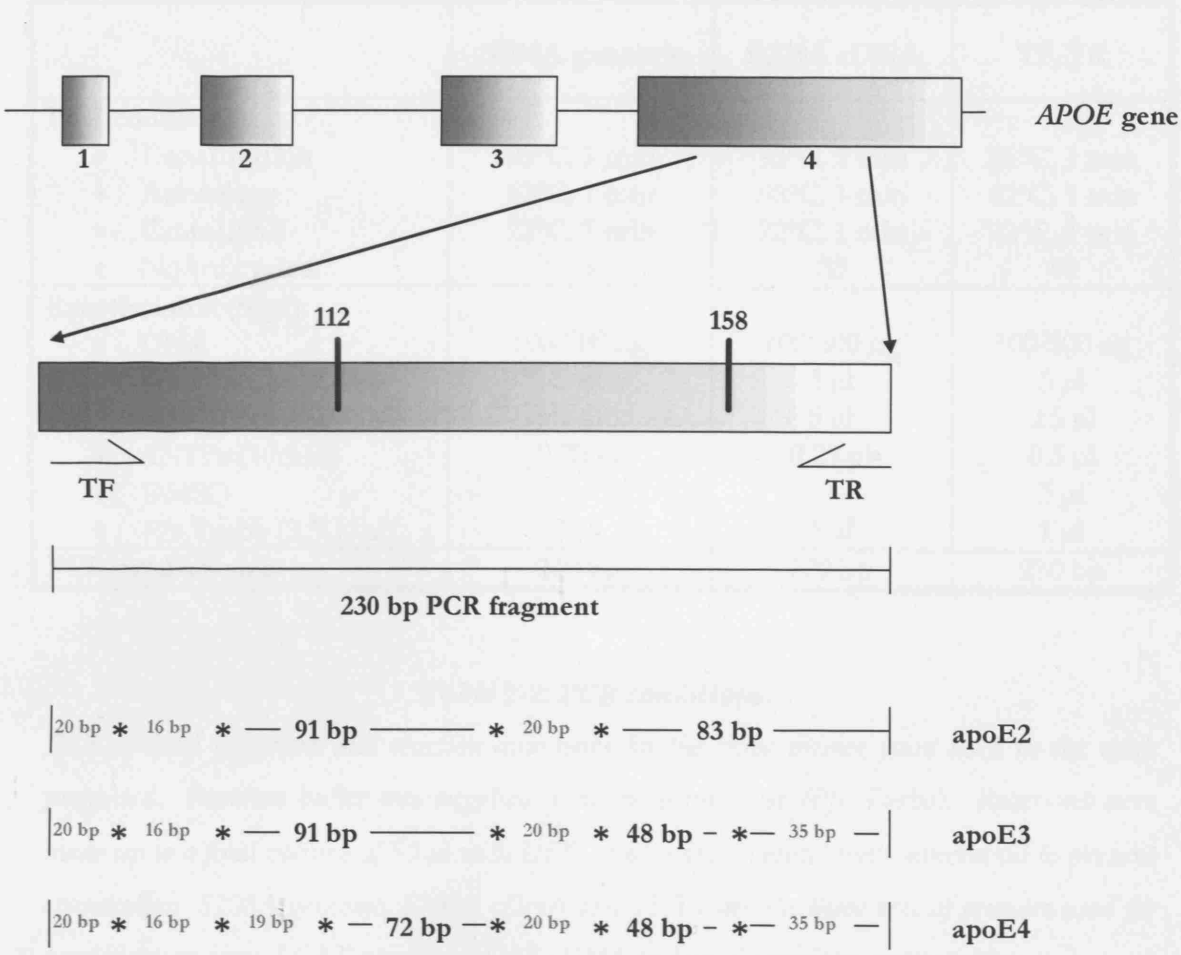

Fig. 2.4: PCR-RFLP for APOE analysis.

The primers TF and TR amplify a region within the fourth exon of the APOE gene (accession number NM_000041) that contains all three genotype sites: apoE2, apoE3 and apoE4, resulting from variations at amino acids 112 or 158. In order to distinguish between them, digest of the 230 bp PCR product with CfoI results in restriction fragments that vary for each genotype. In each case, the two largest digest products are diagnostic: for apoE2 fragments of 91 and 83 bp, for apoE3 91 and 48 bp, and for apoE4 72 and 48 bp. The sizes of the remaining fragments are in grey. TF: forward primer, TR:reverse primer.

	S208A genomic	S208A cDNA	TF, TR
PCR conditions:			
• Denaturation	95°C, 1 min	95°C, 1 min	96°C, 1 min
• Annealing	62°C, 1 min	58°C, 1 min	62°C, 1 min
• Extension	72°C, 1 min	72°C, 1 min	72°C, 1 min
• No. of cycles	35	35	40
Reaction mix (50µl):			
• DNA	100-500 ng	100-500 ng	100-500 ng
• 10x reaction buffer	5 µl	5 µl	5 µl
• Each primer (10 µM)	5 µl	5 µl	2.5 µl
• dNTPs (10mM)	0.25 µl	0.25 µl	0.5 µl
• DMSO	---	---	5 µl
• *Pfu* Turbo (2.5U/µl)	1 µl	1 µl	1 µl
PCR product size	240 bp	229 bp	230 bp

Table 2-2: PCR conditions.

PCR optimal programs and reaction quantities for the three primer pairs used in the work presented. Reaction buffer was supplied with the polymerase (Pfu Turbo). Reactions were made up to a final volume of 50 µl with DEPC water and overlaid with mineral oil to prevent evaporation. S208A genomic, S208A cDNA and TF,TR are the three sets of primers used for amplification from LCAT genomic, LCAT cDNA and apoE templates respectively.

2.1.4 RESTRICTION DIGESTION

This method of cutting double-stranded DNA by using restriction endonucleases was vital in the present work for creating the expression vectors that would make recombinant cell lines, and for restriction fragment length polymorphism (RFLP) analysis of experiments (see ***Figs. 2.2*** to ***2.4***). Restriction endonucleases are enzymes of bacterial origin that are able to cleave DNA at specific recognition sites. Hundreds of these enzymes have been identified so far, each with its own recognition sequence [248]. For the purposes of gene manipulation, an appropriate enzyme can often be found for a specific location where cleavage is required.

DNA was digested with various restriction enzymes, listed in **Table 2-3**. In general, DNA was placed in a 0.5 ml microtube with 1x reaction buffer (provided by the manufacturer with the enzyme), BSA if required by the specific enzyme, deionised water to make up to a set final volume, and the enzyme added last. No more than 10% of the total reaction volume was made up of enzyme in order to avoid star activity. (Star activity is enzymatic cleavage at a site similar but not identical to the defined recognition sequence of that enzyme, occurring during unfavourable reaction conditions.) The tube was then incubated in a water bath at the appropriate temperature for that enzyme for at least 1 h. Digests were then either viewed immediately by agarose gel electrophoresis or stored at -20°C.

2.1.5 PLASMID DEPHOSPHORYLATION

Before ligating fragments of DNA to a linearised plasmid to form a circular vector, dephosphorylation of the vector is necessary in order to remove the 5'-terminal phosphate groups. The purpose of dephosphorylation is to avoid both recircularisation of the vector without insertion of the DNA fragment and plasmid dimer formation. This was achieved with calf intestinal alkaline phosphatase (CIAP; Promega). Following the manufacturer's recommendation, the amount of CIAP required for the reaction was calculated based on the fact that 0.01 units of CIAP are required per pmol ends. To calculate the pmol ends, the following formula was used:

$$\text{pmol ends} = (\mu\text{g plasmid} / \text{kb length plasmid}) \times 3.04 \qquad [249]$$

Enzyme	Recognition sequence	Incubation temperature	Supplier and buffer used
BamHI	5′ - G▼GATCC - 3′ 3′ - CCTAG▲G - 5′	37°C	Promega Buffer E
CfoI	5′ - GCG▼C - 3′ 3′ - C▲GCG - 5′	37°C	Sigma Buffer SM
DpnI	5′ - G^{me}A▼TC - 3′ 3′ - CT^{me}▲AG - 5′	37°C *	Stratagene Universal buffer
DraIII	5′ - CACNNN▼GTG - 3′ 3′ - GTG▲NNNCAC - 5′	37°C **	New England Biolabs Buffer 3
EcoRI	5′ - G▼AATTC - 3′ 3′ - CTTAA▲G - 5′	37°C	Promega Buffer H
HindIII	5′ - A▼AGCTT - 3′ 3′ - TTCGA▲A - 5′	37°C	Promega Buffer E
MwoI	5′ - GCNNNNN▼NNGC - 3′ 3′ - CGNN▲NNNNNCG - 5′	60°C	New England Biolabs MwoI buffer
NdeI	5′ - CA▼TATG - 3′ 3′ - GTAT▲AC - 5′	37°C	Promega Buffer D
NotI	5′ - GC▼GGCCGC - 3′ 3′ - CGCCGG▲CG - 5′	37°C	Promega Buffer D

Table 2-3: Restriction endonucleases.

*List of enzymes used in this thesis and their activity conditions. Symbols ▼ and ▲ indicate the restriction location. * DpnI requires N_6-methylation of the adenine residue for activity. ** DraIII requires the addition of 1 μg/ml BSA to the reaction mix.*

The required amount of plasmid was incubated with the CIAP and 10x reaction buffer (diluted in deionised water) at 37°C for 30 min. The same amount of CIAP was then added again and incubation was continued for a further 30 min. The reaction was stopped by adding 2 µl 0.5 M EDTA and incubating at 65°C for 20 min. The plasmid was then purified by ethanol precipitation (see *Section 2.1.6*), resuspended in deionised water, and then stored at -20°C, following estimation of its concentration by OD_{260}.

2.1.6 ETHANOL PRECIPITATION

This is a method of cleaning up and concentrating DNA that has previously been treated with enzymes. In the course of my work, ethanol precipitation was carried out on plasmids following enzyme treatment. This was achieved by adding 1/10 of the DNA volume of 3 M sodium acetate (pH 5.2) and 2.5 times the combined volume of ethanol. The reagents were mixed and left overnight at -20°C, then centrifuged at 24,000 g for 10 min at 4°C. The supernatant was removed, the pellet washed with 100 µl 70% (v/v) ethanol and centrifuged again for 15 min at 4°C. Ethanol was removed and the pellet allowed to air-dry for several min, then the DNA was resuspended in the appropriate volume of water.

2.1.7 PLASMID LIGATION

Ligation of linearised plasmid and DNA insert was accomplished using T4 DNA ligase (Promega). Quantities of vector and insert were calculated using the following formula:

ng insert = (ng vector x kb insert) / kb vector x ratio (insert/vector)

In general, two insert/vector ratios were tried: 3/1 and 1/1. The reaction mix consisted of vector, insert, 10x ligation buffer supplied with the enzyme (diluted with deionised water) and the ligase in a total volume of 10 µl. Ligation reactions were

either incubated at room temperature for 4 h or left at 4°C overnight, and could be used for transformation into bacteria immediately or stored at -20°C.

2.1.8 SITE-DIRECTED MUTAGENESIS

Site-directed mutagenesis is a technique used to specifically alter a given base in a cloned DNA sequence. Several methods exist using cassettes, oligonucleotides, or PCR. In this case a commercial kit was used: the QuikChange XL Site-Directed Mutagenesis Kit (Stratagene). The method starts by using *Pfu* Turbo DNA polymerase to replicate both plasmid strands, extending from oligonucleotides primers that contain the required mutation. This results in nicked circular DNA strands. The original strands are then digested with DpnI, a restriction enzyme that recognises methylated DNA, such as plasmid DNA originating in E. coli bacteria. Finally, the new plasmid is transformed into XL-Gold ultracompetent cells (Stratagene), where the nick in the mutated plasmid is repaired. Specifically, the mutagenesis kit was used to create the T→G mutation that produces the S208A amino acid change in a plasmid already containing LCAT with the S216A mutation: pLCATHBS216A. This plasmid is a pUC18 vector into which LCAT cDNA was cloned using *Hind*III and *Bam*HI restriction enzymes.

The sequences of the mutagenesis primers are:

MUT208+ : 5′ - CGCTTTATTGATGGCTTCATC<u>G</u>CTCTTGGGGCTCC - 3′

MUT208- : 5′ - GGAGCCCCAAGAG<u>C</u>GATGAAGCCATCAATAAAGCG - 3′

The underlined bases represent the mutation. The primers were designed following the kit's recommendations that they should be 25 to 45 bases long with a melting temperature (Tm) ≥ 78°C, calculated using the formula: Tm = 81.5 + 0.41(%GC) - 675/N - % mismatch, where N is the primer length in bases. Also recommended was that there should be correct sequence for 10-15 bases on either side of the mutation, a minimum GC content of 40%, and that the primer should terminate in one or more C or G bases. Several quantities of plasmid template and various elongation times were tested for the PCR reaction. **Table 2-4** shows the optimal reaction mix and cycling conditions.

The cycling product was then immediately digested with 10 u of DpnI for 1 h at 37°C. Ten microliters of the digest was run on a 1% agarose gel in parallel with linearised pLCATHBS216A (digested with *Bam*HI) to compare plasmid size. Once it was established that the cycling was successful, the remaining digest product was stored at 4°C until ready to transform into bacteria.

	Reaction volumes
DNA (10 ng/µl)	3 µl
10x Pfu Turbo buffer	5 µl
Primer MUT208+ (4 mM)	3 µl
Primer MUT208- (4 mM)	3µl
dNTPs (10 mM)	1 µl
Deionised water	34 µl
***Pfu* Turbo polymerase (2.5 u/µl)**	1 µl
Final volume	50 µl

Denaturation	**Annealing**	**Elongation**
95°C for 30 sec	55°C for 1 min	68°C for 14 min

Table 2-4: Site-directed mutagenesis temperature cycling.

Optimal reaction volumes and cycling conditions. Cycling was started with 30 sec at 95°C followed by 12 cycles of denaturation-annealing-elongation.

2.1.9 BACTERIAL TRANSFORMATION

After cloning DNA into a vector, the resulting plasmid can be amplified in quantity by insertion into competent bacterial cells so that they will be replicated by the host's DNA synthesising machinery. Competence is a state in which bacteria are able to take up recombinant DNA vectors more easily, and can be induced by treatment with ice-cold calcium chloride solutions and brief heating [250].

All recombinant vectors in this thesis were transformed into DH5α E. coli, provided by Dr. A. Manzano (Royal Free & University College Medical School, London, UK) except for the plasmid resulting from site-directed mutagenesis, which was transformed into XL-Gold ultracompetent cells provided with the mutagenesis kit (*Section 2.1.8*), following the manufacturer's instructions.

Competent cells were thawed on ice and 50 µl used for each transformation. Between 20 and 50 ng of ligation mixture were placed in a cold 1.5 ml microtube, the competent cells were added and the tube left on ice for 1 h. The cells were then heated at 42°C for 90 sec and quickly cooled on ice for 5 min. Next 125 µl of LB broth were added to the tube and the bacteria were left to incubate at 37°C for 1 h with shaking at 200 rpm. The mixture was then spread onto LB agar plates containing 100 µg/ml ampicillin to select for transformants. The plates were left at room temperature for 1h, then turned upside-down and incubated in a 37°C incubator overnight. All transformed plasmids included ampicillin resistance and therefore only bacteria containing the transformed DNA would be resistant and could grow on the plate.

To analyse the transformation, colonies were picked from the plate and each colony injected into a 20 ml tube containing 6 ml LB broth with 100 µg/ml ampicillin. The tubes were then incubated at 37°C with shaking at 200 rpm overnight. These cultures were then used to extract plasmid for analysis by restriction digests and sequencing, to determine whether the correct recombinant plasmid was contained in individual colonies.

Once the success of the cloning and transformation was established, bacterial clones were prepared for indefinite storage in glycerol. Tubes containing 200 µl of glycerol were sterilised by autoclaving and 800 µl of a 10 ml overnight culture was

added per tube. The stocks were stored at -80°C and could be used again by spreading onto LB plates and incubating at 37°C.

2.1.10 PLASMID EXTRACTIONS

For small-scale plasmid preparations, the Wizard Plus SV Minipreps DNA Purification System (Promega) was used. Plasmids were extracted from 6 ml overnight culture by first pelleting the bacteria by centrifugation at 24,000 g for 5 min, then suspending the pellet in 250 µl cell resuspension solution [50 mM Tris-HCl, pH 7.5, 10 mM EDTA and 100 µg/ml Rnase A]. This was followed by the addition of 250 µl cell lysis solution [0.2 M NaOH and 1% (w/v) sodium dodecyl sulphate (SDS)], mixing by inversion of the tube 4 times, and incubating until the solution became clear. Then 10 µl of alkaline protease solution was added to inactivate endonucleases and other proteins released during lysis, the tubes were inverted 4 times to mix and incubated at room temperature for 5 min. Next, 350 µl of neutralisation solution [9.04 M guanidine hydrochloride, 0.759 M potassium acetate and 2.12 M glacial acetic acid, pH 4.2] was added, the tubes inverted 4 times and the mixture centrifuged at 24,000 g for 5 min to remove cell debris. To purify the DNA, the cleared lysate was decanted into spin columns sitting in 2 ml collection tubes. The columns were then spun for 1 min and the flow-through discarded from the collection tubes. Next, 750 µl of column wash solution [60% (v/v) ethanol, 60 mM potassium acetate, 8.3 mM Tris-HCl and 0.04 mM EDTA] was added to the columns and spun for 1 min. The flow-through was discarded and washing was repeated with 250 µl column wash solution, again spinning for 1 min. The DNA was then eluted by placing the column in a clean 1.5 ml microtube, adding 100 µl deionised water to the column and centrifuging for 1 min. Plasmids could then be stored at -20°C.

Larger-scale plasmid extractions were prepared using the EndoFree Plasmid Maxi kit (Qiagen). This kit has the ability to extract up to 500 µg of endotoxin-free plasmid DNA, ready to use for transfection into cells. Plasmids were extracted from bacteria resulting from 100 ml overnight culture, following the manufacturer's instructions. The process has the same principle as described for small-scale preparations, except that cell lysates are cleared by passing though a special filter that reduces endotoxin levels instead of by centrifugation, and includes a step of incubation with an endotoxin removal buffer.

2.1.11 CHIMERAPLAST PREPARATION

Three LCAT chimeraplasts were synthesized commercially by MWG-Biotech (Ebersberg, Germany) and one was produced by Eurogentec (Herstal, Belgium). They were delivered in solid form, with the manufacturer's advice for the volume of water in which to dissolve the pellet to give a working concentration of 100 pmol/µl. One fluorescent apoE chimeraplast was produced by MWG-Biotech, with a 5' fluorescein tag, and was delivered already in liquid form at a concentration of 100 pmol/µl. The chimeraplasts were dissolved in RNase/DNase-free distilled water and batched into 20 µl aliquots to avoid repeated freezing and thawing, and stored at -80°C. All handling of chimeraplasts was performed inside a class II microbiological safety cabinet (Envair Ltd., Lancashire, UK) to avoid oligonucleotide degradation. An aliquot of each of the LCAT chimeraplasts were then taken for measurement of the OD_{260}, in order to compare the determined oligonucleotide concentration to the one stated by the manufacturer. Concentrations were calculated in both µg/µl and pmol/µl using the following formulas:

$$\text{Conc. } (\mu g/\mu l) = OD_{260} \times 30\ \mu g/\mu l \times \text{dilution}$$

$$\text{Conc. } (\text{pmol}/\mu l) = \frac{OD_{260} \times 100 \times \text{dilution}}{(1.54 \times A) + (0.75 \times G) + (1.17 \times C) + (0.92 \times T)}$$

where A, G, C and T are the number of each of the four nucleotides adenine, guanine, cytosine and thymidine respectively in the chimeraplast. The second formula was provided by MWG-Biotech and is used by the company to calculate oligonulceotide concentrations. **Table 2-5** summarises the synthesised oligonucleotides and their manufacturer.

Chimeraplast	Length	Manufacturer
LCAT S208A	68-mer	MWG-Biotech
LCAT S216A	68-mer	MWG-Biotech
LCAT S216A	80-mer	MWG-Biotech
apoE3→E2 (5'-fluorescein)	68-mer	MWG-Biotech
LCAT S216A	68-mer	Eurogentec
LCAT S216A	68-mer	Oswel

Table 2-5: List of oligonucleotides synthesised for chimeraplasty studies.
MWG-Biotech produced two 68-mer and one 80-mer LCAT chimeraplast, as well as a fluorescent apoE chimeraplast. Following experimental difficulties, a further 68-mer LCAT chimeraplast was produced by Eurogentec. Due to the poor synthesis quantity, its sister company Oswel produced another identical chimeraplast.

2.1.12 DNA SEQUENCING

All automated fluorescent sequencing reactions were carried out by Cytomyx Sequencing Service (Cambridge, UK) using primers produced by Sigma Genosys.

2.2 PROTEIN DETECTION

2.2.1 SDS-POLYACRYLAMIDE GEL ELECTROPHORESIS (SDS-PAGE)

The principles of protein electrophoresis are the same as described for DNA electrophoresis (*Section 2.1.1*). The polyacrylamide matrix acts in the same way with proteins, but in this case the detergent sodium dodecyl sulphate (SDS) is added in order to remove the proteins' secondary and tertiary structures and coat the proteins with negative charges. This allows the molecules to be separated by their molecular weights. In the work presented here, protein electrophoresis was used to detect LCAT (63 kDa) or apoE (34 kDa). Both were separated on pre-cast Tris-glycine 4-20% gradient Novex gels purchased from Invitrogen. These gels have an increasing acrylamide concentration through the gel, thus allowing a wider range of molecular weights to be covered on the same gel compared to a single percentage gel, as well as producing sharper protein bands.

The sample was mixed 3:1 with 4x SDS-PAGE sample buffer [200 mM Tris-HCl, pH 6.8, 8% (w/v) SDS, 0.2% (w/v) bromophenol blue and 20% (v/v) glycerol]. Beta-mercaptoethanol was added to a final concentration of 2% (v/v) to break disulphide bonds in the proteins, followed by heating at 95°C for 5 min to denature the proteins. The broad range molecular marker (6-175 kDa; New England Biolabs, Hertfordshire, UK) was also heated. The wells of the pre-cast gels were first rinsed with distilled water, then with running buffer [25 mM Tris, pH 8.3, 192 mM glycine and 0.1% (w/v) SDS]. Samples and marker were then loaded into the gel. The electrophoresis chamber was filled with 1x running buffer, which was diluted from a 10x stock (National Diagnostics). Current was applied to the Mini-cell Xcell II gel tank (Invitrogen) following the manufacturer's instructions. The gel was removed when the dye front reached the bottom of the gel and, after removal from its plastic cassette, was either Coomassie stained or used for Western blotting.

2.2.2 COOMASSIE STAINING

This is a method of easily visualising proteins that have been separated by electrophoresis. Coomassie blue reacts with any protein and has a sensitivity of 0.1-0.5 µg protein per band [251]. After electophoresis, a gel can be stained by immersion in a container holding enough Coomassie stain [0.25% (w/v) Coomassie brilliant blue R-250, 50% (v/v) methanol and 10% (v/v) glacial acetic acid] to cover the gel. The gel is stained at room temperature with shaking for at least 30 min. Excess stain is removed by washing the gel with destain [30% (v/v) methanol and 10% (v/v) glacial acetic acid] several times. Finally, the gel is washed in distilled water and dried using the GelAir Drying Frame (Bio-Rad, Hemel Hempstead, UK).

2.2.3 PURIFIED PROTEIN QUANTIFICATION

Purified protein was quantified using the BCA Protein Assay Kit (Perbio Science Ltd, Cheshire, UK). The principle behind this kit is the biuret reaction (reduction of Cu^{2+} to Cu^{1+} by protein in an alkaline medium). When two molecules of bicinchoninic acid (BCA) chelate with one cuprous ion, it produces a purple-coloured reaction with a strong absorbance at 562 nm that is nearly linear with increasing protein concentrations up to 2 mg/ml.

Using bovine serum albumin (BSA) as a standard, a series of dilutions were prepared in triplicate alongside the samples to be quantified, to a total volume of 100 µl. The BCA reagent was prepared according to the manufacturer's instructions, and then 1 ml was added to each sample and incubated at 37°C for 30 min. The samples were transferred to disposable plastic 1 ml microcuvettes and the absorbance was read at 562 nm (OD_{562}) using an Uvikon 930 spectrophotometer (Kontron Instruments). A graph was plotted of the OD_{562} versus the concentrations of the BSA dilutions and used to extrapolate the concentrations of the test samples.

2.2.4 PREPARATION OF SAMPLES FOR WESTERN BLOTTING

In this thesis, Western blotting was used to detect production of apoE or LCAT by recombinant CHO cells carrying the genes coding for these proteins.

Conditioned media was prepared in the same way for all cell lines tested. Cells were grown in 75 cm^2 flasks in their maintenance medium (see ***Section 2.3.1***) to 80% confluency. They were washed in warmed PBS and incubated for 24 h in serum-free maintenance medium. The conditioned medium was then spun at 300 g for 3 min to remove cell debris and concentrated 40 x using Vivaspin concentrators (Vivascience, Hannover, Germany) with a 30,000 kDa MW cutoff by centrifugation at 2,500 g for approximately 20 min. The concentrated medium was then batched into small aliquots and stored at -20°C.

2.2.5 WESTERN BLOTTING

Once proteins in a sample have been separated by electrophoresis, the size of the proteins in the sample is evident but no more information is available when a mixture of proteins is present in the sample. Western blotting is a method of picking out a specific protein on a gel by probing it with a radioactive or enzymatically-labelled antibody. In this thesis, only enzymatically-labelled antibodies were used. Following gel separation, the proteins are transferred to a nitrocellulose membrane, and the protein binding sites on the membrane are blocked with excess protein. The membrane is then exposed to the specific primary antibody. Excess unbound antibody is washed away before the secondary antibody is added. This secondary antibody is directed against the primary antibody and labelled with horseradish peroxidase (HRP), an enzyme required for detection of the protein. After washing away excess secondary antibody, chemiluminescence is used to visualise the target protein. Using the ECL Western Blotting Detection Kit (Amersham Biosciences, Buckinghamshire, UK), the chemical reaction of luminol being oxidized by HRP results in the emission of light at a wavelength of 428 nm, detectable by exposure to blue-light sensitive autoradiography film.

Transfer of protein from gel to solid support was achieved by using Hybond ECL nitrocellulose membranes (Amersham Biosciences) and 3MM absorbent paper (Whatman International, Maidstone, UK) using a wet method. For each transfer, one membrane and two sheets of paper, all cut to the same size as the gel, were pre-soaked in transfer buffer [25 mM Tris, pH 8.3, 192 mM glycine and 20% (v/v) methanol]. They were then stacked in the following order:

CATHODE PLATE
layer of absorbent paper
polyacrylamide gel
nitrocellulose membrane
layer of absorbent paper
ANODE PLATE

The Novex Western Transfer Apparatus (Invitrogen) was used and the transfer sandwich placed in the centre of the Xcell II Blotting Module (Invitrogen) surrounded by pre-soaked sponges. The module was filled with transfer buffer and the blot run for 1h at a constant current of 72 mA. After the transfer, the membrane was blocked in a solution of PBS-T [138 mM NaCl, 10 mM Na_2HPO_4, 1.75 mM KH_2PO_4, 2.7 mM KCl and 0.05% (v/v) Tween 20] and Marvel milk powder. The membrane was immersed in the solution and left on a shaker at room temperature for 1 h or at 4°C overnight, followed by a wash in PBS-T for 10 min on a shaker. The primary antibody was then added and left to incubate for 1 h at room temperature (**Table 2-6**), followed by three 10 min washes is PBS-T. The secondary antibody was added, again incubating for 1 h at room temperature (Table 2-5), followed by three 10 min washes in PBS-T. The membrane was developed using ECL substrate, following the manufacturer's instructions (Amersham Biosciences), secured in a film cassette and exposed to X-ray film (Hyperfilm ECL, Amersham Biosciences).

The mouse anti-human LCAT monoclonal antibody was obtained from sub-clones of LCAT hybridomas kindly provided by Dr. T. Jowell (Monoclonal Antibody Unit, Windeyer Institute of Medical Science, University College London, UK). This was done by growing the cells to confluency in RPMI media supplemented with 1% pyruvate, 0.5% Hepes, 0.5% penicillin (100 U/ml) and 0.5 % streptomycin (100 µg/ml), in two 75 cm^2 flasks and keeping the cells for 2-3 weeks at 37°C with CO_2 until the cells were near dead (demonstrated by the loss of round morphology and adherence to the flask). Media from the cells was then centrifuged at 400 g for 3 min to remove cell debris and the supernatant concentrated 50x to be used as antibody.

The goat anti-human apoE polyclonal antibody was purchased from Biogenesis and the secondary antibodies from Sigma.

Antigen	LCAT	apoE
1° antibody	Mouse anti-human monoclonal	Goat anti-human polyclonal
dilution	1:20	1:2,000
buffer	3% (w/v) BSA/PBS	5% (w/v) milk/PBS-T
2° antibody	Sheep anti-mouse HRP	Rabbit anti-goat HRP
dilution	1:5,000	1:50,000
buffer	10% (w/v) milk/PBS-T	5% (w/v) milk/PBS-T

Table 2-6: Immunoblotting.

Details of antibodies used for Western blotting of LCAT and apoE proteins. BSA: bovine serum albumin. PBS: composition as for PBS-T but without Tween 20.

2.2.6 SCANNING DENSITOMETRY FOR LCAT QUANTIFICATION

As no other method existed at the time (such as ELISA) for quantifying the protein, LCAT production by recombinant CHO cells was estimated by producing Western blotting autoradiographs of various known quantities of pure LCAT (kindly provided by Dr. S. Schepelmann, Royal Free & University College Medical School, London, UK) [252] and LCAT from conditioned media. The pure LCAT was a histidine-6-tagged LCAT molecule with purity checked by SDS-PAGE. Using a scanning densitometer (Bio-Rad Imaging Densitometer Model GS-670), a standard curve could be produced of the pure protein band densities. This curve was then used to extrapolate quantities of secreted LCAT also present on the same autoradiograph. The local background was subtracted from each of the values and the mean 'adjusted volume' was calculated by the densitometer.

2.3 CELL CULTURE

CHO^{dhfr-} is a hamster ovary cell line that lacks the dihydrofolate reductase (*DHFR*) gene. This enzyme catalyses the conversion of dihydrofolate to tetrahydrofolate in the chain of reactions that produces thymidylate (dTMP), one of the essential building blocks of nucleotides. Plasmids transfected into these cells to produce LCAT all contain the *DHFR* gene, therefore only cells that have taken up the plasmid survive in media deficient in hypoxanthine and thymidine (HT). CHO-$LCAT_{WT}$ cells, secreting the wild-type LCAT protein, and CHO-$LCAT_{S216A}$ cells, secreting LCAT containing the S216A mutation, were both provided by Dr. D. Vinogradov (Royal Free & University College Medical School, London, UK). CHO-$LCAT_{2M}$ cells, secreting LCAT containing both S208A and S216A mutations, were produced as described in *Sections 2.1.8* and *2.3.4*. CHO-LE3 cells (containing the *LCAT* gene with a small *APOE* insert) were produced as described in *Section 2.3.4*. These cell lines are based on CHO^{dhfr-} cells.

CHO-K1 cells are the wild-type CHO cell variety expressing the *DHFR* gene, and were used to produce the CHO-EIL cell line (containing both *LCAT* and *APOE* full-length cDNAs). The human hepatoma cell line HepG2 was used for chimeraplasty experiments. CHO^{dhfr-}, CHO-K1 and HepG2 cells were acquired from the European Collection of Animal Cell Culture (ECACC, Wiltshire, UK), with ECACC numbers of 94060607, 85051005, and 85011430, respectively.

2.3.1 CELL MAINTENANCE

All cells were incubated at 37°C and in a 5% CO_2 / 95% air atmosphere (Jencons Millenium CO_2 incubator, Jencons-PLS). Cells were maintained in either 75 cm^2 or 175 cm^2 tissue culture flasks. Cell culture work was performed in a class II microbiological safety cabinet using disposable, sterile plasticware. **Table 2-7** shows the medium used for each cell line used in this thesis.

All cells were grown as adherent monolayers and passaged upon reaching near-confluency, approximately every 5 days. This was done by washing the cells in PBS then incubating them for 3 min with 0.25% (v/v) trypsin-EDTA at 37°C to detach

the cells, followed by neutralisation of the trypsin with fresh medium. The resuspended cells were then split 1:10.

Cell line	Medium	Supplements				
		FBS	Glut	P/S	NEAA	HT
CHO^{dhfr-}	Iscove's modified DMEM (Sigma)	dialysed 10%	1%	1%	1%	2%
CHO-$LCAT_{WT}$	as above	dialysed 5%	1%	1%	1%	---
CHO-$LCAT_{S216A}$	as above	dialysed 5%	1%	1%	1%	---
CHO-$LCAT_{2M}$	as above	dialysed 10%	1%	1%	1%	---
CHO-LE3	as above	dialysed 10%	1%	1%	1%	---
CHO-K1	Ham's F12 (Life Technologies)	10%	1%	1%	---	---
CHO-EIL*	as above	10%	1%	1%	---	---
HepG2	DMEM (Life Technologies)	10%	1%	1%	---	---

Table 2-7: Maintenance medium for cell lines used in this thesis.

*DMEM: Dulbecco's Modified Eagle's Medium. FBS: foetal bovine serum, heat inactivated (Sigma). Glut: glutamine 2 mM. P/S: penicillin 100 U/ml and streptomycin 100 µg/ml. HT: hypoxanthine 0.1 mM and thymidine 16 µM. NEAA: non-essential amino acids. All supplements were purchased from Life Technologies. *Also received 500 µg/ml G-418 sulphate (Invitrogen) for selection.*

2.3.2 CELL COUNTING AND VIABILITY

When cell counts were necessary before seeding for transfection or to assess cell viability, this was achieved by using Trypan Blue stain 0.4%. Live cells are able to pump out the Trypan Blue that they take up, while dead cells are unable to do so, resulting in their appearance as dark circles. An aliquot of cell suspension was added to an equal volume of Trypan Blue and pipetted immediately onto a haemocytometer under a firmly attached coverslip. Cells were counted using an inverted phase-contrast microscope (Nikon TMS, Jencons-PLS) and averaging the number of cells in each of eight 1 mm^2 squares with a total volume of 10^{-4} ml. The number of cells was calculated using this formula:

Cells / ml = (average cell count per square) x dilution / 10^{-4}

2.3.3 CRYOPRESERVATION

Stocks of cells were kept for future use by storage under liquid nitrogen. To do this, a minimum of 10^6 cells were suspended in 1 ml cell culture medium containing 10% (v/v) DMSO. The suspended cells were transferred to a 1.8 ml cryovial (Life Technologies) which was placed in a freezing container (Nalgene Cryo 1°C Freezing Container, Fisher Scientific, Leicestershire, UK) and inserted into a -80°C freezer. The freezing vessel contains isopropanol and when stored at -80°C the temperature of the vials decreases by ~1°C every minute. Once the cryovials reach -80°C they are transferred to liquid nitrogen tanks.

When required, cells were thawed rapidly by dipping a cryovial into a 37°C water bath, and then quickly transferred to a tube containing 10 ml cell culture medium. The cells were pelleted by centrifugation at 300 g for 5 min in a bench-top centrifuge (Heraeus Megafuge 1.0R) and resuspended in fresh medium before being transferred to a 75 cm^2 flask.

2.3.4 PLASMID TRANSFECTION AND CELL CLONING

In the work presented in this thesis, three new recombinant cell lines were produced. CHO-LCAT$_{2M}$ and CHO-LE3 (see *Section 2.3* for description) were made by transfecting CHO^{dhfr-} cells with the pXLCAT$_{2M}$ and pXLE3 expression vectors, respectively. CHO-EIL cells (described in *Section 2.3*) were created by transfecting CHO-K1 cells with the pXEIL expression vector. All transfections were done the same way. The day before transfection, cells were seeded at a density of approximately 3 x 10^5 cells/well in a 6-well plate. The transfections were performed using linear PEI 22-kDa (Exgen 500, TCS Cellworks, Botolph Claydon, UK) as the transfection reagent, each well receiving the combinations in **Table 2-8**. Complexes were incubated for 10 min at room temperature in 0.5 ml tubes before they were added to the wells, already containing 0.5 ml Iscove's medium. The complexes were incubated with the cells for 5 h, after which 2 ml fresh cell culture medium was added to each well to dilute the complexes.

Well	150 nM NaCl	Plasmid	Exgen 500 (PEI)
1	made up to 50 µl	2 µg expression plasmid	5.4 µl
2	"	"	"
3	"	"	"
4	50 µl	---	---
5	made up to 50 µl	---	5.4 µl
6	"	2 µg pGFP	"

Table 2-8: Plasmid transfection mixes.

Complexes were formed in 0.5 ml tubes by adding the above in the order NaCl – plasmid – Exgen 500 and mixed by pipetting. The volume of Exgen 500 used was calculated based on an N:P ratio of 6:1 (see Section 2.3.5 for formula). The plasmid pGFP contains the green fluorescence protein (GFP) gene and transfected cells

therefore produce green fluorescence, which can be used as a control of transfection efficiency.

Twenty-four hours after transfection, the pGFP transfected cells were observed using an inverted fluorescence microscope (Nikon Eclipse TE200) at 20x magnification with a NB2EC filter incident light of wavelength 465-495 nm. This served as a control for the efficiency of transfection with PEI. Wells 1-3 (**Table 2-6**) were treated with trypsin-EDTA, and the detached cells pooled, and transferred to a 75 cm^2 flask. From here on they were given only selection medium. For the CHO^{dhfr-} transfections this was medium without the HT supplement (see ***Section 2.3***). For the CHO-K1 transfection, cells were selected by adding 500 µg/ml G-418 Sulfate (Invitrogen) to the media. G-418 is an antibiotic related to gentamicin, toxic to both prokaryotic and eukaryotic cells [253]. Resistance to G-418 is conferred by the presence of a resistance sequence of bacterial origin in the transfected plasmid. The presence of antibiotic in culture medium creates a selection of only cells that contain the transfected plasmid with the resistance genes. The cells from wells 4 and 5 were also pooled and transferred to a 75 cm^2 flask to serve as a negative control for selection.

After incubation in selection medium it was expected that cells that had not taken up the transfected plasmid would die, as should all cells in the control flask. The resulting cell population could then be used to produce individual clones. A suspension of selected cells was used to make serial dilutions that were seeded into 96-well plates to a final dilution of 0.5 cell per well. After the cells had adhered, wells containing a single cell were marked and left for the cells to divide. Once several divisions had occurred, the clones were trypsinised and transferred to progressively bigger wells to allow for expansion.

2.3.5 CHIMERAPLAST TRANSFECTIONS USING POLYETHYLENIMINES (PEIs)

Linear PEI 22-kDa (Exgen 500) is supplied as a ready-to-use solution stored at 4°C. The solution is 5.47 mM in nitrogen residues, and this number helps calculate the amount of PEI required to transfect a known quantity of DNA, using a formula supplied by the manufacturers:

Quantity of PEI (µl) = (equivalents x µg DNA x 3) / 5.47

where an equivalent is the quantity of PEI needed to get one nitrogen - DNA phosphate grouping, and thus giving the N:P ratio. Chloroquine was obtained from Sigma in solid form and, after dissolving in PBS to a concentration of 10 mM, was sterilized by filtration. Branched PEI 800-kDa, Melittin-PEI 25-kDa, Melittin-PEI 2-kDa, Galactose-PEI 25-kDa, Galactose4-PEI 25-kDa and Transferrin-PEI 25-kDa were kindly provided by Dr. Manfred Ogris (Ludwig-Maximilians-Universität, Munich, Germany).

Transfections of chimeraplasts with linear PEI were performed by first seeding cells in 12-well plates, 24 h prior to transfection at a density of 1.5 x 10^5 cells/well. DNA-PEI complexes were made up by combining chimeraplast, PEI, and 150 nM NaCl in the order NaCl - chimeraplast - PEI to a volume of 50 µl. Complexes were left to form for 10 min at room temperature, after which they were added to the cells, already covered with 200 µl medium. Cells were incubated with the complexes at 37°C for 6 h, after which the medium was removed, the cells washed once in PBS, and fresh medium added. The cells were left to grow, usually for 24 h, and then harvested for DNA isolation and RFLP analysis.

For transfections using the PEI conjugates, **Table 2-9** shows details of concentrations of the different PEI conjugates and the calculated amounts required for transfection. The N:P ratio indicates the number of PEI nitrate groups per DNA phosphate group that interact to form complexes. HepG2 cells plated the day before in 24-well plates (5 x 10^4 cells/well) were targeted using this variety of PEIs as transfection reagent and the E3→2 chimeraplast (*Section 5.2.1*). The medium was removed from the wells and 100 µl fresh medium containing no FBS (plain medium) was added to each well. Each of the PEIs and the chimeraplast were combined in 0.5 µl microtubes in a total volume of 100 µl HBS, the mix vortexed, and left at room temperature for at least 10 min to allow the PEI/DNA complexes to form. **Table 2-10** shows the exact quantities used for each experiment. The complexes were added to the cells, the plates centrifuged for 2 min at 270 g, and the cells incubated at 37°C for approximately 6 h before the complexes were diluted by the addition of 500 µl FBS-containing medium to the wells. Cells were harvested 24 h later for DNA extraction and RFLP analysis. When chloroquine was used, it was added directly to the wells at a final concentration of 100 µM, 5 min before the addition of the PEI/DNA complexes to the cells. Each experimental condition tested was usually performed in triplicate.

PEI	Concentration N^+ residues (mM)	Concentration (mg/ml)	µl to use per µg chimeraplast for N:P ratio of:		
			5:1	7:1	9:1
Linear (22-kDa)	5.47	0.23	2.7	3.8	4.8
Branched (800-kDa)	23	1	0.6	0.9	1.2
Melittin (25-kDa)	22.9	0.92	0.7	1.0	1.2
Melittin (2-kDa)	3.5	0.15	4.2	5.9	7.5
Galactose (25-kDa)	8	2.8	0.2	0.28	0.36
Galactose4 (25-kDa)	50	0.19	0.3	0.4	0.6
Transferrin (25-kDa)	16	0.6	1.1	1.5	2.1

Table 2-9: Concentrations of PEI conjugates and transfection guidelines.

The concentration of N^+ residues indicates how much DNA is required to interact with the PEI at the above ratios.

	24-well plate (total volume 200µl)				6-well plate (total volume 500µl)			
	E3→2	PEI_1	PEI_2	HBS	FE3→2	PEI_1	PEI_2	HBS
Linear	3µl	2µl	---	95µl	1µl	5.4µl	---	93.6µl
Linear + Chloroquine	3µl	2µl	*	90µl	1µl	5.4µl	**	88.6µl
Branched	3µl	0.5µl	---	96.5µl	1µl	1.2µl	---	97.8µl
Melittin2	3µl	3.2µl	---	93.8µl	1µl	8.4µl	---	90.6µl
Linear + melittin2	3µl	1µl	1.6µl	94.4µl	1µl	2.7µl	4.2µl	92.1µl
Melittin25	3µl	0.5µl	---	96.5µl	1µl	1.4µl	---	97.6µl
Linear + melittin25	3µl	1µl	0.3µl	95.7µl	1µl	2.7µl	0.7µl	95.6µl
Galactose	3µl	0.2µl	---	96.8µl	1µl	0.4µl	---	98.6µl
Galactose4	3µl	0.2µl	---	96.8µl	1µl	0.4µl	---	98.6µl
Linear + galactose4	3µl	1µl	0.1µl	95.9µl	1µl	2.7µl	0.2µl	96.1µl
Transferrin	3µl	0.8µl	---	96.2µl	1µl	2.2µl	---	96.8µl

Table 2-10: Chimeraplast-PEI complex formation.

Complexes were formed by combining HBS, chimeraplast and PEIs in one tube (in this order), vortexing the mixture, and incubating at RT for at least 10 min. Complexes were formed in a total volume of 100 µl HBS, the remaining volume being made up by medium on the cells. Chimeraplast concentrations were: ***E3→2*** *- 10 pmol/µl and 0.25 µg/µl with a final concentration of 150 nM;* ***FE3→2*** *- 100 pmol/µl and 2 µg/µl with a final concentration of 200 nM. All calculations are based on an N:P ratio of 5:1. * 2 µl chloroquine (10 mM) or ** 5 µl chloroquine (10 mM) was added to the appropriate wells 5 min before the complexes to a final concentration of 100 µM. Melittin2: Melittin-PEI 2-kDa; Melittin25: Melittin-PEI 25-kDa.*

2.3.6 MICROINJECTION

CHO-LCAT$_{WT}$ and HepG2 cells were microinjected with the 68-mer LCAT chimeraplasts (see *Fig. 4.1* for sequences). First, 12 mm glass coverslips were dipped in 70% ethanol, flamed and then dropped into individual wells of a 12-well plate. The cells were then seeded onto the coverslips in drops of 30 µl, approximately 100 cells per coverslip. The cells were left to adhere for 4 hours, after which 1 ml complete medium was added to each well. The cells were microinjected the next day.

Chimeraplasts were diluted for nuclear injection 3.9 times. This calculation was based on the fact that standard transfections deliver approximately 1.6 µg of chimeraplast per 10^5 cells. This means that theoretically each cell takes up 1.6×10^{-5} µg of chimeraplast. To achieve the same result by microinjection, for 100 cells we would need 1.6×10^{-3} µg in a volume of 2.5 µl, or 0.64 ng/µl. Starting with a chimeraplast concentration of 4.86 ng/µl, the dilution factor is 3.9. The chimeraplasts were diluted in PBS, batched in 5 µl aliquots, and stored at -80°C.

Microinjection was kindly performed by Dr. Maria Dos Santos (Royal Free & University College Medical School, London, UK). Glass pipettes (1.2 mm bore; Clark Electroinstruments, Reading, UK) were used to pull microcapillaries of about 0.5 µm tip diameter using a programmable Pipette Puller (Campden Instruments, Leicester, UK). Two and a half microliters of the chimeraplast solution was loaded into a microcapillary using an Eppendorf microloader tip. Just before microinjection, coverslips were transferred from the 12-well plate to a dish, which was inserted into the enclosed Perspex chamber of the Zeiss-inverted microscope, which is heated to 37°C. Cells were microinjected using an Eppendorf microinjector, with between 1 and 2×10^{-11} ml being delivered to each nucleus. On average, 100-150 cells were injected per coverslip.

The cells were maintained on the coverslips in a 12-well plate for 6 days before being transferred to wells of a 24-well plate. They were left to grow for 14 more days before being harvested for analysis.

2.3.7 EXTRACTION OF DNA FROM CELLS

Following transfection, cells were washed once in PBS and harvested by treatment with 0.25% (v/v) trypsin-EDTA for 3 min at 37°C. Once the cells were detached, the trypsin was neutralized by the addition of fresh medium. Most of the suspended cells were then collected in 1.5 ml microtubes (about 1% were left to grow on) and centrifuged at 24,000 g for 5 min to pellet the cells. The supernatant medium was discarded and the cells used for analysis.

Extraction of DNA was done using the Dneasy Tissue Kit (Qiagen) following the manufacturer's instructions. In summary, the cells are incubated with a lysis buffer and proteinase K for 10 min at 70°C, ethanol is then added, and the lysate is passed by centrifugation through a column that binds the DNA. The DNA is then washed with two other buffers to eliminate any remaining contaminants and enzyme inhibitors, and eluted in a total volume of 200 µl. This genomic DNA was stored at 4°C and used for RFLP analysis.

2.3.8 TRANSFECTIONS WITH FLUORESCENT CHIMERAPLAST AND NUCLEAR ISOLATION

When studying the FE3→2 chimeraplast, 6-well plates were used so that a greater number of cells could be collected and counted by flow cytometry. The transfection method was as described above (see **Table 2-9**), but after the 6 h incubation cells were harvested immediately for nuclear isolation. The cells were detached from their plates using trypsin-EDTA and pelleted by centrifugation. Cells were washed once in 100 µl PBS, resuspended in 100 µl of 0.1% (v/v) Igepal CA-630 (Sigma) in PBS and then incubated on ice for 15 min, during which time the cells were pulled through a 26G needle every 5 min to separate nuclei from outer membranes. The nuclei were pelleted by centrifugation at 12,000 g and washed once in 100 µl PBS to remove remaining detergent, then suspended and fixed in 100 µl ice-cold 50% (v/v) ethanol. Nuclei were stored at 4°C for FACS analysis.

2.3.9 FACS ANALYSIS

Analysis of the nuclei collected after transfection with the FE3→2 chimeraplast was performed on a FACSCalibur flow cytometer (Becton Dickinson, Oxford, UK) equipped with an argon ion laser, which was used to excite the fluorescein at 488 nm (530/30 nm emission bandpass filter). Cells were gated on a dual parameter display of forward and side scattered light using linear amplifications. Data acquisition was programmed to count all nuclei within gate R1 and all fluorescent nuclei emitting fluorescence between 520-530 nm in gate R2, and set to stop once 5,000 events were counted in R2.

Results were calculated using this formula: % transfected cells = 5,000 / R1 where 5,000 is the number of fluorescent events and R1 is the total number of cells counted, fluorescent or not. Each set of transfection conditions was repeated at least 3 times.

2.4 LCAT ACTIVITY ASSAYS

In order to study the enzymatic activity of the different LCAT variants presented in this thesis, it was necessary to create reaction conditions where cholesterol and phosphatidylcholine (lecithin) were available as substrates for LCAT, while being able to monitor the production of cholesteryl esters. For this reaction I used a proteoliposome substrate that contained ^{3}H-cholesterol and phosphatidylcholine and incubated this with conditioned media from LCAT-secreting CHO cells. The protein component of the substrate was apolipoprotein AI (apoAI), which acts as a cofactor to LCAT's enzymatic activity. It was therefore necessary to add apoAI to the substrate for the activity assays. Catalysis by LCAT produced ^{3}H-labelled cholesteryl esters (CE), which were measured by separating the reaction lipids using thin layer chromatography (TLC), isolating the bands corresponding to free cholesterol and CE, and counting radioactivity in both.

2.4.1 ISOLATION OF HUMAN APOLIPOPROTEIN AI

ApoAI was prepared from blood by isolation of HDL followed by delipidation [254], as it is associated with HDL particles. The method of this isolation is based on the principle that when HDL_3 is incubated with delipidated HDL_3 (i.e. apolipoproteins), apoAII will replace apoAI on HDL because it has a higher affinity for HDL particles [255].

HDL is considered to be those lipoproteins that have a density range of 1.063 to 1.21 g/ml. Preparative ultracentrifugation can be used to isolate HDL from plasma by floating it to the surface. In order for this to occur, the density of the plasma solution has to be progressively increased, while at the same time the other lipoproteins are removed sequentially. **Table 1-1** shows the densities of the lipoproteins.

Sodium bromide is used to create solutions of various densities for sequential preparative ultracentrifugation. The sodium bromide density solutions were made by Dr. D. Riddell (Royal Free & University College Medical School, London, UK). A base density solution of 1.006 g/ml was prepared by combining 57 g anhydrous NaCl, 0.5 g EDTA, 5 ml 1 M NaOH and 0.5 g sodium azide in 5.015 L of distilled water. From

this, all other density solutions could be made by adding a specific amount of sodium bromide. Fine adjustments to the density solutions were made by adding ρ1.478 or ρ1.006 solutions.

To calculate the volume of density solution required to float the lipoproteins, the following equation was used:

$$v_1.d_1 + v_2.d_2 = (v_1 + v_2).d_3 \quad [256]$$

where v_1 is the volume of plasma, v_2 is the volume of density solution to be added, d_1 is the density of plasma (assumed to be 1.006 g/ml, which is the protein-free density of plasma), d_2 is the density of the solution used for adjustment, and d_3 is the density required.

Fresh human blood was collected in tubes containing 0.2 M EDTA (pH 7.4) and 0.3 M sodium chloride (pH 7.4) and centrifuged immediately at 1,800 g and 4°C for 30 min. Plasma was collected and the blood cells discarded. One hundred microlitres of 0.5 M magnesium chloride and 100 µl of 4% (w/v) phosphotungstic acid in 0.19 M NaOH were added to each millilitre of plasma to precipitate the apolipoprotein B-containing lipoproteins in a single step. The plasma was stirred, spun at 2,000 g for 20 min, and the supernatant containing the HDL was collected.

In order for the HDL_2 to come to the surface, the density of the solution was brought to 1.125 g/ml with sodium bromide. It was then transferred to 30 ml screw-capped polycarbonate centrifuge tubes (Kontron Instruments Ltd.), and topped up with ρ1.125 density solution made from combining ρ1.006 and ρ1.478 solutions. The tubes were then spun at 37,000 rpm and 16°C for 24 h in a Kontron Centrikon T-2060 ultracentrifuge (using a 12 x 38.5 ml rotor, Kontron TFT 50.38) to separate the HDL_2 and HDL_3. The topmost, dark yellow HDL_2 layer was carefully removed using a syringe and needle. The HDL_3 fraction in the lower phase of the solution was left in the tube, adjusted to ρ1.21 and the solution topped up with ρ1.21 density solution. The HDL was then spun again for 40 h to lift the HDL_3 to the surface. The HDL_3 was carefully collected using a syringe and needle and transferred to two conical membranes sitting on top of plastic 50 ml tubes. The membranes were topped up with PBS and the tubes centrifuged at 2,000 rpm for 20 min. This was repeated twice, topping up with PBS each time and pipetting to mix. This procedure concentrates the HDL_3 and removes traces of other substances such as albumin.

At this stage, 10% of the HDL_3 was put aside and stored at 4°C. The HDL_3 was delipidated by adding it dropwise into a glass tube containing chloroform/methanol (2:1, v/v), while vortexing, to form a milky solution. Next diethyl ether/ethanol (3:2, v/v) was added followed by vortexing and incubating on ice for 10 min. The tubes were then spun at 800 rpm for 5 min and the supernatant removed by aspiration. The washing with diethyl ether/ethanol and centrifugation was repeated twice more. The tubes were then left on a roller mixer to evaporate any remaining diethyl ether, which resulted in a white precipitate in the tube. The precipitate was dissolved in PBS and 4 M guanidine HCl by rolling for 10 min. Next the HDL was dialysed against 150 nM NaCl and 1 mM EDTA six times for 1 h each. To extract the apoAI, the delipidated HDL_3 was mixed with the HDL_3 that was previously put aside and the mixture was left overnight at 4°C. This has the effect of drawing out the apoAI. To separate out the apoAI, the solution was now mixed with ρ1.006 density solution, sodium bromide added to reach ρ1.21 and mixed by gentle inversion, then spun at 43,000 rpm and 16°C for 40 h. The top layer, HDL_3 bound to apoAII, was removed and the apoAI in the lower phase dialysed against 10 mM NH_4HCO_3 overnight. The apoAI was visualised by SDS-PAGE (*Section 2.2.1*) to verify purity and the concentration of the apoAI was determined (*Section 2.2.3*). The apoAI was then concentrated using Vivaspin 20 centrifugal concentrators with a 10,000 kDa MW cutoff, then batched into 4 mg aliquots, frozen to -80°C and freeze-dried (Modulyo Freeze Drier, Edwards).

2.4.2 PREPARATION OF PROTEOLIPOSOME SUBSTRATE

Substrate for the reaction with LCAT was prepared following the method described by Chen and Albers [257]. Each preparation of substrate was made in large batches that were aliquoted and then stored at -20°C for future use. The quantities described below allow the preparation of enough substrate for approximately 350 assays.

In a glass tube with a screw cap, 34.8 mg of L-α-phosphatidylcholine (Sigma, Cat. No. P2772, 100 mg/ml) were mixed with 820 µg cholesterol (Boehringer, 1 mg/ml) and 40 µCi ^{3}H-cholesterol (Sigma, Cat. No. C8794, 1 mCi/ml). The mixture was then evaporated under nitrogen and final traces of solvent removed under vacuum for 30 min. Four milligrams of human apoAI were dissolved in 1 ml PBS and added. The total volume was then adjusted to 10.8 ml with PBS and the mixture

vortexed for 1 min. Next, while vortexing, 1.36 ml of sodium cholate (0.725 M) were added dropwise to the solution to emulsify the proteoliposomes, turning the solution clear. The solution was then transferred to pre-treated, washed 10-kDa MW cutoff dialysis tubing (Medicell International, London, UK) and dialysed against 150 mM NaCl at 4°C with stirring, six times for 90 min and once overnight, changing the NaCl solution each time.

Half a gram of fatty acid free bovine serum albumin (BSA; Sigma) was dissolved in 25 ml PBS and heat-inactivated at 56°C for 30 min. The solution was sterile filtered using a 0.2 µ syringe filter (Corning) and 22.5 ml was transferred into a plastic beaker. This was stirred magnetically while the dialysed proteoliposomes were added. This had the effect of removing fatty acids from the substrate, as these bind lysophosphatidylcholine during the LCAT reaction. The beaker was then weighed again and the weight adjusted to 64.8 g with PBS, then the solution was stirred again.

As an extra step in order to thoroughly remove any remaining sodium cholate (an inhibitor of LCAT), the solution was incubated with amberlite XAD-2 beads (20-60 mesh, Aldrich). The beads were prepared by adding 1 g of beads to each of four 50 ml tubes and washing with methanol (30 ml) for 15 mins using a roller mixer. The methanol was then decanted and the beads washed with water (30 ml) three times for 5 min followed by three 5 min washes with PBS (30 ml).

The proteoliposomes were divided between two tubes of amberlite beads and incubated for 90 min at room temperature on the roller mixer. The substrate was then transferred to the other two tubes of amberlite and the incubation repeated. The substrate was then pooled and β-mercaptoethanol was added to a final concentration of 5 mM. The solution was divided into 2.5 ml aliquots and stored at -20°C.

2.4.3 LCAT ACTIVITY ASSAY

Samples of conditioned media from LCAT secreting CHO cells were prepared by adding 15 ml of serum-free fresh medium (see **Table 2-6**) to a 75 cm^2 flask of confluent CHO cells. After 24 h the medium was collected and concentrated 20 times using Vivaspin 20 centrifugal concentrators with a 30-kDa MW cutoff. The samples were then batched into 50 µl aliquots and stored at -20°C. As a negative control,

conditioned medium from CHO^{dhfr-} cells was also collected and treated in the same way. The positive control for these experiments was plasma obtained as described in *Section 2.4.1.* As a negative control for the plasma, PBS was used.

The substrate was thawed in a 37°C water bath, gently mixed by vortexing, and kept on ice until the reaction mixes were ready. In a 1.5 ml tube, 242.5 µl of proteoliposome substrate was added to and 8 µl of test sample (plasma, PBS, LCAT conditioned medium or control medium). The reaction mixes were incubated at 37°C for 1 h. The reaction was then stopped by transferring the tubes onto ice. To extract the lipids, the reaction mixes were transferred into glass screw-cap tubes containing 4 ml chloroform / methanol (1:1) and the tubes vortexed. Next, 1.2 ml of water were added to each tube and the tubes vortexed again. The samples were centrifuged at 2,000 rpm and 4°C for 10 min (MSE Mistral). The lower, organic phase of each tube was then transferred using a plastic micropipette to a clean flat-bottomed glass tube containing 5 drops of methanol. The samples were dried in a 40°C heating block under nitrogen. Then 200 µl chloroform / methanol (1:1) was added to each tube, the tube walls rinsed with the solution, and the samples dried again.

The dried samples were then dissolved in 30 µl chloroform, carefully rinsing the bottom of the tube, and the samples were transferred onto the application zones of 250 µm silica gel TLC plates (60 Å; 20 x 20 cm, layer thickness 250 µm; Whatman). One lane of the plate was reserved for running 5 mg lipid standard (Sigma) as a marker. The plate was allowed to dry briefly and was then placed in a TLC chamber containing a layer approximately 1 cm high of hexane / diethylether / acetic acid in (90:10:1 by volume). The lipids were allowed to separate until the solvent front reached nearly the top of the plate. The plate was then air-dried briefly and the lipids stained in a chamber containing iodine crystals. The plate was removed from the iodine chamber and the UC and CE bands were marked with a pencil.

The plate was sprayed with water and the UC and CE bands scraped off into a scintillation vial containing 8 ml of scintillation fluid (Ecoscint A, National Diagnostics). The vials were briefly vortex-mixed and their radioactivity measured. LCAT activity was expressed as the % cholesterol esterified/hour:

% cholesterol esterified / hour = CE dpm / (CE dpm + UC dpm) x 100

Negative controls (control medium and PBS) were calculated initially and their values subtracted from the corresponding test samples.

2.5 STATISTICAL ANALYSIS

Values in the text and figures are expressed as the mean ± S.D., when appropriate. Statistical differences between means was determined using Student's *t*-test and considered significant if $P < 0.05$. All analyses were performed using Microsoft Excel (Microsoft Office XP).

Chapter 3 –

Comparison of wild-type LCAT and LCAT with potentially atheroprotective mutations

3.1 INTRODUCTION

In the Introduction (*Section 1.2.5*), I discussed point mutations in the LCAT gene that are believed to increase the enzyme's catalytic activity. Site-directed mutagenesis was used to produce a variety of LCAT mutants with Ser→Ala amino acid changes. These were transiently expressed in COS-6 cells and analysis of the LCAT secreted by the recombinant cells showed that Ser_{208}→Ala and Ser_{216}→Ala mutations had increased enzymatic activity [125]. In pursuing the idea that the S208A and S216A mutations have the potential to be anti-atherogenic, my first goal was to ascertain that these variants do have higher specific activities compared to wild-type LCAT, and in the setting of stable expression. I already had available to me two recombinant CHO cell lines: one that expressed the LCAT wild-type gene (CHO-$LCAT_{WT}$), and one that expressed LCAT with the Ser→Ala mutation at amino acid 216 (CHO-$LCAT_{S216A}$), both previously created in our laboratory. CHO cells do not normally express LCAT [258] and are therefore useful vehicles for studying the human protein. I decided that it would be interesting to establish whether LCAT containing two mutations: both S208A and S216A, would also have increased activity by comparing this double mutant enzyme to wild-type LCAT and $LCAT_{S216A}$.

This chapter describes my work using site-directed mutagenesis to produce a plasmid vector carrying the double-mutated LCAT cDNA, transferring the cDNA into an expression vector, and producing recombinant CHO cells expressiong this LCAT variant. I looked at comparable levels of enzymic activity sufficient to measure the specific activities of wild-type LCAT, $LCAT_{S216A}$ and LCAT with the double mutation.

3.2 RESULTS

3.2.1 GENERATION OF RECOMBINANT CHO CELLS EXPRESSING LCAT WITH THE DOUBLE MUTATION (SER208ALA AND SER216ALA)

3.2.1.1 Mutagenesis to produce the expression vector

Site-directed mutagenesis was performed as described in *Section 2.1.8*. The template was pLCATHBS216A, a pUC18 plasmid containing LCAT cDNA with the S216A mutation (***Fig. 3.1***). The mutagenic process had the purpose of introducing a T→G mutation which would result in the S208A amino acid change (***Fig. 3.2***). Although the manufacturer of the mutagenesis kit suggests a PCR elongation time of 2 min/kb of plasmid, which in this case would mean an elongation time of 8 min, this proved to be insufficient. An elongation time of 14 min was found to give a better result. Ten percent of the PCR reaction was visualised on a 1% agarose gel against linearised pLCATHBS216A, to verify that the PCR product was of the correct size (***Fig. 3.3A***).

Next the PCR product was digested with DpnI (***Fig. 3.3B***). This restriction enzyme recognises the methylated, nonmutated DNA template. Digesting the PCR product left only the new, mutated plasmid, which was then transformed into ultracompetent cells and grown on a LB agar plate containing ampicillin for selection of bacteria containing the transformed plasmid. Twelve colonies were picked from the plate and grown in minicultures, after which DNA was extracted. Only one of the colonies appeared to contain the correct plasmid when viewed by electrophoresis against the linearised original plasmid, and this clone was digested with HindIII and BamHI for further confirmation (***Fig. 3.3C***). In order to ascertain that the mutagenesis was successful, the plasmid was also analysed by RFLP for both S208A and S216A mutations (see *Section 2.1.3* and ***Fig. 3.4*** for expected RFLP pattern). The two mutations were found to be present (***Fig. 3.5A***). Sequencing of the cDNA portion of the plasmid was then performed to exclude the presence of any other unwanted mutations, and also provided another form of confirmation of the presence of both mutations (***Fig. 3.5B***). No other mutations were found within the cDNA. The newly created plasmid was termed pLCAT2M.

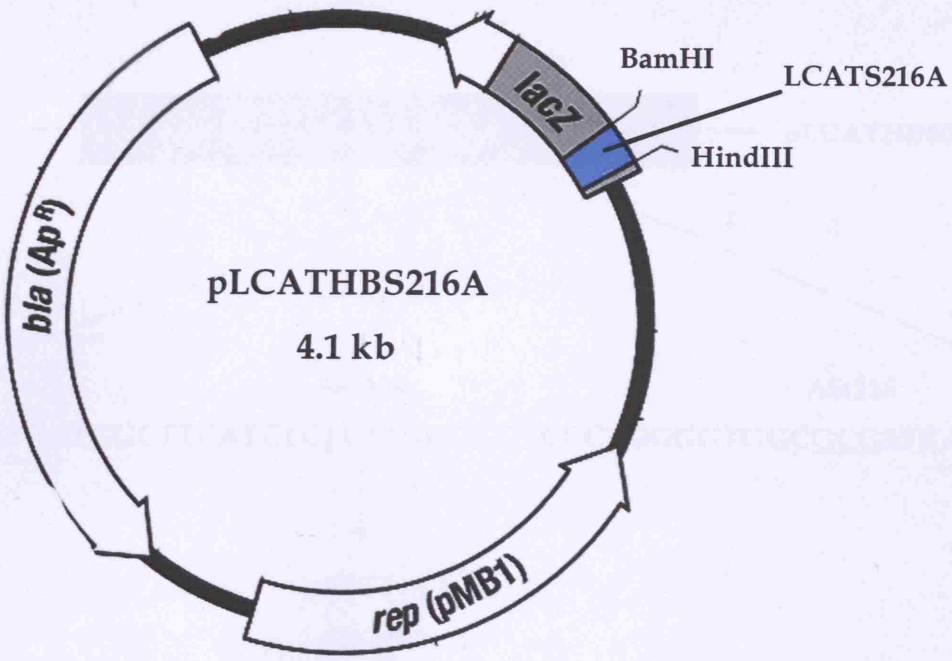

Fig. 3.1: Plasmid pLCATHBS216A.

The pUC18-based plasmid was used as template for mutagenesis within the LCAT cDNA. The 1.5 kb full-length LCAT cDNA was cloned into the vector using HindIII and BamHI. The plasmid carries the gene coding for beta-lactamase (bla), conferring ampicillin resistance to bacteria and therefore ampicillin was used as a selection agent for successfully transformed bacterial colonies after mutagenesis. The original figure (reproduced from the catalogue of Fermentas International, Canada) was modified to include the LCAT cDNA. rep: pMB1 replicon, responsible for plasmid replication; lacZ: gene whose expression results in the formation of blue colonies. When cloning into the lacZ gene, this feature is abolished, resulting in white colonies, allowing for the identification of recombinant plasmids following bacterial transformation.

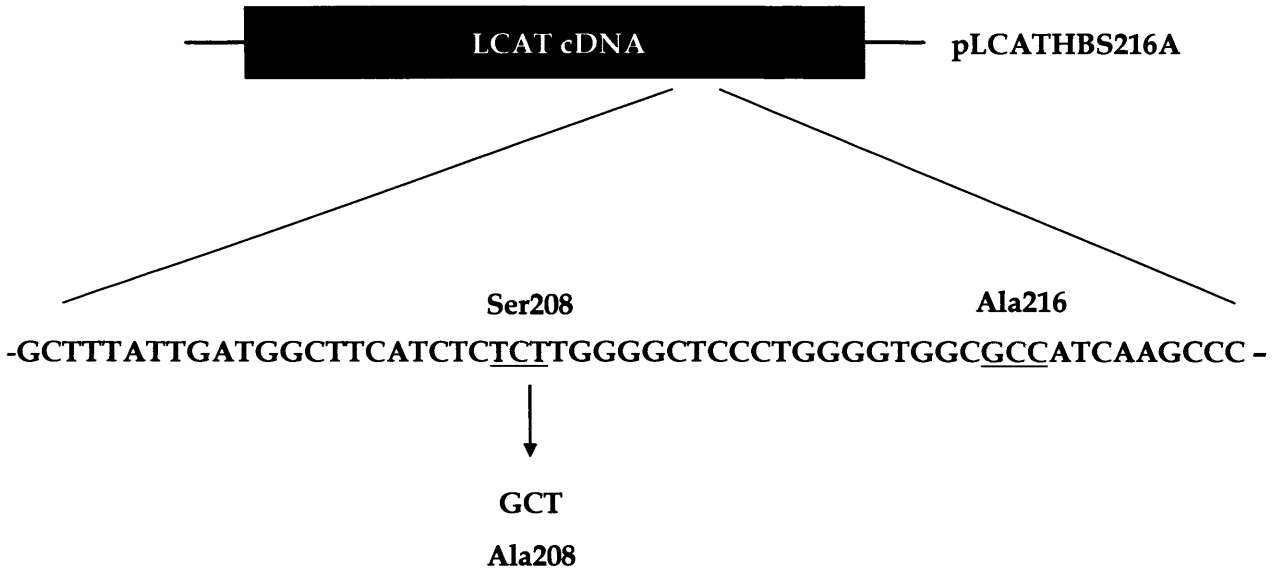

Fig. 3.2: Diagram depicting the LCAT cDNA in pLCATHBS216A.

Amino acids 208 and 216 are serines in wild-type LCAT. The plasmid pLCATHBS216A contains LCAT cDNA with the Ser→Ala mutation at position 216. The nucleotides that code for amino acids 208 and 216 are underlined. Mutagenesis on this plasmid added the Ser→Ala mutation at position 208 by changing T to G.

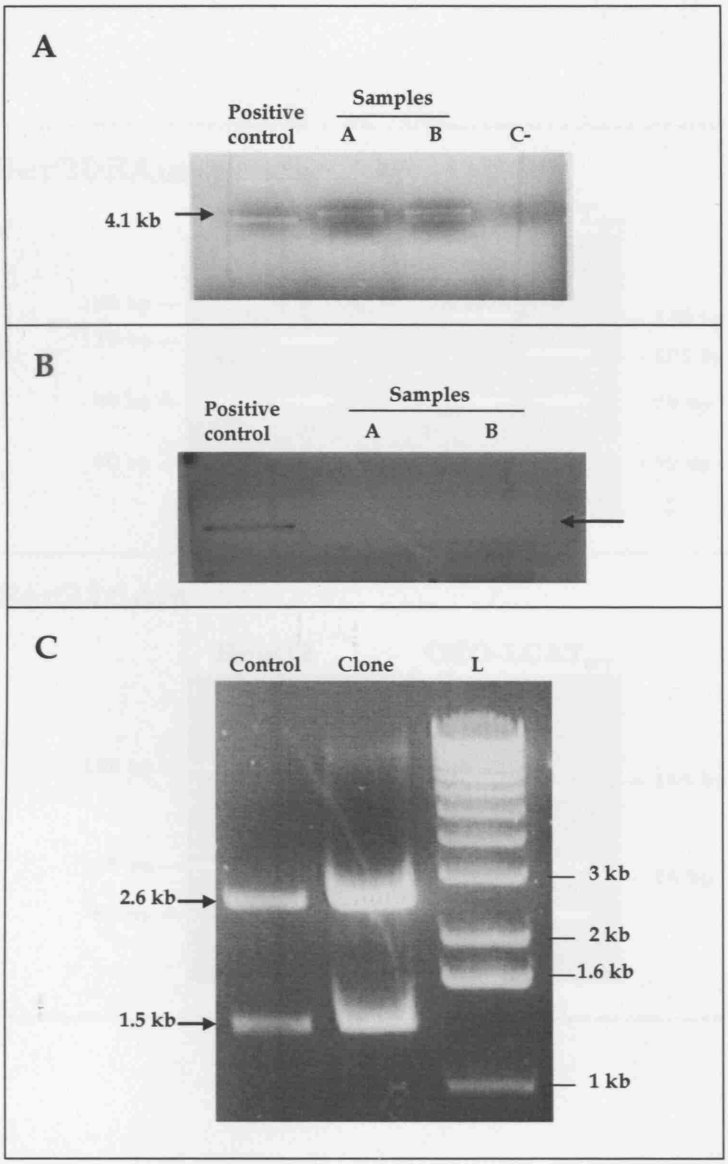

Fig. 3.3: Site-directed mutagenesis on plasmid pLCATHBS216A.

A: *Agarose gel showing the mutagenesis PCR products (A and B) against the linearised plasmid that was used as PCR template (positive control). C-: PCR negative control.* ***B:*** *Agarose gel of the PCR reactions after digestion with DpnI. The arrow indicates the correct band of 4.1 kb, confirmed by the linearised plasmid in the first lane.* ***C:*** *Digest products after treatment of mutagenesis plasmid with HindIII and BamHI, showing the same pattern as control. Control: pLCATHBS216A digested with the same enzymes. L: 1 kb ladder.*

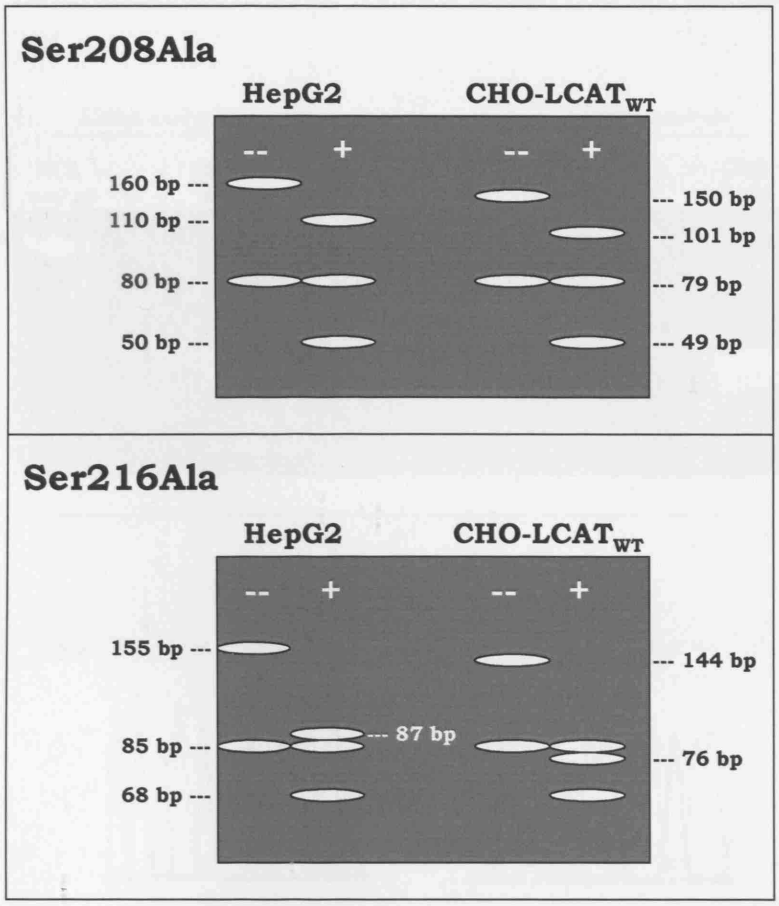

Fig. 3.4: Diagram of RFLP pattern following LCAT chimeraplasty.

Representation of gel patterns following restriction digest of PCR products obtained from DNA extracted from cells treated with either Ser208Ala or Ser216Ala chimeraplasts. DNA from cells receiving the S208A chimeraplast were cut with MwoI and those receiving the S216A chimeraplast were cut with CfoI (see Figs. 2.2 and 2.3). When no base change is present (--) only one restriction site exists in the PCR product and therefore there are two restriction fragments. Following successful chimeraplasty, a new restriction site is created by the base change (+) resulting in the disappearance of the largest band and appearance of 2 smaller bands. Due to the fact that different primers were used for genomic DNA or cDNA, the restriction patterns are slightly different on analysis of transfections of HepG2 cells or recombinant CHO cells.

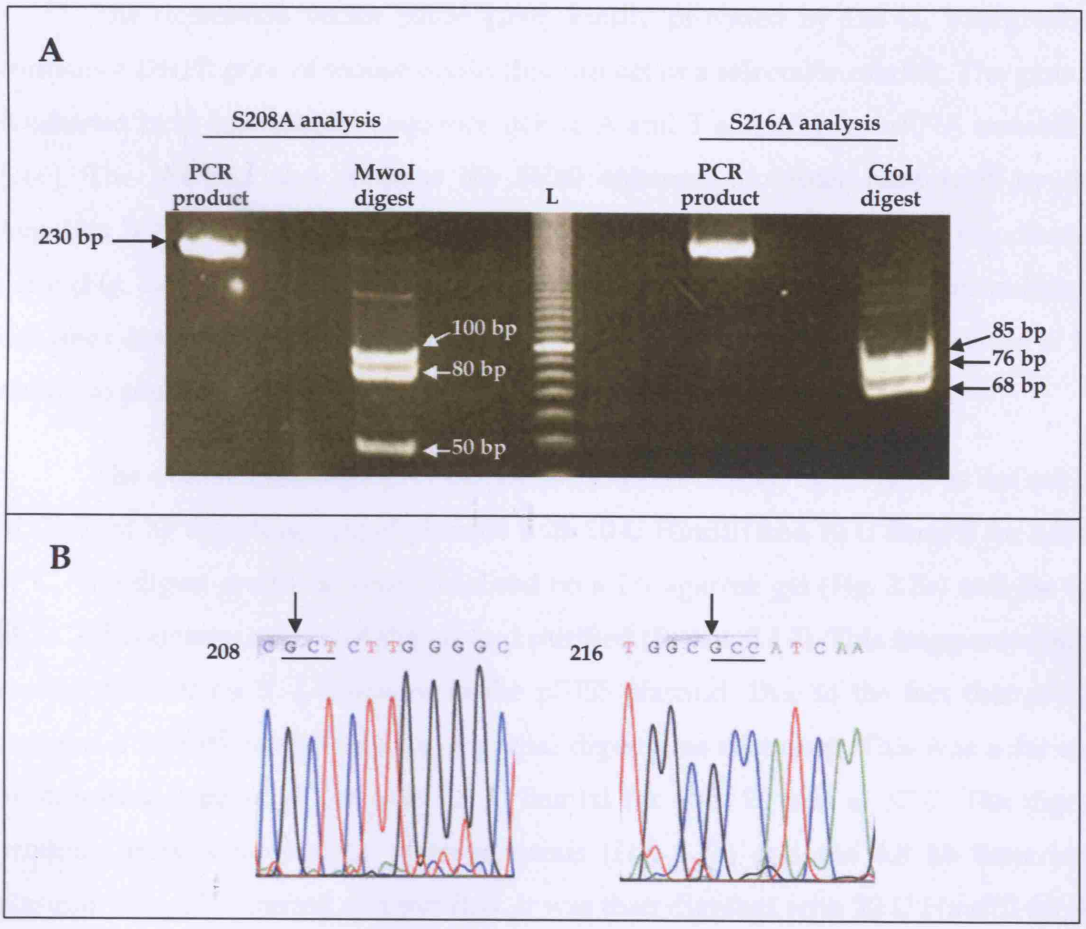

Fig. 3.5: Analysis of mutagenesis on plasmid pLCATHBS216A.

A: *Analytic RFLP for S208A and S216A mutations confirming the success of mutagenesis at position 208. For the S208A analysis, no mutation results in two restriction fragments of 150 bp and 80 bp, whereas when the mutation is present an additional digest site within the 150 bp fragment results in its cleavage into 100 bp and 50 bp. Likewise, for the S216A mutation, in the presence of the mutation the 144 bp band splits into 76 bp and 68 bp bands. L: 10 bp ladder (100 bp band is boldest).* ***B:*** *Sequencing confirmation of the presence of both T→G mutations (indicated by arrows) at amino acid sites 208 and 216 (underlined).*

3.2.1.2 *Production of $LCAT_{2M}$ expression plasmid*

The expression vector p7055 [259], kindly provided by Dr. D. Vinogradov, contains a *DHFR* gene of mouse origin that can act as a selectable marker. The gene is weakened by a downstream sequence rich in A and T resulting in mRNA instability [260]. The plasmid also contains the SV40 enhancer-promoter reinforced by the hepatitis B virus X transactivator (HBV-X), allowing high expression of the desired gene (***Fig. 3.6***). This plasmid was used to create this and the two other recombinant cell lines described in this chapter, CHO-$LCAT_{WT}$ and CHO-$LCAT_{S216A}$, because of its ability to produce high gene expression and its selection ability via dhfr.

The double-mutated LCAT cDNA (henceforth termed $LCAT_{2M}$) was cut out of pLCAT2M by digesting 5 µg of plasmid with 10 U HindIII and 10 U BamHI for 3 h at 37°C. The digest products were visualised on a 1% agarose gel (***Fig. 3.7a***) and the 1.5 kb LCAT fragment cut out of the gel and purified (*Section 2.1.2*). This fragment would replace the 500 bp IL-2 fragment in the p7055 plasmid. Due to the fact that p7055 contains 2 BamHI restriction sites, a partial digest was necessary. This was achieved by digesting 3 µg of p7055 with 0.6 U BamHI for only 20 min at 37°C. The digest products were separated by electrophoresis (***Fig. 3.7b***) and the 6.8 kb linearised plasmid was gel extracted and purified. It was then digested with 20 U HindIII for 90 min at 37°C. Digest products were again separated by electrophoresis (***Fig. 3.7c***) and the 6.3 kb fragment representing the plasmid without the IL-2 insert was gel purified. Both LCAT insert and empty vector were quantified by measurement of the OD_{260}.

The vector was dephosphorylated as described in *Section 2.1.5* and ethanol precipitated prior to ligation with the LCAT insert. Ligation was performed as described in *Section 2.1.7*, using a 5:1 insert to vector ratio (250 ng LCAT insert and 50 ng p7055) and 3 U ligase. The reaction was carried out for 1 h at room temperature, then left overnight at 4°C. Half of the ligation mix was transformed into DH5α bacteria as described in *Section 2.1.9* and plated on LB agar with ampicillin. After 24 h 12 colonies were picked for analysis, grown overnight in small cultures and DNA was extracted. One fifth of the DNA from each of the 12 plasmids was digested with 5 U ClaI, as was pXLCAT (p7055 containing wild-type LCAT) to serve as a positive control. ClaI has several restriction sites within p7055 and LCAT. All plasmids showed the same restriction pattern as the digested pXLCAT. Another digest was performed on 3 of the 12 plasmids (colonies 1, 8, and 11: chosen because they had the

highest DNA concentrations), this time with HindIII and BamHI to ascertain that the IL-2 fragment had been successfully removed (represented by a 500 bp band). All three plasmids showed the correct restriction pattern for p7055 containing LCAT cDNA and no IL-2 (***Fig. 3.8***). Culture 11 was chosen for expansion into a larger culture (*Section 2.1.10*) to produce purer and larger amounts of plasmid for transfection into CHO cells.

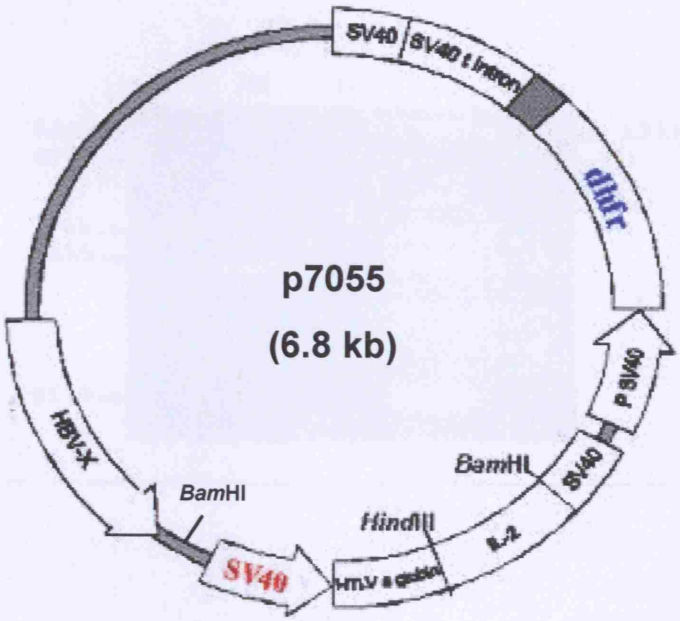

Fig. 3.6: Plasmid p7055.

The plasmid was digested with HindIII and partially digested with BamHI to cut out the interleukin-2 (IL-2) fragment. The resulting 6.3 kb open vector was then ligated with the double-mutated LCAT cDNA producted by mutagenesis. SV40 enhancer-promoter and HBV-X (the gene coding for hepatitis B virus X transactivator) allow high levels of expression of the cloned gene. dhrf: gene coding for dihydrofolate reductase; HTLV1 a globin: 5' UTR R+U5 region from HTLV1 and an intron containing the splice sites from the dital intron of the mouse x-globin gene; IL-2: 500 bp gene coding for interleukin-2, which was removed and replaced by the LCAT gene.

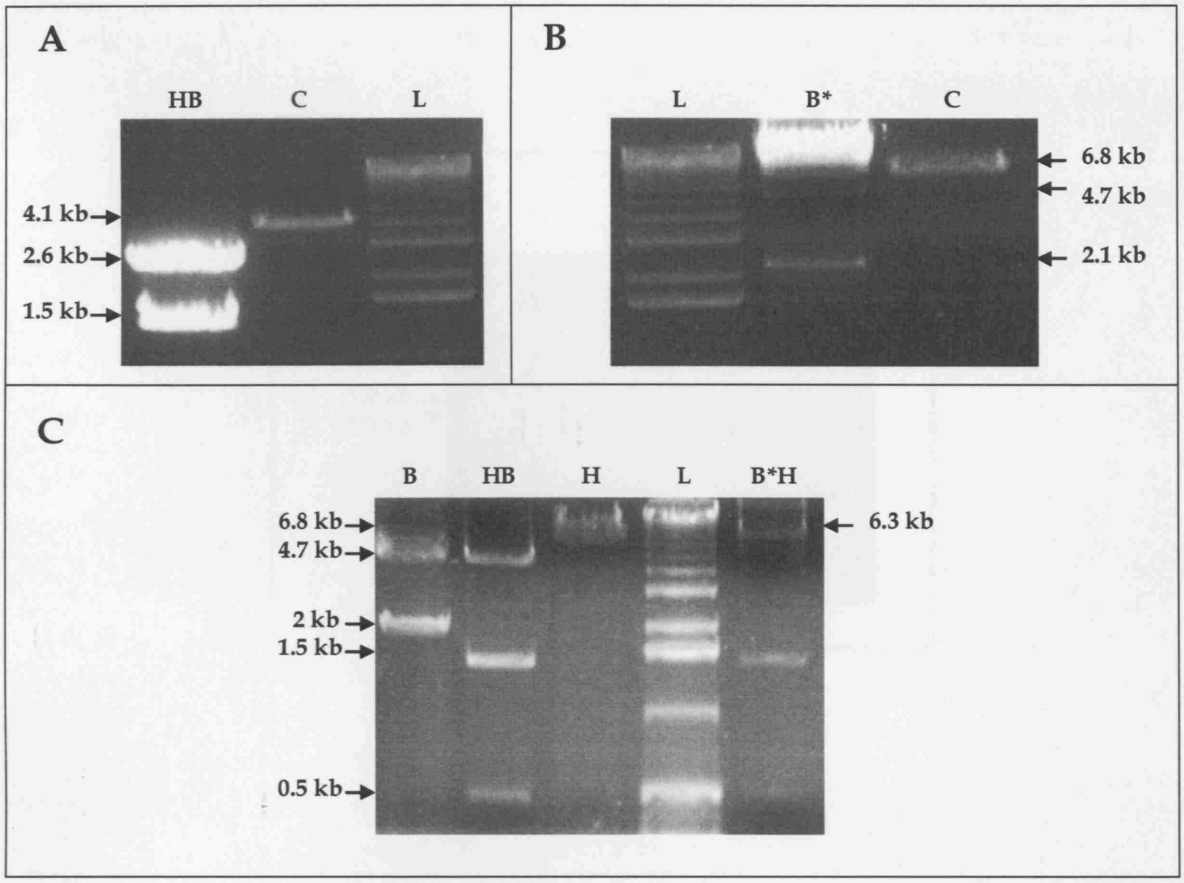

Fig. 3.7: Preparation of $LCAT_{2M}$ and p7055 for ligation.

A: *Digest of pLCAT2M with HindIII and BamHI (HB). The LCAT2M fragment of 1.5 kb was purified from the gel for use in the ligation. C: control, pLCAT2M linearised with BamHI; L: 1 kb ladder.* ***B:*** *Partial digest of p7055 with BamHI (B*), in order to linearise the plasmid without cutting at both BamHI sites. The 6.8 kb linearised plasmid was gel purified for use in further digests. L: 1 kb ladder; C: control, p7055 linearised with HindIII.* ***C:*** *The BamHI partial digest product was digested with HindIII (B*H). The 6.3 kb fragment was purified from the gel for ligation. B: p7055 digested with 1 U BamHI. HB: p7055 digested with 10 U HindIII and 10 U BamHI. H: p7055 linearised with HindIII. L: 1 kb ladder.*

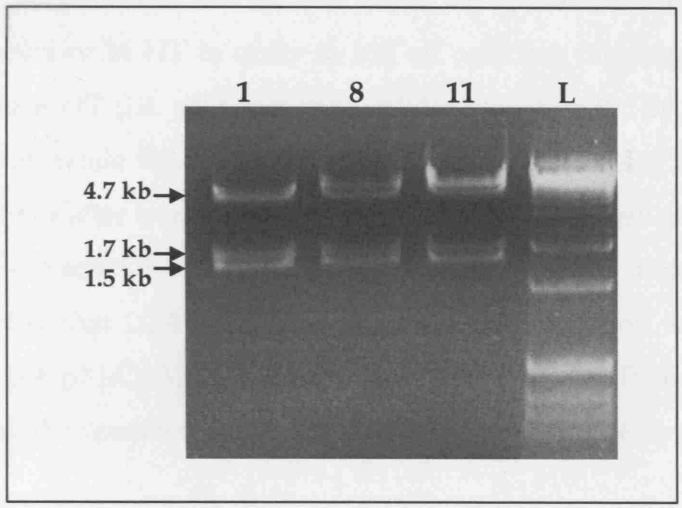

Fig. 3.8: Analysis of plasmids from picked bacterial colonies.

Three chosen plasmids (from colonies 1, 8, and 11) were digested with HindIII and BamHI. All showed a digest pattern consistent with fragmentation of p7055 (fragments of 4.7 kb and 1.7 kb) containing LCAT (1.5 kb). L: 1 kb ladder.

3.2.1.3 *Transfection of pXLCAT$_{2M}$ into CHO^{dhfr-} cells*

The pXLCAT$_{2M}$ plasmid was transfected into CHO^{dhfr-} cells as described in *Section 2.3.4*. The day after transfection, cells that received the pGFP plasmid, as a visual control of transfection efficiency, showed that the transfection was only approximately 10% successful. The pXLCAT$_{2M}$ transfected cells were transferred to a 75 cm^2 flask and selection was started (see Table 2-6 for selection medium used) by using medium deficient of HT in order to kill off cells not carrying the *DHFR* gene required to produce HT (i.e. cells not successfully transfected). By the 12th day the flask was confluent, while in the control flask (untransfected cells) only 40% of cells survived. Thirty days after transfection, all cells in the control flask were dead. At this stage DNA was extracted from some of the transfected cells and PCR-RFLP was performed to verifiy that LCAT cDNA with the double mutation was present. As a positive control, the pXLCAT2M plasmid was used. PCR-RFLP confirmed that the cells were carrying the double mutated LCAT gene (results not shown).

3.2.1.4 *Cloning of recombinant CHO-LCAT$_{2M}$ cells*

Cloning of the cells was performed by limiting dilution in a 96-well plate. The day after cloning had begun, wells containing individual cells were marked. The cells were then left for 10 days, after which they were trypsinised and transferred to a 24-well plate. As the cells reached confluency they were transferred again to 6-well plates and finally into 75 cm^2 flasks.

3.2.1.5 *Analysis of CHO-LCAT$_{2M}$ clones*

Once sufficient cells were available, 10% of each clone was taken for DNA extraction and PCR-RFLP analysis. DNA was amplified using the S208A cDNA primers (*Section 2.1.3*) and the PCR products digested with CfoI to identify the Ser216Ala mutation (see *Fig. 3.4* for RFLP pattern). Analysis for the Ser208Ala mutation was considered unnecessary at this preliminary screening stage as the presence of one shows the presence of the other because they are carried together in the transfected cDNA. RFLP confirmed that all picked cells do contain the S216A

mutation (***Fig. 3.9A***), seen as the presence of three restriction fragments (85, 76 and 68 bp) rather than two (144 and 85 bp). It was therefore considered that all the clones contained the double-mutated LCAT cDNA. All clones were then grown on for collection of conditioned medium over a 24 h period as described in *Section 2.2.4.* Briefly, near-confluent 6-well plates received serum-free medium that was collected after 24 h, concentrated 40 times and snap-frozen. The presence of LCAT protein in medium was analysed by Western blotting (*Section 2.2.5*) using a mouse monoclonal anti-human LCAT primary antibody and sheep anti-mouse HRP secondary antibody, followed by ECL detection. Blots revealed that all 8 clones were secreting a protein of the correct size for LCAT (63-kDa), and that with a comparable number of cells for each clone, the three best secretors were clones A, D and E (***Fig. 3.9B***). Clone 'D' was producing the highest level of protein and consequently, CHO-$LCAT_{2M}$(D) was the cell line used for subsequent experiments.

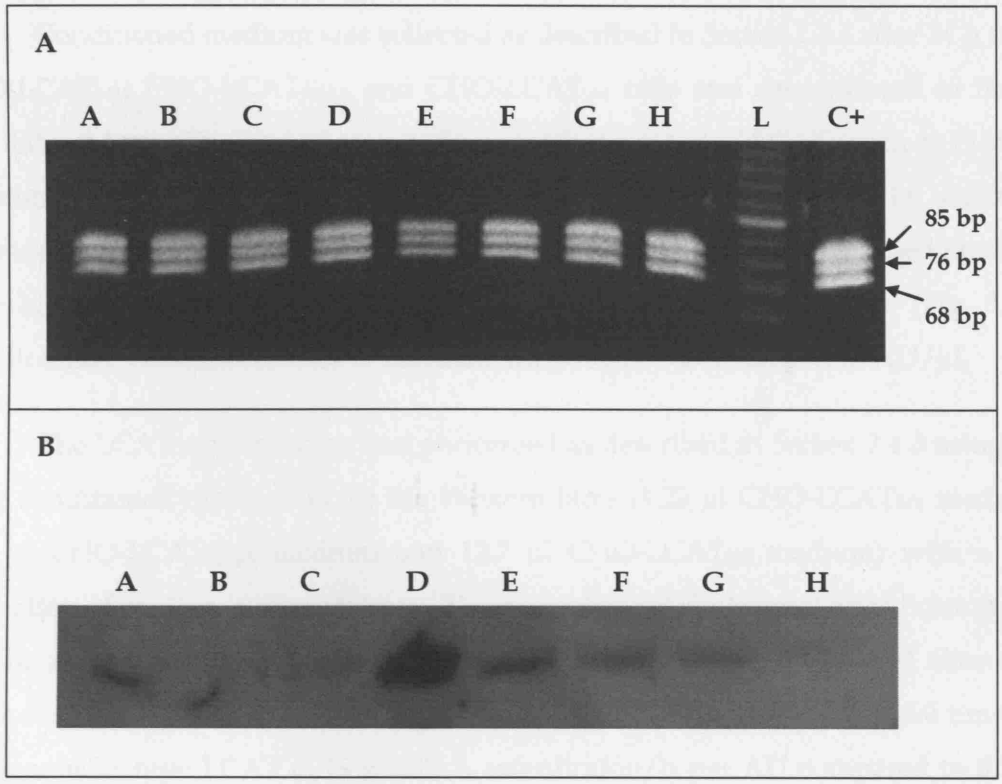

Fig. 3.9: Analysis of 8 CHO-LCAT$_{2M}$ clones.

***A**: PCR amplification of DNA from clone cells (A to H) using the S208A cDNA primers followed by digest with CfoI to verify the presence of the Ser216Ala mutation. All 8 clones show the expected digest pattern (presence of three bands of 85, 76, and 68 bp rather than an 85 bp and an undigested 144 bp band), identical to the same analysis from amplified plasmid pLCAT2M (C+). L: 10 bp ladder. **B**: One of two Western blots showing LCAT secretion in 40 X concentrated conditioned medium collected after 24 h. The protein was detected using mouse anti-human LCAT primary and sheep anti-mouse HRP secondary antibodies followed by ECL. All clones produced a protein of 63-kDa. LCAT production varied greatly, with the highest levels in clones A, D and E. Clone D was considered to be the best LCAT producer and used for subsequent experiments.*

3.2.2 PRELIMINARY COMPARISON OF SPECIFIC ACTIVITIES OF THE THREE LCAT VARIANTS

Conditioned medium was collected as described in *Section 2.2.4* after 24 h from CHO-LCAT$_{WT}$, CHO-LCAT$_{S216A}$ and CHO-LCAT$_{2M}$ cells and concentrated 40 times. As I did not have a method of accurately quantifying secreted LCAT (such as ELISA), an estimation was made of protein quantity in arbitrary units (AU) by scanning densitometry of Western blots. Three dilutions of CHO-LCAT$_{WT}$ conditioned medium were blotted against medium from the two other cell lines as before (***Fig. 3.10***). Densitometry values were used to calculate the protein concentration in AU/µl.

The LCAT activity assay was performed as described in *Section 2.4.3* using the same conditioned medium as for the Western blots (1.27 µl CHO-LCAT$_{WT}$ medium, 12.7 µl CHO-LCAT$_{S216A}$ medium and 12.7 µl CHO-LCAT$_{2M}$ medium) with a 1 h incubation of medium with substrate. The percentage of cholesterol esterification and specific activity for the three LCAT variants are listed in **Table 3-1** and shown in graph form in ***Fig. 3.11***. The calculated results indicate that LCAT$_{S216A}$ is 8.9 times as active as wild-type LCAT (3.19 ± 2.52 % esterificaton/h per AU compared to 0.36 ± 0.22 % respectively). The double mutation also confers higher activity than wild-type (0.71 ± 0.55 % esterification/h per AU compared to 0.36 ± 0.22 % respectively), though it is only 1.9 times greater. Results are the mean of duplicate experiments on the same protein samples. Unfortunately, these results have to be regarded as preliminary because the sample size was not large enough to provide statistically significant results. A larger sample size was not possible because of the low concentration of LCAT protein secreted by the mutated LCAT-secreting cells. As Fig. 3.10 shows, the LCAT content of the conditioned medium from CHO-LCAT$_{S216A}$ and CHO-LCAT$_{2M}$ cells was very low in comparison with medium from CHO-LCAT$_{WT}$ cells. Consequently, relatively large volumes of medium (even when concentrated 40 times) had to be used for the activity assays.

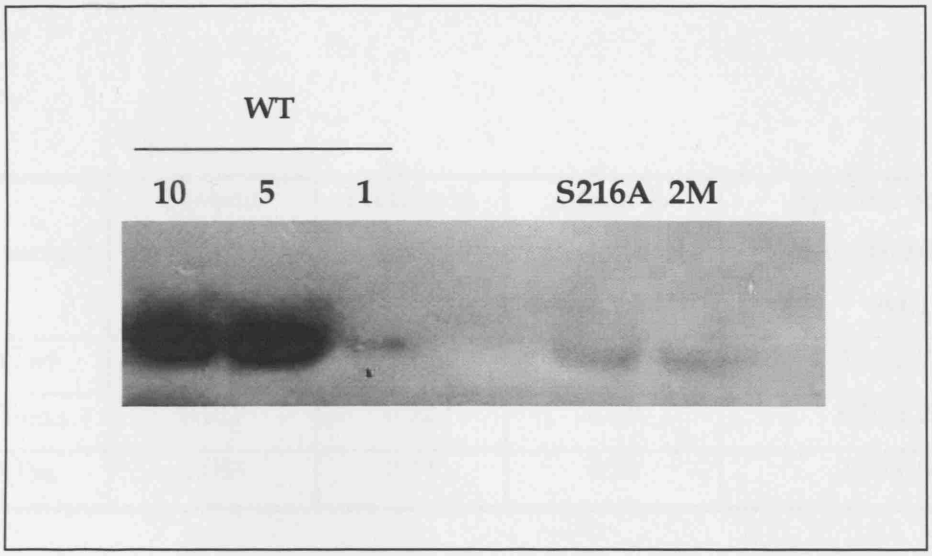

Fig. 3.10: Western blotting of conditioned medium from LCAT-secreting cells.
Conditioned medium was collected after 24 h from CHO-LCAT$_{WT}$, CHO-LCAT$_{S216A}$ and CHO-LCAT$_{2M}$ cells and concentrated 40 times. Known volumes from each cell line were visualised on the same blot for estimation of concentration in the form of AU/µl by scanning densitometry compared to background. These values were used to calculate the specific activity of the LCAT variants following activity assays performed using the same conditioned medium. WT: LCAT$_{WT}$ showing three dilutions of medium, S216A: LCAT$_{S216A}$, 2M: LCAT$_{2M}$ (medium from clone D).

LCAT variant	Protein concentration (AU/µl)	Protein in assay (AU)	Mean % cholesterol esterified/h	Specific activity (% esterification/h per AU)
$LCAT_{WT}$	4.15	5.14	1.95	0.36 ± 0.22
$LCAT_{S216A}$	0.017	0.22	0.70	3.19 ± 2.52
$LCAT_{2M}$	0.033	0.14	0.29	0.71 ± 0.55

Table 3-1: Specific activity data for three LCAT variants.

These results were derived from analysis of protein secreted into medium by CHO-$LCAT_{WT}$, CHO-$LCAT_{S216A}$ and CHO-$LCAT_{2M}$ cells. Protein concentration was estimated by scanning densitometry of Western blots and expressed as arbitrary units (AU/µl). Following incubation of the medium with ^{3}H-cholesterol labelled substrate, the percentage of cholesterol esterified/h was calculated by comparing radioactive counts in unesterified cholesterol and cholesteryl esters. Specific activity is expressed ± SD (n=2). LCAT containing the Ser216Ala mutation appears to have the highest LCAT activity (8.9 times that of $LCAT_{WT}$), followed by the double-mutated LCAT (1.9 times higher than $LCAT_{WT}$).

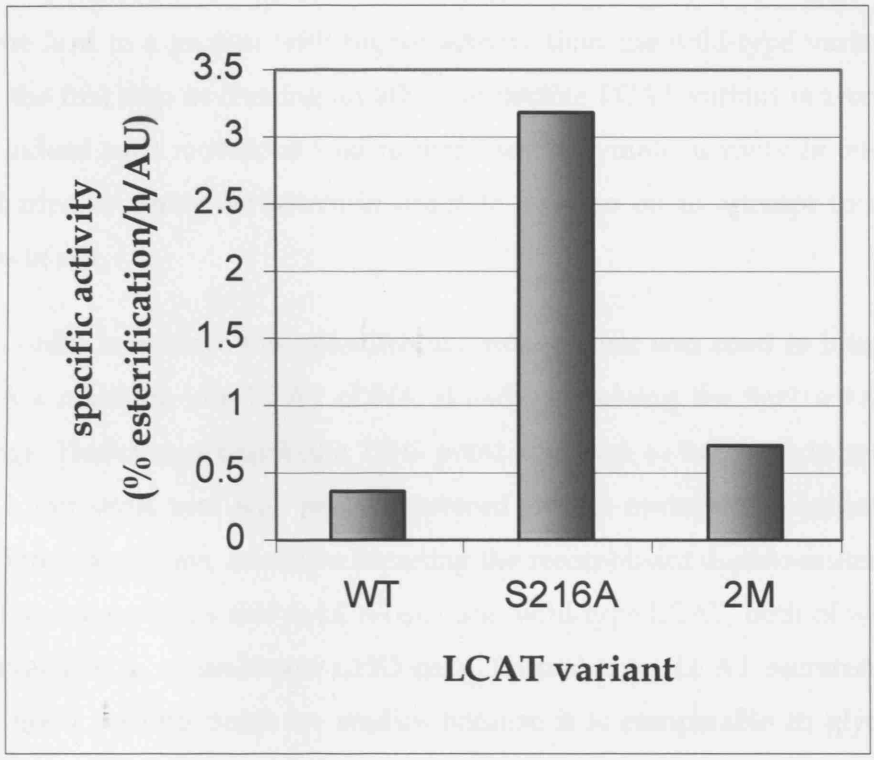

Fig. 3.11: Specific activity of the three LCAT variants.

Results from Table 3-1 represented as a bar graph, showing that the order of esterification acivity from highest to lowest is $LCAT_{S216A}$, $LCAT_{2M}$, and $LCAT_{WT}$. The S216A mutation appears to result in LCAT activity that is almost 9 times that of wild-type LCAT, whereas the double-mutant is 2-fold higher. WT: $LCAT_{WT}$, S216A: $LCAT_{S216A}$, 2M: $LCAT_{2M}$.

3.3 DISCUSSION

The primary subject of this thesis revolves around the hypothesis that increasing the activity of the enzyme LCAT will result in an atheroprotective lipoprotein profile. Furthermore, it has been shown that certain mutations in the *LCAT* gene lead to a protein with higher activity than the wild-type variant. Taken together, the first step in creating an atheroprotective LCAT variant *in vivo* is to test whether indeed such mutations lead to increased enzymatic activity *in vitro*. In this chapter I tried to verify the above in order to then go on to attempt to create the mutations *in situ*.

In order to achieve this, site-directed mutagenesis was used to introduce the Ser208→Ala mutation into LCAT cDNA already containing the Ser216→Ala amino acid change. This change required a T→G point mutation, as had been introduced for the S216A mutation, and was easily produced by the mutagenesis technique. The purpose here was to have a cell line secreting the recombinant double-mutated LCAT ($LCAT_{2M}$) and to compare this to $LCAT_{S216A}$ and wild-type LCAT, both of which were already available in recombinant CHO cells. Recombinant LCAT secreted by CHO cells is a good starting point for studies because it is comparable in glycosylation structure and activity to human plasma LCAT [258].

The double-mutated cDNA was cloned into an expression vector containing the *DHFR* gene and transfected into CHO cells deficient in this gene, so that this property of the vector could be used as a selection method. The selected cells were analysed by RFLP to confirm the presence of the double-mutated LCAT cDNA, then eight single cells were successfully expanded. All eight clones were analysed for LCAT secretion by Western blotting and the highest producer selected for further studies.

Once all three cell lines were ready, conditioned medium was collected for analysis of secreted LCAT. The first observation that can be made regarding the recombinant cells is that there is a great variation in LCAT production between $LCAT_{WT}$ and the mutated LCAT variants. There are several possible explanations for this phenomenon. The first has to do with the fact that transfected DNA can integrate into genomic DNA at different locations or more than one location [261]. Moreover, it

is difficult to know how many copies of cDNA exist in a recombinant cell line or if they are transcriptionally active. The second reason for lower protein quantity could be related to changes in the secondary structure of the protein resulting from the amino acid substitution, leading to reduced secretion. Francone and Fielding [122] mention that the S216A substitution leads to loss of a turn preceding the sequence containing amino acid 216, though this does not cause a reduction in protein secretion. Qu *et al.* [125] also found no significant difference in secretion from wild-type LCAT when the serines were replaced. Furthermore, they state that the serine to alanine replacements have no effect on N-glycosylation of adjacent asparagines residues. One way of testing this possibility would have been to perform Western blotting on lysates of the recombinant CHO cells. Detection of greater amounts of LCAT protein in lysates would have suggested that LCAT is being synthesised but secretion is hampered by structural changes. Another possible reason for reduced protein secretion could be that the mutant proteins are more unstable, and are therefore degraded more rapidly, though, again, Francone and Qu's work examining the S208A and S216A mutations did not find this to be the case. Also, the only O-glycosylation sites in LCAT are at Thr407 and Ser409 [261a], distant from the 208 and 216 sites, and therefore unlikely to be affected by amino acid changes here. It appears to be most likely that the cause of protein quantity differences is due to variation in cDNA copy between the three cell lines.

The results acquired by the activity assays performed here are not ideal. The specific activities, though different for each LCAT variant, are numerically low. The most likely reason for this is a suboptimal substrate. For the estimation of LCAT activity, different substrate methods exist, but two main types are commonly used. The endogenous self-substrate method uses plasma as substrate and enzyme to measure the endogenous cholesterol esterification rate, and therefore is not appropriate for the purposes of the work presented here. The exogenous common-substrate method uses heat-inactived plasma or artificial liposomes as substrate, as was done in this study.

It has been shown that plasma is not an efficient substrate for LCAT [262], besides which components can change from sample to sample, therefore resulting in inconsistent measurements. Thus the most appropriate substrate for testing recombinant LCAT is an artificial one formed by combining PC, cholesterol and apoAI, essentially reconstituted HDL (rHDL). In order to be able to track the

conversion of free cholesterol to cholesteryl esters, a ^{3}H-labelled cholesterol is also included in the proteoliposome mix.

The molar ratios of PC:cholesterol:apoAI have been varied in many publications in attempts to produce a good substrate [263, 264] but the protocol used for the experiments presented here is adapted from that of Chen and Albers [257]. They found that the best LCAT activity was evident with an egg-PC:cholesterol:apoAI molar ratio of 250:12.5:0.8. They showed that varying the lecithin:cholesterol ratio had a direct effect on LCAT activity. Matz and Jonas [265] showed that varying the PC type also has an effect on the enzyme's activity, with egg-PC being a superior acyl donor to dipalmitoyl-PC or dimyristoyl-PC.

Cholate is used in substrate formation to disperse the apoAI and is then removed by dialysis, as it is an inhibitor of LCAT. Complete removal of cholate from the substrate is therefore very important, and Chen and Albers found that after 18 h of dialysis 99.9% of cholate was removed. Our protocol has approximately 20 h of dialysis followed by incubation of the substrate with amberlite XAD-2 ion exchange beads to ensure complete removal of the cholate. This step was added because prolonging the dialysis time can result in unstable liposomes. Nevertheless, tests of the substrate performed in our lab before and after use of the amberlite beads did not show a significant improvement.

Another possible reason for reduced activity with the substrate is an extended storage time. Our substrate was kept at -20°C for many months, which may have had an effect on the stability of the liposomes. Undisturbed substrate should remain unchanged if stored frozen, but the longest time period that has been examined is 5 weeks [257]. Although our method of substrate preparation should produce liposome vesicles when vortexing the mixture with cholate, sonication could possibly improve particle formation and thus substrate quality. This method has been used in the past for LCAT substrate preparation [266] and could be of benefit where improved performance of substrate is necessary.

In conclusion, modification of the substrate formation protocol may have resulted in higher LCAT activities than the ones observed for the comparative experiments performed in this chapter. Additionally, a larger sample size may have helped give statistically significant data. Despite this fact and the differences in quantity of protein secreted, the mutated LCAT variants appeared to be active. The

method used to determine the specific activities of each enzyme was meant to give purely comparative insight into the effect of the mutations. It is therefore not possible to draw a parallel between published activity levels and these individual results. Nevertheless, the specific activities obtained here point in the direction of previously reported findings. Qu *et al.* [125] found that the S216A mutation doubled the specific activity compared to wild-type, whereas Francone and Fielding [122] observed a 14-fold increase of activity for the same mutation. The results of this study were somewhere between the two, with approximately 9 times higher specific activity observed for $LCAT_{S216A}$.

With regards to the S208A + S216A double mutation, no publications currently exist to corroborate my findings. Although again, higher activity was found here, this was not as dramatic as the increase seen for the S216A mutation alone. The protein region of the Ser208 and Ser216 is adjacent to the active site of the enzyme. It has already been postulated that changing a serine to a more hydrophobic alanine may aid binding of substrate [125], but the addition of a further alanine may alter binding to phospholipids in an unfavourable manner. This would explain the reduction in activity from the higher level seen with the S216A mutation alone, though the reduction does not eliminate the beneficial presence of alanine at amino acid 216 completely. This is supported by the fact that there is still a nearly 2-fold increase activity for the double mutant compared to wild-type.

Even though protein production was lower in the cell lines expressing the mutants compared to wild-type LCAT, the same may not necessarily be true *in vivo*. As discussed earlier, *in vitro* work leads to recombinant cell lines carrying undetermined numbers of LCAT gene copies, which is not the case *in vivo*. Therefore, the findings of higher specific activities for the mutant LCAT proteins could prove realistic *in vivo* despite reduced LCAT secretion by recombinant cells *in vitro*.

The main aim of this project was to introduce the S208A and/or S216A mutations into target cells *in-situ* using the technique of chimeraplasty, followed by analysis of the properties and specific activities of LCAT secreted by these cells. The project therefore began with experiments targeting HepG2 and $CHO\text{-}LCAT_{WT}$ cells with chimeraplasts aimed at mutating the LCAT gene (see Chapter 4). These mutations proved difficult to achieve by chimeraplasty, and led me back to mutagenesis as a method of creating mutations. Production of the LCAT double-mutant allowed me to compare specific activities of three LCAT variants.

Unfortunately, by this stage time was limited and problems in generating good quality substrate did not allow me to delve deeper into analysis of the three LCAT variants described in this chapter. Nevertheless, the experiments performed here sufficiently support published findings on the LCAT S208A and S216A mutations to justify attempting to create these mutations *in situ* using chimeraplasty.

Chapter 4 –

Targeting the LCAT gene by chimeraplasty using standard procedures

4.1 INTRODUCTION

As outlined in *Section 1.3*, two mutations in the LCAT gene were found to cause structural and functional changes in the enzyme that result in an increase in its activity [125]. These published findings were based on site-directed mutagenesis of human LCAT cDNA and transient expression and analysis of the protein in CHO cells. In Chapter 3 I followed the same method and my results support previous findings that showed that the Ser208Ala and Ser216Ala mutations do indeed increase LCAT enzymatic activity. Although this gives valuable insight into these two mutations and expression in CHO cells makes it easier to study the protein, more information can be gained by looking at expression of mutated LCAT *in situ* in a human cell line.

One of the greatest advantages of the technology of chimeraplasty is its ability to mutate genes *in situ* [199]. This eliminates the need to use site-directed mutagenesis, avoids time wasted in constructing vectors containing the mutated cDNA, and allows the cell to use the machinery that would naturally be used to express and regulate the gene. Along with these merits is the fact that chimeraplasty can correct the pre-existing gene rather than allow the errant gene to exist in the cell while a corrected gene is added that would be expressed alongside the original one (gene addition).

In this segment of my work, I attempted to use chimeraplasty to create the Ser208Ala and Ser216Ala mutations, both in human LCAT cDNA in CHO cells and in the LCAT gene in the human hepatoblastoma cell line, HepG2. This was done with a standard transfection protocol using PEI as the delivery agent. The aim was to mutate the gene, collect the protein secreted into the culture medium, and then analyse the enzyme to see whether indeed any increase in catalytic activity is observed, as was done in Chapter 3 with LCAT from recombinant cells.

The standard protocol for transfection of chimeraplasts resulted from work in our laboratory to target the apoE gene [191]. Recombinant CHO cells secreting human apoE2 (containing amino acids Cys112 and Cys158) were converted to apoE3 (Cys112 and Arg 158) using a chimeraplast that creates the mutation T→C resulting in an amino acid change from cysteine to arginine. Concentrations of 100 to 1000 nM of

a 68-mer or 88-mer chimeraplast, preincubated with PEI, were used to transfect the CHO cells, which were harvested for analysis 24 hours later. RFLP analysis resulted in several findings: 1) there is a dose-dependent response: 400 nM chimeraplast results in a higher conversion than 200 nM; 2) repeat targeting of the same cells can increase the conversion; and 3) increasing the length of the chimeraplast can increase the conversion. These conclusions led to the design of my experiments with the LCAT chimeraplasts.

4.2 RESULTS

4.2.1 CHIMERAPLAST DESIGN

The chimeraplasts that were designed to target the 208 and 216 sites of the *LCAT* gene followed the scheme previously used by this laboratory [186]. Previous publications [179-183] and our own experience have shown that this structure was adequate to achieve a nucleotide change of almost 40% with a concentration of 400 nM. The molecule is made up of 68 nucleotides, mostly DNA, with two 2'-O-methyl RNA regions of 10 nucleotides each to stabilize hybridization with one strand of the gene while the DNA segment starts the base exchange event of the gene repair on the other strand. There is sequence complementarity between the RNA and DNA segments so that the molecule can fold into a double-hairpin configuration, thus avoiding nuclease digestion and concatenation of double-stranded molecules when the chimeraplasts are transfected into cells. The oligonucleotide also contains a GC clamp at the 3' end, a short region supposed to confer a high melting temperature, and four T residues at each end of the double-stranded part of the molecule to allow the hairpin to form. The mutator base lies in the middle of the five DNA nucleotides between the two RNA regions (***Fig. 4.1***). A BLAST search of the hybridizing sequence was performed for the two chimeraplasts and found that there is a 100% match only for human and monkey LCAT. In addition, a longer 80-mer molecule was produced, extending the RNA regions and complementary DNA in both directions by 3 nucleotides.

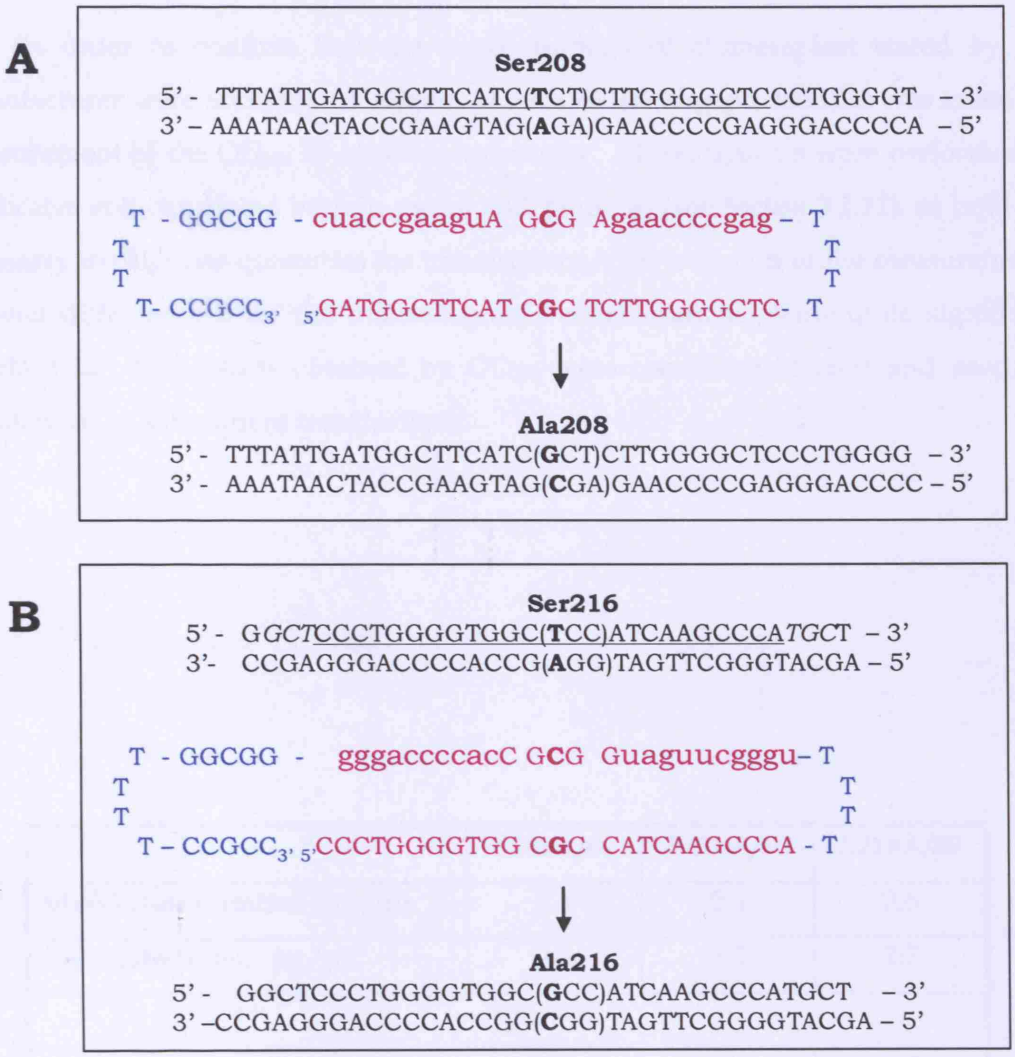

Fig. 4.1: LCAT chimeraplast sequences.

Alignment of the synthetic 68-mer oligonucleotides with the target sequences in the human LCAT gene (in black). The 2'-O-methyl RNA residues are in lowercase and the DNA residues in capital letters. Nucleotides corresponding to the LCAT gene are in pink. Centre mutator nucleotides within the chimeraplast are in bold. The targeted nucleotides in the LCAT gene are underlined. Chimeraplast structure is discussed in Section 1.3.3.2. ***A****: Ser208Ala chimeraplast.* ***B****: Ser216Ala chimeraplast. The three nucleotides in italics on either side of the underlined segment in the gene represent the ones added to make the 80-mer Ser216Ala chimeraplast.*

4.2.2 ESTIMATION OF CHIMERAPLAST CONCENTRATION

In order to confirm that the concentrations of chimeraplast stated by the manufacturer were accurate, an aliquot of each of the oligonucleotides was taken for measurement of the OD_{260} by spectrophotometry. Measurements were performed in duplicates and calculated both in µg/µl and pmol/µl (see *Section 2.1.11*), as both are necessary to calculate quantities for transfections. The averages of the measurements showed differences from the manufacturer's concentrations, some quite significant (**Table 4-1**). The results obtained by OD_{260} were considered correct and used for calculations in subsequent transfections.

	S208A/68	**S216A/68**	**S216A/80**
MWG concentration (µg/µl)	2.5	2.4	2.6
Calculated conc. µg/µl	2.6	3.3	2.7
MWG concentration (pmol/µl)	100	100	100
Calculated conc. pmol/µl	159	127	114

Table 4-1: Chimeraplast concentrations.

OD_{260} calculated concentrations of the three LCAT chimeraplasts in comparison with the concentrations stated by the manufacturer (MWG). S208A/68 and S216A/68 refer to the 68-mer chimeraplasts, while S216A/80 refers to the 80-mer chimeraplast.

4.2.3 TRANSFECTIONS USING THE FIRST BATCHES OF SER208ALA AND SER216ALA 68-MER CHIMERAPLASTS

4.2.3.1 Preliminary transfections using a standard protocol

The first experiments used a protocol previously shown to work in our laboratory, and found adequate to induce gene conversion when targeting the *APOE* gene. HepG2 cells were seeded in 12-well plates 24 h before transfection. On the day of transfection cells were approximately 70% confluent. The transfection complexes were made up of 400 nM of either of the two oligonucleotides (Ser208Ala or Ser216Ala), L-PEI at an N:P ratio of 5:1, and 150 nM NaCl. These were mixed together and left to incubate at room temperature for 10 min, then added to the cells. After 6 h, the cells were washed once in PBS and maintenance medium was added. Analysis of the transfection was accomplished by harvesting the cells after 24 h, extracting DNA, and performing PCR-RFLP. Tagalakis and colleagues [186] showed that PCR results of chimeraplasty experiments (here, to convert apoE4 to apoE3) are not artefactual by spiking PCR reactions with either intact chimeraplasts or with DNA from CHO cells secreting apoE4. PCR-RFLP analysis was therefore considered a valid method of analysis for chimeraplasty experiments.

PCR was performed using the LCAT genomic primers for HepG2 DNA and generated a 240 bp band (see Section *2.1.3*). PCR products from DNA of cells treated with the Ser208Ala chimeraplast were digested with the restriction endonuclease MwoI, while those from DNA of cells treated with the Ser216Ala chimeraplast were digested with CfoI. For the RFLP, in each case a base change results in the addition of a restriction site. The expected electrophoresis patterns are illustrated in ***Fig. 3.4*** (Chapter 3). No base change was observed for targeting in HepG2 cells with either of the two chimeraplasts (results not shown).

HepG2 cells were thought to possibly be more difficult to transfect than CHO cells, therefore the experiment was repeated in CHO-LCAT$_{WT}$ cells. Cells were prepared and treated in the same way as the HepG2 cells, and collected for analysis after 24 h. PCR used the LCAT cDNA primers and generated a 230 bp band. Digests of the PCR products were performed as before (for pattern see ***Fig. 3.4***). Again, no conversion was detected using either of the chimeraplasts (***Fig. 4.2***).

4.2.3.2 *Transfections with the addition of chloroquine*

The standard protocol having failed, it was thought that the addition of chloroquine would improve transfection efficiency by raising lysosomal pH and therefore protecting endocytosed DNA from degradation [221]. CHO-LCAT$_{WT}$ cells were prepared as before, as were the transfection complexes (400 nM chimeraplast and L-PEI at an N:P ratio of 5:1), but chloroquine at a final concentration of 100 μM was added to the cells 5 min prior to the addition of the oligonucleotide-PEI mix. Cells were then incubated for 6 h with the mix and harvested 24 h later. PCR-RFLP analysis again showed a failure to produce a base change with either of the chimeraplasts (results not shown).

4.2.3.3 *Transfections with chimeraplasts at various concentrations*

In order to determine whether a higher concentration is necessary for chimeraplast activity to become apparent, both CHO-LCAT$_{WT}$ and HepG2 cells were targeted with the two chimeraplasts separately at concentrations ranging from 300 to 1200 nM, with PEI used at an N:P ratio of 5:1. Cells were treated with the oligonucleotide-PEI complexes for 6 h, then harvested after 24 hours and DNA was extracted. RFLP results showed that no base mutation had occurred at any of the concentrations of chimeraplast used, in neither of the two cell lines targeted, and with neither of the two 68-mer chimeraplasts (***Fig. 4.3***).

4.2.3.4 *Transfections at various N:P ratios of PEI*

Linear polyethylenemine (PEI) is a transfection reagent that has been shown to work with relatively low toxicity and high efficiency. As was discussed in *Section 1.3.4.3*, the molecules are "proton sponges" with every third atom a protonable amino nitrogen atom. This property allows the number of DNA molecules that can associate with a molecule of PEI to vary greatly and the complexes produced when they are mixed together can range from neutral to very positive. The variation in charge has an effect on the delivery efficiency of PEI [208], but higher doses of PEI also lead to increased toxicity for the cells. As the LCAT chimeraplast/PEI complexes failed to produce a conversion at a N:P ratio of 5:1, I wondered whether this was not a lack of

chimeraplast activity, but rather poor delivery caused by a sub-optimal N:P ratio for the chimeraplast transfection.

Both HepG2 cells and CHO-LCAT$_{WT}$ cells were targeted with 400 nM chimeraplast (either Ser208Ala or Ser216Ala) with a PEI N:P ratio ranging from 4:1 to 9:1. The cells were transfected as before and incubated for 6 h, followed by harvesting for RFLP analysis after 24 h. All samples were analysed, except for the cells targeted with the 9:1 ratio, because by 4 h incubation over 95% of the cells had died. RFLP analysis showed that again no mutation had occurred at any of the N:P ratios, in neither of the cell lines, and with neither of the chimeraplasts (results not shown).

To ensure that there was no combined N:P ratio and chimeraplast concentration effect, cells were also targeted with up to 1000 nM of oligonucleotide while varying the N:P ratio. Unfortunately this again had no effect in producing gene conversion (results not shown).

4.2.3.5 Transfections with the addition of centrifugation

Gentle centrifugation of the cells after addition of chimeraplast-PEI complexes has the purpose of increasing contact between the complexes and the cell surface. Cells were transfected with either 400 nM or 800 nM chimeraplast (either Ser208Ala or Ser216Ala) and L-PEI at a N:P ratio of 5:1, as before. Immediately after the addition of the complexes to the cells, the plate was spun at 400 g for 5 min. Incubation was then continued for 6 h as previously done. PCR-RFLP analysis again showed no success in converting the gene with either of the chimeraplasts (results not shown).

4.2.3.6 Repeated targeting of cells with chimeraplasts

The next experiment tried to determine whether repeated targets on the same cells would result in a conversion due to a cumulative effect of the chimeraplast's action. If a conversion occurred, it would show that transfection efficiency was indeed the problem in the first series of experiments, or that the chimeraplasts have a very poor activity, which can be improved by repetitive treatments.

For this experiment, HepG2 cells were targeted 5 times using 800 nM of each chimeraplast, at a PEI N:P ratio of 5:1. Cells were detached from their wells by trypsinisation after 24 h, 10% were re-plated to grow on, and the rest were harvested for analysis. The retained cells were allowed to grow for at least 7 days between each targeting, with the same transfection conditions repeated each time. Again, even after the 5th targeting no conversions were detected by RFLP (***Fig. 4.4A***). This was confirmed by sequencing, which showed no evidence of a conversion from T→G (***Fig. 4.4B***).

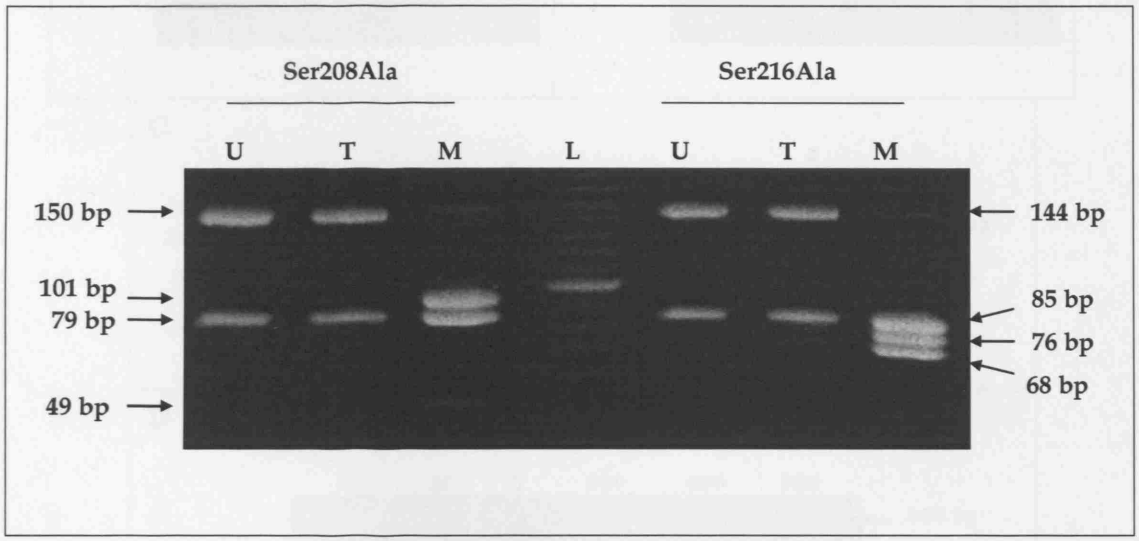

Fig. 4.2: Preliminary targeting of CHO-LCAT$_{WT}$ cells with Ser208Ala and Ser216Ala chimeraplasts.

Cells were targeted with 400 nM of each oligonucleotide in combination with L-PEI (N:P ratio = 5:1), incubated for 6 h, and harvested for analysis after 24 h. The gel shows that for each of the chimeraplasts there is no appearance of the diagnostic third band, indicating failure of the chimeraplast to create a mutation. L: 10 bp ladder. U: untreated cells. T: chimeraplast-treated cells. M: RFLP of CHO-LCAT$_{2M}$ cells (containing both Ser208Ala and Ser216Ala mutations) as a positive control.

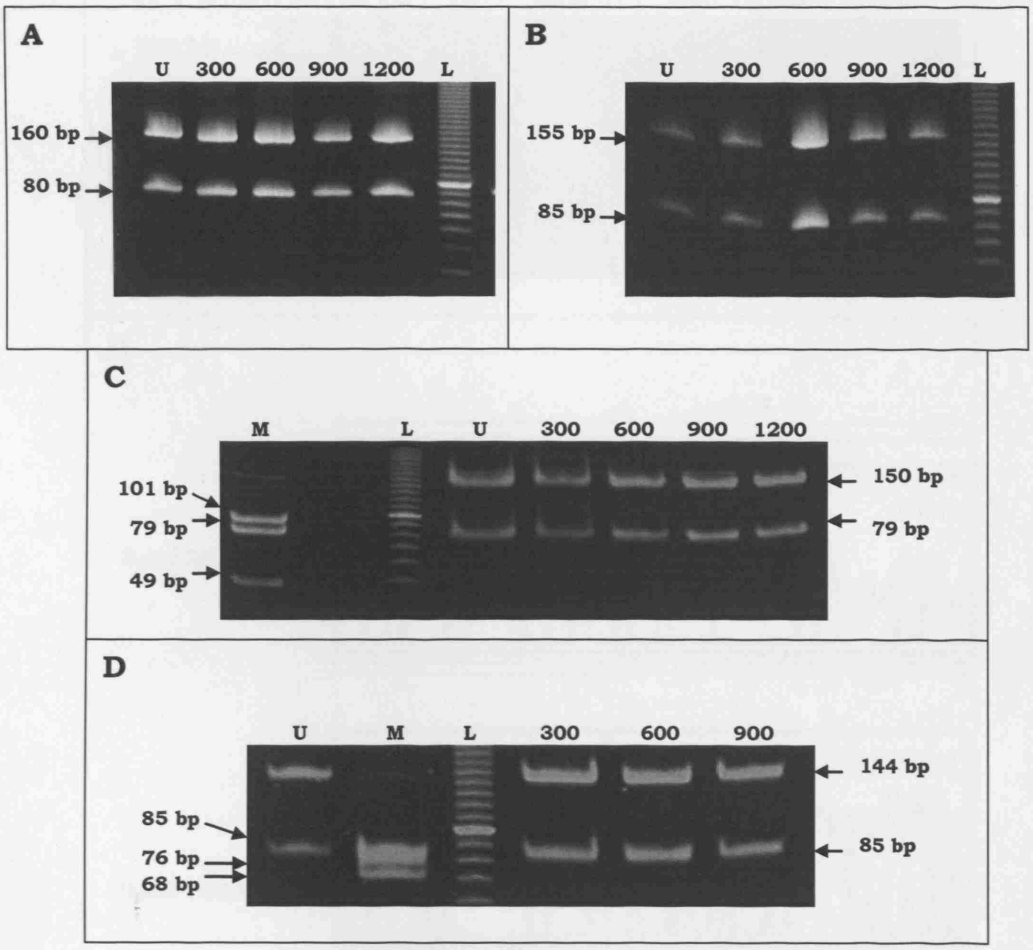

Fig. 4.3: Transfections at increasing concentrations.

HepG2 and CHO-LCAT$_{WT}$ cells were targeted with 300, 600, 900 and 1200 nM of chimeraplasts Ser208Ala/68 and Ser216Ala/68, which has been complexed with L-PEI. The cells were incubated with the complexes for 6 h, then harvested for analysis 24 h later. The gels show the results of RFLP analyses. ***A****: HepG2 cells targeted with Ser208Ala/68.* ***B****: HepG2 cells targeted with Ser216Ala/68.* ***C****: CHO-LCAT$_{WT}$ cells targeted with Ser208Ala/68.* ***D****: CHO-LCAT$_{WT}$ cells targeted with Ser216Ala/68. L: 10 bp ladder. U: untreated cells. M: CHO-LCAT$_{2M}$ cells (containing both Ser208Ala and Ser216Ala mutations) as a positive control. All four images show absence of a diagnostic third band, indicating failure to mutate the gene.*

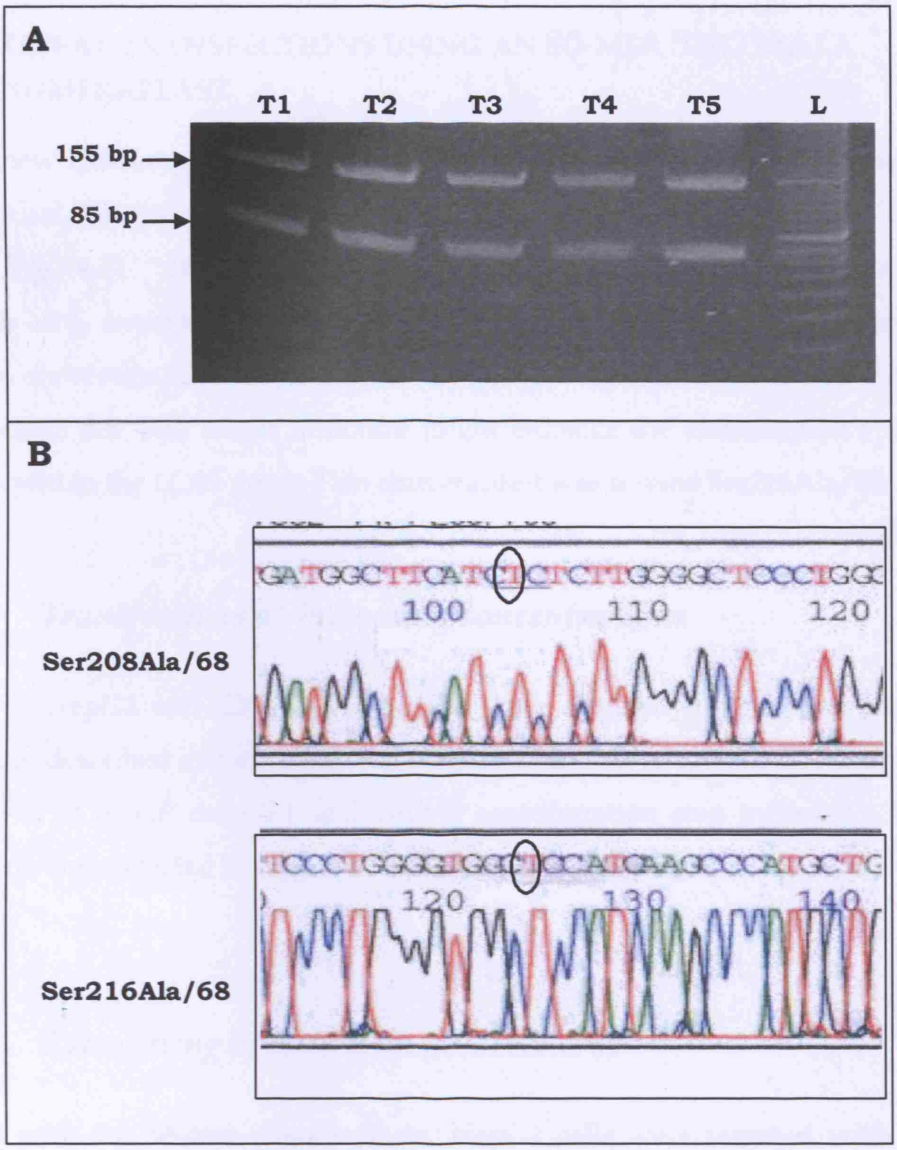

Fig. 4.4: Retargeting of HepG2 cells with LCAT chimeraplasts.

***A**: RFLP results of the repeated (T1 to T5) transfection of HepG2 cells with S216A/68 chimeraplast. Cells were targeted with 800 nM chimeraplast and L-PEI (N:P ratio = 5:1). Twenty-four hours after each target, 10% of cells were left to grow on for at least a week before retargeting. The diagnostic third restriction fragment is missing, indicating failure to mutate. L: 10 bp ladder. **B**: Sequencing of PCR products from analysis of cells following the 5th retarget with either Ser208Ala/68 or Ser216Ala/68. Gene correction by the chimeraplasts would have changed the T (circled) to a G at both 208 and 216 sites.*

4.2.4 REPEAT TRANSFECTIONS USING AN 80-MER SER216ALA CHIMERAPLAST

A new chimeraplast was ordered, of a similar structure to the 68-mer S216A chimeraplast, but containing 3 more nucleotides at each end of the LCAT targeting region (***Fig. 4.1***). It was previously shown in our laboratory that for apoE chimeraplasty, extending the length of the chimeraplast from 68-mer to 88-mer increases conversion efficiency by almost 10% [191]. Therefore, in the case of LCAT, it was thought that this longer structure might enhance the chimeraplast's ability to function within the *LCAT* gene. This chimeraplast was termed Ser216Ala/80.

4.2.4.1 Transfections at increasing concentrations

Both HepG2 and CHO-LCAT$_{WT}$ cells were targeted in the same manner as previously described at concentrations ranging from 300 to 1200 nM of chimeraplast, with L-PEI at a N:P ratio 5:1 and with a centrifugation step included. No gene conversion was detected in either cell line by PCR-RFLP (results not shown).

4.2.4.2 Retargeting of cells with Ser216Ala/80

As with the 68-mer chimeraplasts, HepG2 cells were targeted with 800 nM Ser216Ala/80 at a PEI N:P ratio of 5:1. After 24 h, 10% of the cells were left to grow on and retargeted after 7 days. This was repeated 5 times. Again, there was no success at conversion as judged by RFLP analysis (results not shown).

4.2.5 ANALYSIS OF CHIMERAPLASTS BY ELECTROPHORESIS

The chimeraplasts were resolved on a TBE-urea gel as described in *Section 2.1.1* in order to assess whether the structures were intact. A single band of the correct size (68 or 80 nt) would suggest that the chimeraplast molecules are not degraded. If degradation of the molecules were observed, this might explain why no gene mutating activity had yet been observed for the 3 chimeraplasts tested. Degraded oligonucleotides would appear as a smear rather than a distinct band.

Aliquots of the oligonucleotides were prepared as described in *Section 2.1.1.* ***Fig. 4.5*** shows the resulting gel. None of the chimeraplasts appeared as distinct single bands that would represent intact molecules all of the same size. Moreover, the 80-mer chimeraplast was expected to appear slightly higher on the gel than the 68-mer molecules because of its larger size; this was in fact not observed (***Fig. 4.5***).

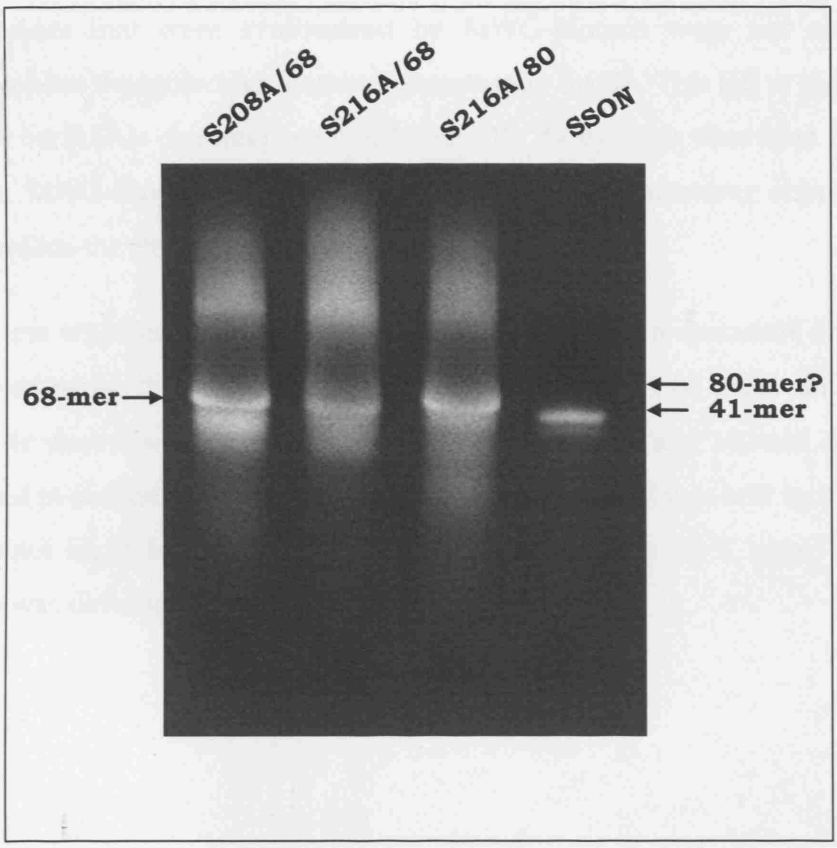

Fig. 4.5 : TBE-urea gel of the LCAT chimeraplasts.

Chimeraplasts were mixed with sample buffer, heated at 96°C for 10 min and then loaded into a precast 15% TBE-urea gel. The samples were run in parallel with a 41-mer single-stranded oligonucleotide (SSON). All three chimeraplasts show signs of degradation, with smearing above and below the 68-mer level. The 80-mer chimeraplast shows the densest band at the 68-mer level, rather than at a higher level consistent with its larger size. Molecules of good quality should appear as distinct bands with no smearing, as seen for the SSON.

4.2.6 TRANSFECTIONS WITH A SECOND BATCH OF SER216ALA 68-MER CHIMERAPLAST

The results of the previous section lead to the assumption that the oligonucleotides that were synthesized by MWG-Biotech were not active, most probably because the molecules were not structurally intact. This led to the order of a new 68-mer Ser216Ala chimeraplast (Ser216Ala/II), though this time from Eurogentec rather than MWG-Biotech. A gel produced by the manufacturer shows a single distinct band for the chimeraplast (***Fig. 4.6***).

To test whether this oligonucleotide could produce a mutation, HepG2 cells were targeted using chimeraplast concentrations up to 1500 nM with a PEI N:P ratio of 5 :1. Cells were also targeted with 800 nM chimeraplast and 100 μM chloroquine (as described in *Section 4.2.3.2*). Cells were spun at 275 g for 2 min and incubated with the complexes for 4 h before being harvested for analysis 24 h later. Again, no conversion was detected by PCR-RFLP (results not shown).

4.2.7 TRANSFECTIONS WITH A THIRD BATCH OF SER216ALA 68-MER CHIMERAPLAST

The Eurogentec synthesis yielded a low quantity of chimeraplast (approximately 500 μg whereas previously the yield was at least double this amount). The manufacturer's sister company, Oswel, therefore offered to synthesize another batch of the Ser216Ala chimeraplast (Ser216Ala/III) to make up the difference. As this was a completely new synthesis, it could not be assumed that the activity of the new reagent would be the same, therefore the same experiments that were described in *Section 4.2.6* were repeated with the new batch. Once more, the reagent failed to generate a mutation in HepG2 cells, even at high concentrations (results not shown).

In order to gain further insight into a possible reason for repeated failures, the Eurogentec and Oswel chimeraplasts were also visualised by electrophoresis. Interestingly, when viewed in parallel with a 68-mer chimeraplast aimed at targeting a different gene, both the Ser216Ala reagents appear to have the densest band slightly lower than the level expected for 68-mer (***Fig. 4.7***).

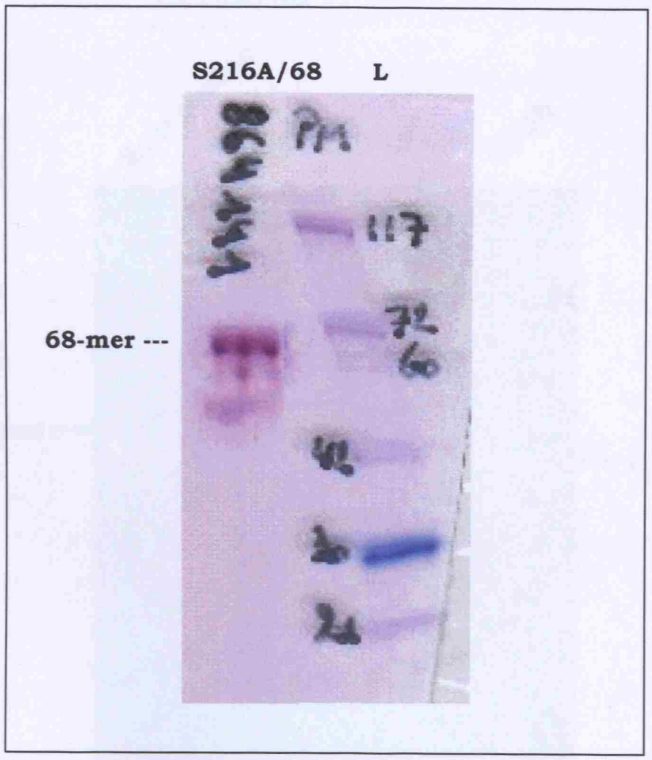

Fig. 4.6: Electrophoresis of Eurogentec Ser216Ala/68 chimeraplast.

Gel provided by the manufacturer on delivery of the synthesized chimeraplast. The oligonucleotide appears to be of relatively good quality, with little smearing and a distinct band consistent with a molecule size of 68-mer. L, ladder.

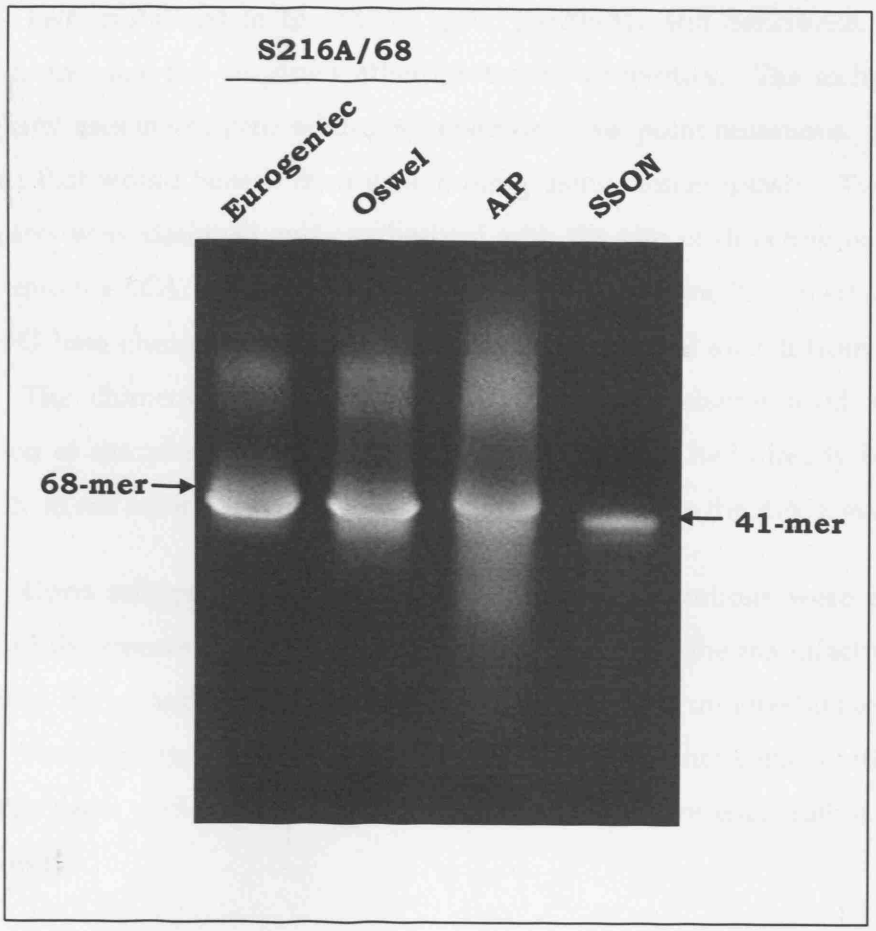

Fig. 4.7: Electrophoresis of 2nd and 3rd batches of Ser216Ala/68 chimeraplasts. *Chimeraplasts were again visualised on a 15% TBE-urea gel. The Eurogentec and Oswel reagents appear as dense bands with not much smearing, but at a level slightly lower than that of the 68-mer chimeraplast to target the apolipoprotein AI gene (AIP). SSON: 41-mer single-stranded oligonucleotide.*

4.3 DISCUSSION

Two mutations in the LCAT gene, Ser208Ala and Ser216Ala, have the potential to increase the enzyme's atheroprotective properties. The technology of chimeraplasty uses *in situ* gene editing to repair or create point mutations. *LCAT* is a target gene that would benefit from gene editing using chimeraplasty. Two 68-mer chimeraplasts were designed and synthesized with the aim of directing *in situ* gene editing within the *LCAT* gene at two sites, serine 208 and serine 216, to effect in each case a T→G base change that would result in an amino acid switch from serine to alanine. The chimeraplast design followed the same scheme used since the introduction of chimeraplasty in 1996 [179], and this design had already been used successfully in our laboratory on a molecule destined to mutate the *APOE* gene [191].

Upon receipt of the chimeraplasts, their concentrations were measured and showed differences from the expected ones as stated by the manufacturer. It is possible that the quantity of chimeraplast synthesized was underestimated by the producer. Nevertheless, the new concentrations were taken into consideration when transfections were performed and my calculated values were used rather than the manufacturer's.

A protocol that was successful in targeting the *APOE* gene by chimeraplasty was followed to perform a preliminary transfection of HepG2 cells with each of the LCAT chimeraplasts. The first transfections attempted to establish whether the molecules were able to create the intended mutations using conditions that were optimal for the ApoE chimeraplasts. At 400 nM concentration and a standard amount of L-PEI, neither of the two oligonucleotides managed to show a mutation using RFLP analysis. Due to the fact that transfection efficiencies can vary between cell types, recombinant CHO cells carrying LCAT cDNA (CHO-$LCAT_{WT}$) were also transfected, but again the results were negative. Experimentally, transfection efficiency was difficult to estimate. Performing pGFP transfections in parallel would not necessarily be an indicator of efficiency for a chimeraplast transfection. The lack of success could have been attributed to problems at the level of delivery or at the level of chimeraplast action within the gene.

To try to improve delivery, chloroquine was added to the next transfection. This reagent raises the pH of lysosomes, therefore inactivating

lysosomal enzymes and in so doing protecting DNA that has been taken up by the cell [221]. Chloroquine has been shown to improve transfection efficiency by up to 20 times in both HepG2 and CHO cells [221, 226]. Nevertheless, when used to try to enhance the efficiency of transfection of oligonucleotides into CHO-LCAT$_{WT}$ cells, results remained negative.

The next logical experiment was to evaluate a range of chimeraplast concentrations. Until now the only concentration used was 400 nM, which could be insufficient to mutate the *LCAT* gene. Cells were transfected with increasing concentrations of the two oligonucleotides, up to 1200 nM. This limit was set because the amount of PEI that was required to produce the transfection complexes at higher concentrations became toxic to the cells. While chimeraplasts directed at other genes showed activity at 200 and 400 nM [182, 183, 191], here no mutation appeared even at concentrations as high as 1200 nM. The problem did not appear to be a matter of cell type, because both HepG2 and CHO-LCAT$_{WT}$ cells produced the same result.

At this stage, several explanations could be envisaged to explain the results. Firstly, failure could have been at the level of DNA delivery into the cell. If transfection efficiency was the problem, modifications to the way the DNA/PEI complexes were formed might help. It is widely accepted that different cell lines can have different transfection efficiencies with the same delivery reagent [267,268]. A second difficulty might be at the level of the chimeraplast's interaction with the gene in the nucleus. The conformation of the gene within that section of chromosome might create physical barriers to the oligonucleotide hybridising with the target region. This is a possible explanation for failure to mutate in HepG2 cells, but is more difficult to explain in the case of CHO-LCAT$_{WT}$ cells because here the location of the LCAT cDNA is different to the genomic location and cells may even contain more than one copy of the cDNA in several locations. Alternatively, the sequence to which the target region was to be mutated (e.g. TCT→GCT) could be the reason for failure to mutate, as studies have shown that certain mismatches are more readily repaired than others [193]. Table 1-5 lists all major publications with successfully chimeraplast-mutated genes and the specific nucleotide change involved in each one. None of these involves a T→G mutation such as in LCAT and therefore it may be that this mutation is one that is less amenable to chimeraplast action. Thirdly, the fault may lie with the chimeraplast itself, as its quality may be poor and thus it may be non-functional even though it is able to make its way into the nucleus.

In order to tackle the first of these possibilities, a series of transfections were performed where the only variable was the amount of PEI used in the DNA/PEI complexes, with the concentration of chimeraplast remaining constant. The decision to use L-PEI as the delivery reagent was based on results shown in several recent papers [228, 231, 269, 270] as well as successful chimeraplasty work performed in our laboratory. Although the manufacturers of Exgen 500 state that transfections can be performed with a N:P ratio of up to 12, experiments performed here showed that at a ratio of 9:1 significant toxicity was evident. Furthermore, the cells that did survive (at ratios 8:1 and below) still showed no signs of having been affected by the chimeraplasts. A further small modification, the addition of a centrifugation step after addition of the DNA/PEI complexes in order to enhance contact of the complexes with the cells, also proved futile. At this stage it was still not clear where the problem lay: with transport, gene, or chimeraplast.

The next idea was to see whether the activity of these chimeraplasts was so weak that a mutation was present but below the detection level picked up by RFLP. Several groups reported very low conversion rates that were below the sensitivity of RFLP analysis [184, 187, 271]. Could amplification by repeatedly targeting the same cells to create a cumulative effect bring the mutation level up high enough to be detectable by RFLP? HepG2 cells were targeted 5 times over, but even though cells were analysed after each retarget, by the fifth time there was still no apparent mutation, and this was confirmed by sequencing. Assuming the oligonucleotide molecules were reaching the nucleus, three scenarios were now possible: 1) failure to see gene mutation was still due to conversion levels being below RFLP detectability; 2) at each target most of the successfully transfected cells died because of DNA/PEI toxicity, leaving only the untransfected cells to be retargeted, and thus each targeting event was individual, not cumulative; 3) the chimeraplasts had no gene correction ability.

Having attempted variations of all the elements involved in the transfection, it was now time to look at the chimeraplast itself. In order to tackle the possible failure of the experiments due to lack of chimeraplast activity, a longer oligonucleotide was designed for the Ser216 target because it had been shown with the apoE2→E3 chimeraplast that elongating the oligonucleotides to 80-mer increases the strength of the hybridisation with the target site and therefore improves chances of a mutation occurring [191]. With this intention, transfections were repeated using

similar conditions as were done with the 68-mer oligonucleotides. Unfortunately, the improved hybridisation ability did not aid in achieving a gene conversion at the serine 216 site, despite high concentrations of reagent being put on the cells. Retargeting up to 5 times also showed no improvement by a cumulative effect.

To go back to the three possible reasons for lack of success in targeting the *LCAT* gene so far, delivery was still an option. Though chloroquine and various DNA/PEI complex charges were looked at, uptake of DNA by the cell nucleus is still poorly understood. It could therefore be assumed that there was still place for optimisation of delivery into the cell. If indeed the limiting factor in achieving gene conversion is poor access to the target within the nucleus or sequence-specific poor hybridisation, then more investigation is necessary to gain better understanding of gene location and interaction of oligonucleotides with target sequences, though this is a difficult task.

I decided to first look at the third option, quality of the synthesized oligonucleotides. The simplest way to do this initially was by visualising the molecules on a gel. A synthesis of good quality should contain molecules that are all the same size, demonstrated on electrophoresis by a single band. The appearance of several bands or smudges would indicate that there are molecules that have become degraded. When I examined my three chimeraplasts (two 68-mer and one 80-mer) I found that the 68-mer oligonucleotides were partially intact but also showed signs of degradation, while the 80-mer reagent showed few molecules at the electrophoresis level that should correspond with 80 nt. This result could partially explain the failure of the previous experiments. If this was the condition of the reagents when they were transfected into cells, only a percentage of all the molecules present were structurally intact, therefore reducing the chances of gene correction occurring. Synthesis of RNA/DNA oligonucleotides as they are designed for chimeraplasty is more complicated than the synthesis of DNA oligonucleotides because of the modified RNA segments. It may be that the process of purification following synthesis somehow damages the molecules and renders them inactive.

In order to verify whether indeed reagent quality was the limiting element, a new Ser216Ala chimeraplast was ordered, though from a different company this time (Eurogentec), to see whether synthesis and purification method differences had an effect on the activity of the oligonucleotides. Experiments were repeated in HepG2 cells: increasing concentrations up to 1500 nM, using chloroquine and introducing a

centrifugation step, but again gene correction failed. Due to the fact that the Eurogentec synthesis resulted in a small batch, the company offered us the opportunity to acquire another batch of the Ser216Ala chimeraplast, this time synthesised by their sister company, Oswel. The same experiments were once again undertaken in HepG2 cells, with failure resulting once more.

Electrophoresis of the Eurogentec and Oswel reagents revealed that once again there was a problem with the molecules. Although smearing was not widespread, the densest band visible for both oligonucleotides was just below where it should have been for a molecule of 68-mer length. Again, this could explain the lack of gene correction due to a very low number of intact and hence viable molecules reaching their expected destination. Nevertheless, other chimeraplasts have been shown to work at quite low transfection concentrations. If at high concentrations, for example 1500 nM, of poor quality reagent chimeraplast activity is still not seen, could optimising delivery be the key? In this case, it would be worthwhile to do this specifically for HepG2 cells targeted with chimeraplasts. The next chapter deals with this subject.

Chapter 5 –

Optimisation of chimeraplast delivery

5.1 INTRODUCTION

In *Section 1.4* of the introduction chapter it was noted that transfection efficiencies with a given reagent can vary from cell line to cell line. Ultimately, the target cells of this study are hepatic cells, and *in vitro* the cell line that was most used was the human hepatoma cell line HepG2. In the last chapter I showed that transfecting these cells with the LCAT chimeraplasts using a standard protocol was unsuccessful. Therefore it was considered important to determine which transfection reagent could produce optimal conditions for transfections with chimeraplasts.

To this end, polyethylenimine (PEI) and several of its conjugates were examined with regards to transfection efficiency. PEI has been the subject of many papers, but the great majority discuss its ability to transfect plasmid DNA. Only a few publications show the value of using a modified PEI to transfect cells with RNA/DNA oligonucleotides [197,273]. My investigation began by looking at basic PEIs: comparing linear PEI (most commonly used) and branched PEI. Next, I looked at the value of treating cells with chloroquine before transfection. Conjugated PEIs that enter the cell via receptors were also examined: Galactose-PEI and Galactose4-PEI via the asialoglycoprotein receptor [238], and Transferrin-PEI via the transferrin receptor [234]. Lastly, PEI conjugated to melittin was examined to see whether this might enhance nuclear access.

Analysis of these experiments was by two methods: RFLP and fluorescence activated cell sorter (FACS). RFLP examined the ability of a chimeraplast of known activity to create the required point mutation using the various transfection reagents. FACS analysis investigated the delivery aspect of transfection, by targeting cells with a fluorescently-labelled chimeraplast, isolating the cell nuclei after a number of hours, and counting the number of fluorescent nuclei to indicate the percentage of cells successfully transfected.

5.2 RESULTS

5.2.1 CHIMERAPLAST DESIGN

In order to perform gene conversion experiments that were reproducible, a chimeraplast of validated activity was necessary. Two chimeraplasts were chosen that target the apolipoprotein E (*APOE*) gene, converting it from the wild-type genotype apoE3 to either the apoE2 genotype, a C→T mutation at amino acid 158, or to the apoE4 genotype, with a T→C mutation at amino acid 112. The chimeraplasts were designed based on the E2→E3 chimeraplast published by Tagalakis *et al.* [191] and were termed E3→E2 and E3→E4 respectively. ***Fig. 5.1*** shows the sequence of apoE in the genomic target region and the sequence of the E3→E2 and E3→E4 chimeraplasts. The E3→E2 chimeraplast was already established to be active in experiments previously performed by Dr. Zahra Mohri in our laboratory, targeting HepG2 cells amongst other cells, with conversion demonstrated by RFLP at concentrations as low as 200 nM of similar efficiency as the E2→E3 chimeraplast.

For the chimeraplast uptake studies, a similar chimeraplast was used, bearing an identical sequence to E3→E2, with the addition of fluorescein at the 3′ end of the oligonucleotide (termed FE3→E2). The fluorescence would enable a study of chimeraplast uptake into the nucleus, measured by flow cytometry counting of fluorescent nuclei. All three chimeraplasts were synthesized by MWG-Biotech. Oligonucleotides were delivered in powder form and suspended in nuclease-free distilled water to a concentration of 100 µM, gently mixed, then batched into small aliquots and stored at -80°C.

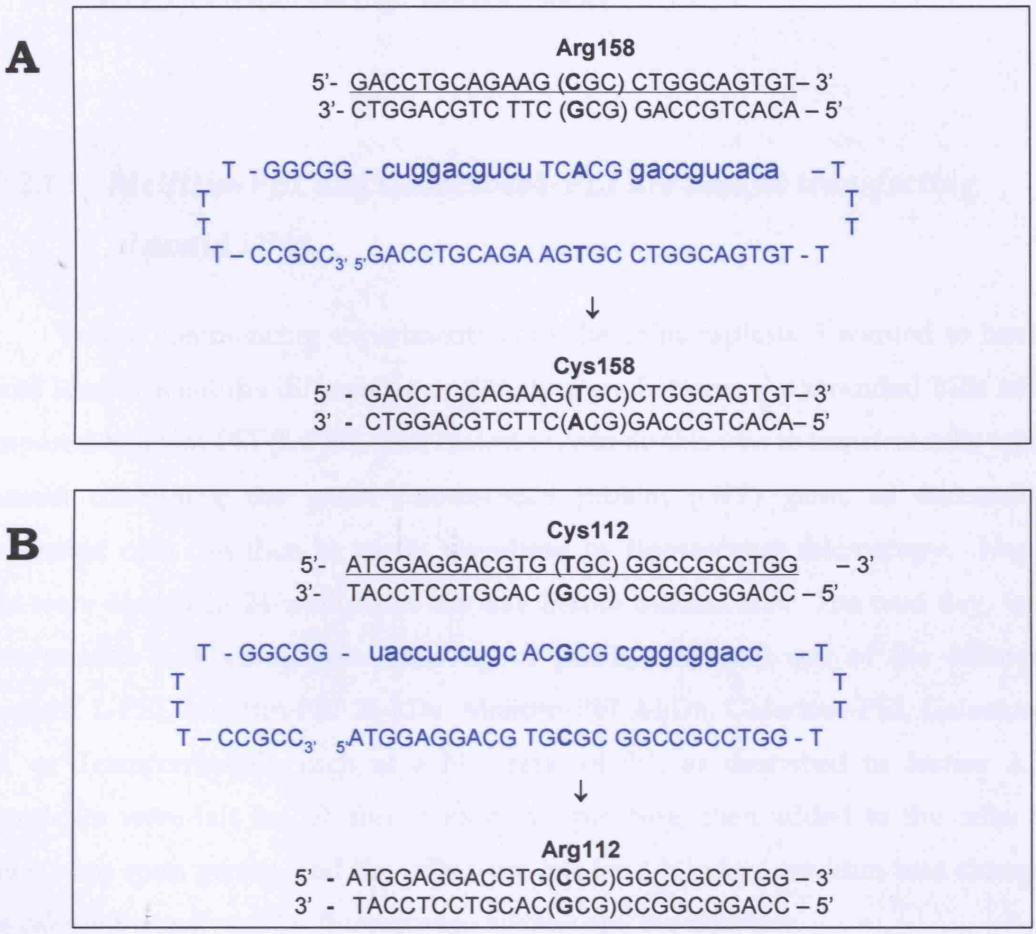

Figure 5.1: Sequence of the E3→E2 and E3→E4 chimeraplasts.

The chimeraplasts are 68-mer oligonucleotides (in blue) that can fold onto themselves using the two gene-specific regions that are homologous to the underlined area of the human apoE sequence (in black). The 5′ end of the chimeraplast is the complementary region to the target DNA. Further past the first polyT loop are two 2′-O-methyl RNA regions (lowercase) separated by the DNA mutator region, with the required nucleotide change (bold) at its centre. At the 3′ end is the GC clamp. ***A****: The E3→E2 chimeraplast, where the C→T mutation changes an arginine to a cysteine.* ***B****: The E3→E4 chimeraplast, where the reverse occurs at a different gene location: T→C mutation resulting in a change from cysteine to arginine.*

5.2.2 PRELIMINARY ANALYSIS OF TRANSFECTION REAGENT EFFICIENCY USING FLUORESCENCE MICROSCOPY

5.2.2.1 *Melittin-PEI and Galactose4-PEI are best at transfecting plasmid DNA*

Before commencing experiments with the chimeraplasts, I wanted to have a visual idea of what the differences in activity were between the modified PEIs when compared to linear PEI (L-PEI). The easiest way to do this was to transfect cells with a plasmid containing the green fluorescence protein (*GFP*) gene, as successfully transfected cells can then be easily visualised by fluorescence microscopy. HepG2 cells were seeded in 24-well plates the day before transfection. The next day, wells were treated with complexes made up of pGFP, HBS and one of the following reagents: L-PEI, Melittin-PEI 25-kDa, Melittin-PEI 2-kDa, Galactose-PEI, Galactose4-PEI, or Transferrin-PEI, each at a N:P ratio of 5:1, as described in *Section 2.3.5.* Complexes were left for 20 min at room temperature, then added to the cells, the plates were spun gently, and the cells were left for 4 h before medium was changed. The cells were analysed by fluorescence microscopy the next day.

Fig. 5.2 shows that for the 6 reagents used for transfecting plasmids, clear differences were visible in numbers of fluorescent cells. Melittin-PEI 25-kDa (Mel-PEI/25) and Galactose4-PEI (Gal4-PEI) appear to be the most efficient delivery agents, with L-PEI following behind. Melittin-PEI 2-kDa (Mel-PEI/2), Galactose-PEI (Gal-PEI) and Transferrin-PEI (Tf-PEI) were the weakest reagents.

5.2.2.2 *Linear PEI is superior to branched PEI at delivering plasmid DNA*

The only non-conjugated reagent to be examined other than L-PEI was an 800-kDa branched PEI (B-PEI). In general, polymers of such a large size are regarded as having a lower transfection efficiency than reagents under 70-kDa [249], but all experiments were previously conducted on plasmid DNA. I began here by verifying these findings and then looking at whether chimeraplast transfections showed similar

results. Again, HepG2 cells were transfected 24 h after seeding, with complexes made of pGFP, HBS and either L-PEI or B-PEI, which were allowed to form for 20 min before being added to the cells. Cells were then spun as before, incubated for 4 h, and after changing the medium, cells were observed the next day. Fluorescence microscopy clearly showed a larger number of fluorescent cells in the well transfected with L-PEI than with B-PEI (***Fig. 5.3A***).

5.2.2.3 *Large DNA/PEI aggregates result in better gene delivery than smaller particles*

It has been shown that when certain solutions are used to create DNA/PEI complexes the result is small particles, while others tend to form large aggregates. This can have an effect on delivery efficiency [250]. When HEPES is used for this purpose, it creates small particles of DNA and PEI, while HEPES buffered saline (HBS) creates larger complexes. In parallel to the experiment described in *Section 5.2.2.2*, I looked at the same factors but changed the HBS to HEPES to see if a difference would be visible. ***Fig. 5.3B*** shows that using HBS clearly results in a better transfection, therefore proving that for plasmid transfections larger aggregates result in higher uptake of DNA/PEI complexes. For this reason, it was assumed that chimeraplast DNA/PEI particles act in the same way and all further transfection experiments in this chapter used HBS as complexing buffer.

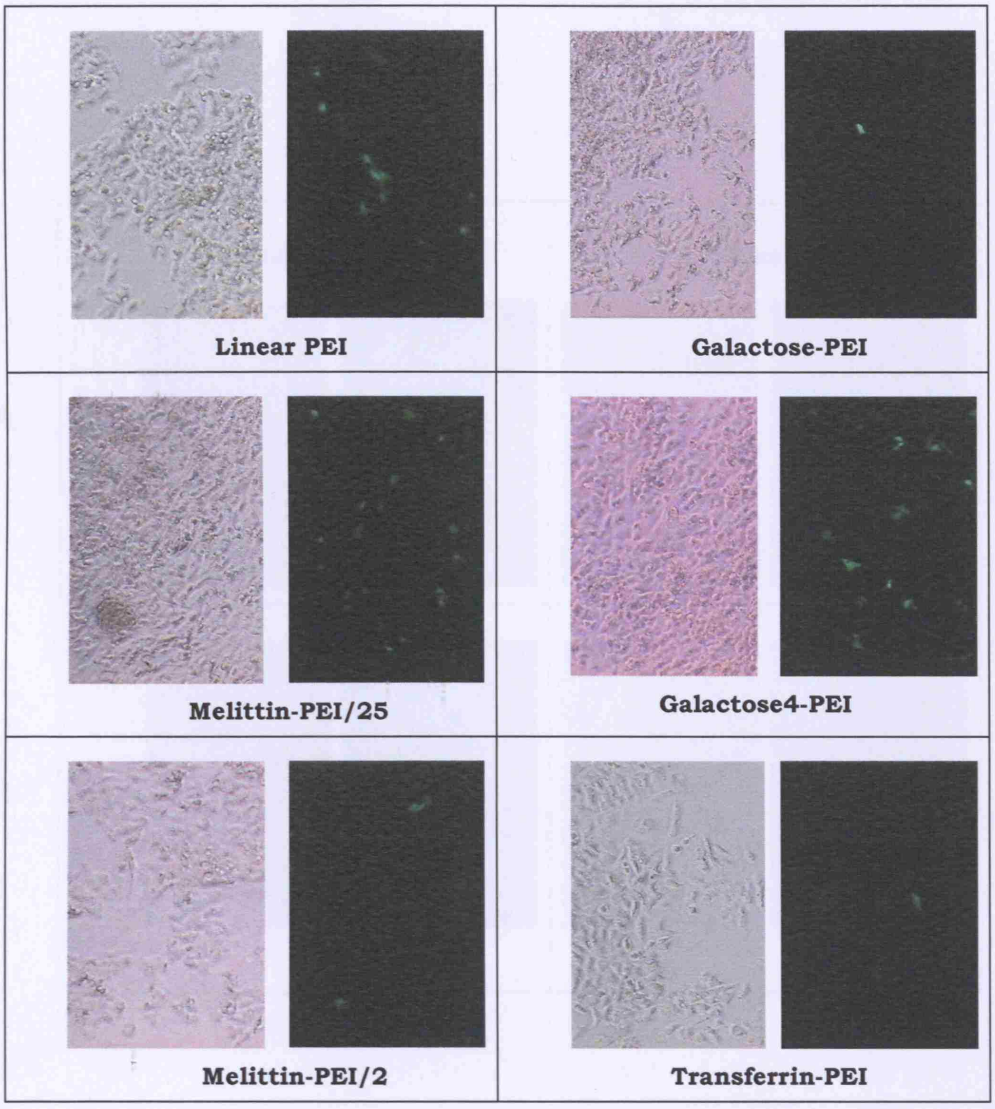

Fig. 5.2: HepG2 cells transfected with pGFP and various PEI-based reagents.

DNA/PEI complexes were made by mixing 1.5 μg pGFP, HBS and one of the 6 reagents (N:P ratio 5:1), allowing them to incubate for 20 min before addition to the cells. Plates were spun at 275 g for 3 min then left for 4 h before medium was changed. Cells were examined by phase-contrast microscopy (left image of each panel) and fluorescence microscopy with incident blue light of 465-495 nm wavelength (right image of each panel) both at 20 X magnification. Melittin-PEI/25 and Galactose4-PEI show the best transfection efficiency of the 6, followed by linear PEI. Melittin-PEI/25: 25-kDa, Melittin-PEI/2: 2-kDa.

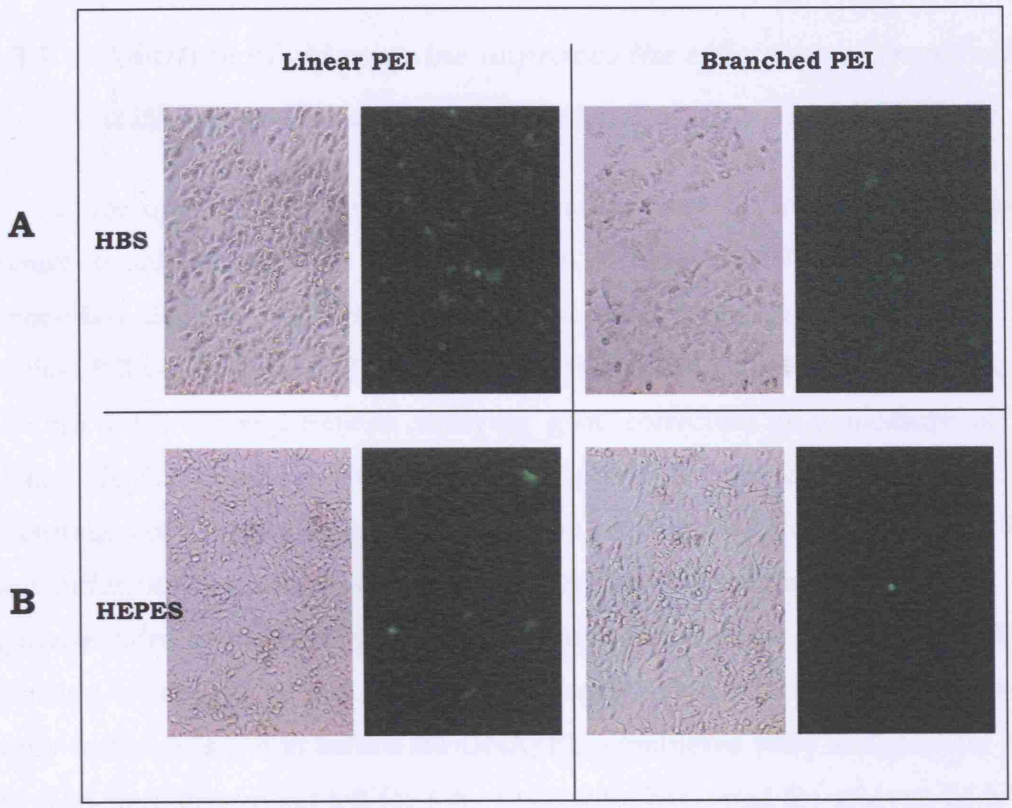

Fig. 5.3: Effect of branched PEI and complexing buffer on transfection of HepG2 cells with pGFP.

DNA/PEI complexes were formed by mixing 1.5 μg pGFP with either linear PEI or branched PEI (N:P ratio 5:1), and in each case with either HBS or HEPES. The complexes were left to form for 20 min, then added to the cells and the plates were spun at 275 g for 3 min before being left for 4 h, after which the medium was changed. Phase-contrast and fluorescence microscopy images were captured 24 h later. Panel ***A*** *shows that in HBS, linear PEI is a superior transfection reagent. When compared to panel* ***B****, it is clear that complexing the DNA and PEI with HBS results in more successful gene delivery, regardless of which of the two transfection reagents is used.*

5.2.3 ANALYSIS OF TRANSFECTION REAGENT EFFICIENCY BY RFLP

5.2.3.1 *Addition of chloroquine improves the efficiency of transfection with linear PEI and is also better than branched PEI alone*

Chloroquine is known to enhance transfections by inactivating lysosomal enzymes in order to decrease the degradation of transfected DNA [242]. The first chimeraplast delivery conditions I examined dealt with the unconjugated PEIs: branched PEI versus linear PEI, and L-PEI with or without chloroquine. As described in *Section 2.3.5*, for experiments studying gene correction as a measure of gene delivery, HepG2 cells were seeded in 24-well plates 24 h prior to transfection. The concentration of E3→E2 chimeraplast used was 150 nM, intentionally low in order to detect differences between the activities of the various reagents in question. The oligonucleotides were combined with HBS and either linear or branched PEI by incubating for at least 10 min. For the chloroquine studies, the reagent was added directly to the cells 5 min before the DNA/PEI complexes were added. The plates were then spun gently and left for 6 h. Cells were harvested for analysis 24 h later. DNA was then extracted as explained in *Section 2.3.7* followed by RFLP, as described in *Section 2.1.3*.

Electrophoresis of the final restriction digest products showed a weak but visible conversion from apoE3 to apoE2 indicated by the appearance of a diagnostic 83 bp band for the transfections using both chloroquine and L-PEI, whereas conversions for both L-PEI alone and B-PEI alone were undetectable (***Fig. 5.4***).

5.2.3.2 *Melittin-PEI 25-kDa is more efficient than melittin-PEI 2-kDa*

Section 5.2.2.2 mentioned that there can be a difference in transfection efficiency based on the size of the polymer used [249]. I was provided with two sizes of PEI linked to melittin: 2-kDa and 25-kDa. I transfected HepG2 cells under the same conditions as before, with the E3→E2 chimeraplast and each of these PEI conjugates to determine whether indeed there was any difference in gene delivery. ***Fig. 5.5A*** shows the RFLP result, which indicated that the larger of the two molecules (25-kDa)

delivered more DNA into the cell, based on the stronger conversion indicated by the 83 bp band.

5.2.3.3 *Transfections with melittin-PEI can be improved by mixing with linear PEI*

In order to evaluate whether the conversion efficiency of Melittin-PEI 25-kDa could be improved further, I tried combining it in equal proportions with L-PEI. HepG2 cells were prepared as before and complexes made up with the E3→E2 chimeraplast, HBS and Mel-PEI alone or 1:1 with L-PEI. Incubation times were as before and RFLP analysis after 24 h. Results show that although there is a conversion visible for both conditions, a stronger one is apparent for the Mel-PEI/L-PEI combination (***Fig. 5.5B***).

5.2.3.4 *Receptor-specific conjugated PEIs are of value when targeting hepatic cells*

Certain cells can be targeted by using receptors specific to that cell line. Hepatocytes carry the asialoglycoprotein receptor that can bind with certain sugars and glycoproteins, such as galactose [218], and therefore delivering DNA specifically to the liver can be accomplished by using a reagent such as Galactose-PEI. The transferrin receptor, a glycoprotein whose function is to mediate cellular uptake of iron from transferrin [251], is expressed by all human cells and thus transferrin-PEI (Tf-PEI) can be used to improve gene delivery by utilising this receptor as a gateway into the cell.

HepG2 cells were targeted with Galactose-PEI (where 5% of PEI nitrogens are modified by galactose), Galactose4-PEI (where 5% of PEI nitrogens are modified by linear tetragalactose) or Transferrin-PEI. Cells and complexes were prepared as for the previous experiments, again at a N:P ratio of 5:1, and after incubation for 6 h with the complexes, cells were analysed for gene conversion 24 h later. In comparing the three reagents, RFLP did not detect any conversion with Gal-PEI, while both Gal4-PEI

and Tf-PEI succeeded in delivering enough chimeraplast into the cell to create the required mutation at a level high enough for detection by RFLP (***Fig. 5.6***).

Another chimeraplast was available to use in our laboratory, also targeting the apolipoprotein E gene, but converting the apoE3 genotype to apoE4 (E3→E4 chimeraplast; see Fig. 5.1). Like the LCAT chimeraplasts, this oligonucleotide did not produce conversions using the standard protocol, and therefore enhanced transfection conditions were attempted. HepG2 cells were targeted with this chimeraplast using either Gal4-PEI on its own or a combination of Gal4-PEI and L-PEI, as a mixed reagent appeared to produce a better result when tried with melittin-PEI (see *Section 5.2.3.3*). The RFLP analysis (see Fig. 2.3 for restriction pattern) indicates that although Gal4-PEI on its own did not produce a gene conversion, in combination with L-PEI the conversion was successful. Even though the gel shows a weak conversion at 600 nM of chimeraplast, the result was confirmed by sequencing, where the T→C mutation is evident by the double peak (***Fig. 5.7***).

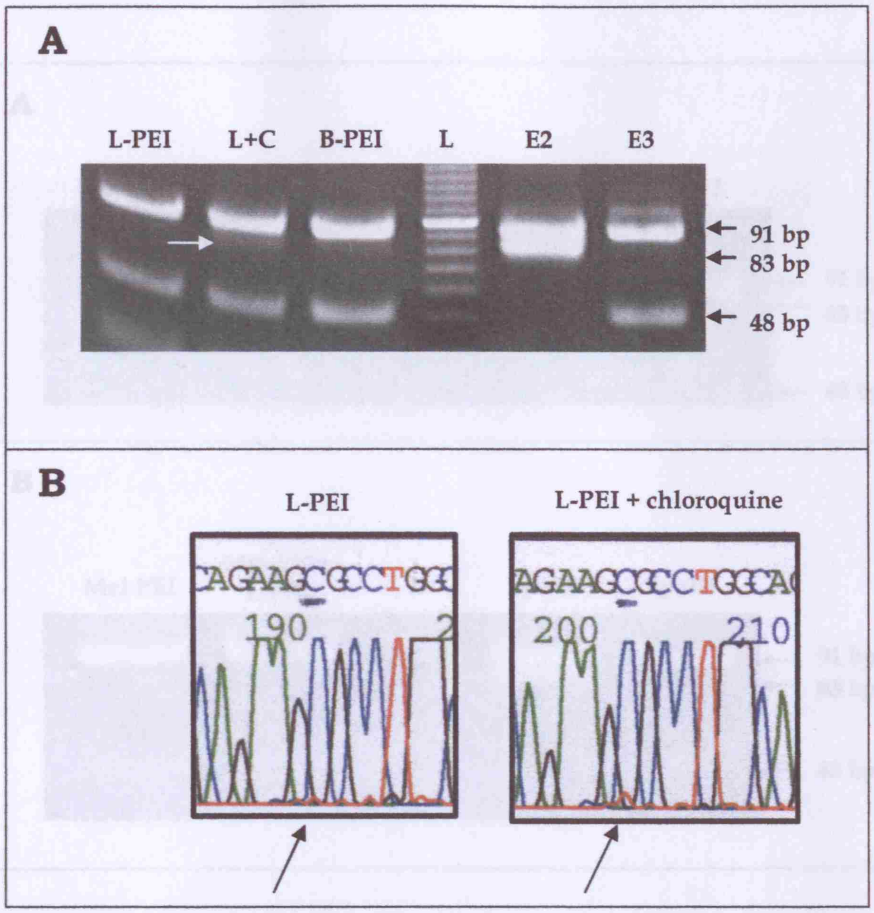

Fig. 5.4: RFLP analysis of HepG2 cells transfected with the E3→E2 chimeraplast using L-PEI +/- chloroquine, or B-PEI.

Transfection complexes were made of 150 nM chimeraplast, HBS, and L-PEI or B-PEI (N:P=5:1), and incubated for at least 10 min. To add chloroquine to L-PEI transfected cells, the reagent was added to wells 5 min before the DNA/PEI complexes to a final concentration of 100 μM. The cells were spun at 275 g for 3 min then left for 6 h before the medium was changed. Cells were analysed 24 h later. Results are shown from a single experiment. ***A****: RFLP result showing a very weak conversion from apoE3 to apoE2 (white arrow) only when chloroquine was added to cells before transfection with L-PEI and no visible conversion for L-PEI or B-PEI alone.* ***B****: Confirmation of the RFLP result by sequencing. The C→T mutation is only visible for L-PEI combined with chloroquine (black arrows). L-PEI: linear PEI, L+C: linear PEI and chloroquine, B-PEI: branched PEI, L: 10 bp ladder, E2: apoE2 control, E3: untreated cells.*

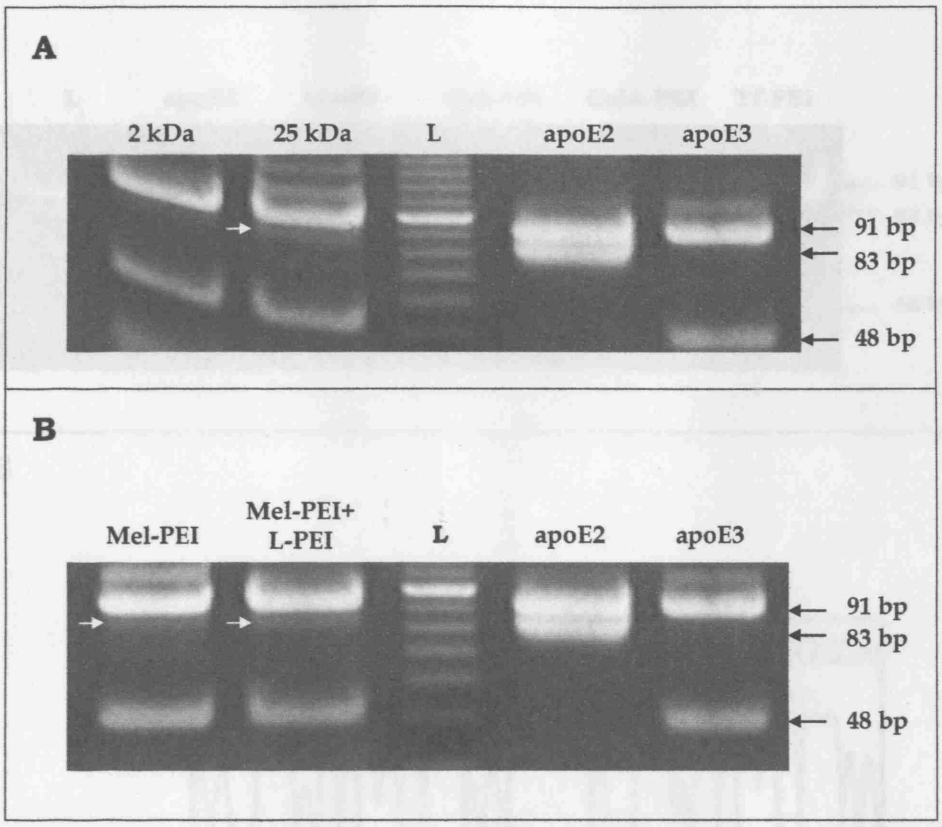

Fig. 5.5: Transfection of HepG2 cells with theE3→E2 chimeraplast using Melittin-PEI.

Transfection complexes were made up of 150 nM E3→E2 chimeraplast, HBS, and either melittin-PEI 2-kDa, melittin-PEI 25-kDa, or melittin-PEI 25-kDa in a 1:1 combination with L-PEI. All complexes had a final N:P ratio of 5:1 and were incubated for at least 10 min. Cells were spun at 275 g for 3 min and treated for 6 h, then harvested for analysis 24 h later. ***A****: When comparing melittin-PEIs of different molecular weights, the larger of the two appears to give a higher conversion, as indicated by the appearance of the 83 bp band (white arrow).* ***B****: Both melittin-PEI 25-kDa alone and combined with L-PEI can deliver enough DNA to cause a conversion, but it appears that the addition of L-PEI enhances the effect, as the 83 bp band appears stronger (compare white arrows). Results are from a single experiment. L: 10 bp ladder, apoE2: apoE2 control, apoE3: untreated cells.*

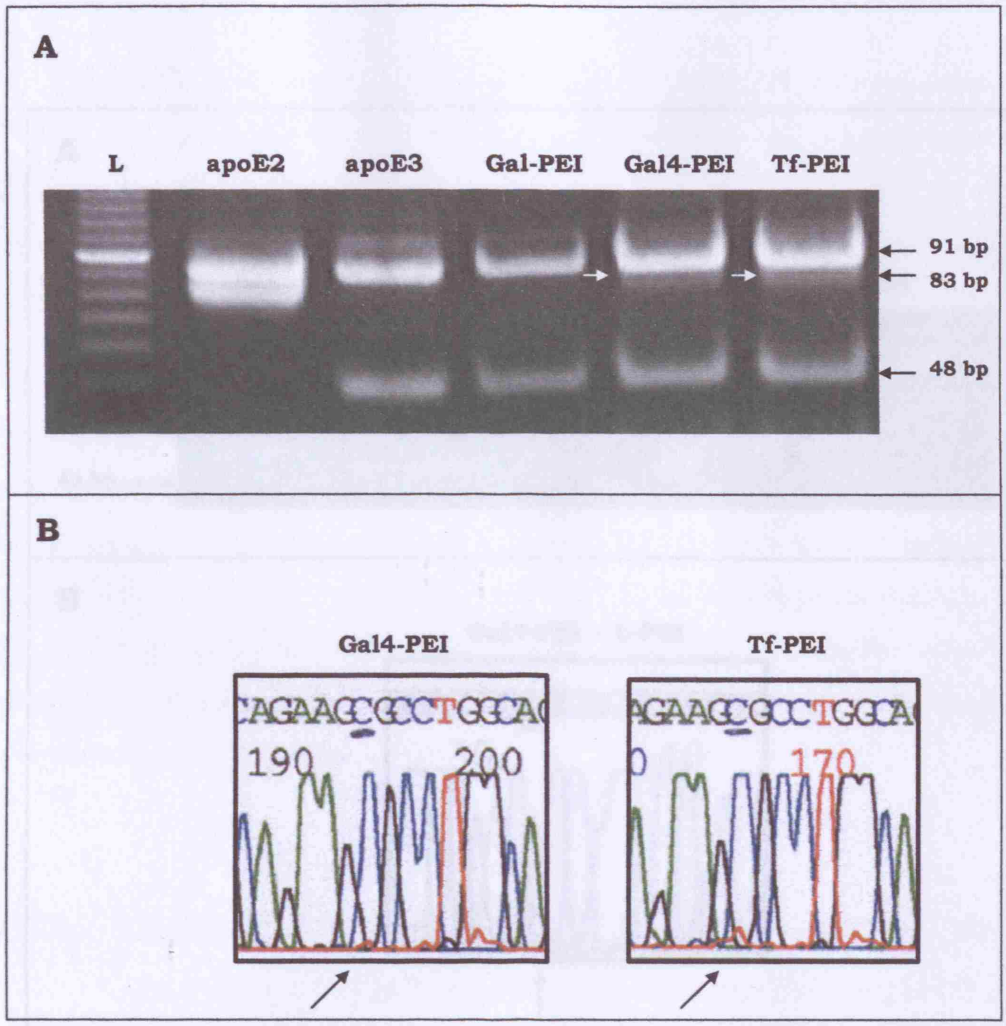

Fig. 5.6: HepG2 cells transfected with receptor-specific conjugated PEIs.

DNA/PEI complexes were composed of 150 nM E3→E2 chimeraplast, HBS, and either Gal-PEI, Gal4-PEI or Tf-PEI at an N:P ratio of 5:1. Complexes were allowed to form for at least 10 min. Cells were transfected with the complexes, followed by centrifugation at 275 g for 3 min and incubation for 6 h. Analysis was begun 24 h after transfection. ***A****: RFLP analysis showing successful gene conversion using Gal4-PEI and Tf-PEI, indicated by the appearance of the 83 bp band (white arrows), but not with Gal-PEI. L: 10 bp ladder, apoE2: apoE2 control, apoE3: untreated cells.* ***B****: Sequencing result showing small T peaks (black arrows) confirming the C→T conversion for the transfections using Gal4-PEI and Tf-PEI. These are results of a single experiment.*

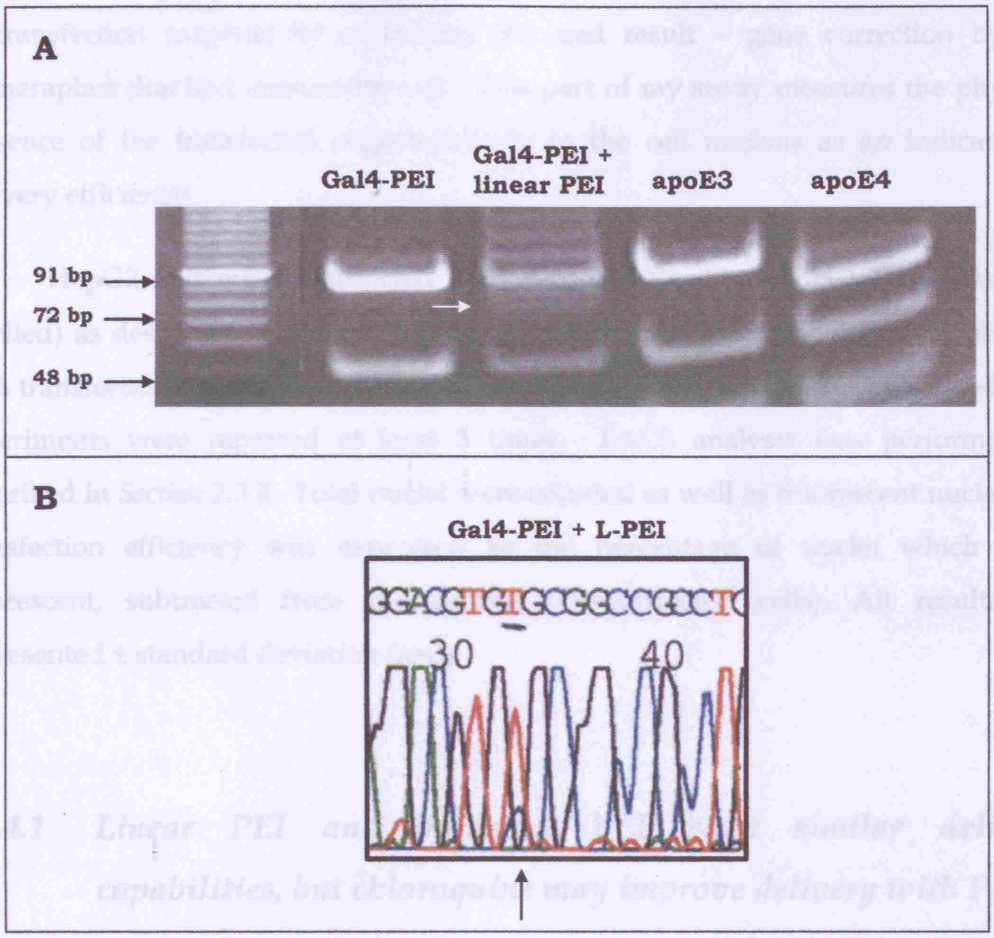

Fig. 5.7: RFLP analysis of HepG2 transfection with Galactose4-PEI in combination with L-PEI.

*DNA/PEI complexes were composed of 600 nM E3→E4 chimeraplast, HBS, and either Gal4-PEI or a 1:1 combination of Gal4-PEI with L-PEI at an N:P ratio of 5:1 and left to form for 10 min. The complexes were added to the cells, the plates centrifuged at 275 g for 3 min, and incubated for 6 h. Cells were harvested for analysis 24 h later. The gel shows no visible conversion when using galactose4-PEI alone, but the appearance of the diagnostic 72 bp band for the transfection where L-PEI was also present (**A**). This result was confirmed by sequencing, which shows the nucleotide conversion from T→C (**B**). apoE3: untreated cells, apoE4: apoE4 control. These results represent a single experiment.*

5.2.4 ANALYSIS OF TRANSFECTION REAGENT EFFICIENCY BY FACS

The analysis of transfection efficiency conducted by RFLP assessed the ability of transfection reagents by examining the end result - gene correction by the chimeraplast that had entered the cell. This part of my study measures the physical presence of the transfected oligonucleotide in the cell nucleus as an indicator of delivery efficiency.

HepG2 cells were transfected with the FE3→E2 chimeraplast (3′ fluorescein-labelled) as described in *Section 2.3.8*, in 6-well plates. Following 6 h of incubation with transfection complexes, cells were immediately collected and nuclei isolated. All experiments were repeated at least 3 times. FACS analysis was performed as described in *Section 2.3.9*. Total nuclei were counted as well as fluorescent nuclei and transfection efficiency was expressed as the percentage of nuclei which were fluorescent, subtracted from the control (untransfected cells). All results are represented ± standard deviation (n=3).

5.2.4.1 *Linear PEI and branched PEI have similar delivery capabilities, but chloroquine may improve delivery with PEI*

HepG2 cells were transfected either with L-PEI or branched PEI, or were pretreated with chloroquine and transfected with L-PEI. Quantitative measurement of nuclei by FACS showed that L-PEI and branched PEI delivered oligonucleotides successfully to approximately the same number of nuclei (11.7 ± 0.7 % and 11.9 ± 4.8 % fluorescent nuclei, respectively) but that the addition of chloroquine to cells before transfection raised delivery to the nucleus (17.6 ± 7.2 % fluorescent nuclei), although neither of these results showed statistical significance as calculated using Student's *t*-test. The results are shown in *Fig. 5.8*.

5.2.4.2 *The transfection efficiency of Melittin-PEI can is improved by mixing with linear PEI*

The next delivery vehicle to be examined was melittin-PEI, the reagent conjugated to the peptide melittin, known for its ability to increase transfection efficiency by up to 30% by aiding intracellular travel of DNA to the nucleus [242]. HepG2 cells were transfected as before, with either Melittin-PEI 25-kDa alone as transfection reagent, or a 1:1 combination of Melittin-PEI and L-PEI. ***Fig. 5.9*** shows that L-PEI delivered DNA to as many nuclei as Melittin-PEI (11.4 ± 0.7 % compared to 11.7 ± 7.0 % fluorescent nuclei, though not statistically significant), but when the two reagents are combined the result is a 27% increase in nuclear delivery (16 ± 1.8 % compared to 11.7 ± 7.0 % fluorescent nuclei, $P<0.05$).

5.2.4.3 *Galactose4-PEI is superior to linear PEI for transfecting hepatic cells*

It has been shown that there is value in using transfection reagents carrying ligands that specifically bind cell-surface receptors in order to increase DNA uptake into the cell [238, 239, 240]. Gal-PEI and Gal4-PEI were used to transfect HepG2 cells, as was described earlier (*Section 2.3.8*). FACS analysis showed that Gal-PEI was not as effective as L-PEI (9.4 ± 1.6 % compared to 11.7 ± 0.7 % transfected nuclei, $P<0.05$), but Gal4-PEI delivered 24% more chimeraplast to nuclei than L-PEI (15.4 ± 0.1 % compared to 11.7 ± 0.7 % transfected nuclei, $P<0.05$), and 39% more than Gal-PEI ($P<0.05$), shown in ***Fig. 5.10***.

As combining Melittin-PEI with L-PEI produced a positive effect on delivery, this was also attempted with Gal4-PEI. The reagent was mixed 1:1 with L-PEI and used to transfect HepG2 cells. The result was to raise the transfection efficiency even further to 17.7 ± 1.5 % fluorescent nuclei (***Fig. 5.10***), or 34% higher than L-PEI alone ($P<0.05$). The specificity of Gal4-PEI for the asialoglycoprotein receptor was then tested by repeating the L-PEI and L-PEI + Gal4-PEI experiments in CHO cells, as they do not express this receptor. Here, FACS analysis showed a greater transfection activity in CHO cells for L-PEI alone than for the Gal4-PEI + L-PEI combination (13.2 ± 1.2 % compared to 11.6 ± 6.35 % fluorescent nuclei), as demonstrated in ***Fig. 5.11***. The presence of Gal4-PEI appears to have increased delivery of chimeraplast in

HepG2 cells (17.7 ± 1.5 % in HepG2 cells compared with 11.6 ± 6.35 % in CHO cells), whereas when added to CHO cells delivery was slightly reduced (13.2 ± 1.2 % L-PEI alone and 11.6 ± 6.35 % with Gal4-PEI), although it is not possible to interpret these findings as they were not statistically significant.

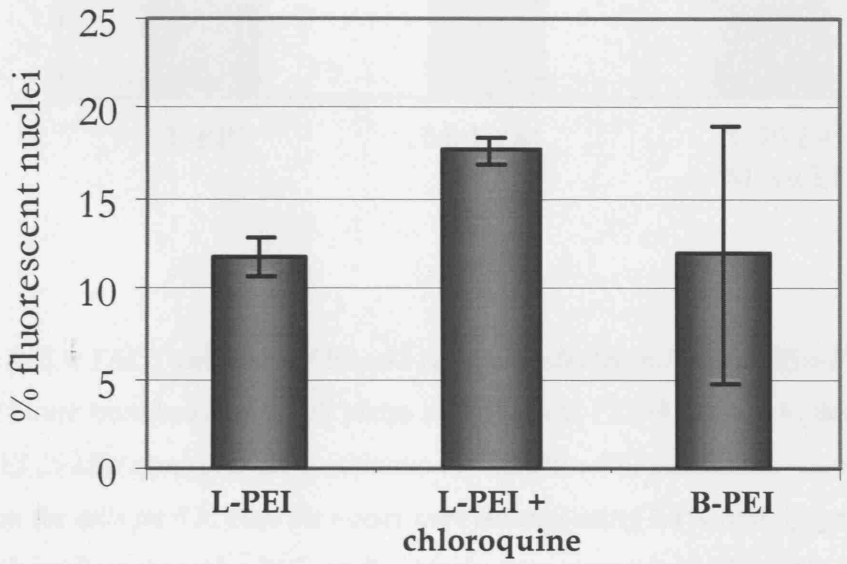

Fig. 5.8: FACS analysis of HepG2 cells transfected with linear and branched PEI. *Cells were transfected in 6-well plates with 200 nM FE3→E2 chimeraplast and either L-PEI or B-PEI at an N:P ratio of 5:1. Complexes were left to form for at least 10 min. Additional cells were treated with chloroquine and received a final concentration of 100 μM 5 min before addition of transfection complexes. After 6 h incubation, cells were harvested and nuclei isolated using 0.1% (v/v) Igepal CA-630 in PBS on ice by pulling through a 26G needle. Nuclei were suspended and fixed in ice-cold 50% (v/v) ethanol and counted using FACS. Transfection efficiency is expressed as the percentage of fluorescent nuclei. Mean percentage values are from triplicate experiments ± SD. L-PEI used in conjunction with chloroquine transfected the most nuclei, although results were not significant when assessed by Student's t-test (P=0.12). L-PEI: linear PEI, B-PEI: branched PEI.*

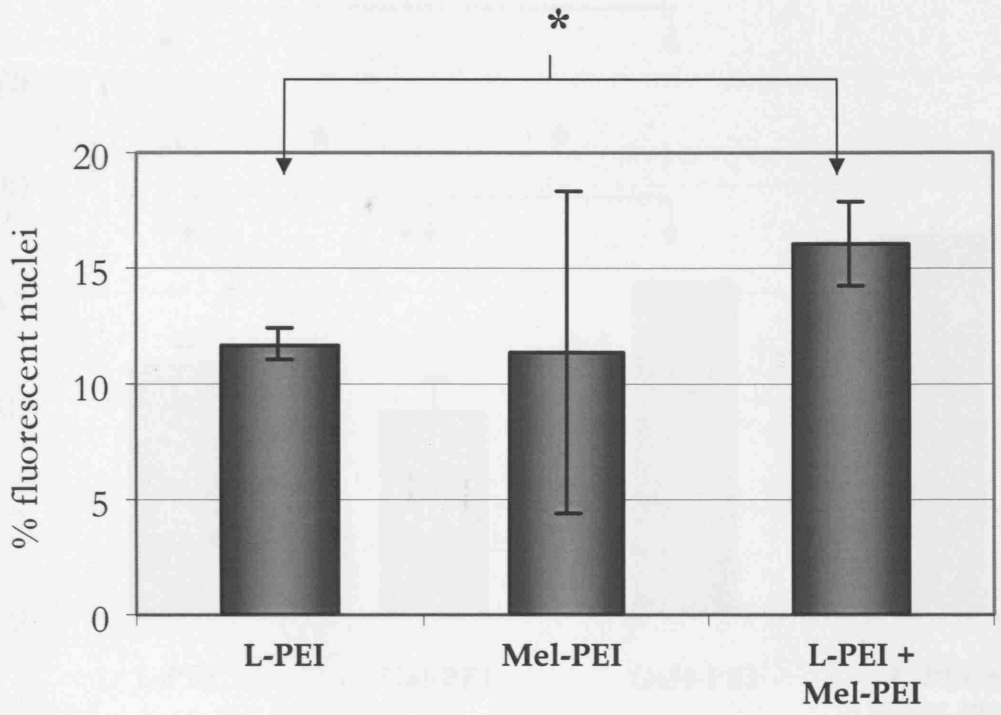

Fig. 5.9: FACS analysis of HepG2 cells transfected with Melittin-PEI.

*HepG2 cells were transfected in 6-well plates with 200 nM FE3→E2 chimeraplast and either Melittin-PEI 25-kDa alone or a 1:1 combination of Melittin-PEI and L-PEI. Complexes were incubated on the cells for 6 h, then the nuclei were isolated using 0.1% (v/v) Igepal CA-630 in PBS on ice by pulling through a 26G needle. Nuclei were suspended and fixed in ice-cold 50% (v/v) ethanol and counted using FACS. Transfection efficiency is expressed as the percentage of fluorescent nuclei. Mean percentage values are from triplicate experiments ± SD. The combination of L-PEI with Melittin-PEI resulted in a more efficient transfection when compared to L-PEI alone (*P<0.05 as assessed by Student's t-test). L-PEI: linear PEI, Mel-PEI: Melittin-PEI.*

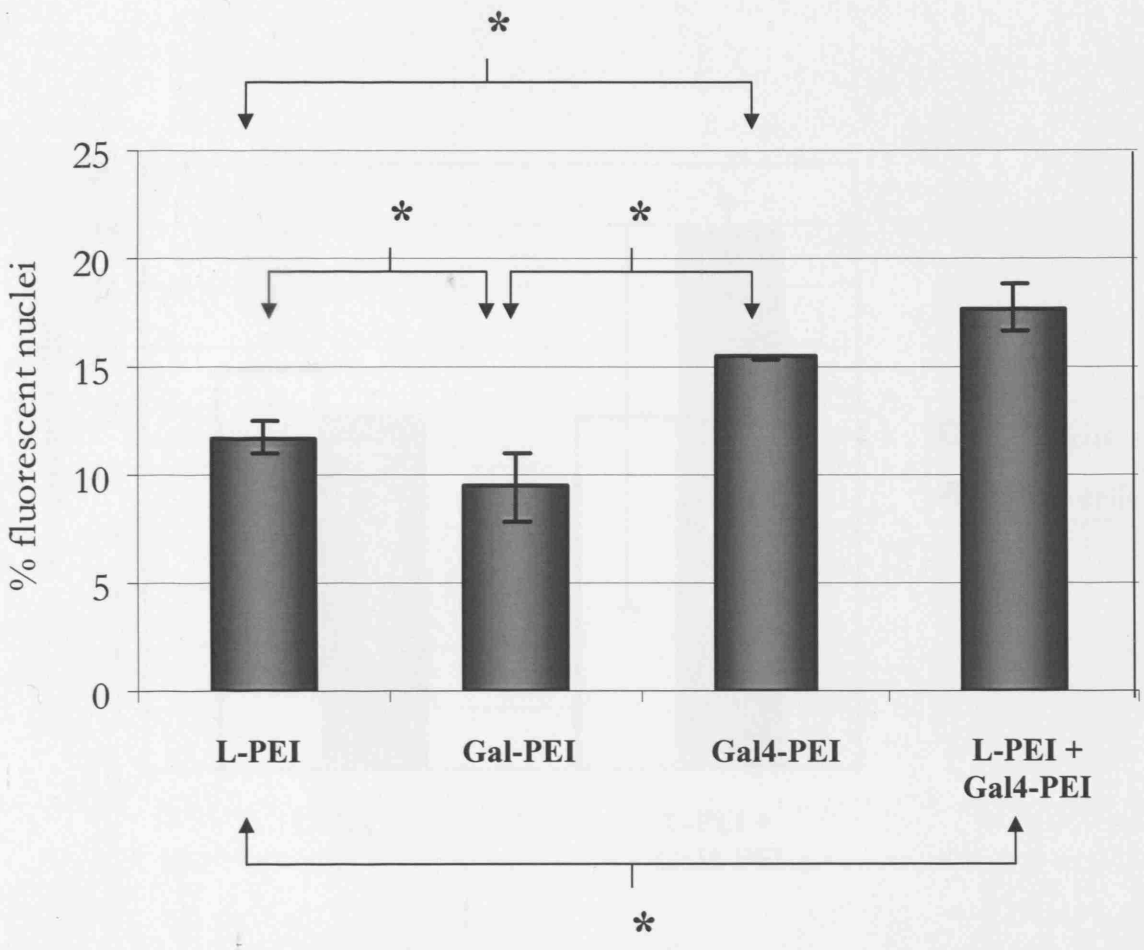

Fig. 5.10: FACS analysis of HepG2 cells transfected with reagents using the asialoglycoprotein receptor.

Transfection complexes were made up of 200 nM FE3→E2 chimeraplast and either Galactose-PEI, Galactose4-PEI, or a 1:1 combination of L-PEI and Galactose4-PEI. Complexes were incubated for 10 min, then incubated with HepG2 cells for 6 h. The cells were then harvested and nuclei isolated using 0.1% (v/v) Igepal CA-630 in PBS on ice by pulling through a 26G needle. Nuclei were suspended and fixed in ice-cold 50% (v/v) ethanol and counted using FACS. Transfection efficiency is expressed as the percentage of fluorescent nuclei. Mean percentage values are from triplicate experiments ± SD. These results show that compared to L-PEI, Gal4-PEI is 24% more efficient as a delivery agent for chimeraplasts, and that the addition of L-PEI to Gal4-PEI further improves delivery by 10%. Also, the use of Gal4-PEI rather than Gal-PEI can raise the transfection efficiency by 39% ($P<0.05$ as assessed by Student's t-test). L-PEI: linear PEI, Gal-PEI: Galactose-PEI, Gal4-PEI: Galactose4-PEI.*

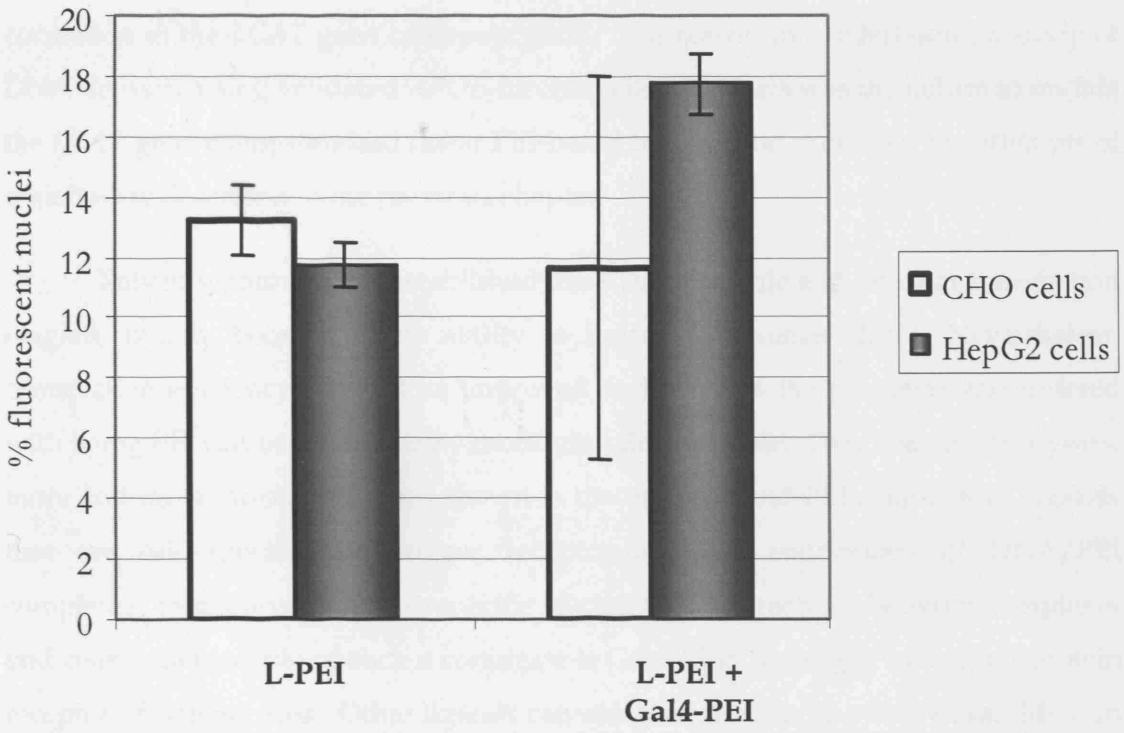

Fig. 5.11: Comparison of Galactose4-PEI transfections of CHO and HepG2 cells by FACS analysis.

CHO cells, that do not express the asialoglycoprotein receptor, were transfected as for HepG2 cells using 200 nM FE3→E2 chimeraplast and either L-PEI alone or a 1:1 combination with Gal4-PEI. Complexes were incubated with the cells for 6 h, then harvested for nuclei isolation using 0.1% (v/v) Igepal CA-630 in PBS on ice by pulling through a 26G needle. Nuclei were suspended and fixed in ice-cold 50% (v/v) ethanol and counted using FACS. Transfection efficiency is expressed as the percentage of fluorescent nuclei. Mean percentage values are from triplicate experiments ± SD. The combination of L-PEI and Gal4-PEI resulted in the delivery of chimeraplasts to more HepG2 cells than CHO cells, although values were not significant when assessed by Student's t-test. L-PEI: linear PEI, Gal-PEI: galactose-PEI, Gal4-PEI: galactose4-PEI.

5.3 DISCUSSION

The experiments described in this chapter were aimed at improving the delivery of chimeraplasts in the hope of identifying a way to successfully direct gene correction in the *LCAT* gene of hepatic cells. The reason for undertaking a study of DNA delivery using validated *APOE*-directed chimeraplasts was the failure to mutate the *LCAT* gene using standard linear PEI-based transfection protocols, the attempts of which were described in the previous chapter.

Polyethylenimine has established itself as a versatile and efficient transfection reagent, mainly because of its ability to buffer endosomes [228]. Nevertheless, transfection efficiency can still be improved and some of the problems encountered with using PEI can be overcome by modifying the molecule. Over the past few years, more and more interest has been shown in the use of ligand-PEI conjugates. Ligands that are cell specific can trigger receptor-mediated endocytosis of DNA/PEI complexes, thus preventing non-specific electrostatic interactions between complexes and cells. An example of such a conjugate is Gal-PEI to target the asialoglycoprotein receptor of hepatocytes. Other ligands can aid gene transfer in other ways. Melittin increases endosomal release of DNA, as well as improving transfer of DNA/PEI complexes to the nucleus [242].

While the interest in improving DNA delivery using PEI is considerable, the majority of studies have used plasmid DNA complexed to PEI rather than synthetic oligonucleotides. Plasmids are several kilobases in size, a great difference from RNA/DNA oligonucleotides of 68 to 80 nucleotides. For this reason, it cannot be assumed that the delivery of these molecules would be the same with PEI as for the delivery of plasmids.

My initial investigations confirmed the findings that were previously published regarding transfection of plasmids using PEI. I transfected the plasmid pGFP into HepG2 cells using a variety of PEIs and looked at the expression of green fluorescence protein under the microscope, as an indication of successful DNA/PEI uptake. Before examining the conjugated PEIs, I examined the difference between a 22-kDa linear PEI and a much bigger 800-kDa branched PEI. I found that transfection with the 800-kDa branched PEI resulted in less fluorescent cells than following

transfection with the 22-kDa L-PEI. There are two aspects to this finding: the difference in PEI size and the fact that one is linear and the other branched.

Several studies have shown that a lower molecular weight PEI transfects more efficiently than one with a higher molecular weight [232,277], though an explanation for this fact is still lacking. Godbey and colleagues [278] believe that, based on their findings, the smaller DNA/PEI particles created using smaller PEI molecules dissociate more easily, resulting in a lower transfection efficiency, but the group only tested PEIs up to 70-kDa. Thus, their findings cannot be directly related to experiments that used an 800-kDa PEI. On the subject of linear vs. branched PEI, Wightman *et al.* [277] found that in most cell lines transfected, the 22-kDa linear PEI was more efficient than the 800-kDa branched PEI. Additionally, on microscopy they found that DNA/L-PEI complexes were found close to the nucleus faster than DNA/branched PEI complexes. Nevertheless, they could not offer an explanation for these findings. Brunner *et al.* [279] compared 22-kDa L-PEI to 25-kDa branched PEI and also found L-PEI to have higher transfection efficiency, but Godbey *et al.* [274] believe that branched PEI should be more efficient at delivering DNA. They postulated that the layer of PEI surrounding the DNA is much thicker in branched PEI and able to bind more protons, as well as providing a better physical barrier to DNases, thus offering better protection to the DNA molecules it is carrying. The discrepancy between these observations is yet to be elucidated.

Using the same pGFP/PEI transfection method, I also observed by microscopy that Gal4-PEI and Mel-PEI seemed to transfect more efficiently than L-PEI, for reasons mentioned above. Finally, I examined the choice of complexing buffer. Ogris and colleagues [275] showed that complexing DNA/PEI in HBS results in large, aggregated particles, while using HEPES generates small particles. The difference in size of DNA/PEI particles formed has an influence on transfection efficiency because smaller particles are more readily taken up into the cell, while the larger aggregates tend to stick onto the cell surface. At the same time, the group found that despite reduced cellular uptake of aggregates, gene expression was higher in experiments using HBS as buffer, which parallels my observations. They explain the higher gene transfer by the fact that the total cell association of aggregates is higher than that of small particles, and by postulating that aggregates have a higher ability to lyse endosomes.

In order to study chimeraplast delivery I chose two methods - transfection with a fluorescent oligonucleotide to look at physical entry of DNA into the cell nucleus, and RFLP analysis to determine whether gene conversion had occurred as a measure of DNA entry into the nucleus. The results obtained from both these methods support each other.

Chloroquine is a chemical known to increase transfection efficiency, with a maximum activity when present at 100 μM in the culture medium of cells [267]. The proposed mechanism of action of chloroquine is by protecting DNA taken up into endosomes by neutralising acidic compartments and decreasing delivery of endosomal contents to lysosomes, thus limiting DNA degradation. Both RFLP and FACS analysis confirmed that this is the case for smaller DNA molecules as well as plasmids. Qualitative and quantitative evidence showed that treating cells with chloroquine prior to transfection using L-PEI helped protect chimeraplasts and therefore allowed them a greater opportunity to reach the nucleus than when using L-PEI alone.

Before embarking on experiments using the conjugated PEIs, I wanted to determine whether there was a difference between using 22-kDa L-PEI and 800-kDa B-PEI. Both modes of investigation suggest that L-PEI and B-PEI have similar activities when transfecting chimeraplasts, although the quantitative data acquired by FACS was not statistically significant. Therefore, it would be necessary to conduct further studies comparing the two reagents to be able to provide a definite conclusion.

Our laboratory had available Mel-PEI in two forms: one conjugated to a 25-kDa PEI, the other to a 2-kDa PEI. As mentioned earlier, it has been shown that PEIs of higher molecular weight up to 70-kDa have better transfection activities than those of lower molecular weights. It therefore makes sense that experiments performed here to compare the two reagents found that the 25-kDa Mel-PEI was a more efficient transfection reagent for both pGFP and chimeraplasts. My findings are supported by a recent study that examined PEI molecules of 2 to 750-kDa [280]. This study showed that 25 kDa linear PEI was the most efficient transfection agent, with 2-kDa PEI being unable to transfect COS-7 or CHO-K1 cells. On the other hand, Kunath *et al.* [281] showed that 5-kDa PEI has superior transfection qualities to PEI of high molecular weight, and these smaller molecules are being used to deliver small oligonucleotides [282].

The advantage of using Mel-PEI is thought to reflect the ligand's lytic activity and its ability to enhance nuclear accumulation of the transfected DNA. Ogris *et al.* [242] showed that Mel-PEI makes a significant difference to transfection of plasmid DNA. In my experiments though, I was not able to show an increased activity of Mel-PEI over that of unmodified L-PEI. This could possibly be accounted for by the fact that there may be different factors involved in chimeraplast transfections that are not currently apparent. One such factor is the interaction of DNA with PEI within the complex. One study examined the secondary structure of DNA in such a complex and found no alteration to the helical form of plasmid DNA [280]. This does not mean that a smaller oligonucleotide would react the same way. Additionally, no publications have shown use of Mel-PEI to deliver oligonucleotides, therefore their stability with this reagent may be different to that of plasmid DNA.

Wightman *et al.* [277] showed that there is a difference in aggregate formation between 22-kDa PEI and 25-kDa PEI, with 22-kDa being better at both aggregating and delivering genes. Though the reason for this difference in behaviour has not yet been elucidated, this fact led me to add L-PEI (22-kDa) to Mel-PEI (25-kDa) to determine whether the superior ability of L-PEI could enhance the effect already shown with Mel-PEI alone. Both RFLP analysis, and more impressively, FACS analysis demonstrated this to be true. This reasoning seems to hold for other conjugated PEIs also, as adding L-PEI to 25-kDa Gal4-PEI again improved transfection efficiency.

The most striking of the benefits of adding L-PEI to a conjugated reagent was shown in the transfection with the apoE3→E4 chimeraplast (Fig. 5.7). The contribution of L-PEI to the success of gene conversion in this case was unmistakable: when even high concentrations of chimeraplast (600 nM) were previously unable to accomplish gene correction using L-PEI alone, the combination of both Gal4-PEI and L-PEI showed successful action of the oligonucleotide.

The receptor-specific conjugated PEIs certainly have benefits in targeting key tissues *in vivo*, but my experiments showed that this is also the case for delivering chimeraplasts *in vitro*. For correcting the *LCAT* gene in the liver, the asialoglycoprotein receptor is an attractive target, which made the investigation of Gal-PEI seem worthwhile. Interestingly, both RFLP and FACS data showed that PEI linked to tetragalactose (Gal4-PEI) was a more efficient transfection reagent than PEI linked to just galactose (Gal-PEI). Bettinger and colleagues [283] showed that Gal4-

PEI results in the formation of small, more stable particles when complexed with plasmid DNA, and this may contribute to the improved delivery of DNA.

The conclusion of the study presented in this chapter is that overall, the best transfection conditions for delivering chimeraplasts to hepatocytes are Gal4-PEI + L-PEI > L-PEI + chloroquine > Mel-PEI + L-PEI. The results shown with the previously troublesome E3→E4 chimeraplast provide hope of possibly finding adequate delivery conditions to see success in targeting the *LCAT* gene with chimeraplasts.

Chapter 6 –

LCAT chimeraplasty at optimal conditions

6.1 INTRODUCTION

In the previous chapter, due to the problems I encountered when attempting to target the *LCAT* gene with chimeraplasts aimed at two separate sites, I tried to determine if the conditions for transfecting cells with chimeraplasts can be improved beyond the standard protocol used in our laboratory. Using a chimeraplast aimed at the *APOE* gene, I compared the transfection efficiencies of several PEI-based reagents, as well as the benefits of using chloroquine, by meauring success of gene conversion and nuclear uptake of DNA/PEI complexes. Having established that transfection efficiency can be improved by using chloroquine and a combination of L-PEI with Gal4-PEI, I now go back to my LCAT chimeraplasts and transfect cells using these reagents. The results are presented in the first section of this chapter, but unfortunately were also negative.

My next course of action was to try to explain the discrepancy between success in targeting the *APOE* gene but failure in converting *LCAT*. I looked at the intracellular course of the transfection complexes by transfecting cells simultaneously with an ApoE chimeraplast and an LCAT chimeraplast. Again, the ApoE oligonucleotide was successful, while the LCAT one was not. My final experiment was to circumvent any problems due to ineffective delivery by microinjecting the LCAT chimeraplasts directly into cell nuclei. However, this again gave a negative result.

Following this, I studied the possibility that lack of accessibility to the gene target region was the reason for the consistent failure to accomplish gene conversion. I created two recombinant CHO cell lines containing the targeting areas of the ApoE and LCAT genes, one with both complete cDNAs, the other with a complete LCAT cDNA but just the targeting segment of ApoE cDNA. I then cotargeted these cells with both apoE and LCAT gene-converting chimeraplasts.

Finally, towards the end of my time in the lab, a single-stranded oligonucleotide constructed to create the Ser216Ala mutation became available through a collaboration with Tapestry Pharmaceuticals and I was able to do some preliminary experiments with this molecule. SSONs are all-DNA short oligonucleotides with phosphorothioate linkages at both ends and were found to have almost 4 times higher

correctional activity than chimeraplasts [198]. My results show that delivery was probably not a limiting factor to gene repair mediated by chimeraplasts, as the SSON was able to create the S216A mutation when delivered with L-PEI alone.

6.2 RESULTS

6.2.1 CHIMERAPLASTY WITH SER208ALA AND SER216A OLIGONUCLEOTIDES USING OPTIMAL TRANSFECTION CONDITIONS

Firstly, CHO-LCAT$_{WT}$ cells were transfected as described in *Section 2.3.5* with the Ser216Ala chimeraplasts, both 68-mer (first batch) and 80-mer, at a concentration of 600 nM. The transfections were performed using L-PEI and chloroquine or L-PEI and Mel-PEI (1:1). Cells were incubated with DNA/PEI complexes for 4 h, then harvested for analysis after 48 h. RFLP analysis (*Section 2.1.3*) showed that none of the conditions produced a successful conversion (***Fig. 6.1A***), which would have been evident by the appearance of two smaller bands of 76 and 68 bp.

Next, HepG2 cells were targeted with the Ser216Ala 68-mer chimeraplast at a concentration of 800 nM using L-PEI and chloroquine, L-PEI and Mel-PEI (1:1), Tf-PEI, or L-PEI and Gal4-PEI (1:1). Cells were incubated with complexes for 4 h and harvested 36 h later. RFLP analysis again showed that even at this high concentration and using more efficient transfection reagents, there was no gene correction (results not shown). Targeting in both CHO-LCAT$_{WT}$ and HepG2 cells was repeated using the Ser208Ala chimeraplast with no success at mutating the gene (***Fig. 6.1B***).

6.2.2 CO-TARGETING OF LCAT AND APOE GENES IN HEPG2 CELLS

In the last chapter, we saw that it is possible to create a mutation in the *APOE* gene using the apoE3→E2 chimeraplast. The success of this chimeraplast indicates that the molecule is both able to make its way into the nucleus and to correct the gene.

By mixing both apoE3→E2 and Ser216Ala chimeraplasts with PEI, complexes can be formed theoretically carrying both oligonucleotides. It is not certain that their intracellular path would be identical, but it would be interesting to see what mutations result.

HepG2 cells were simultaneously transfected with 400 nM apoE3→E2 chimeraplast and 400 nM Ser216Ala chimeraplast using L-PEI. Cells were incubated with complexes for 6 h, then harvested after 24 h. Analysis of the transfection showed that a conversion was detected in the apoE gene by the appearance of a weak but definite 83 bp band compared to control (***Fig. 6.2B***). On the other hand, no conversion was found in the LCAT gene, where a mutation would be detected by the presence of two bands of 87 and 68 bp (***Fig. 6.2A***), as LCAT genomic DNA follows a different RFLP analysis than LCAT cDNA (*Section 2.1.3*).

6.2.3 MICROINJECTION OF SER208ALA AND SER216ALA CHIMERAPLASTS

Though at this stage it seemed unlikely that failure to reach the nucleus was the reason behind the LCAT chimeraplasts' inability to correct the gene, the final test was to physically insert the oligonucleotides into the cell nucleus. This was done by microinjection as described in *Section 2.3.6*. Cells were seeded onto coverslips and about 100 cells injected per coverslip. Each cell received approximately 1.6×10^{-5} μg of chimeraplast. Both CHO-$LCAT_{WT}$ cells and HepG2 cells were microinjected with either Ser208Ala or Ser216Ala (68-mer) chimeraplasts. Additionally, as a positive control, HepG2 cells were also microinjected with the apoE3→E2 chimeraplast. After microinjection, the cells were left to grow for 20 days before being harvested for analysis by RFLP. ***Fig. 6.3*** shows that once again neither of the LCAT chimeraplasts mutated the gene, while the apoE chimeraplast was successful.

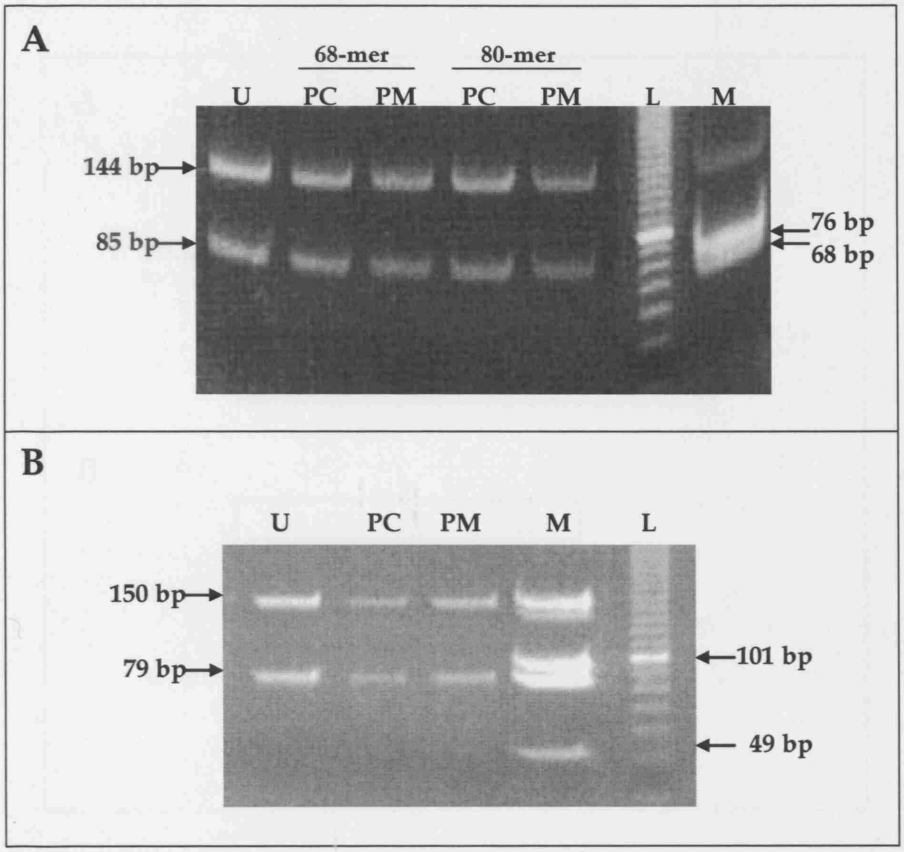

Fig. 6.1: LCAT chimeraplasty at optimal transfection conditions.

***A**: CHO-LCAT$_{WT}$ cells were transfected with 600 nM of either the 68-mer (first batch) or 80-mer Ser216Ala chimeraplast, in complex with either L-PEI (cells pre-treated with 100 μM chloroquine) or L-PEI and Mel-PEI (1:1). The amine:phosphate (N:P) ratio was 5:1. Cells were incubated for 4 h, then harvested for RFLP analysis 48 h later. Electrophoresis shows that there was no appearance of the two smaller diagnostic bands of 76 and 68 bp that would indicate the mutation from T→G, at either of the conditions and with neither of the chimeraplasts. **B**: CHO-LCAT$_{WT}$ cells were also targeted with 600 nM of Ser208Ala chimeraplast, using the same transfection conditions as above. A nucleotide conversion would have appeared as two bands of 101 and 49 bp, but again this was not detected. U: untreated cells. PC: L-PEI + chloroquine. PM: L-PEI + Mel-PEI. L: 10 bp ladder. M: CHO-LCAT$_{2M}$ cells (containing both Ser208Ala and Ser216Ala mutations) as a positive control.*

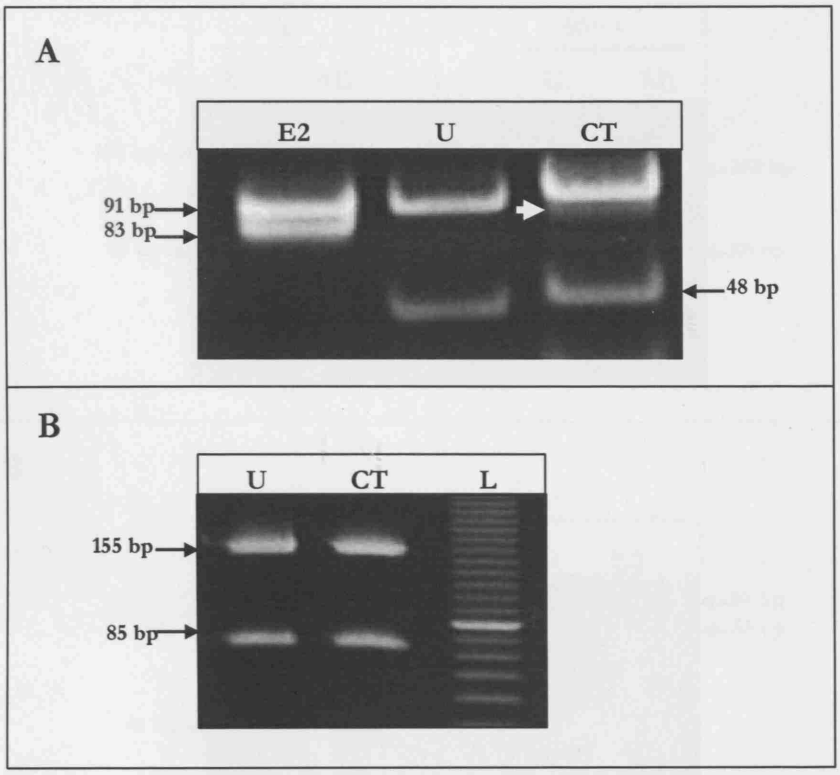

Fig. 6.2: Co-transfection of HepG2 cells with apoE3→E2 and Ser216Ala chimeraplasts.

HepG2 cells were targeted with DNA/PEI complexes composed of 400 nM apoE3→E2 chimeraplast, 400 nM Ser216Ala (68-mer, first batch) chimeraplast, 150 nM NaCl, and L-PEI at an N:P ratio of 5:1. ***A****: RFLP analysis of the apoE gene. Mutation to the apoE2 genotype is detected by the appearance of the 83 bp band (white arrow). U: untreated cells. CT: co-transfected cells. L: 10 bp ladder. E2: apoE2 genotype control.* ***B****: RFLP analysis for the LCAT gene. A mutation would result in disappearance of the 155 bp band and appearance of two smaller bands of 87 and 68 bp. No such mutation is visible here.*

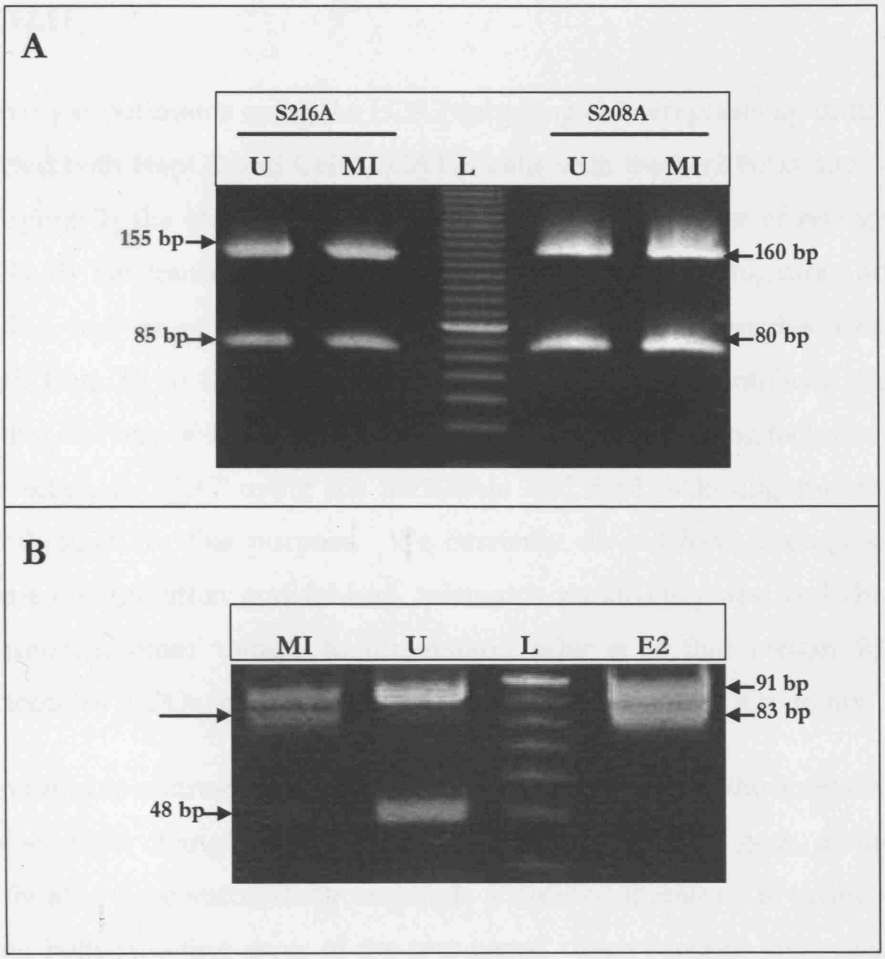

Fig. 6.3: Microinjection of LCAT and apoE chimeraplasts into HepG2 cells.

HepG2 cells were seeded onto coverslips (approximately 100 cells/coverslip) the day before microinjection. Each cell was microinjected with about 1.6 x 10^{-5} μg chimeraplast, either Ser208Ala, Ser216Ala (both first batch), or apoE3→E2. On average 100-150 cells were injected per coverslip. Cells were maintained on coverslips for 6 days, then transferred to progressively larger wells. Analysis began 20 days after microinjection. ***A****: RFLP analysis for the LCAT chimeraplasts. For the Ser216Ala (S216A) mutation, a conversion would be indicated by the appearance of two smaller bands of 87 and 68 bp. For the Ser208Ala (S208A) mutation, a conversion would appear with two smaller bands of 110 and 50 bp. These are not visible here.* ***B****: Successful conversion on RFLP analysis of the apoE chimeraplast, noted by the appearance of the 83 bp diagnostic band (arrowed). U: untreated cells. MI: microinjected cells. L: 10 bp ladder. E2: apoE2 genotype control.*

6.2.4 TARGETING OF LCAT IN LCAT-APOE RECOMBINANT CHO CELLS

In my experiments using the LCAT-targeting chimeraplasts up until this point I transfected both HepG2 and CHO-LCAT$_{WT}$ cells with the Ser208Ala and Ser216Ala; while varying: 1) the chimeraplast concentration; 2) the number of retargets on the same cells; 3) the transfection conditions - addition of centrifugation, addition of chloroquine, and use of modified PEIs; and 4) the size of chimeraplast by increasing the length from 68 to 80-mer. The results of all these chimeraplasty experiments suggest that delivery of DNA to the cell nucleus is not the limiting factor in achieving gene correction in *LCAT* using the Ser208Ala and Ser216Ala oligonucleotides that were synthesized for this purpose. We currently do not have enough knowledge about gene configuration and folding, mismatch repair enzymes, and chimeraplast purity, amongst other things, to understand why it is that certain RNA/DNA oligonucleotides (RDOs) easily mutate a target gene but other RDOs do not.

In order to address this question, I investigated whether the accessibility of the *LCAT* gene might change if it was in proximity to the *APOE* gene, as the latter is apparently able to be successfully targeted. I decided therefore, to create a plasmid containing both targeting areas of the two genes. Two versions were made, one in which the full LCAT cDNA was present with just the targeting segment of the APOE gene immediately upstream of the LCAT targeting region, the other containing complete cDNAs of both genes.

6.2.4.1 Production of the pXLE3 plasmid

In order to generate the plasmid containing the apoE targeting region within the complete LCAT cDNA, firstly, it was necessary to produce the apoE segment to ligate into the LCAT gene. To do this, a 341 bp apoE3 fragment was generated by PCR of p7055.E3, a plasmid containing the apoE3 cDNA (***Fig. 6.4***). The primers were designed using Vector NTI, based on the apoE cDNA (accession number NM_000041). These primers contain DraIII adaptors at their 5′ ends for ligation into LCAT (***Fig. 6.5***). The reaction and temperature gradient programme are shown in **Table 6-1**. It was found that the best product was obtained at 62°C annealing (***Fig.***

6.6) as at this temperature the PCR product was the most specific, indicated on the gel by one sharp band with minimal smearing. This temperature was used in subsequent PCR reactions to generate the DNA fragment.

Next, the PCR product was gel purified as described in *Section 2.1.2* and digested with 20 units of the restriction enzyme DraIII, at 37°C overnight. It was then gel purified again and quantified by OD measurement at 260 nm (1 OD_{260} = 50 µg/ml). Plasmid pXLCAT (p7055 containing the LCAT cDNA, ampicillin resistance and the *DHFR* gene) was also treated with DraIII in order to linearise the vector (***Fig. 6.7A***): approximately 10 µg of the plasmid were digested with 20 units of the enzyme at 37°C for 3 h. The linearised plasmid was then gel purified.

The linearised plasmid was dephosphorylated as described in *Section 2.1.5.* The plasmid was then ethanol precipitated, resuspended in 15 µl dH_2O, and quantified by OD measurement at 260 nm. Ligation of the apoE3 fragment and vector was accomplished as described in *Section 2.1.7.* Two insert to vector ratios were tried, 3/1 and 1/1. The reaction mix was left at 4°C overnight.

The next morning, the ligated plasmid was transformed into DH5α bacterial cells as described in *Section 2.1.9* and incubated at 37°C overnight. Colony growth was found on both 3/1 and 1/1 plates. Six colonies were picked using a sterile pipette tip from each plate and cultured in 5 ml LB broth containing 50 µg/ml ampicillin overnight at 37°C with shaking. Plasmid DNA was extracted from bacteria as described in *Section 2.1.10.*

Twenty microliters of each miniprep DNA was run on a 1% agarose gel to check for presence of DNA and to estimate the quantity obtained from the pellets. Then 30 µl of each plasmid was digested with 5 units restriction enzyme BamHI (Promega) at 37°C for 3 h, which was expected to give fragments of sizes 3280 bp and 4730 bp. Digests were run on a 1% agarose gel, which showed that of the 6 minipreps only culture '16' contained the correct plasmid (***Fig. 6.8***).

The remaining bacteria from culture 16 were recultured to prepare a larger plasmid preparation (see *Section 2.1.10*). Two microliters of the resulting DNA was run on a 1% agarose gel to verify the presence of the correct plasmid and the plasmid was quantified by spectrophotometry. One microgram of the plasmid was then digested with 5 units BamHI at 37°C for 3 hours, which showed the correct fragment

sizes for this plasmid: 4.3 and 3.5 kb (result not shown). A further 1 μg of the plasmid was sequenced using both an LCAT and an apoE PCR primer (for sequences see *Section 2.1.3*), to verify that both LCAT and apoE cDNAs were present in the plasmid (result not shown). At this stage, the plasmid, henceforth termed pXLE3, was ready for transfection into Chinese hamster ovary (CHO) cells (***Fig. 6.7B***).

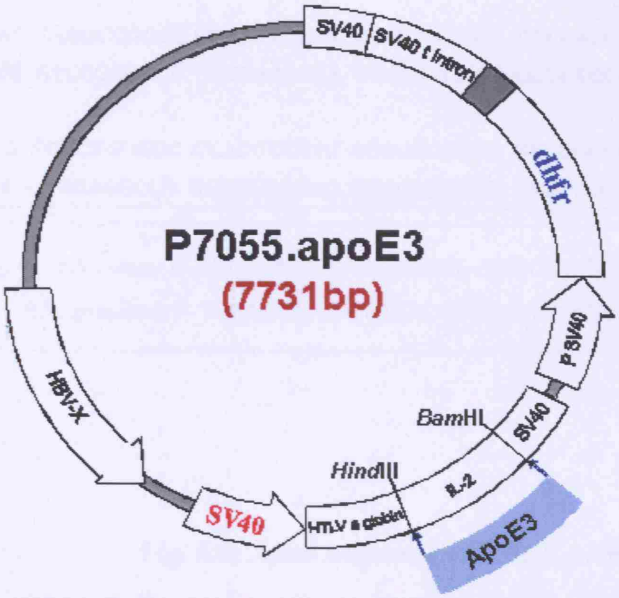

Fig. 6.4: Plasmid p7055.E3.

This plasmid is based on the p7055 vector, with exchange of the interleukin-2 (IL-2) cDNA for apoE3 cDNA. The plasmid contains ampicillin resistance for bacterial selection and the DHFR gene for selection in cultured cells. It was used here as a PCR template to generate the apoE3 fragment that would be ligated into the LCAT gene in pXLCAT.

Fig. 6.5: ApoE sequence and PCR primers.

Sequence of the section of the apoE3 gene to be amplified for ligation with LCAT cDNA. Underlined are the parts of the sequence matching the primers, and the full primer sequences are in the bottom box. Circled is the C→T point of mutation that changes the genotype from apoE3 to apoE2.

	Volume (µl)	Final concentration
10 x Taq buffer	5	1x
50 mM $MgCl_2$ stock	1.5	1.5 mM
10 µM E3L sense primer	2.5	0.5 µM
10 µM E3L antisense primer	2.5	0.5 µM
100 mM dNTP mix stock	1	2 mM
plasmid	6	10 ng/µl
dH_2O	31	
Taq polymerase	0.5	5 units/µl
Total volume	50	

Denaturation	Annealing	Elongation
96°C for 45 seconds	58/60/62°C for 45 seconds	72°C for 1½ minutes

Table 6-1: E3L PCR reaction and programme.

The top table shows the quantities and final concentrations used for a 50 µl reaction. The table below it shows the thermocycler programme, which began with 5 min at 96°C followed by 30 cycles of the above, ending with 10 min at 72°C.

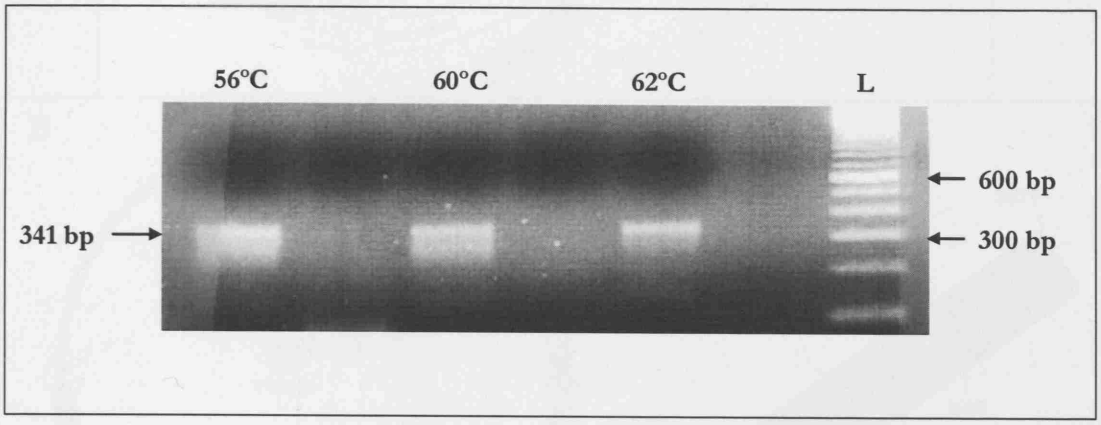

Fig. 6.6: PCR to generate apoE3 fragment with primers E3L.

*Gradient PCR products on a 2% agarose gel alongside a 100 bp ladder (**L**). The 341 bp fragment was most specifically produced at 62°C annealing temperature, as indicated by the sharper band with less non-specific product (smearing), and this temperature was used in subsequent PCR reactions to generate the apoE3 fragment for ligation into LCAT cDNA.*

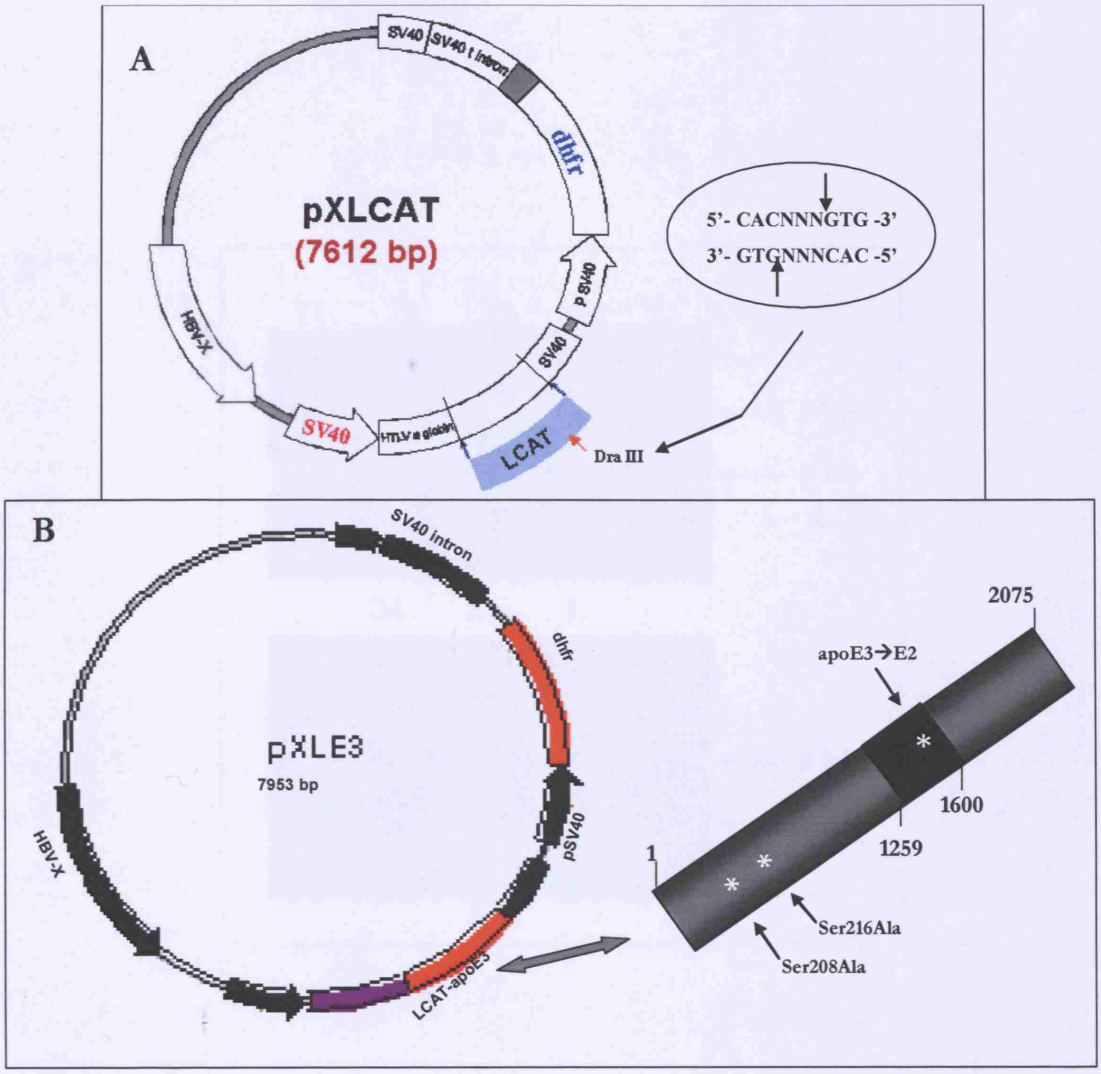

Fig. 6.7: Vector pXLCAT and the resulting plasmid pXLE3.

***A**: The expression vector carrying the LCAT cDNA into which the apoE3 targeting region was inserted. The vector was linearised using restriction enzyme DraIII so that the apoE3 fragment with its DraIII adaptors could be ligated in. **B**: The plasmid that results, pXLE3, after ligation of the 341 bp apoE3 fragment and schematic representation of the location of the apoE fragment within the LCAT cDNA (nucleotides 1259 to 1590), as well as the approximate locations of the targets for chimeraplasty (shown as stars).*

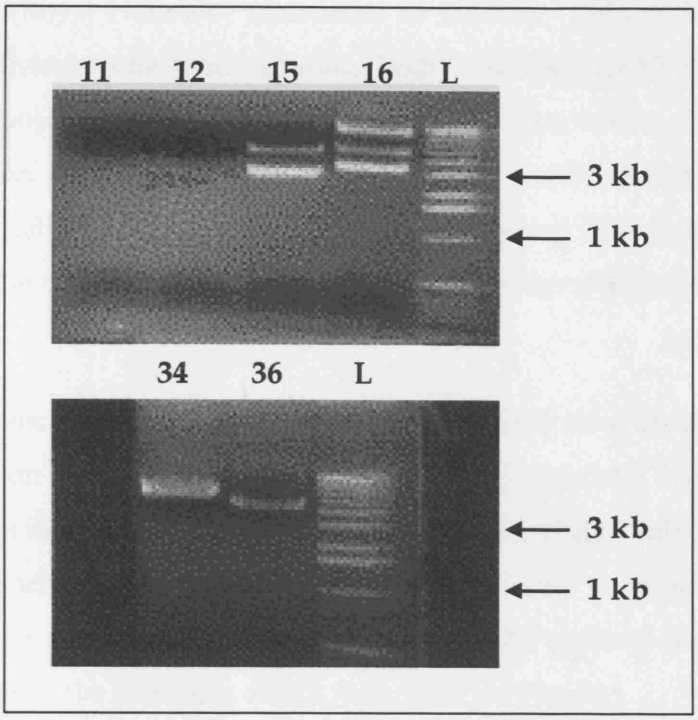

Fig. 6.8: Bacterial clones transformed with pXLE3 and digested with BamHI.

1% agarose gel of digests of DNA extracted from 6 picked bacterial colonies, resolved against a 1 kb ladder. The numbers indicate individual colonies. Colony 16 was the only one to produce the correct BamHI digestion fragments of 3280 bp and 4730 bp. L: 1 kb ladder.

6.2.4.2 *Production of the pXEIL plasmid*

This plasmid was created to contain both complete cDNAs of apoE and LCAT. The plasmid was based on pAAV.EIL (***Fig. 6.9A***), kindly provided by Dr. T. Athanasopoulos (Royal Holloway University of London. Egham, Surrey). It is an adeno-associated viral vector which contains both LCAT and apoE3 cDNAs separated by an internal ribosomal entry site (IRES) region. The aim was to cut out the apoE-IRES-LCAT region (termed EIL) and insert it into a vector that is selectable after transfection into cells in culture. The vector chosen was pcDNA3 (***Fig. 6.9B***), which contains ampicillin resistance (for bacterial culture) and neomycin resistance (for cell culture).

The sequences for both pAAV.EIL and pcDNA3 were studied to establish common restriction sites which could be used for digestion and re-ligation of the 2 fragments. It was found that the restriction enzymes NdeI and EcoRI both had only 1 restriction site each and were in a convenient location in both vectors. Five microliters of each plasmid were first digested with 30 units of NdeI overnight at 37°C. This linearised the plasmids, which were then gel purified.

Next, the linearised plasmids were digested with 20 units of EcoRI at 37°C overnight. Again, the required fragments were isolated by gel purification. The resulting sizes of the fragments to be isolated were 4.4 kb for EIL and 4.9 kb for pcDNA3. At this stage, the open pcDNA3 was dephosphorylated as described in *Section 2.1.5* with 0.018 unit of calf intestinal alkaline phosphatase (CIAP) each time. The dephosphorylated vector was then ethanol precipitated and resuspended in 24 µl dH_2O.

The two fragments were now ready for ligation and their concentrations estimated by measuring their OD at 260 nm. As described in the previous section, both 3/1 and 1/1 ratios of insert to vector were tried for the ligation, using the formula described in *Section 2.1.7.* The ligation reaction was carried out at 4°C overnight. The next day, transformation into DH5α cells was performed, using the same protocol as previously mentioned and plating bacteria on LB agar/ampicillin plates.

The next day 5 colonies were picked from each plate and cultured overnight in 5 ml LB broth containing 50 µg/ml ampicillin, at 37°C with shaking.

Growth was found in 8 of the 10 cultures (labelled C2, C3, C4, C5, C6, C7, C9, C10), and the plasmids from these were purified as previously described. Twenty microliters of each plasmid preparation was run on a 1% agarose gel, and 6 of the 8 were found to have visible amounts of DNA, all of the same size (above 8 kb). Equal amounts of all 8 preparations were digested with 10 units NotI, which was expected to produce 2 fragments from the plasmid, with sizes of 6.0 and 3.4 kb. Five of the 8 plasmids gave the correct digest products (***Fig. 6.10***). Preparation 'C3' was picked to culture for maxipreparation. This was done as for pXLE3 and the resulting plasmid preparation was quantified by OD_{260}. At this stage the plasmid was ready for transformation into CHO cells, and is henceforth referred to as pXEIL.

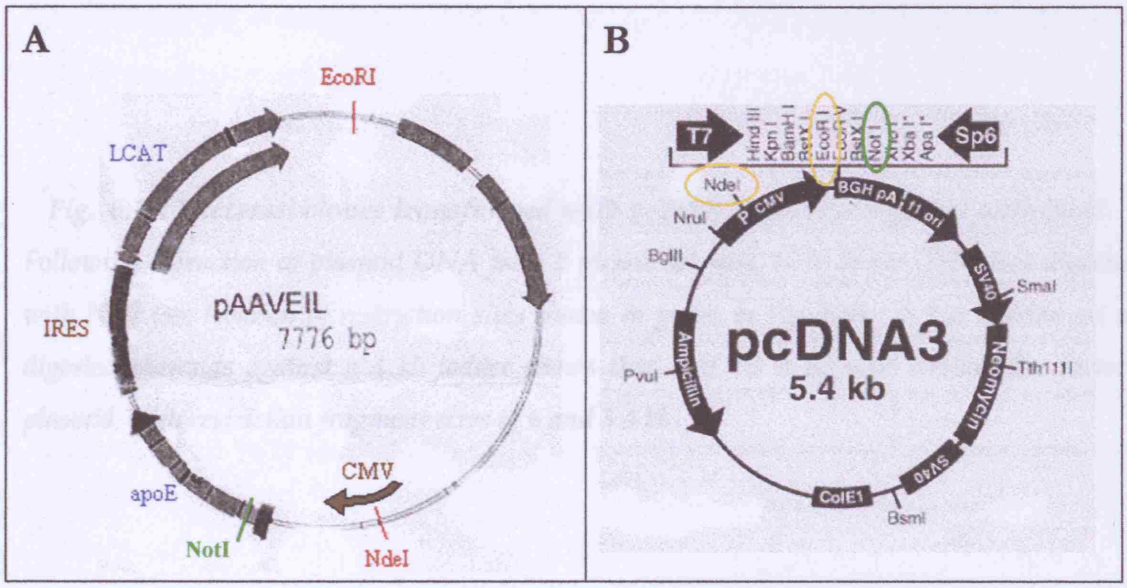

Fig. 6.9: Vectors digested to construct the pXEIL plasmid.

***A**: pAAV.EIL plasmid showing the EcoRI and NdeI restriction sites (red) which were used to isolate the apoE-IRES-LCAT section (4.4 kb). **B**: pcDNA3 plasmid with EcoRI and NdeI sites circled in yellow. The open vector is 4.9 kb. The apoE-IRES-LCAT fragment was cloned into the vector at these sites.*

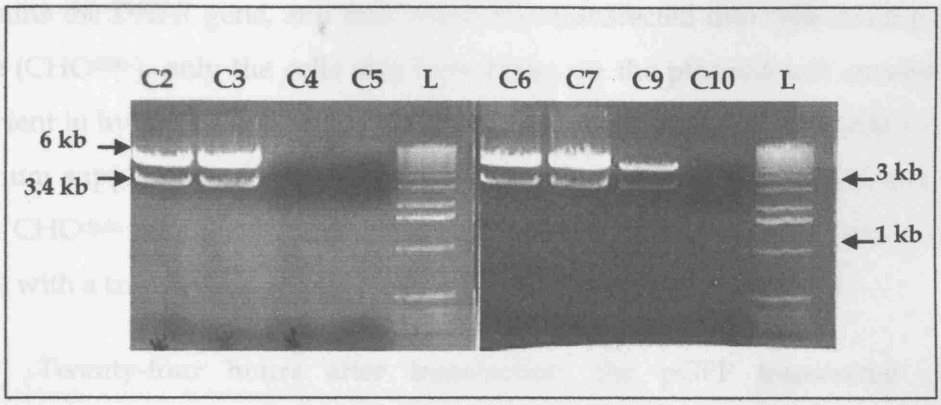

Fig. 6.10: Bacterial clones transformed with pcDNA3-EIL and digested with NotI. *Following extraction of plasmid DNA from 8 picked colonies, 10% of the DNA was digested with NotI (see location of restriction sites shown in green in Fig. 6.9). A 1% agarose gel of digested plasmids against a 1 kb ladder shows that 5 of the 8 colonies contain the correct plasmid, with restriction fragment sizes of 6 and 3.4 kb.*

6.2.4.3 *Production of CHO-LE3 cells and targeting with the LCAT chimeraplasts*

Dihydrofolate reductase (dhfr) is an enzyme which catalyses the conversion of dihydrofolate to tetrahydrofolate in the chain of reactions that produces thymidylate (dTMP), one of the essential building blocks of nucleotides [284]. Plasmid pXLE3 contains the *DHFR* gene, and thus when it is transfected into cells lacking the *DHFR* gene (CHO^{dhfr-}), only the cells that have taken up the plasmid will survive in media deficient in hypoxanthine and thymidine (HT). Therefore, CHO^{dhfr-} cells are grown in medium supplemented with HT (see Table 2-6), whereas the selection medium lacks HT. CHO^{dhfr-} cells were transfected with the pXLE3 plasmid as described in *Section 2.3.4*, with a transfection of pGFP as a control of delivery efficiency.

Twenty-four hours after transfection, the pGFP transfected cells were observed using a fluorescence microscope for GFP production and the pXLE3 transfection estimated as being 30-40% efficient. The plasmid transfected cells (wells 1-3) were trypsinized from their wells, pooled, and transferred to a 75 cm^2 flask containing selection medium. The cells from wells 4 and 5 were also pooled and transferred to a 75 cm^2 flask, to serve as a negative control for selection - the cells in this flask should all die because of the lack of HT in the medium, as they were not transfected with pXLE3 containing the *DHFR* gene. The transfected cells began to die off after approximately one week in selection medium, then quickly reached confluency over a period of 3 days. Success of transfection was verified by DNA extraction and PCR and RFLP to analyse the target regions of LCAT and apoE (***Fig. 6.11***).

Cloning of the cells was considered to be unnecessary for the purposes of the chimeraplasty experiments intended for these cells. Mutation is readily detected provided that all cells contain the relevant cDNAs, which can be achieved by maintaining constant selection pressure.

For the chimeraplasty experiments, CHO-LE3 cells were seeded in 12-well plates (1.5×10^{-5} cells/well) 24 h prior to transfection (*Section 2.3.5*). Targeting complexes were made up of 800 nM of S216A/68 chimeraplast (first batch), 600 nM of apoE3→E2 chimeraplast, and either L-PEI alone, L-PEI + Mel-PEI (1:1), or Tf-PEI with N:P ratio of 5:1 in all cases. The complexes were incubated for 10 min at room

temperature, then added to the cells. After 3 h the complex solution and medium were removed and replaced with fresh medium. Cells were harvested 24 h later for DNA extraction and RFLP analysis. Although no conversion was detected at the apoE location (data not shown), the S216A chimeraplast had successfully mutated the gene at all three conditions (***Fig. 6.12A***), with the highest conversion for the L-PEI/Mel-PEI mix. These results were confirmed by sequencing, where two peaks are visible as there is a mixed population of unconverted cells and cells with the T→G mutation (***Fig. 6.12B***).

6.2.4.4 *Production of CHO-EIL cells and targeting with the LCAT chimeraplasts*

CHO-KI cells were used in transfections with the pXEIL vector (*Section 2.3.4*) and were cultured in the medium shown in Table 2-6. Selection was accomplished using G-418, an antibiotic related to gentamicin, which is toxic to both prokaryotic and eukaryotic cells [253]. Resistance to G-418 is conferred by the presence of the *NEO* gene in the transfected plasmid. Thus, addition of the antibiotic to the culture medium allows a selection of only the cells which contain the transfected plasmid with the *NEO* gene. Transfection of plasmid pGFP was again performed as a control of delivery efficiency.

The day after transfection pGFP-transfected cells were observed under the microscope and delivery was estimated at being 40-50% efficient. The pXEIL-transfected cells were pooled and selected as was described above for pXLE3, and were kept under constant selection pressure. These cells were analysed by RFLP for confirmation of the presence of LCAT and apoE cDNAs (***Fig. 6.11***).

Transfections with the S216A/68 (first batch) chimeraplast were performed exactly as for the CHO-LE3 cells. Analysis of the extracted DNA again showed successful conversion in the LCAT cDNA, with the best gene correction in cells into which chimeraplast was delivered using Tf-PEI (***Fig. 6.12A***), though no conversion in apoE cDNA (data not shown). Sequencing of these DNA samples confirmed a very good T→G mutation using Tf-PEI as the delivery agent (***Fig. 6.12B***).

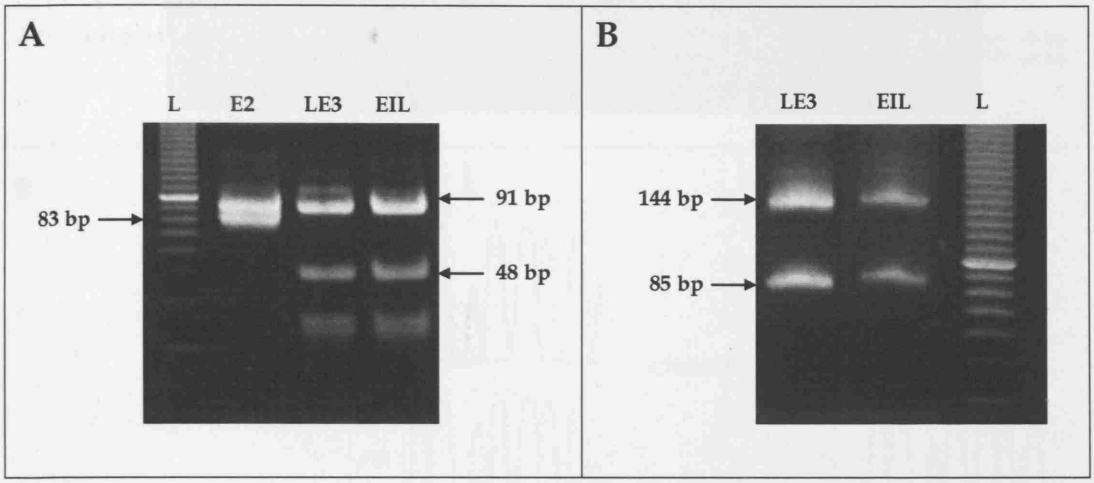

Fig. 6.11: RFLP analysis of CHO-LE3 and CHO-EIL cells.

Following selection, DNA was extracted from cells of each cell line and analysed for the presence of apoE and LCAT cDNAs. ***A****: ApoE RFLP showing correct digest pattern for the apoE3 genotype contained in both cell lines (91 and 48 bp), compared to digestion of DNA with the apoE2 genotype (E2: 91 and 83 bp).* ***B****: LCAT RFLP analysis of the Ser216 site confirming the presence of* $LCAT_{WT}$ *cDNA (144 and 85 bp). L: 10 bp ladder.*

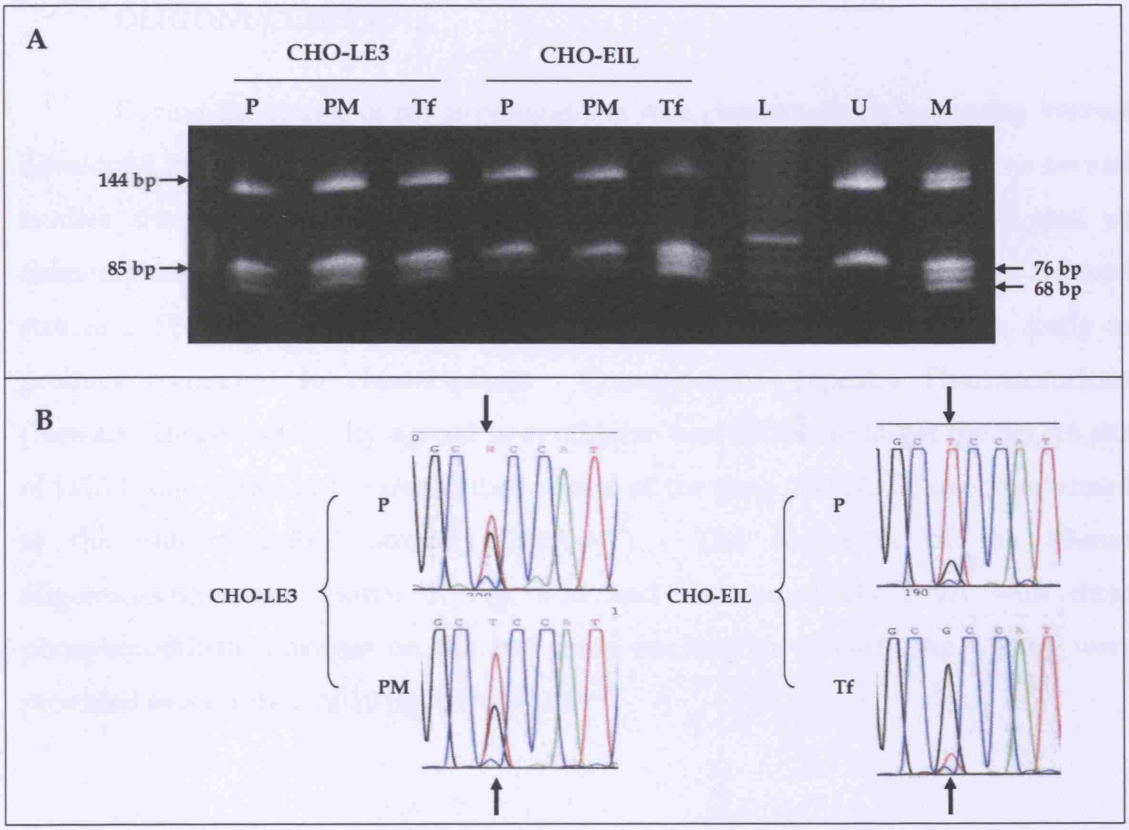

Fig. 6.12: Targeting of CHO-EIL and CHO-LE3 cells with S216A/68.

*Both cell lines were transfected with 800 nM of the S216A/68 (first batch) chimeraplast and 600 nM of apoE3→E2 chimeraplast. Complexes were formed using either L-PEI, L-PEI/Mel-PEI (1:1) or Tf-PEI (all N:P=5:1) and left on the cells for 3 h. Cells were harvested for analysis 24 h later. RFLP indicates conversion from T→G at all transfection conditions in both cell lines, by the appearance of two extra bands of 76 and 68 bp size (**A**). The successful gene mutation was confirmed by sequencing (**B**). P: L-PEI; PM: L-PEI + Mel-PEI; Tf: Tf-PEI; L: 10 bp ladder; U: untreated cells; M: CHO-LCAT$_{2M}$ cells (containing both Ser208Ala and Ser216Ala mutations) as a positive control.*

6.2.5 GENE REPAIR WITH A SER216ALA SINGLE-STRANDED OLIGONUCLEOTIDE

During the course of my investigations with chimeraplasts, increasing interest developed in gene repair using single-stranded oligonucleotides (SSONs), as several studies showed that these shorter molecules could achieve the same goal as chimeraplasts (see *Section 1.3.3.3* of the Introduction). As a result of their reduced structure, SSONs have the advantage of being easier to purify and less costly to produce compared to chimeraplasts. Consequently, Tapestry Pharmaceuticals (Newark, Delaware) kindly agreed to synthesize two SSONs to target the Ser216 site of LCAT, one aimed at the transcribed strand of the gene (S216A-T), the other aimed at the non-transcribed strand (S216A-NT). The sequences of the 49-mer oligonucleotides are shown in ***Fig. 6.13*** and are completely DNA with three phosphorothioate linkages on the last three nucleotides at each end. They were provided as a solution of 10 µg/µl in water.

S216A-T: 5'-TCTCTTGGGGCTCCCTGGGGTGGC**G**CCATCAAGCCCATGCTGGTCTTGG-3'

S216A-NT: 5'-CCAAGACCAGCATGGGCTTGATGG**C**GCCACCCCAGGGAGCCCCAAGAGA-3'

Fig. 6.13: Sequences of the LCAT Ser216Ala SSONs.

*The oligonucleotides each target either the transcribed strand (**S216A-T**) or non-transcribed strand (**S216A-NT**) of the gene. Each molecule is a 49-mer and contains the mutation at its centre (underlined) with the last three bases at each end protected with phosphorothioate linkages.*

Based on data published by Parekh-Olmedo *et al.* [285], CHO-EIL cells were transfected with each of the SSONs at three different doses (2, 6 or 12 µg per 2 x 10^5 cells) using L-PEI (N:P=5:1) following the same process as for chimeraplast transfections. Cells were incubated with transfection complexes for 5 h and harvested

for analysis 24 h later. Control cells targeted in parallel with pGFP were viewed the day after transfection by fluorescence microscopy for GFP production, which showed a transfection efficiency of approximately 10%. Despite this low result, RFLP analysis of the SSON-transfected cells showed successful mutation with 6 and 12 μg doses of the S216A-NT oligonucleotide, although no gene correction was detected using S216A-T (***Fig. 6.14***).

Fig. 6.14: CHO-EIL cells transfected with S216A SSONs.

CHO-EIL cells were transfected with increasing quantities (2, 6, or 12 μg) of oligonucleotide S216A-T or S216A-NT in complex with L-PEI (N:P=5:1) for 5 h. Cells were analysed 24 h later and RFLP shows that S216A-NT is able to mutate the gene at the two higher doses (as judged by appearance of the 76 and 68 bp bands). U: untreated cells; M: CHO-LCAT$_{2M}$ cells (containing both Ser208Ala and Ser216Ala mutations) as a positive control.

6.3 DISCUSSION

Comparative investigations into the delivery of chimeraplasts using PEI-based reagents into cells in culture (Chapter 5) showed that the standard protocol, using L-PEI alone, can be improved by supplementing the PEI/DNA complexes with Mel-PEI or Gal4-PEI. This was evident from both a gene delivery point of view (uptake of chimeraplast molecules into the nucleus) and a gene correction one (genotypic proof of chimeraplast action). Using this information, I went back to my LCAT-mutating chimeraplasts and targeted CHO-$LCAT_{WT}$ and HepG2 cells in order to generate the S208A and S216A mutations. For improved delivery into CHO cells, a combination of L-PEI and Mel-PEI was used, while in HepG2 cells delivery was optimised by using L-PEI with Gal4-PEI to exploit uptake via the asialoglycoprotein receptor.

Despite these efforts, along with attempts at delivery with other modifications (pre-incubation of cells with chloroquine or use of Tf-PEI), RFLP analysis repeatedly showed unmutated targets. The likelihood of failure to see a nucleotide change being due to a delivery barrier now appeared less likely as the increased efficiency of these vehicles had been verified by targeting the *APOE* gene, but another experiment to support this assumption was performed. HepG2 cells, which express both *LCAT* and *APOE* genes, were co-targeted simultaneously with the Ser216Ala chimeraplast and the apoE3→E2 chimeraplast, complexed together with L-PEI. When fluorescently-labelled, the latter was previously seen to enter the nucleus. By complexing the two chimeraplasts together, I hoped that the apoE chimeraplast would act as a "piggy back" for the LCAT chimeraplast into the nucleus. Again, a mutation was found in the *APOE* gene but not in *LCAT*.

Finally, nuclear microinjection of the chimeraplasts was performed to completely eliminate the possibility of delivery being an insurmountable hurdle for these oligonucleotides. As a control for the process, an apoE chimeraplast was also microinjected in parallel. While a clear mutation was achieved with the apoE chimeraplast, neither of the LCAT chimeraplasts managed to produce a mutation. This last transfection in the series put to rest the question of DNA delivery, as this time there was no doubt that the molecules were physically present in the nucleus. Kren *et al.* [182] showed that nuclear uptake of chimeraplasts is independent of

sequence by transfecting 5 different fluorescently-labelled molecules aimed at different genes into the same cells. Therefore the query now was why can one chimeraplast direct mutation, but not another?

One possible explanation for the apparent failure of the LCAT chimeraplasts is that some gene conversion does occur, but at such a low frequency that it is not detectable by PCR. Numerous chimeraplasty studies support such an idea. For example, a chimeraplast aimed at mutating the tyrosinase gene in melanocytes (resulting in a change of pigmentation from white to black) was successful at a frequency of 0.01-15% [184]. The method by which these results were obtained was simply by counting pigmented cells under a microscope. In a separate study, mutation of the β-galactosidase gene to restore enzymatic activity was successful at levels of 0.1-1% as determined by histochemical staining and colour selection of bacteria transformed with Hirt DNA [272]. Other quantitative methods, such as scanning densitometry of RFLP bands on polyacrylamide gels is only able to pick up conversions of 5% or over, while detection of ^{32}P-dCTP incorporated into PCR reactions is only reliably measured above 1% conversion [187]. If indeed the gene correction mediated by the S208A and S216A chimeraplasts was at the low levels described above, then a method of detection other than PCR-RFLP would be beneficial in future experiments. On the other hand, assuming low but successful mutations were occurring, the usefulness of such weak conversions would have to be questioned when the ultimate goal is use as a clinical gene therapeutic.

Another matter which has been addressed in the past is whether transcriptional activity influences the ability to target a gene. Early on in chimeraplasty's history it was shown that this was unlikely to be a factor in gene correction, as the β-globin gene was successfully mutated in hepatocytes, where it is not expressed [182]. On the other hand, others suggest that transcriptional activity does play a role in gene repair [200, 286], though these studies were conducted on single-stranded oligonucleotide-mediated repair.

Additional considerations for successful chimeraplasty are the quality of the reagent and whether the molecules may be toxic to the transfected cells. The first point was addressed in Chapter 4, where visual evidence of chimeraplast quality was seen and showed that there is an inter-batch difference in synthesis quality. With regards to toxicity, it is difficult to judge in transfections with chimeraplast/PEI mixtures whether any observed toxicity is due to the oligonucleotide or to the PEI.

Evidence against chimeraplasts themselves being toxic is that when I microinjected naked molecules into cell nuclei there was no more cell death than when PEI transfection was used. Nevertheless, we do not know if DNA and PEI stay complexed the whole time they are in the cell, and free PEI may be cytotoxic. Clamme *et al.* [287] studied the intracellular fate of PEI and observed that 80% of PEI molecules in DNA/PEI complexes are free, and that there is a great accumulation of free PEI in the nucleus.

Chimeraplast stability before and after transfection is another factor that may affect successful gene correction. Once inside the cell, PEI-associated chimeraplasts are protected from degradation, but it is not certain that all molecules remain complexed with PEI the whole time that they are inside the cytoplasm and nucleus. If a proportion of molecules were being degraded at some point, this might also account for very low gene correction activity. To counter this possibility, one study transfected cells with labelled molecules, then isolated them from cell lysates and showed on a polyacrylamide gel that the chimeraplasts were intact 24 h after transfection as before transfection [179].

My next line of investigation was concerned with gene location as an explanation for the lack of detectable mutation in the *LCAT* gene. Little is known at this stage about the exact conformation of most genes and their relationship with surrounding structures. It is therefore difficult to compare genes while trying to determine if one is more accessible to gene targeting than another. HepG2 cells were targeted because they express the *LCAT* gene [288] and represent an *in vitro* model of gene repair in the liver, which would be the *in vivo* aim for LCAT chimeraplasty. As a comparison, recombinant CHO cells stably expressing LCAT would not have the cDNA integrated in the same location as the gene in a human cell line. Nevertheless, these different targeting locations did not give an obvious difference when transfecting the two cell lines with the LCAT chimeraplasts, as in both results were negative.

The availability of the apoE chimeraplast (E3→E2), an oligonucleotide previously shown to be active, was useful as a positive control for experiments with the LCAT chimeraplasts. With this in mind, I constructed two plasmids that contained both LCAT and apoE targeting regions adjacent to each other, and used these to produce the cell lines CHO-LE3 (where just the targeting area of apoE was inserted downstream of the LCAT targeting area) and CHO-EIL (containing complete

cDNAs for both proteins). If these two recombinant cell lines were also susceptible to apoE targeting, then logically it implies that the transfected DNA, co-harbouring the LCAT gene, is accessible to a mutagenic chimeraplast. The results of my experiments showed, for the first time, the required T→G mutation at the amino acid 216 site of LCAT in both cell lines.

An explanation now needs to be found for the reason that LCAT in this context was accessible to gene correction but was not in HepG2 or CHO-LCAT$_{WT}$ cells. It has been shown that one chimeraplast can have different mutation frequencies in different cell lines [187]. Other than transfection efficiency, no clear reason is yet available for this finding, but a possibility is that the recombinational ability of each cell type is different and therefore leads to variations in gene correction frequencies. This idea was supported by enhanced gene correction by up to 70% after transfections of chimeraplast into cells that overexpress RAD51, the protein that is thought to stabilise the double D-loop structure needed for chimeraplast interaction with its target [196], compared to transfection into the same cells without RAD51 [197]. In the case of my experiments, this might only be the true when comparing CHO-EIL and CHO-LE3 cells to HepG2 cells, but would not explain differences between these two cell lines and CHO-LCAT$_{WT}$ cells, as they are essentially all based on the same Chinese hamster ovary cell.

To return to my "piggy back" idea of apoE chimeraplasts carrying LCAT chimeraplasts, I cannot say for certain that it is the presence of the apoE chimeraplast in transfection complexes that caused the LCAT mutation to be successful. Unfortunately, time limitations did not allow me to investigate this finding further, but the next experiment to do would have been targeting of the CHO-EIL and CHO-LE3 cells with the S216A chimeraplast alone, to observe whether the presence of the apoE chimeraplast really has any influence on successful mutation in LCAT.

Successful gene correction in the CHO-EIL recombinant cell line with the S216A SSON shows that these shorter oligonucleotides probably have an advantage over chimeraplasts in mediating gene repair. Various publications have shown that when targeting the same sequence with a corresponding chimeraplast and SSON, the SSON showed higher activity [197,198]. Again, time limitations did not allow me to verify that this was true for LCAT by transfecting HepG2 cells or CHO-LCAT$_{WT}$ cells.

An interesting feature of SSONs is that although both strands of a gene can be targeted, the non-transcribed strand is more amenable to gene correction. This was apparent in my last experiment, where the oligonucleotide targeting the non-transcribed strand proved to have mediated gene conversion, while the other oligonucleotide did not. It has been postulated that the reason for this strand preference stems from the interactions of RNA polymerase with the target gene. The polymerase molecules associate to the transcribed strand, and it is possible that this creates competition for the target sequence, with the result that the SSON corresponding to the transcribed strand is displaced by the polymerase. By contrast, the non-transcribed strand being relatively undisturbed, it is more open to hybridisation with its corresponding SSON. Support for this hypothesis has been shown by Liu *et al.* [200], who used ^{32}P-labelled oligonucleotides to target a site within a plasmid, and observed the interaction between the two once RNA polymerase was added. They found that the labelled gene repair molecule was displaced from the strand that was the object of transcription. Consequently, this means that SSONs have a major difference from chimeraplasts: SSON activity appears to be influenced by the cell's transcriptional status, whereas chimeraplasts are not.

The recent appearance of strategies to enhance gene repair mediated by SSONs would be of interest to test using both LCAT chimeraplasts and SSONs. One such strategy is the overexpression of RAD51 in cells prior to transfection [183], for reasons discussed above. Another is treatment of cells with DNA damaging agents such as hydroxyurea or thymidine before transfection with gene correction oligonucleotides, as this has been shown to induce homologous recombination and therefore facilitates mutation by an SSON [289]. Finally, it has also been demonstrated that elongation of the S phase using camptothecin [202] slows replication forks and thus increases the frequency of gene repair with SSONs.

In summary, more work needs to be done to elucidate the extent of success of the S216A chimeraplast and SSON: whether LCAT in hepatic cells can be mutated, whether such a mutation is stable after repeated passaging of cells, and whether it would be successful *in vivo*. In conclusion, there are still many mysteries regarding the exact intracellular movements and mechanisms of action of chimeraplasts and SSONs, but the preliminary success in mutating the *LCAT* gene brings hope of this technique eventually being used as a gene therapeutic.

Chapter 7 –

General Discussion

7.1 AIMS OF THE THESIS

Atherosclerosis is a multifactorial process (*Section 1.1.1*), and therefore many possible gene therapy targets exist to combat this entity. An important physiological process in atheroprotection is reverse cholesterol transport, the pathway by which excess cholesterol is gathered from peripheral cells and taken to the liver for degradation. One of the key steps in RCT is the esterification of cholesterol by LCAT, leading to maturation of HDL particles [37]. Besides this function, LCAT has also been shown to be able to reverse the oxidation of LDL [95], an important contributor to the generation of atheromas. Therefore, LCAT can be regarded as an important factor in the prevention of atherosclerosis. Indeed, the absence of LCAT can result in an abnormal lipid profile and atherosclerosis [110]. The benefits of functional LCAT are evident from overexpression in transgenic rabbits [113], where these animals showed resistance to atherosclerotic changes on a cholesterol-rich diet, and even diminished atheromas. This line of reason has led to the development of anti-atherogenic therapy by LCAT gene addition, using mainly adenoviral and retroviral vectors [117-119].

In broad terms, atherosclerosis can either be prevented or existing lesions reversed. Gene therapy strategies aim to do this locally at the site of atheromas or systemically by targeting genes involved in the regulation of atherogenesis. Most of the human trials so far have involved viral vectors to deliver genes locally. For example, the vascular endothelial growth factor (*VEGF*) gene was successfully injected into the myocardium of patients with CHD using an adenoviral vector [290]. In a slightly different approach, retrovirus-*LDLR* cDNA was transfected *ex vivo* into resected hepatocytes of patients with familial hypercholesterolaemia and transplanted back into the liver [291]. Systemic treatment for atherosclerosis has not yet appeared in clinical gene therapy trials, but shows promise when attempted in animal models. Examples of these are the intravenous administration of adenovirus-*eNOS* (the endothelial nitric oxide synthase gene) [292] and AAV-*IL-10* (the interleukin-10 gene) [293] into apoE-deficient mice, both of which showed inhibition of progression of atherosclerotic lesions. The common factor in all the current lines of investigation is that the great majority use a gene addition strategy, whereas only our laboratory has utilised a gene repair approach [191].

If the presence of a higher number of LCAT molecules by overexpression of the gene leads to atheroprotection, then in theory the same should be true for LCAT molecules with an increased specific activity. In order for this to be possible, gain-of-function mutations in the *LCAT* gene are necessary. Two such mutations have been shown *in vitro*: Ser208Ala and Ser216Ala, with increased activities up to 14-fold that of wild-type LCAT [122, 125]. In order to introduce these mutations with the aim of creating a form of gene therapy, a method of gene repair is required, such as the technique of chimeraplasty. This method involves targeting the *LCAT* gene *in situ* with an RNA/DNA oligonucleotide that would recruit DNA repair mechanisms intrinsic to the cell in order to promote the required mutations [179]. To date, no such method has been used to target the *LCAT* gene with the goal of treating atherosclerosis. Chimeraplasty is an attractive procedure because, unlike gene addition, it allows the target gene to remain in its natural position and interact with surrounding regulatory elements, something which does not occur when cDNA is inserted into a cell.

The main aim of this thesis was to edit the *LCAT* gene using chimeraplasty in order to produce the potentially atheroprotective mutations Ser208Ala and Ser216Ala *in vitro*. As part of this study, I created a recombinant cell line expressing LCAT containing both Ser208Ala and Ser216Ala, and compared the specific activity of this variant with $LCAT_{Ser216Ala}$ and wild-type LCAT, to determine whether indeed these mutations lead to increased activity of the protein. Next, I studied the nuclear uptake of a validated chimeraplast that targets the *APOE* gene in order to develop the most efficient DNA delivery protocol for the transfection of chimeraplasts into cells in culture. I did this by testing the transfection efficiency of a variety of PEI-based reagents, using PCR-RFLP for monitoring gene correction and FACS for assessing nuclear uptake. I then went on to use this optimised protocol to target the *LCAT* gene with chimeraplasts in HepG2 and recombinant CHO cells.

7.2 $LCAT_{S216A}$ AND $LCAT_{S208A+S216A}$ HAVE HIGHER ENZYMATIC ACTIVITY THAN WILD-TYPE LCAT

The experiments previously conducted to test the specific activity of LCAT mutants [106,109] followed a similar method to those carried out here. LCAT cDNA was mutated by site-directed mutagenesis and transfected into cells. The main difference is that the published studies used transiently transfected cells, whereas

here the transfections were stable. Additionally, the combined effect of mutating both 208 and 216 sites to alanine had not previously been examined.

In this study, I used site-directed mutagenesis to produce a T→G mutation resulting in the Ser208Ala amino acid change in a plasmid already containing LCAT cDNA with the Ser216Ala mutation. This double-mutated cDNA ($LCAT_{2M}$) was then transferred to an expression vector and stably transfected into CHO cells. These recombinant cells were selected and cloned. The highest LCAT secreter of the resulting clones was used to produce $LCAT_{2M}$ for comparison with $LCAT_{S216A}$ and $LCAT_{WT}$ proteins. The specific activities of the three LCAT variants were compared by measuring the cholesterol esterification rate of the enzyme using a proteoliposome substrate containing ^{3}H-cholesterol and estimating protein mass using scanning densitometry of bands on Western blots. Although my experiments were only of a preliminary nature, because of the suboptimal substrate used for the reaction, it appeared that the Ser216Ala mutation did confer higher activity (approximately 9-fold greater) than the wild-type variant. The double-mutation also resulted in higher activity, though only about twice that of wild-type LCAT.

Although my results only give a rough indication of differences between the three LCAT variants, Francone and Fielding [122] had shown $LCAT_{S216A}$ to be 14 times more active than wild-type LCAT, while Qu *et al.* [125] found it had almost twice the activity. Thus, my activity assay for the Ser216Ala variant confirm these reports, if not quantitatively, then at least in a qualitative manner that this mutation results in superior LCAT enzymatic activity. The 2-fold increase in activity shown in my assays of the double-mutated LCAT variant is less noteworthy and would probably not be worth pursuing. Nevertheless, because my investigation was preliminary, it is still useful to verify this increased activity properly. It is thought that the increased hydrophobicity provided by an alanine residue at a location close to the enzyme's active site (i.e. amino acid 216) may help bind substrate [125]. It is difficult to explain why the presence of two alanines in this region (i.e. also at amino acid 208) would result in lower activity than just one. No studies have appeared that examined mutations of the two sites together, but if indeed an alanine aids phospholipids binding, one possibility could be that the second alanine somehow interferes with substrate binding.

Given more time to devote to this part of my thesis, I would have worked on developing better substrate and carried out more extensive comparisons of the LCAT

variants to generate statistically significant values. I would have also verified the acquired specific activities by examining several clones of each LCAT variant. Other studies can also be conducted to exploit the recombinant cell lines that now exist. The roles of LCAT in RCT and as an anti-oxidant can be further investigated by examining the three variants. Additionally, the mutated cDNAs may be incorporated into viral vectors, as a method of "enhanced" gene addition.

7.3 DELIVERY OF CHIMERAPLASTS INTO CELLS IS IMPROVED BY CHLOROQUINE, MEL-PEI AND GAL4-PEI

Most gene delivery methods involved viral or liposomal vectors until the appearance of PEI. This versatile polycation was shown to be an efficient DNA carrier both *in vitro* and *in vivo* [228]. The degree of protonation of PEI's amine residues increases as the pH decreases [294]. This unique quality allows PEI to buffer endosomes by a "proton sponge" effect and leads to endosomal rupture, freeing DNA/PEI complexes and preventing degradation [295]. Therefore, PEI has an advantage over viral vectors because it lacks immunogenicity, and is superior to liposomes because it can avoid lysosomal degradation.

Additionally, PEI can be easily modified to enhance delivery or target specific cells. Linking the peptide melittin to PEI results in better complex uptake due to its membrane lytic activity, but also improves nuclear accumulation. Ogris and colleagues believe this is due to a nuclear localisation signal-like sequence contained in melittin's primary structure [242]. Several ligands exist that can target specific cell types: mannose for macrophages [239], transferrin for rapidly dividing cells [240], and galactose (and lactose) for hepatic cells [238]. Also, intracellular survival of DNA/PEI complexes can be improved by the use of chloroquine, as this reagent can inhibit lysosomal degradation of complexes by raising their pH [221].

In order to study uptake of chimeraplasts into hepatic cells for the purposes of finding an optimal delivery protocol, I tested several PEI variants as well as the use of chloroquine. I found that this was important to assess as most publications on the subject of delivery agents used plasmids, whereas RNA/DNA oligonucleotides may act differently when complexed with PEI. I used a validated chimeraplast that targets the *APOE* gene to measure delivery efficiency into HepG2 cells in two ways: 1) gene conversion activity of the chimeraplast (i.e. successful access and action of

oligonucleotides to target DNA) was investigated by RFLP; 2) the uptake of DNA/PEI complexes into the nucleus was examined by counting nuclei transfected with a fluorescent chimeraplast using FACS.

The varieties of PEI that were used in these experiments were linear PEI, branched PEI, Melittin-PEI (25-kDa), Melittin-PEI (2-kDa), Galactose-PEI, Galactose4-PEI and Transferrin-PEI. Preliminary transfections with the plasmid pGFP showed that of these reagents, Mel-PEI (25-kDa) and Gal4-PEI were the most promising, and appeared to transfect more cells than L-PEI. From the properties of Mel-PEI and Gal-PEI mentioned above, this seems a logical finding.

Investigations using the apoE chimeraplast were more detailed. Transfections to examine gene conversion were performed using the minimal quantity of oligonucleotide so that performance differences between reagents would be detectable by RFLP analysis. Comparison of L-PEI, L-PEI + chloroquine, and B-PEI showed that of the three, L-PEI with chloroquine gave the best conversion. This result demonstrates that even though L-PEI has the ability to protect the chimeraplast intracellularly, the action of chloroquine must reduce degradation even further. Another finding was that the receptor-specific PEIs were of value. While Gal-PEI did not produce results obviously better than L-PEI, both Gal4-PEI and Tf-PEI increased the conversion. The most remarkable results were observed when L-PEI was combined 1:1 with either Mel-PEI or Gal4-PEI. For example, the addition of Gal4-PEI resulted in successful gene conversion using a chimeraplast that had previously been unsuccessful when delivered with L-PEI alone.

In order to obtain additional, quantitative support for the RFLP findings, experiments were repeated and fluorescent oligonucleotide-transfected nuclei counted by FACS. The first significant finding was that although Mel-PEI alone did not improve transfection efficiency, its combination with L-PEI resulted in a 27% increase in nuclear delivery of chimeraplast. There could be several explanations for this result. The interaction of Mel-PEI with chimeraplasts may be different than with plasmids, and no investigation into this matter has yet been published. Additionally, Mel-PEI is 25-kDa while L-PEI is 22-kDa, an apparently significant difference when it comes to delivery ability [277], and therefore when the two were combined the condensing ability of L-PEI was used, while nuclear delivery was exploited by Mel-PEI.

When examining the reagents that utilise the asialoglycoprotein receptor to target hepatic cells, I found that although Gal-PEI was inferior in transfection efficiency to L-PEI, Gal4-PEI improved delivery by 24%. Furthermore, combining L-PEI with Gal4-PEI raised chimeraplast delivery by another 10%. The reason for the tetragalactose (Gal4-PEI) variant being more useful than Gal-PEI may be because Gal4-PEI is able to form smaller, more stable DNA/PEI complexes, resulting in more efficient delivery [283]. Here, again, the improved performance afforded by the addition of L-PEI can be explained by the fact that Gal4-PEI is 25-kDa, like the Mel-PEI.

FACS analyses of transfections using chloroquine showed an increase in nuclear delivery compared to cells that did not receive chloroquine, but the values were not statistically significant. The same was true for experiments using Gal4-PEI. In HepG2 cells, which carry the ASGPR, FACS values indicated that more HepG2 nuclei were transfected with L-PEI + Gal4-PEI than nuclei from CHO cells (which lack the ASPGR), but these were not statistically significant.

In conclusion, taking both RFLP and FACS data together, the best transfection conditions for delivery of chimeraplasts into HepG2 cells are L-PEI + Gal4-PEI > L-PEI + chloroquine > L-PEI +Mel-PEI. While the results of this study were useful for the continuation of my work of targeting the *LCAT* gene by chimeraplasty, they can also be applied to future experiments where chimeraplasts are used to target other genes. This includes improving chimeraplast delivery for *in vivo* trials, especially to target the liver, as with a hepatic receptor-specific feature it may be possible to bypass DNA/PEI complex trapping in the lungs after intravenous injection [235]. Furthermore, it could be useful to transfect fluorescently-labelled oligonucleotides in order to separate out transfected cells using FACS so that RFLP analysis is only of successfully transfected cells, which may lead to seeing a higher conversion than if DNA is collected from a mixed culture of transfected and untransfected cells.

7.4 LCAT CAN BE EDITED AT THE SER216 SITE BY BOTH CHIMERAPLASTS AND SINGLE-STRANDED OLIGONUCLEOTIDES

I began my attempts to edit the LCAT gene by transfecting two chimeraplasts, each causing a T→G mutation, to create the Ser208Ala or Ser216Ala phenotypes. The

delivery vehicle was L-PEI and a standard protocol that had previously worked well [191] was used to target HepG2 cells and CHO-LCAT$_{WT}$ cells. Unfortunately, this method failed, and so different aspects of the basic method were modified: 1) the concentration of chimeraplast was increased up to 1200 nM (whereas previously a concentration of 400 nM was sufficient to mediate mutation in our laboratory); 2) the N:P ratio of PEI was varied from 4:1 to 9:1 because the standard 5:1 ratio did not show a conversion; 3) a centrifugation step was added to increase the contact of complexes with cells; 4) cells were retargeted to generate a cumulative effect of chimeraplast action; 5) an 80-mer chimeraplast was used instead of the standard 68-mer length to improve oligonucleotide-target hybridisation; and 6) several new batches were synthesised to address possible problems of chimeraplast quality. Unfortunately, none of these variations to experimental conditions resulted in successful chimeraplast action.

Having established the best transfection conditions for chimeraplasts (above), I then repeated the experiments using L-PEI + chloroquine or L-PEI + Mel-PEI on CHO-LCAT$_{WT}$ cells, and those combinations plus L-PEI + Gal4-PEI on HepG2 cells. Again, no gene conversion was noted by RFLP analysis. In order to eliminate the possibility of oligonucleotide delivery as the limiting step, HepG2 cell nuclei were mincroinjected with the chimeraplasts. Again, no mutation was observed. As a transfection control, I cotargeted HepG2 cells with an apoE chimeraplast as well as an LCAT chimeraplast; this resulted in successful conversion in the *APOE* gene but none in the *LCAT* gene. At this point, it seemed less likely that delivery was the barrier to successful chimeraplasty, but that the oligonucleotides themselves were the problem.

One of the possible explanations for LCAT chimeraplasty mutations being undetectable by RFLP analysis is that this method is not sensitive enough to detect low levels of mutation. Successful chimeraplasty experiments have been previously shown at frequencies of as low as 0.01% [184], whereas scanning densitometry of RFLP bands can only detect conversions of about 5% [187]. Chimeraplast quality is another area of concern, as visualisation of the reagents by electrophoresis showed that there is a difference between each synthesis. Synthesis of these long molecules involves coupling reactions and deprotection, which are not totally efficient and can result in impure products. Additionally, we do not know the exact fate of chimeraplasts once inside the cell. Though apparently intact RDOs have been

detected [179], and I have demonstrated that they do migrate into the nucleus, we cannot be sure that there is no major degradation.

Finally, we do not know why certain genes appear amenable to mutation by chimeraplasts and not others. Zhang and colleagues [185] looked at six different loci and targeted them with 42 chimeraplast variants. The group designed standard 68-mer RNA-DNA oligonucleotides as well as RDOs with varying lengths of DNA or RNA segments and RDOs with no complementary region to the target DNA. All chimeraplasts were introduced *in vitro* using liposome carriers mainly into lymphoblastoid cells, fibroblasts, or hepatocytes. Additionally, they attempted electroporation and microinjection, but PCR-based analysis and sequencing showed no reproducible success. Diaz-Font *et al.* [296] tried to use a chimeraplast to correct a mutation that causes Gaucher disease and found no evidence of success by RFLP analysis. Although currently gene conformation and interaction with surrounding structures is not fully understood, this aspect of gene repair may be the answer to inter-gene differences in targeting success.

With this in mind, I wanted to examine the effect of the proximity of the apoE targeting region to the LCAT targeting region. In order to do this, I generated two recombinant cell lines expressing apoE-LCAT cDNA: one had both full-length cDNAs next to each other (CHO-EIL), while the other was a hybrid sequence with the apoE targeting section just downstream of the LCAT targeting region (CHO-LE3). I then co-transfected these cells with the apoE3→E2 and LCAT Ser216Ala chimeraplasts and found that the Ser216Ala oligonucleotide successfully mutated the gene in both cell lines. Time limitations did not allow me to transfect these cells with the Ser216Ala chimeraplast alone, in order to assess whether the presence of the apoE chimeraplast somehow potentiated its effect. Nevertheless, the fact that these recombinant CHO cells were targetable whereas the CHO-LCAT$_{WT}$ cells were not may indicate that the location of cDNA integration in the nucleus does influence accessibility of chimeraplasts to target genes.

Successful mutation was once again seen when targeting CHO-EIL cells with single-stranded oligonucleotides aimed at the Ser216 location of LCAT. These molecules have been shown to be better at mediating gene correction than chimeraplasts [197,198], but are believed to use the same basic mechanisms. I also comfirmed the published findings that SSONs aimed at the non-transcribed strand result in up to nearly 20 times higher mutation frequencies than those aimed at the

transcribed strand [200]. The authors showed that this is due to less interference by RNA polymerase on the non-transcribed strand.

There are many more points to investigate in LCAT gene repair. My successful preliminary targeting work with the Ser216Ala chimeraplast in CHO-EIL and CHO-LE3 cells needs to be repeated with no apoE chimeraplast present, for reasons explained above, as well as targeting these cells with the Ser208Ala chimeraplast. Once successful targeting is established, the stability of the mutations needs to be assessed by passaging the cells and re-analysing for retention of the mutation. The SSONs need to be transfected into HepG2 cells, to see whether hepatocytes are sensitive to their effect, and if so, again to check the stability of the mutation after passaging. Once this has been established, mutated cells can be cloned and secreted LCAT studied for levels of activity as was done for the recombinant CHO cells.

The ultimate aim of this project was to test the viability of the chimeraplasty method in targeting the *LCAT* gene, and if successful to generate a HepG2 cell line expressing $LCAT_{S208A}$ or $LCAT_{S216A}$ with assumed higher enzymatic activity than wild-type LCAT. Previously published studies have shown LCAT variants resulting in reduced enzymatic activity that were naturally occurring or created by mutagenesis. Gain-of-function mutations in LCAT have so far only been the result of mutagenesis in recombinant cells. To have a human hepatocyte cell line expressing an LCAT gain-of-function mutation *in situ* is a novelty and of clear scientific value. In particular, the cells will be useful for studying LCAT structure-function relationships in a setting that is not engineered, such as when plasmids carrying cDNA are inserted into cells.

Moreover, the fact that this is achievable by the gene repair techniques used in this thesis encourages studies into *in vivo* gene manipulation. There are obvious advantages to using RDOs and SSONs rather than a viral vector approach. The molecules are relatively inexpensive to produce, are non-immunogenic and, as they target the endogenous gene, do not have the problem of producing low expression sometimes found with viral vectors. Successful *in situ* gene editing of LCAT in an animal model could open up a new avenue of anti-atherogenic treatment and has the potential to become a real gene therapy approach to atherosclerosis.

BIBLIOGRAPHY

1. British Heart Foundation 2004 Coronary Heart Disease Statistics Factsheet (available at: http://www.bhf.org.uk/professionals)
2. Stocker, R. and Keaney, J.F. Jr (2004) Role of oxidative modifications in atherosclerosis. *Physiol. Rev.* **84**, 1381-1478.
3. Libby, P. (2000) Changing concepts of atherogenesis. *J. Int. Med.* **247**,349-358.
4. Gu, L., Okada, Y., Clinton, S., Gerard, C., Sukhova, G.K., Libby, P., and Rollins, B.J. (1998) Absence of monocyte chemoattractant protein-1 reduces atherosclerosis in low-density lipoprotein deficient mice. *Mol. Cell.* **2**, 275-281.
5. Watson, A.D., Leitinger, N., Navab, M., Faull, K.F., Horkko, S., Witztum, J.L., Palinski, W., *et al.* (1997) Structural identification by mass spectrometry of oxidized phospholipids in minimally oxidized low density lipoprotein that induce monocyte/endothelial interactions and evidence for their presence in vivo. *J. Biol. Chem.* **272**, 597-607.
6. Witztum, J.L. and Berliner, J.A. (1998) Oxidized phospholipids and isoprostanes in atherosclerosis. *Curr. Opin. Lipidol.* **9**, 441-448.
7. Stary, H.C., Chandler, A.B., Glagov, S., Guyton, J.R., Insull, W. Jr, Rosenfeld, M.E., Schaffer, A., *et al.* (1994) A definition of initial, fatty streak, and intermediate lesions of atherosclerosis: a report from the Committee on Vascular Lesions of the Council on Atherosclerosis, American Heart Association. Special report. *Arterioscler. Thromb.* **14**, 840-856.
8. Stary, H.C., Chandler, A.B., Dinsmore, R.E., Fuster, V., Glagov, S., Insull, W. Jr, Rosenfeld, M.E., *et al.* (1995) A definition of advanced types of atherosclerotic lesions and a histologic classification of atherosclerosis. A report from the Committee on Vascular Lesions of the Council on Atherosclerosis, American Heart Association. *Arterioscler. Thromb. Vasc. Biol.* **15**, 1512-1531.
9. Corti, R., Hutter, R., Badimon, J.J., and Fuster, V. (2004) Evolving concepts in the triad of atherosclerosis, inflammation and thrombosis. *J. Thromb. Thrombolysis* **17**, 35-44.
10. Guzik, T.J., West, N.E., Black, E., McDonald, D., Ratnatunga, C., Pillai, R., and Channon, K.M. (2000) Vascular superoxide production by NAD(P)H oxidase: association with endothelial dysfunction and clinical risk factors. *Circ. Res.* **86**, E85-E90.
11. Podrez, E.A., Abu-Soud, H.M., and Hazen, S.L. (2000) Myeloperoxidase-generated oxidants and atherosclerosis. *Free Radic. Biol. Med.* **28**, 1717-1725.
12. Ylä-Herttuala, S., Rosenfeld, M.E., Parthasarathy, S., Glass, C.K., Sigal, E., Witztum, J.L., and Steinberg, D. (1990) Colocalization of 15-lipoxygenase mRNA and protein with epitopes of oxidized low density lipoprotein in macrophage-rich areas of atherosclerotic lesions. *Proc. Natl. Acad. Sci. U.S.A.* **87**, 6959-6963.
13. Garner, B., van Reyk, D., Dean R.T., and Jessup, W. (1997) Direct copper reduction by macrophages. Its role in low density lipoprotein oxidation. *J. Biol. Chem.* **272**, 6927-6935.
14. Brown, A.J. and Jessup, W. (1999) Oxysterols and atherosclerosis. *Atherosclerosis* **142**, 1-28.
15. Fu, S., Davies, M.J., Stocker, R., and Dean R.T. (1998) Evidence for roles of radicals in protein oxidation in advanced human atherosclerotic plaque. *Biochem J* **333**, 519-525.
16. Holvoet, P., Collen, D., and van de Werf, F. (1999) Malondialdehyde-modified LDL as a marker of acute coronary syndromes. *J.A.M.A.* **281**, 1721.

17. Aviram, M. (1996) Interaction of oxidized low density lipoprotein with macrophages in atherosclerosis, and the antiatherogenicity of antioxidants. *Eur. J. Clin. Chem. Clin. Biochem.* **34**, 599-608.
18. Chen, M., Masaki, T., and Sawamura, T. (2002) LOX-1, the receptor for oxidized low-density lipoprotein identified from endothelial cells: implications in endothelial dysfunction and atherosclerosis. *Pharmacol. Ther.* **95**, 89.
19. Mirami, M., Kume, N., Shimaoka, T., Kataoka, H., Hayashida, K., Yonehara, S., and Kita, T. (2001) Expression of scavenger receptor for phosphatidylserine and oxidized lipoprotein (SR-PSOX) in human atheroma. *Ann. N.Y. Acad. Sci.* **947**, 373-376.
20. Endemann, G., Stanton, L.W., Madden, K.S., Bryant, C.M., White, R.T., and Protter, A.A. (1993) CD36 is a receptor for oxidized low density lipoproteins. *J. Biol. Chem.* **268**, 11811-11816.
21. Acton, S.L., Scherer, P.E., Lodish, H.F., and Krieger, M. (1994) Expression cloning of SR-BI, a CD-36-related class B scavenger receptor. *J. Biol. Chem.* **269**, 21003-21009.
22. Silva, A.R., de Assis, E.F., Caiado, L.F., Marathe, G.K., Bozza, M.T., McIntyre, T.M., Zimmerman, G.A., *et al.* (2002) Monocyte chemoattractant protein-1 and 5-lipoxygenase products recruit leukocytes in response to platelet-activating factor-like lipids in oxidized low-density lipoprotein. *J. Immunol.* **168**, 4112-4120.
23. Lui, S.X., Chen, Y., Zhou, M., and Wan, J. (1998) Oxidized cholesterol in oxidized low density lipoproteins may be responsible for the inhibition of LPS-induced nitric oxide production in macrophages. *Atherosclerosis* **136**, 43-49.
24. Tsimikas, S. and Witztum, J.L. (200) The oxidative modification hypothesis of atherosclerosis. In Oxidative Stress and Vascular Disease, edited by Keaney, J.F. Kluwer, Boston, p. 49–74.
25. Mahley, R.W., Innerarity, T.L., Rall, S.C., and Weisgraber, K.H. (1984) Plasma lipoproteins: apolipopotein structure and function. *J. Lipid Res.* **25**, 1277-1294.
26. Li, W.H., Tanimura, M., Luo, C.C., Datta, S., and Chan, L. (1988) The apolipoprotein multigene family: biosynthesis, structure, structure-function relationships, and evolution. *J. Lipid Res.* **29**, 245-71.
27. Machness, M.I. and Durrington, P.N. (1992) Lipoprotein separation and analysis for clinical studies. In Lipoprotein Analysis, A Practical Approach, edited by Converse, C.A. and Skinner, E.R., Oxford University Press, Oxford, p. 1-2.
28. Kinnunen, P.K., Jackson, R.L., Smith, L.C., Gotto, A.M. Jr, and Sparrow, J.T. (1977) Activation of lipoprotein lipase by native and synthetic fragments of human plasma apolipoprotein C-II. *Proc. Natl. Acad. Sci. U.S.A.* **74**, 4848-4851.
29. Cooper, A.D. (1997) Hepatic uptake of chylomicron remnants. *J. Lipid Res.* **38**, 2173-2192.
30. McIlhargey, T.L., Yang, Y., Wong, H., and Hill, J.S. (2003) Identification of a lipoprotein lipase cofactor-binding site by chemical cross-linking and transfer of apolipoprotein C-II-responsive lipolysis from lipoprotein lipase to hepatic lipase. *J. Biol. Chem.* **278**, 23027-35.
31. Griffin, B.A., and Packard, C.J. (1994) Metabolism of VLDL and LDL subclasses. *Curr. Opin. Lipidol.* **5**,200-6.
32. Goldstein, J.L., and Brown, M.S. (1984) Progress in understanding the LDL receptor and HMG-CoA reductase, two membrane proteins that regulate the plasma cholesterol. *J. Lipid Res.* **25**, 1450-61.
33. Björkhem, I. (1992) Mechanism of degradation of the steroid side chain in the formation of bile acids. *J. Lipid Res.* **33**, 455-471.
34. Fredrickson, D. S., Altrocchi, P. H., Avioli, L. V., Goodman, D. S., and Goodman, H. C. (1961) Tangier disease. *Ann. Intern. Med.* **55**, 1016-1031.
35. Brooks-Wilson, A., Marcil, M., Clee, S. M., Zhang, L.-H., Roomp, K., van Dam, M., Yu, L., *et al.* (1999) Mutations in ABC1 in Tangier disease and familial high-density lipoprotein deficiency. *Nature Genet.* **22**, 336-345.

36. Wang, N., Silver, D.L., Thiele, C., and Tall, A.R. (2001) ATP-binding cassette transporter A1 (ABCA1) functions as a cholesterol efflux regulatory protein. *J. Biol. Chem.* **276**, 23742-23747.
37. Fielding, C.J., and Fielding, P.E. (1995) Molecular physiology of reverse cholesterol transport. *J. Lipid Res.* **36**, 211-228.
38. Out, R., Hoekstra, M., Spijkers, J.A.A., Kruijt, J.K., van Eck, M., Bos, I.S.T., Twisk, J., *et al.* (2004) Scavenger receptor class B type I is solely responsible for the selective uptake of cholesteryl esters from HDL by the liver and the adrenals in mice. *J. Lipid Res.* **45**, 2088-2095.
39. Wilson, P.W., Abbott, R.D., and Castelli, W.P. (1988) High density lipoprotein cholesterol and mortality. The Framingham Heart Study. *Arteriosclerosis* **8**, 737-741.
40. Assmann, G., Schulte, H., von Eckardstein, A., and Huang, Y. (1996) High-density lipoprotein cholesterol as a predictor of coronary heart disease risk. The PROCAM experience and pathophysiological implications for reverse cholesterol transport. *Atherosclerosis* **124**, 11-20.
41. Gordon, D.J., Probstfield, J.L., Garrison, R.J., Neaton, J.D., Castelli, W.P., Knoke, J.D., Jacobs, D.R. Jr, *et al.* (1989) High-density lipoprotein cholesterol and cardiovascular disease. Four prospective American studies. *Circulation* **79**, 8-15.
42. Rubens, H.B., Robins, S.J., Collins, D., Fye, C.L., Anderson, J.W., Elam, M.B., Faas, F.H., *et al.* (1999) Gemfibrozil for the secondary prevention of coronary heart disease in men with low levels of high-density lipoprotein cholesterol. Veterans Affairs High-Density Lipoprotein Cholesterol Interventions Trial Study Group. *N. Engl. J. Med.* **341**, 410-418.
43. Li, X.P., Zhao, S.P., Zhang, X.Y., Liu, L., Gao, M., and Zhou, Q.C. (2000) Protective effect of high density lipoproteins on endothelium-dependent vasodilatation. *Int. J. Cardiol.* **73**, 231-236.
44. Ota, Y., Kugiyama, K., Sugiyama, S., Matsumura, T., Terano, T., and Yasue, H. (1997) Complexes of apoA-I with phosphatidylcholine suppress dysregulation of arterial tone by oxidized LDL. *Ann. Physiol.* **273**, H1215-1222.
45. Uittenbogaard, A., Shaul, P.W., Yuhanna, I.S., Blair, A., and Smart, E.J. (2000) High density lipoprotein prevents oxidized low density lipoprotein-induced inhibition of endothelial nitric-oxide synthase localization and activation in caveolae. *J. Biol. Chem.* **275**, 11278-11283.
46. Nofer, J.-R., Kehrel, B., Fobker, M., Levkau, B., Assmann, G., and von Eckardstein, A. (2002) HDL and arteriosclerosis: beyond reverse cholesterol transport. *Atherosclerosis* **161**, 1-16.
47. Cockerill, G.W., Rye, K.A., Gamble, J.R., Vadas, M.A., and Barter, P.J. (1995) High-density lipoproteins inhibit cytokine-induced expression of endothelial cell adhesion molecules. *Arterioscler. Thromb. Vasc. Biol.* **15**, 1987-1994.
48. Riddell, D.R., Graham, A., and Owen, J.S. (1997) Apolipoprotein E inhibits platelet aggregation through the L-Arginine : nitric oxide pathway. *J. Biol. Chem.* **272**, 89-95.
49. Riddell, D.R., Vinogradov, D.V., Stannard, A.K., Chadwick, N., and Owen, J.S. (1999) Identification and characterisation of LRP8 (apoER2) in human blood platelets. *J. Lipid Res.* **40**, 1925-1930.
50. Nazih, H., Nazih-Sanderson, F., Magret, V., Caron, B., Goudemand, J., Fruchart, J.C., and Delbart, C. (1994) Protein kinase C-dependent desensitization of HDL_3 activated phospholipase C in human platelets. *Arterioscler. Thromb.* **14**: 1321-1326.
51. Nofer, J.-R., Tepel, M., Kehrel, B., Walter, M., Wierwille, S., Seedorf, U., Assmann, G., *et al.* (1996) High density lipoproteins enhance the Na^+/H^+ antiport in human platelets. *Thromb. Haemost.* **75**, 635-641.
52. Parthasarathy, S., Barnett, J., and Fong, L.G. (1990) High-density lipoprotein inhibits the oxidative modification of low-density lipoprotein. *Biochem. Biophys. Acta.* **1044**, 275-283.

53. Hayek, Y., Oiknine, J., Dankner, G., Brook, J.G., and Aviram, M. (1995) HDL apolipoprotein A-I attenuates oxidative modification of low density lipoprotein: studies in transgenic mice. *Eur. J. Clin. Chem. Clin. Bioch.* **33**, 721-725.
54. Mackness, M.I., Arrol, S., and Durrington, P.N. (1991) Paroxonase prevents accumulation of lipoperoxides in low-density lipoproteins. *FEBS Lett.* **286**, 152-154.
55. Aviram, M., Hardak, E., Vaya, J., Mahmood, S., Milo, S., Hoffmann, A., Billicke, S., *et al.* (2000) Human serum paraoxonase (PON1) Q and R selectively decrease lipid peroxides in human coronary artery and carotid atherosclerotic lesions: PON1 esterase and peroxide-like activities. *Circulation* **101**, 2510-2517.
56. Glomset, J.A. (1962) The mechanism of the plasma cholesterol esterification reaction: plasma fatty acid transferase. *Biochim. Biophys. Acta* **65**, 128-135.
57. Ollis, D.L., Cheah, E., Cygler, M., Dijkstra, B., Frolow, F., Franken, S., Harel, M., *et al.* (1992) The alpha/beta hydrolase fold. *Protein Eng.* **5**, 197-211.
58. Peelman, F., Vanaimont, N., Verhee, A., Vanloo, B., Verschelde, J.L., Labeur, C., Seguret-Mace, S., *et al.* (1998) A proposed architecture for lecithin:cholesterol acyl transferase (LCAT): identification of the catalytic triad and molecular modelling. *Protein Sci.* **7**, 587-599.
59. Adimoolam, S. and Jonas, A. (1997) Identification of a domain of lecithin-cholesterol acyltransferase that is involved in interfacial recognition. *Biochem. Biophys. Res. Commun.* **232**, 783-787.
60. Van Tilbeurgh, H., Egloff, M.-P., Martinez, C., Rugani, N., Verger, R., and Cambillau, C. (1993) Interfacial activation of the lipase-procolipase complex by mixed micelles revealed by x-ray crystallography. *Nature* **362**, 814-820.
61. Yang, Y.C. and Lowe, M.E. (2000) The open lid mediates pancreatic lipase function. *J. Lipid Res.* **41**, 48-57.
62. Francone, O.L., Evangelista, L., and Fielding, C.J. (1993). Lecithin-cholesterol acyltransferase: effects of mutagenesis at N-linked oligosaccharide attachment sites on acyl acceptor specificity. *Biochim. Biophys. Acta* **1166**, 301-304.
63. Qu, S.J., Fan, H.-Z., Blanco-Vaca, F., and Pownall, H.J. (1993) Roles of cysteines in human lecithin:cholesterol acyltransferase. *Biochemistry* **32**, 8732-8736.
64. Jonas, A. (2000) Lecithin cholesterol acyltransferase. *Biochim. Biophys. Acta* **1529**, 245-256.
65. Parks, J.S. and Gebre, A.K. (1997) Long-chain polyunsaturated fatty acids in the sn-2 position of phosphatidylcholine decrease the stability of recombinant high density lipoprotein apolipoprotein A-I and the activation energy of the lecithin:cholesterol acyltransferase reaction. *J. Lipid Res.* **38**, 266-275.
66. Zhao, Y., Gebre, A.K., and Parks, J.S. (2004) Amino acids 149 and 294 of human lecithin:cholesterol acyltransferase affect fatty acyl specificity. *J. Lipid Res.* **45**, 2310-2316.
67. Jin, L., Shieh, J.J., Grabbe, E., Adimoolam, S., Durbin, D., and Jonas, A. (1999) Surface plasmon resonance biosensor studies of human wild-type and mutant lecithin cholesterol acyltransferase interactions with lipoproteins. *Biochemistry* **38**, 15659-15665.
68. Adimoolam, S., Jin, L., Grabbe, E., Shieh, J.J., and Jonas, A. (1998). Structural and functional properties of two mutants of lecithin-cholesterol acyltransferase (T123I and N228K). *J. Biol. Chem.* **273**, 32561-32567.
69. Fielding, C.J., Shore, V.G., and Fielding, P.E. (1972) A protein cofactor of lecithin:cholesterol acyltransferase. *Biochem. Biophys. Res. Commun.* **46**, 1493-1498.
70. Daum, U., Leren, T.P., Langer, C., Chirazi, A., Cullen, P., Pritchard, P.H., Assmann, G., *et al.* (1999) Multiple dysfunctions of two apolipoprotein A-I variants, apoA-I (R160L) Oslo and apoA-I (P165R), that are associated with hypoalphalipoproteinemia in heterozygous carriers. *J. Lipid Res.* **40**, 486-494.

71. Roosbeek, S., Vanloo, B., Duverger, N., Caster, H., Breyne, J., De Beun, I., Patel, H., *et al.* (2001) Three arginine residues in apolipoprotein A-I are critical for activation of lecithin:cholesterol acyltransferase. *J. Lipid Res.* **42**, 31-40.
72. Kuivenhoven, J.A., Pritchard, H., Hill, J., Frohlich, J., Assmann, G., and Katelein, J. (1997). The molecular pathology of lecithin:cholesterol acyltransferase (LCAT) deficiency syndromes. J. *Lipid Res.* **38**, 191-205.
73. Liu, M., Subramanian, V.S., and Subbaiah, P.V. (1998) Modulation of the positional specificity of lecithin-cholesterol acyltransferase by the acyl group composition of its phosphatidylcholine substrate: role of the sn-1-acyl group. *Biochemistry* **37**, 13626-13633.
74. Szedlacsek, S.E., Wasowicz, E., Hulea, S.A., Nishida, H.I., Kummerow, F.A., and Nishida, T. (1995) Esterification of oxysterols by human plasma lecithin-cholesterol acyltransferase. *J. Biol. Chem.* **270**, 11812-11819.
75. Albers, J.J., Bergelin, R.O., Adolphson, J.L., and Wahl, P.W. (1982) Population-based reference values for lecithin-cholesterol acyltransferase (LCAT). *Atherosclerosis* **43**, 369-379.
76. Jonas, A. (1998) Regulation of lecithin cholesterol acyltransferase activity. *Prog. Lipid Res.* **37**, 209-234.
77. Kosek, A.B., Durbin, D., and Jonas, A. (1999) Binding affinity and reactivity of lecithin cholesterol acyltransferase with native lipoproteins. *Biochem. Biophys. Res. Commun.* **258**, 548-51.
78. Jonas, A., Zorich, N.L., Kezdy, K.E., and Trick, W.E. (1987) Reaction of discoidal complexes of apolipoprotein A-I and various phosphatidylcholines with lecithin cholesterol acyltransferase. Interfacial effects. *J. Biol. Chem.* **262**, 3969-3974.
79. Pownall, H.J., Pao, Q., and Massey, J.B. (1985) Acyl chain and headgroup specificity of human plasma lecithin:cholesterol acyltransferase. Separation of matrix and molecular specificities. *J. Biol. Chem.* **260**, 2146-2152.
80. Hoang, A., Huang, W., Sasaki, J., and Sviridov, D. (2003) Natural mutations of apolipoprotein A-I impairing activation of lecithin:cholesterol acyltransferase. *Biochim. Biophys. Acta* **1631**, 72-76.
81. Martin-Campos, J.M., Julve, J., Escola, J.C., Ordonez-Llanos, J., Gomez, J., Binimelis, J., Gonzalez-Sastre, F., *et al.* (2002) ApoA-I (MALLORCA) impairs LCAT activation and induces dominant familial hypoaplhalipoproteinemia. *J. Lipid Res.* **43**, 115-123.
82. Scott, B.R., McManus, D.C., Franklin, V., McKenzie, A.G., Neville, T., Sparks, D.L., and Marcel, Y.L. (2001) The N-terminal globular domain and the first class A amphipathic helix of apolipoprotein A-I are important for lecithin:cholesterol acyltransferase activation and the maturation of high density lipoprotein in vivo. *J. Biol. Chem.* **276**, 48716-48724.
83. Durbin, D.M., and Jonas, A. (1997) The effect of apolipoprotein A-II on the structure and function of apolipoprotein A-I in a homogeneous reconstituted high density lipoprotein particle. *J. Biol. Chem.* **272**, 31333-31339.
84. Lavallee, B., Provest, P.R., and Belanger, A. (1996) Formation of pregnenolone- and dehydroepiandrosterone-fatty acid esters by lecithin-cholesterol acyltransferase in human plasma high density lipoproteins. *Biochim. Biophys. Acta* **1299**, 306-312.
85. Lin, C.Y., and Morel, D.W. (1996) Esterification of oxysterols in human serum: effects on distribution and cellular uptake. *J. Lipid Res.* **37**, 168-178.
86. Czarnecka, H., and Yokoyama, S. (1993) Regulation of lecithin-cholesterol acyltransferase reaction by acyl acceptors and demonstration of its "idling" reaction. *J. Biol. Chem.* **268**, 19334-19340.
87. Atger, V., Kellner-Weibel, G., Williams, D.L., and Phillips, M.C. (1999) Cell cholesterol efflux: integration of old and new observations provides new insights. *J. Lipid Res.* **40**, 781-796.

88. Chung, B., Franklin, F., SimonCho, B., Segrest, J., Hart, K., and Darnell, B. (1998) Potencies of lipoproteins in fasting and postprandial plasma to accept additional cholesterol molecules released from cell membranes. *Arterioscler. Thromb. Vasc. Biol.* **18**, 1217-1230.
89. Miida, T., Fielding, C.J., and Fielding, P.E. (1990) Mechanism of transfer of LDL-derived free cholesterol to HDL subfractions in human plasma. *Biochemistry* **29**, 10469-10474.
90. Huang, Y., von Eckardstein, A., and Assmann, G. (1993) Cell-derived unesterified cholesterol cycles between different HDLs and LDL for its effective esterification in plasma. *Arterioscler. Thromb.* **13**, 445-458.
91. Francone, O.L., and Fielding, C.J. (1990) Initial steps in reverse cholesterol transport: the role of short-lived cholesterol acceptors. *Eur. Heart J.* **11**(Suppl E), 218-224.
92. Dobiasova, M., and Frohlich, J.J. (1999) Advances in understanding of the role of lecithin cholesterol acyltransferase (LCAT) in cholesterol transport. *Clin. Chim. Acta* **286**, 257-271.
93. Francone, O.L., Gurakar, A., and Fielding, C. (1989) Distribution and function of lecithin:cholesterol acyltransferase and cholesteryl ester transfer protein in plasma lipoproteins. *J. Biol. Chem.* **264**, 7066-7072.
94. Francone, O.L., Haghpassand, M., Bennett, J.A., Royer, L., and McNeish, J. (1997) Expression of human lecithin:cholesterol acyltransferase in transgenic mice: effects on cholesterol efflux, esterification, and transport. *J. Lipid Res.* **38**, 813-822.
95. Goyal, J., Wang, K., Liu, M., and Subbaiah, P.V. (1997) Novel function of lecithin-cholesterol acyltransferase. Hydrolysis of oxidized polar phospholipids generated during lipoprotein oxidation. *J. Biol. Chem.* **272**, 16231-16239.
96. Howlander, Z.H., Kamiyama, S., Shirakawa, H., Murakami, Y., Ito, M., Komai, M., Muramoto, K., *et al.* (2002) Detoxification of oxidized LDL by transferring its oxidation product(s) to lecithin:cholesterol acyltransferase. *Biochem. Biophys. Res. Commun.* **291**, 758-763.
97. Vohl, M.C., Neville, T.A.M., Kumarathasan, R., Braschi, S., and Sparks, D.L. (1999) A novel lecithin-cholesterol acyltransferase antioxidant acitivity prevents the formation of oxidized lipids during lipoprotein oxidation. *Biochemistry* **38**, 5976-5981.
98. Kamiyama, S., Yamato, T., and Furukawa, Y. (1998) Inhibitory effects of lipid oxidation on the activity of plasma lecithin-cholesterol acyltransferase. *Biosci. Biotechnol. Biochem.* **62**, 941-946.
99. Wang, K., and Subbaiah, P.V. (2000) Importance of the free sulfhydryl groups of lecithin-cholesterol acyltransferase for its sensitivity to oxidative inactivation. *Biochim. Biophys. Acta* **1488**, 268-277.
100. Wang, K., and Subbaiah, P.V. (2002) Role of the interfacial binding domain in the oxidative susceptibility of lecithin:cholesterol acyltransferase. *Biochem. J.* **365**, 649-657.
101. McLean, J., Fielding, C., Drayna, D., Dieplinger, H., Baer, B., Kohr, W., Henzel, W., *et al.* (1986) Cloning and expression of human lecithin-cholesterol acyltransferase cDNA. *Proc. Nat. Acad. Sci.* **83**, 2335-2339.
102. McLean, J., Wion, K., Drayna, D., Fielding, C., and Lawn, R. (1986) Human lecithin-cholesterol acyltransferase gene: complete gene sequence and sites of expression. *Nucleic Acids Res.* **14**, 9397-9406.
103. Azoulay, M., Henry, I., Tata, F., Weil, D., Grzeschik, K.H., Chaves, E., McIntyre, N., *et al.* (1987) The structural gene for lecithin:cholesterol acyltransferase (LCAT) maps to 16q22. *Ann. Hum. Genet.* **5**, 129-136.
104. Warden, C.H., Langner, C.A., Gordon, J.I., Taylor, B.A., McLean, J.W., and Lusis, A.J. (1989) Tissue-specific expression, developmental regulation, and chromosomal mapping of the lecithin:cholesterol acyltransferase gene. Evidence for expression in brain and testis as well as liver. *J. Biol. Chem.* **264**, 21573-21581.

104a. Hoppe, K.L and Francone, O.L. (1998) Binding and functional effects of transcription factors Sp1 and Sp3 on the proximal human lecithin:cholesterol acyltransferase promoter. *J. Lipid Res.* **39**, 969-977.
104b. Feister, H.A., Auerbach, B.J., Cole, L.A., Krause, B.R., and Karathanasis, S.K. (2002) Identification of an IL-6 response element in the human LCAT promoter. *J. Lipid Res.* **43**, 960-970.
105. Staels. B., van Tol, A., Skretting, G., and Auwerx, J. (1992) Lecithin:cholesterol acyltransferase gene expression is regulated in a tissue-specific manner by fibrates. *J. Lipid Res.* **33**, 727-735.
106. Skretting, G., Gjernes, E., and Pryde, H. (1995) Regulation of lecithin:cholesterol acyltransferase by TGF-beta and interleukin-6. *Biochim. Biophys. Acta* **1255**, 267-272.
107. Ly, H., Francone, O.L., Fielding, C.J., Shigenaga, J.K., Moser, A.H., Grunfeld, C., and Feingold, K.R. (1995). Endotoxin and TNF lead to reduced plasma LCAT activity and decreased hepatic LCAT mRNA in Syrian hamsters. *J. Lipid Res.* **36**, 1254-1263.
108. Gotoda, T., Yamada, N., Murase, T., Sakuma, M., Murayama, N., Shimano, H., Kozaki, K., *et al.* (1991) Differential phenotypic expression by three mutant alleles in familial lecithin:cholesterol acyltransferase deficiency. *Lancet* **338**, 778-781.
109. Norum, K.R., and Gjore, E. (1967) Familial plasma lecithin:cholesterol acyltransferase deficiency. *Scand. J. Clin. Lab. Invest.* **20**, 231-243.
110. Ayyobi, A.F., McGladdery, S.H., Chan, S., Mancini, G.B., Hill, J.S., and Frohlich, J.J. (2004) Lecithin:cholesterol acyltransferase (LCAT) deficiency and risk of vascular disease: 25 year follow-up. *Atherosclerosis* **177**, 361-366.
111. Carlson, L.A., and Philipson, B. (1979) Fish-eye disease: a new familial condition with massive corneal opacities and dyslipoproteinemia. *Lancet* **2**, 922-924.
112. Sakai, N., Vaisman, B.L., Koch, C.A., Hoyt, R.F., Meyn, S.M., Talley, G.D., Paiz, J.A., *et al.* (1997) Targeted disruption of the mouse lecithin:cholesterol acyltransferase (LCAT) gene. *J. Biol. Chem.* **272**, 7506-7510.
113. Hoeg, J.M., Santamarina-Fojo, S., Berard, A.M., Cornhill, J.F., Henderick, E.E., Feldman, S.H., Haudenschild, C.C., *et al.* (1996) Overexpression of lecithin:cholesterol acyltransferase in transgenic rabbits prevents diet-induced atherosclerosis. *Proc. Natl. Acad. Sci.* **93**, 11448-11453.
114. Brousseau, M.E., Kauffman, R.D., Henderick, E.E., Demosky, S.J. Jr, Evans, W., Marcovina, S., Santamarina-Fojo, S., *et al.* (2000) LCAT modulates atherogenic plasma lipoproteins and the extent of atherosclerosis only in the presence of normal LDL receptors in transgenic rabbits. *Arterioscler. Thromb. Vasc. Biol.* **20**, 450-458.
115. Berard, A.M., Foger, B., Remaley, A., Shamburek, R., Vaisman, B.L., Talley, G., Paigen, B., *et al.* (1997) High plasma HDL concentrations associated with enhanced atherosclerosis in transgenic mice overexpressing lecithin-cholesterol acyltransferase. *Nat. Med.* **3**, 744-749.
116. Foger, B., Chase, M., Amar, M.J., Vaisman, B.L., Shamburek, R.D., Paigen, B., Fruchard-Najib, J., *et al.* (1999). Cholesteryl ester transfer protein corrects dysfunctional high density lipoproteins and reduces aortic atherosclerosis in lecithin:cholesterol acyltransferase transgenic mice. *J. Biol. Chem.* **274**, 36912-36920.
117. Seguret-Mace, S., Latta-Mahieu, M., Castro, G., Luc, G., Fruchart, J.C., Rubin, E., Denefle, P., *et al.* (1996) Potential gene therapy for lecithin-cholesterol acyltransferase (LCAT)-deficient and hypoalphalipoproteinemic patients with adenovirus-mediated transfer of human LCAT gene. *Circulation* **94**, 2177-2184.
118. Fan, L., Drew, J., Dunckley, M.G., Owen, J.S., and Dickson, G. (1998) Efficient coexpression and secretion of anti-atherogenic human apolipoprotein AI and lecithin-cholesterol acyltransferase by cultured muscle cells using adeno-associated virus plasmid vectors. *Gene Ther.* **5**, 1434-1440.
119. Fan, L., Owen, J.S., and Dickson, G. (1999). Construction and characterization of polycystronic retrovirus vectors for sustained and high-level co-expression of

apolipoprotein A-I and lecithin-cholesterol acyltransferase. *Atherosclerosis* **147**, 139-145.
120. Miettinen, H.E., Gylling, H., Tenhunen, J., Virtamo, J., Jauhianen, M., Huttunen, J.L., Kantola, I., *et al.* (1998) Molecular genetic study of Finns with hypoalphalipoproteinemia and hyperalphalipoproteinemia - a novel Gly(230)Arg mutation (LCAT(Fin)) of lecithin:cholesterol acyltransferase (LCAT) accounts for 5% of cases with very low serum HDL cholesterol levels. *Arterioscler Thromb Vasc Biol* **18**, 591-198.
121. Kasid, A., Rhyne, J., Zeller, K., Pritchard, H., and Miller, M. (2001) A novel TC deletion resulting in Pro^{260}→Stop in the human LCAT gene is associated with a dominant effect on HDL-cholesterol. *Atherosclerosis* **156**, 127-132.
122. Francone, O.L., and Fielding, C.J. (1991) Structure-function relationships in human lecithin:cholesterol acyltransferase. Site-directed mutagenesis at serine residues 181 and 216. *Biochemistry* **30**, 10074-10077.
123. Farooqui, J.Z., Wohl, R., Kezdy, F.J., and Scanu, A.M. (1988) Identification of the active-site serine in human lecithin:cholesterol acyltransferase. *Arch. Biochem. Biophys.* **261**, 330-335.
124. Park, Y.B., Yuksel, K.U., Gracy, R.W., and Lacko, A.G. (1987) The catalytic center of lecithin:cholesterol acyltransferase: isolation and sequence of diisopropyl fluorophosphates-labelled particles. *Biochem. Biophys. Res. Commun.* **143**, 360-363.
125. Qu, S.-J., Fan, H.-Z., Blanco-Vaca, F., and Pownall, H.J. (1994) Effects of site-directed mutagenesis on the serine residues of human lecithin:cholesterol acyltransferase. *Lipids* **29**, 803-809.
126. Peelman, F., Vanloo, B., Verschelde, J.-L., Labeur, C., Caster, H., Taveirne, J., Vanhee, A., *et al.* (2001) Effect of mutations of N- and C-terminal charged residues on the activity of LCAT. *J. Lipid Res.* **42**, 471-479.
127. Stocks, J., Cooke, C.J., and Miller, N.E. (2000) A common lecithin:cholesterol acyltransferase gene variant (Ser^{208}→Thr). *Atherosclerosis* **149**, 219-220.
128. Pownall, H., Pao, Q., and Massey, J. (1985) Isolation and specificity of rat lecithin:cholesterol acyltransferase: comparison with the human enzyme using reassembled high-density lipoprotein containing ether analogs of phosphatidylcholine. *Biochem. Biophys. Acta* **833**, 456-462.
129. Wang, J., Gebre, A., Anderson R., and Parks, J. (1997) Amino acid residue 149 of lecithin:cholesterol acyltransferase determines phospholipase A2 and transacylase fatty acyl specificity. *J. Biol. Chem.* **272**, 280-286.
130. Furbee, J.W., Francone, O., and Parks, J.S. (2001) Alteration of plasma HDL cholesteryl ester composition with transgenic expression of a point mutation (E149A) of human LCAT. *J. Lipid Res.* **42**, 1626-1635.
131. Ryther, R.C.C., Flynt, A.S., Phillips, J.A. III, and Patton, J.G. (2005) siRNA therapeutics: big potential from small RNAs. *Gene Ther.* **12**, 5-11.
132. Wilda, M., Fuchs, U., Wossmann, W., and Borkhardt, A. (2002) Killing of leukemic cells with a BCR/ABL fusion gene by RNA interference (RNAi). *Oncogene* **21**, 5716-5724.
133. Crooke, R.M., Graham, M.J., Lemonidis, K.M., Whipple, C.P., Koo, S., and Perera, R.J. (2005) An apolipoprotein B antisense oligonucleotide lowers LDL cholesterol in hyperlipidaemic mice without causing hepatic steatosis. *J. Lipid Res.* **46**, 872-884.
134. Edelstein, M.L., Abedi, M.R., Wixon, J., and Edelstein, R.M. (2004) Gene therapy clinical trials worldwide 1989-2004 - an overview. *J. Gene Med.* **6**, 597-602.
135. Burns, J.C., Friedmann, T., Driever, W., Burrascano, M., and Yee, J.K. (1993) Vesicular stomatitis virus G glycoprotein pseudotyped retroviral vectors: concentration to very high titer and efficient gene transfer into mammalian and nonmammalian cell. *Proc. Natl. Acad. Sci.* **90**, 8033-8037.

136. Miller, D.G., Adam, M.A., and Miller, A.D. (1990) Gene transfer by retrovirus vectors occurs only in cells that are actively replicating at the time of infection. *Mol. Cell. Biol.* **10**, 4239-4242.
137. Cavazzana-Calvo, M., Hacein-Bey, S., and deSaint, B. (2000) Gene therapy of human severe combined immunodeficiency (SCID)-X1 disease. *Science* **288**, 669-672.
138. Hacein-Bey-Abina, S., von Kalle, C., Schmidt, M., McCormack, M.P., Wulffraat, N., Leboulch, P., Lim, A., *et al.* (2003) LMO2-associated clonal T cell proliferation in two patients after gene therapy for SCID-X1. *Science* **302**, 415-419.
139. Kaiser, J. (2005) Gene therapy. Panel urges limits on X-SCID trials. *Science* **307**, 1544-1545.
140. Bukrinsky, M.I., and Haffar, O.K. (1999) HIV-1 nuclear import: in search of a leader. *Front. Biosci.* **4**, 772-781.
141. Vigna, E., and Naldini, L. (2000) Lentiviral vectors: excellent tools for experimental gene transfer and promising candidates for gene therapy. *J. Gene Med.* **5**, 308-316.
142. Zufferey, R., Dull, T., Mandel, R.J., Bukovsky, A., Quiroz, D., Naldini, L., and Trono, D. (1998) Self-inactivating lentivirus vector for safe and efficient in vivo gene delivery. *J. Virol.* **72**, 9873-9880.
143. Kordower, J.H., Emborg, M.E., Bloch, J., Ma, S.Y., Chu, Y., Leventhal, L., McBride, J. *et al.* (2000) Neurodegeneration prevented by lentiviral vector delivery of GDNF in primate models of Parkinson's disease. *Science* **290**, 767-773.
144. Bosch, A., Perret, E., Desmaris, N., Trono, D., and Heard, J.M. (2000) Reversal of pathology in the entire brain of mucopolysaccharidosis type VII mice after lentivirus-mediated gene transfer. *Hum. Gene Ther.* **11**, 1139-1150.
145. Benihoud, K., Yeh, P., and Perricaudet, M. (1999). Adenovirus vectors for gene delivery. *Curr. Opin. Biotechnol.* **10**, 440-447.
146. Graham, F.L., Smiley, J., Russell, W.C., and Naim, R. (1977). Characteristics of a human cell line transformed by DNA from human adenovirus type 5. *J. Gen. Virol.* **36**, 59-74.
147. Lusky, M., Christ, M., Rittner, K., Dieterle, A., Dreyer, D., Mourot, B., Schultz, H., *et al.* (1998) In vitro and in vivo biology of recombinant adenovirus vectors with E1, E1/E2A, or E1/E4 deleted. *J. Virol.* **72**, 2022-2032.
148. Morsey, M.A. and Caskey, C.T. (1999) Expanded-capacity adenoviral vectors - the helper-dependent vectors. *Mol. Med. Today* **5**, 18-24.
149. Crystal, R., McElvaney, M., Rosenfeld, M., Chu, C., Mastrangeli, A., Hay, J., Brody, S., *et al.* (1994) Administration of an adenovirus containing the human CFTR cDNA to the respiratory tract of individuals with cystic fibrosis. *Nat. Genet.* **8**, 42-50.
150. Rosengart, T.K., Lee, L.Y., Patel, S.R., Sanborn, T.A., Parikh, M., Bergman, G.W., Hachamovitch, M., *et al.* (1999) Angiogenesis gene therapy: phase I assessment of direct intramyocardial administration of an adenovirus vector expressing VEGF121 cDNA to individuals with clinically significant severe coronary artery disease. *Circulation* **100**, 468-74.
151. NIH website. Available at: http://www4.od.nih.gov/oba/rac/clinicaltrial.htm
152. Raper, S.E., Chirmule, N., Lee, F.S., Wivel, N.A., Bagg, A., Gao, G.P., Wilson, J.M. *et al.* (2003) Fatal systemic inflammatory response syndrome in a ornithine transcarbamylase deficient patient following adenoviral gene transfer. *Mol. Genet. Metab.* **80**, 148-158.
153. Tal, J. (2000) Adeno-associated virus-based vectors in gene therapy. *J. Biomed. Sci.* **7**, 279-291.
154. Monahan, P.E. and Samulski, R.J. (2000) Adeno-associated virus vectors for gene therapy: more pros than cons? *Mol. Med. Today* **11**, 433-440.
155. Nakai, H., Yant, S.R., Storm, T.A., Fuess, S., Meuse, L., and Kay, M.A. (2001) Extrachromosomal recombinant adeno-associated virus vector genomes are primarily responsible for stable liver transduction in vivo. *J. Virol.* **75**, 6969-6976.

156. Rabinowitz, J.E., Rolling, F., Li, C., Conrath, H., Xiao, W., Xiao, X., and Samulski, R.J. (2002) Cross-packaging of a single adeno-associated virus (AAV) type 2 vector genome into multiple AAV serotypes enables transduction with broad specificity. *J. Virol.* **76**, 791-801.
157. Kay, M.A., Manno, C.S., Ragni, M.V., Larson, P.J., Couto, L.B., McClelland, A., Glader, B. *et al.* (2000) Evidence for gene transfer and expression of blood coagulation factor IX in patients with severe hemophilia B treated with an AAV vector. *Nat. Genet.* **24**, 257-261.
158. Stedman, H., Wilson, J.M., Finke, R., Kleckner, A.L., and Mendell, J. (2000) Phase I clinical trial utilizing gene therapy for limb girdle muscular dystrophy: α-, β-, or γ- or Δ-sarcoglycan gene delivered with intramuscular instillations of adeno-associated vectors. *Hum. Gen. Ther.* **11**, 777-790.
159. Wagner, J.A., Messner, A.H., Moran, M.L., Daifuku, R., Kouyama, K., Desch, J.K., Manley, S. *et al.* (1999) Safety and biological efficacy of an adeno-associated virus vector-cystic fibrosis transmembrane regulator (AAV-CFTR) in the cystic fibrosis maxillary sinus. *Laryngoscope* **109**, 266-274.
160. Krisky, D.M., Marconi, P.C., Oligino, T.J., Rouse, R.J., Fink, D.J., Cohen, J.B., Watkins, S.C. *et al.* (1998) Development of herpes simplex virus replication-defective multigene vectors for combination gene therapy applications. *Gene Ther.* **5**, 1517-1530.
161. Spaete, R., and Frenkel, N. (1982) The herpes simplex virus amplicon: a new eukaryotic defective-virus cloning amplifying vector. *Cell* **30**, 295-304.
162. Burton, E.A., and Glorioso, J.C. (2000) Herpes simplex vector-based gene therapy for malignant glioma. *Gene Ther. Mol. Biol.* **5**, 1-17.
163. Goss, J., Goins, W., Lacomis, D., Glorioso, J., and Fink, D. (1999) Effect of a modified herpes simplex virus expressing nerve growth factor on taxol-induced neuropathy in mice. *Ann Meet Soc Neurosci Absts* **29**, 2280.
164. Athanasopoulos, T., Owen, J.S., Hassall, D., Dunckley, M.G., Drew, J., Goodman, J., Tagalakis, A.D. *et al.* (2000) Intramuscular injection of a plasmid vector expressing human apolipoprotein E limits progression of xanthoma and aortic atheroma in apoE-deficient mice. *Hum. Mol. Genet.* **9**, 2545-2551.
165. Lekutis, C., Shriver, J.W., Liu, M.A., and Letvin, N.L. (1997) HIV-1 env DNA vaccine administered to rhesus monkeys elicits MHC class II-restricted CD4+ T helper cells that secrete IFN-gamma and TNF-alpha. *J. Immunol.* **158**, 4471-4477.
166. Izsvak, Z., and Ivics, Z. (2004) *Sleeping Beauty* transposition: biology and aaplications for molecular therapy. *Mol. Ther.* **9**, 147-156.
167. Yant, S.R., Meuse, L., Chiu, W., Ivics, Z., Izsvak, Z., and Kay, M.A. (2000) Somatic integration and long-term transgene expression in normal and haemophiliac mice using a DNA transposon system. *Nat. Genet.* **25**, 35-41.
168. Belur, L.R., Frandsen, J.L., Dupuy, A.J., Ingbar, D.H., Largaespada, D.A., Hackett, P.B., and Scott McIvor, R. (2003) Gene insertion and long-term expression in lung mediated by the *Sleeping Beauty* transposon system. *Mol. Ther.* **8**, 501-507.
169. Montini, E., Held, P.K., Noll, M., Morcinek, N., Al-Dhalimy, M., Finegold, M., Yant, S.R. *et al.* (2002) *In vivo* correction of murine tyrosinemia type I by DNA-mediated transposition. *Mol. Ther.* **6**, 759-769.
170. Hunger-Bertling, K., Harrer, P., and Bertling, W. (1990) Short DNA fragments induce site specific recombination in mammalian cells. *Mol. Cell. Biochem.* **92**, 107-116.
171. Sangiuolo, F., Bruscia, E., Serafino, A., Nardone, A.M., Bonifazi, E., Lais, M., Gruenert, D.C. *et al.* (2002) In vitro correction of cystic fibrosis epithelial cell lines by small fragment homologous replacement (SFHR) technique. *B.M.C. Med. Genet.* **3**, 8-19.

172. Goncz, K.K., Prokopishyn, N.L., Chow, B.L., Davis, B.R., and Gruenert, D.C. (2002). Application of SFHR to gene therapy of monogenic disorders. *Gene Ther.* **9**, 691-694.
173. Kapsa, R., Quigley, A., Lynch, G.S., Steeper, K., Kornberg, A.J., Gregorevic, P., Austin, L. *et al.* (2001) In vivo and in vitro correction of the mdx dystrophin gene nonsense mutation by short-fragment homologous replacement. *Hum. Gene Ther.* **12**, 629-642.
174. Richardson, P.D., Kren, B.T., and Steer, C.J. (2002) Gene repair in the new age of gene therapy. *Hepatology* **35**, 512-518.
175. Strobel, S.A. and Dervan, P.B. (1992) Triple helix-mediated single-site enzymatic cleavage of megabase genomic DNA. *Methods Enzymol.* **216**, 309-321.
176. Wang, G., Seidman, M.M., and Glazer, P.M. (1996) Mutagenesis in mammalian cells induced by triple helix formation and transcription-coupled repair. *Science* **271**, 802-805.
177. Ebbinghaus, S.W., Vigneswaran, N., Miller, C.R., Chee-Awai, R.A., Mayfield, C.A., Curiel, D.T., and Miller, D.M. (1996) Efficient delivery of triplex forming oligonucleotides to tumor cells by adenovirus-polylysine complexes. *Gene Ther.* **3**, 287-297.
178. Goñi, J.R., de la Cruz, G., and Orozco, M. (2004) Triplex-forming oligonucleotide target sequences in the human genome. *Nucleic Acids Res.* **32**: 354-360.
179. Yoon, K., Cole-Strauss, A., and Kmiec, E.B. (1996) Targeted gene correction of episomal DNA in mammalian cells mediated by a chimeric RNA.DNA oligonucleotide. *Proc. Natl. Acad. Sci. U.S.A.* **93**, 2071-2076.
180. Kotani, H., Germann, M.W., Andrus, A., Vinayak, R., Mullah, B., and Kmiec, E.B. (1996) RNA facilitates RecA-mediated DNA pairing and strand transfer between molecules bearing limited regions of homology. *Mol. Gen. Genet.* **250**, 626-634.
181. Cole-Strauss, A., Yoon, K., Xiang, Y., Byrne, B.C., Rice, M.C., Gryn, J., Holloman, W.K., and Kmiec, E.B. (1996) Correction of the mutation responsible for sickle cell anemia by an RNA-DNA oligonucleotide. *Science* **273**, 1386-1389.
182. Kren, B.T., Cole-Strauss, A., Kmiec, E.B., and Steer, C.J. (1997) Targeted nucleotide exchange in the alkaline phosphatase gene of Huh-7 cells mediated by a chimeric RNA/DNA oligonucleotide. *Hepatology* **25**, 1462-1468.
183. Kren, B.T., Bandyopadhyay, P., and Steer, C.J. (1998) In vivo site-directed mutagenesis of the factor IX gene by chimeric RNA/DNA oligonucleotides. *Nat. Med.* **4**, 285-290.
184. Alexeev, V., and Yoon, K. (1998) Stable and inheritable changes in genotype and phenotype of albino melanocytes induced by an RNA-DNA oligonucleotide. *Nat. Biotechnol.* **16**, 1343-1346.
185. Zhang, Z., Erriksson, M., Falke, G., Graff, C., Presnell, S.C., Read, M.S., Nichols, T.C., *et al.* (1998) Failure to achieve gene conversion with chimeric circular oloigonucleotides: Potentially misleading PCR artefacts observed. *Antisense and Nucl. Av. Drug. Dev.* **8**, 531-536.
186. Tagalakis, A.D., Dickson, J.G., Owen, J.S., and Simons, J.P. (2005) Correction of the neuropathogenic human apolipoprotein E4 (APOE4) gene to APOE3 in vitro using synthetic RNA/DNA oligonucleotides (chimeraplasts). *J. Mol. Neurosci.* **25**, 95-104.
187. Santana, E., Peritz, A.E., Iyer, S., Uitto, J., and Yoon, K. (1998) Different frequency of gene targeting events by the RNA-DNA oligonucleotide among epithelial cells. *J. Invest. Dermatol.* **111**, 1172-1177.
188. Kren, B.T., Parashar, B., Bandyopadhyay, P., Chowdhury, N.R., Chowdhury, J.R., and Steer, C.J. (1999) Correction of the UDP-glucuronosyltransferase gene defect in the Gunn rat model of Crigler-Najjar syndrome type I with a chimeric oligonucleotide. *Proc. Natl. Acad. Sci. U.S.A.* **96**, 10349-10354.
189. Bartlett, R.J., Stockinger, S., Denis, M.M., Bartlett, W.T., Inverardi, L., Le, T.T., thi Man, N. *et al.* (2000) In vivo targeted repair of a point mutation in the canine

dystrophin gene by a chimeric RNA/DNA oligonucleotide. *Nat. Biotechnol.* **18**, 615-622.
190. Beetham, P.R., Kipp, P.B., Sawycky, X.L., Arnzen, C.J., and May, G.D. (1999) A tool for functional plant genomics: Chimeric RNA/DNA oligonucleotides cause in vivo gene-specific mutations. *Proc. Natl. Acad. Sci. U.S.A.* **96**, 8774-8778.
191. Tagalakis, A.D., Graham, I.R., Riddell, D.R., Dickson, J.G., and Owen, J.S. (2001) Gene correction of the apolipoprotein (apo)E2 phenotype to wild-type apoE3 by in situ chimeraplasty. *J. Biol. Chem.* **276**, 13226-13230.
192. Cole-Strauss, A., Gamper, H., Holloman, W.K., Munoz, M., Cheng, N., and Kmiec, E.B. (1999) Targeted gene repair directed by the chimeric RNA/DNA oligonucleotide in a mammalian cell-free extract. *Nucleic Acids Res.* **27**, 1323-1330.
193. Gamper, H.B., Cole-Strauss, A., Metz, R., Parekh, H., Kumar, R., and Kmiec, E.B. (2000) A plausible mechanism for gene correction by chimeric oligonucleotides. *Biochemistry* **39**, 5808-5816.
194. Rice, M.C., Bruner, M., Czymmek, K., and Kmiec, E.B. (2001) *In vitro* and *in vivo* nucleotide exchange directed by chimeric RNA/DNA oligonucleotides in *Saccharomyces cerevisiae*. *Mol. Microbiol.* **40**, 857-868.
195. Igoucheva, O., Alexeev, V., and Yoon, K. (2002). Nuclear extracts promote gene correction and strand pairing of oligonucleotides to the homologous plasmid. *Antisense Nucleic Acids Drug Dev.* **12**, 235-246.
196. Rice, M.C., Czymmek, K., and Kmiec, E.B. (2001) The potential of nucleic acid repair in functional genomics. *Nat. Biotechnol.* **19**, 19321-19326.
197. Thorpe, P.H., Stevenson, B.J., and Porteous, D.J. (2002) Functional correction of episomal mutations with short DNA fragments and RNA-DNA oligonucleotides. *J. Gene Med.* **4**, 195-204.
198. Gamper, H.B., Parekh, H., Rice, M.C., Bruner, M., Youkey, H., and Kmiec, E.B. (2000) The DNA strand of RNA/DNA oligonucleotides can direct gene repair/conversion activity in mammalian and plant cell-free extracts. *Nucleic Acids Res.* **28**, 4332-4339.
199. Liu, L., Rice, M.C., and Kmiec, E.B. (2001) In vivo gene repair of point and frameshift mutations directed by chimeric RNA/DNA oligonucleotides and modified single-stranded oligonucleotides. *Nucleic Acids Res.* **29**, 4238-4250.
200. Liu, L., Rice, M.C., Drury, M., Cheng, S., Gamper, H., and Kmiec, E.B. (2002) Strand bias in targeted gene repair is influenced by transcriptional activity. *Mol. Cell Biol.* **22**, 3852-3863.
201. Ferrera, L. and Kmiec, E.B. (2004) Camptothecin enhances the frequency of oligonucleotide-directed gene repair in mammalian cells by inducing DNA damage and activating homologous recombination. *Nucleic Acids Res.* **32**, 5239-5248.
202. Brachman, E.E. and Kmiec, E.B. (2005) Gene repair in mammalian cells is stimulated by the elongation of S phase and transient stalling of replication forks. *DNA Repair* **4**, 445-457.
203. Liu, L., Maguire, K.K., and Kmiec, E.B. (2004) Genetic re-engineering of *Saccharomyces cerevisiae* RAD51 leads to a significant increase in the frequency of gene repair *in vivo*. *Nucleic Acids Res.* **32**, 2093-2101.
204. Parekh-Olmedo, H. and Kmiec, E.B. (2003) Targeted nucleotide exchange in the CAG repeat region of the human HD gene. *Biochem. Biophys. Res. Commun.* **310**, 660-666.
205. Yin, W., Kren, B.T., and Steer, C.J. (2005) Site-directed base changes in the coding or promoter region of the human beta and gamma globin genes by single-stranded oligonucleotides. *Biochem. J.* [epub only at time of print].
206. Danko, I., Jia, Z., and Zhang, G. (2004) Nonviral gene transfer into liver and muscle for treatment of hyperbilirubinemia in the gunn rat. *Hum. Gene Ther.* **15**, 1279-1286.

207. Inoue, S., Hakamata, Y., Kaneko, M., and Kobayashi, E. (2004) Gene therapy for organ grafts using rapid injection of naked DNA: application to the rat liver. *Transplantation* **15**, 997-1003.
208. Chesnoy, S. and Huang, L. (2002) Enhanced cutaneous gene delivery following intradermal injection of naked DNA in a high ionic strength solution. *Mol. Ther.* **5**, 57-62.
209. Kawase, A., Nomura, T., Yasuda, K., Kobayashi, N., Hashida, M., and Takakura, Y. (2003) Disposition and gene expression characteristics in solid tumors and skeletal muscle after direct injection of naked plasmid DNA in mice. *J. Pharm. Sci.* **92**, 1295-1304.
210. Gehl, J. (2003) Electroporation: theory and methods, perspectives for drug delivery, gene therapy and research. *Acta Physiol. Scand.* **177**, 437-447.
211. Heller, R., Schultz, J., Lucas, M.I., Jaroszeski, M.J., Heller, L.C., Gilbert, R.A., Moelling, K. *et al.* (2001) Intradermal delivery of interleukin-12 plasmid DNA by in vivo electroporation. *DNA Cell Biol.* **20**, 21-26.
212. Mir, L.M., Bureau, M.F., Gehl, J., Rangara, R., Rouy, D., Caillaud, J.M., Delaere, P., *et al.* (1999) High efficiency gene transfer into skeletal muscle mediated by electric pulses. *Proc. Natl. Acad. Sci. U.S.A.* **96**, 4262-4267.
213. Heller, R., Jaroszeski, M., Atkin, A., Moradpour, D., Gilbert, R., Wands, J., and Nicolau, C. (1996) In vivo gene electroinjection and expression in rat liver. *FEBS Lett.* **389**, 225-228.
214. Lawrie, A., Brisken, A.F., Francis, S.E., Tayler, D.I., Chamberlain, J., Crossman, D.C., Cumberland, D.C., and Newman, C.M. (1999) Ultrasound enhanced reporter gene expression after transfection of vascular cells in vitro. *Circulation* **99**, 2617-2620.
215. Klein, T.M., Wolf, E.D., Wu, R., and Sanford, J.C. (1987) High-velocity microprojectiles for delivering nucleic acids into living cells. *Nature* **327**, 70-73.
216. Zelenin. A.V., Kolesnikov, V.A., Tarasenko, O.A., Shafei, R.A., Zelenina, I.A., Mikhailov, V.V., Semenova, M.L., *et al.* (1997) Bacterial beta-galactosidase and human dystrophin genes are expressed in mouse skeletal muscle fibers after ballistic transfection. *FEBS Lett.* **414**, 319-322.
217. Gnirke, A., Huxley, C., Peterson, K., and Olson, M.V. (1993) Microinjection of intact 200- to 500-kb fragments of YAC DNA into mammalian cells. *Genomics* **15**, 659-667.
218. Gordon, J.W. and Ruddle, F.H. (1981) Integration and stable germ line transmission of genes injected into mouse pronuclei. *Science* **214**, 1244-1246.
219. Perry, A.C., Wakayama, T., Kishikawa, H., Kasai, T., Okabe, M., Toyoda, Y., and Yanagimachi, R. (1999) Mammalian transgenesis by intracytoplasmic sperm injection. *Science* **284**, 1180-1183.
220. Orrantia, E. and Chang, P.L. (1990) Intracellular distribution of DNA internalized through calcium phosphate precipitation. *Exp. Cell Res.* **190**, 170-174.
221. Hasan, M.T., Subbaroyan, R., and Chang, T.Y. (1991) High-efficiency stable gene transfection using chloroquine-treated Chinese hamster ovary cells. *Somat. Cell Mol. Genet.* **17**, 513-517.
222. Liu, F., Qi, H., Huang, L., and Liu, D. (1997) Factors controlling the efficiency of cationic lipid-mediated transfection in vivo via intravenous administration. *Gene Ther.* **4**, 517-523.
223. Meyer, O., Kirpotin, K., Hong, B., Sternberg, J.W., Park, M.C., Woodle, D., and Papahadjopoulos, D. (1998) Cationic liposomes coated with polyethylene glycol as carriers for oligonucleotides. *J. Biol. Chem.* **273**, 15621-15627.
224. Dass, C.R. (2004) Lipoplex-mediated delivery of nucleic acids: factors affecting in vivo transfection. *J. Mol. Med.* **82**, 579-591.
225. Bloomfield, V.A. (1996) DNA condensation. *Curr. Opin. Struc. Biol.* **6**, 334-341.
226. Pouton, C.W., Lucas, P., Thomas, B.J., Uduehi, A.N., Milroy, D.A., and Moss, S.H. (1998) Polycation-DNA complexes for gene delivery: a comparison of the

biopharmaceutical properties of cationic polypeptides and cationic lipids. *J. Control. Release* **53**, 289-299.
227. Tang, M.X. and Szoka, F.C. (1997) The influence of polymer structure on the interactions of cationic polymers with DNA and morphology of the resulting complexes. *Gene Ther.* **4**, 823-832.
228. Boussif, O., Lezoualc'h, F., Zanta, M.A., Mergny, M.D., Scherman, D., Demeneix, B., and Behr, J.P. (1995) A versatile vector for gene and oligonucleotide transfer into cells in culture and *in vivo*: Polyethylenimine. *Proc. Natl. Acad. Sci. U.S.A.* **92**, 7297-7301.
229. Godbey, W.T., Wu, K.K., and Mikos, A.G. (1999) Tracking the intracellular path of poly(ethylenimine)/DNA complexes for gene delivery. *Proc. Natl. Acad. Sci. U.S.A.* **96**, 5177-5181.
230. Bieber, T., Messner, W., Kostin, S., Niemann, A., and Elsasser, H.P. (2002) Intracellular route and transcriptional competence of polyethylenimine-DNA complexes. *J. Contol. Release* **82**, 441-454.
231. Boussif, O., Zanta, M.A., and Behr, J.-P. (1996) Optimized galenics improve *in vitro* gene transfer with cationic molecules up to 1000-fold. *Gene Ther.* **3**, 1074-1080.
232. Abdallah, B., Hassan, A., Benoist, C., Goula, D., Behr, J.P., and Demeneix, B.A. (1996) A powerful non-viral vector for *in vivo* gene transfer into the adult mammalian brain: polyethylenimine. *Hum. Gene Ther.* **7**, 1947-1954.
233. Miskick, K.A. and Baldeschweiler, J.D. (1996) Evidence for the role of proteoglycans in cationic-mediated gene transfer. *Proc. Natl. Acad. Sci. U.S.A.* **93**, 12349-12354.
234. Ogris, M., Brunner, S., Schuller, S., Kircheis, R., and Wagner, E. (1999) PEGylated DNA/transferrin-PEI complexes: reduced interaction with blood components, extended circulation in blood and potential for systemic gene delivery. *Gene Ther.* **6**, 595-605.
235. Chollet, P., Favrot, M.C., Hubrin, A., and Coll, J.L. (2002) Side-effects of a systemic injection of linear polyethylenimine-DNA complexes. *J. Gene Med.* **4**, 84-91.
236. Petersen, H., Fechner, P.M., Martin, A.L., Kunath, K., Stolnik, S., Roberts, C.J., Fischer, D. *et al.* (2002) Polyethylenimine-graft-poly(ethylene glycol) copolymers: influence of copolymer block structure on DNA complexation and biological activities as gene delivery system. *Bioconjug. Chem.* **13**, 845-854.
237. Kichler, A., Chillon, M., Leborgne, C., Danos, O., and Frisch, B. (2002) Intranasal gene delivery with a polyethylenimine-PEG conjugate. *J. Control. Release* **81**, 379-388.
238. Zanta, M.A., Boussif, O., Adib, A., and Behr, J.-P. (1997) In vitro gene delivery to hepatocytes with galactosylated polyethylenimine. *Bioconjug. Chem.* **8**, 839-844.
239. Diebold, S.S., Lehrmann, H., Kursa, M., Wagner, E., Cotton, M., and Zenke, M. (1999) Efficient gene delivery into human dendritic cells by adenovirus polyethylenimine and mannose polyethylenimine transfection. *Hum. Gene Ther.* **10**, 775-786.
240. Rudolph, C., Schillinger, U., Plank, C., Gessner, A., Nicklaus, P., Muller, R., and Rosenecker, J. (2002) Nonviral gene delivery to the lung with copolymer-protected and transferrin-modified polyethylenimine. *Biochim. Biophys. Acta* **1573**, 75-83.
241. Blessing, T., Kursa, M., Holzhauer, R., Kircheis, R., and Wagner, E. (2001) Different strategies for formation of pegylated EGF-conjugated PEI/DNA complexes for targeted gene delivery. *Bioconjug. Chem.* **12**, 529-537.
242. Ogris, M., Carlisle, R.C., Bettinger, T., and Seymour, L.W. (2001) Melittin enables efficient vesicular escape and enhanced nuclear access of nonviral gene delivery vectors. *J. Biol. Chem.* **276**, 47550-47555.
243. Sochanik, A., Cichon, T., Makselon, M., Strozyk, M., Smolarczyk, R., Jazowiecka-Rakus, J., and Szala, S. (2004) In vivo gene transfer using cetylated polyethylenimine. *Acta Biochim. Pol.* **51**, 693-702.

244. Furgeson, D.Y., Yockman, J.W., Janat, M.M., and Kim, S.W. (2004) Tumor efficacy and biodistribution of linear polyethylenimine-cholesterol/DNA complexes. *Mol. Ther.* **9**, 837-845.
245. Kim, H.W., Park, I.K., Cho, C.S., Lee, K.H., Beck, G.R. Jr, Colburn, N.H., and Cho, M.H. (2004) Aerosol delivery of glucosylated polyethylenimine/phosphatase and tensin homologue deleted on chromosome 10 complex suppresses Akt downstream pathways in the lung of K-ras null mice. *Cancer Res.* **64**, 7971-7976.
246. Sambrook, J., Fritsch, E.F., and Maniatis, T. (1989) Gel electrophoresis of DNA. In Molecular Cloning: A Laboratory Manual. Cold Harbor Springs Publications, New York, p 6.1-6.62.
247. Sambrook, J., Fritsch, E.F., and Maniatis, T. (1989) In vitro amplification of DNA by the polymerase chain reaction. In Molecular Cloning: A Laboratory Manual. Cold Harbor Springs Publications, New York, p 14.1-14.22.
248. Sambrook, J., Fritsch, E.F., and Maniatis, T. (1989) Enzymes used in molecular cloning. In Molecular Cloning: A Laboratory Manual. Cold Harbor Springs Publications, New York, p 5.3-5.32.
249. Promega Subcloning Notebook, available at: http://www.promega.com/guides/subcloning_guide/_euro/subcloning_notebook_euro.pdf.
250. Hanahan, D. (1983) Studies on transformation of Escherichia coli with plasmids. *J. Mol. Biol.* **166**, 557-580.
251. Hames, B. D., ed. (1998) Gel Electrophoresis of Proteins: A Practical Approach 3rd ed., Oxford University Press, New York.
252. Vinogradov, D.V., Hongqun, L., and Owen, J.S. (1998) C-terminal His6-tagged lecithin-cholesterol acyltransferase (LCAT) is catalytically active. *Biochem. Soc. Trans.* **26**, S146.
253. Colbere-Garapin, F., Horodniceanu, F., Kourilsky, P., and Garapin, A. (1981) A new dominant selective marker for higher eukaryotic cells. *J. Mol. Biol.* **150**, 1-14.
254. Koizumi, J., Kano, M., Okabayashi, K., Jadhav, A., and Thompson, G.R. (1988) Behavior of human apolipoprotein A-I:phospholipids and apoHDL:phospholipids complexes in vitro and after injection into rabbits. *J. Lipid Res.* **29**, 1405-1415.
255. Vadiveloo, P.K. and Fidge, N.H. (1990) Studies on the interaction between apolipoprotein A-II enriched HDL3 and cultured bovine endothelial (BAE) cells. *Biochim. Biophys. Acta* **1045**, 135-141.
256. Mackness, M.I. and Durrington, P.N. (1992) Lipoprotein separation and analysis for clinical studies. In Lipoprotein Analysis - A Practical Approach. Oxford University Press, Oxford.
257. Chen, C. and Albers, J.J. (1982) Characterization of proteoliposomes containing apolipoprotein A-I: a new substrate for the measurement of lecithin:cholesterol acyltransferase activity. *J. Lipid Res.* **23**, 680-691.
258. Miller, K.R., Wang, J., Sorci-Thomas, M., Anderson, R.A., and Parks, J.S. (1996) Glycosylation structure and enzyme activity of lecithin:cholesterol acyltransferase from human plasma, HepG2 cells, and baculoviral and Chinese hamster ovary cell expression systems. *J. Lipid Res.* **37**, 551-561.
259. Miloux, B. and Lupker, J.H. (1994) Rapid isolation of highly productive recombinant Chinese Hamster Ovary cell lines. *Gene* **149**, 341-344.
260. Shaw, G. and Kamen, R. (1986) A conserved AU sequence from the 3' untranslated region of GM-CSF mRNA mediates selective mRNA degradation. Cell **46**, 659-667.
261. Old, R.W. and Primrose, S.B. (1994) Introducing genes into animal cells. In Principles of Gene Manipulation. Blackwell Science, Oxford, p 302-345.
261a. Schindler, P.A., Settineri, C.A., Collet, X., Fielding, C.J., and Burlingame, A.L. (1995) Site-specific detection and structural characterization of the glycosylation of human plasma proteins lecithin:cholesterol acyltransferase and apolipoprotein D using

HPLC/electrospray mass spectrometry and sequential glycosidase digestion. *Protein Sci.* **4**, 719-803.
262. Fielding, C.J. and Fielding, P.E. (1971) Purification and substrate specificity of lecithin:cholesterol acyltransferase from human plasma. *FEBS Lett.* **15**, 355-358.
263. Adimoolam, S., Jin, L., Grabbe, E., Shieh, J.J., and Jonas, A. (1998) Structural and functional properties of two mutants of lecithin-cholesterol acyltransferase (T123I and N228K). *J. Biol. Chem.* **273**, 32561-32567.
264. Kosek, A.B., Durbin, D., and Jonas, A. (1999) Binding affinity and reactivity of lecithin cholesterol acyltransferase with native lipoproteins. *Biochem. Biophys. Res. Commun.* **285**, 548-551.
265. Matz, C. and Jonas, A. (1982) Reaction of human lecithin cholesterol acyltransferase with synthetic micellar complexes of apolipoprotein A-I, phosphatidylcholine, and cholesterol. *J. Biol. Chem.* **257**, 4541-4546.
266. Nichols, A.V. and Gong, E.L. (1971) Use of sonicated dispersions of mixtures of cholesterol with lecithin as substrates for lecithin:cholesterol acyltransferase. *Biochim. Biophys. Acta* **231**, 175-184.
267. Erbacher, P., Roche, A.C., Monsigny, M., and Midoux, P. (1996) Putative role of chloroquine in gene transfer into a human hepatoma cell line by DNA/lactosylated polylysine complexes. *Exp. Cell Res.* **225**, 186-194.
268. Kim, A., Lee, E.H., Choi, S.H., and Kim, C.K. (2004) In vitro and in vivo transfection efficiency of a novel ultradeformable cationic liposome. *Biomaterials* **25**, 305-313.
269. Pelisek, J., Engelmann, M.G., Golda, A., Fuchs, A., Armeanu, S., Shimizu, M., Mekkaoui, C., Rolland, P.H., and Nikol, S. (2002) Optimization of nonviral transfection: variables influencing liposome-mediated gene transfer in proliferating vs. quiescent cells in culture and in vivo using a porcine restenosis model. *J. Mol. Med.* **80**, 724-736.
270. Kichler, A., Leborgne, C., Coeytaux, E., and Danos, O. (2001) Polyethylenimine-mediated gene delivery: a mechanistic approach. *J. Gene Med.* **3**, 135-144.
271. Godbey, W.T., Barry, M.A., Saggau, P., Wu, K.K., and Mikos, A.G. (2000) Poly(ethylenimine)-mediated transfection: A new paradigm for gene delivery. *J. Biomed. Mater. Res.* **51**, 321-328.
272. Igoucheva, O., Peritz, A.E., Levy, D., and Yoon, K. (1999) A sequence-specific gene correction by an RNA-DNA oligonucleotide in mammalian cells characterized by transfection and nuclear extract using a lacZ shuttle system. *Gene Ther.* **6**, 1960-1971.
273. de Semir, D., Petriz, J., Avinyo, A., Larriba, S., Nunes, V., Casals, T., Estivill, X., *et al.* (2002) Non-viral vector-mediated uptake, distribution, and stability of chimeraplasts in human airway epithelial cells. *J. Gene Med.* **4**, 308-322.
274. Godbey, W.T., Wu, K.K., and Mikos, A.G. (1999) Size matters: Molecular weight affects the efficiency of poly(ethylenimine) as a gene delivery vehicle. *J. Biomed. Mater. Res.* **45**, 268-275.
275. Ogris, M., Steinlein, P., Carotta, S., Brunner, S., and Wagner, E. (2001) DNA/polyethylenimine transfection particles: Influence of ligands, polymer size, and PEGylation on internalization and gene expression. *A.A.P.S. Pharm.Sci.* **3**, E21.
276. Ponka, P. and Lok, C.N. (1999) The transferrin receptor: role in health and disease. *Int. J. Biochem. Cell Biol.* **31**, 1111-1137.
277. Wightman, L., Kircheis, R., Rössler, V., Carotta, S., Ruzicka, R., Kursa, M., and Wagner, E. (2001) Different behaviour of branched and linear polyethylenimine for gene delivery *in vitro* and *in vivo*. *J. Gene Med.* **3**, 362-372.
278. Godbey, W.T., Wu, K.K., and Mikos, A.G. (1999) Poly(ethyleneimine) and its role in gene delivery. *J. Control. Release* **60**, 149-160.
279. Brunner, S., Furtbauer, E., Sauer, T., Kursa, M., and Wagner, E. (2002) Overcoming the nuclear barrier: cell cycle independent nonviral gene transfer with linear polyethylenimine or electroporation. *Mol. Ther.* **5**, 80-86.

280. Choosakoonkriang, S., Lobo, B.A., Koe, G.S., Koe, J.G., and Middaugh, C.R. (2003) Biophysical characterization of PEI/DNA complexes. *J. Pharm. Sci.* **92**, 1710-1722.
281. Kunath, K., von Harpe, A., Fischer, D., Petersen, H., Bickel, U., Voigt, K., and Kissel, T. (2003) Low-molecular-weight polyethylenimine as a non-viral vector for DNA delivery: comparison of physicochemical properties, transfection efficiency and in vivo distribution with high-molecular-weight polyethylenimine. *J. Control. Release* **89**, 113-125.
282. Urban-Klein, B., Werth, S., Abuharbeid, S., Czubayko, F., and Aigner, A. (2005) RNAi-mediated gene-targeting through systemic application of polyethylenimine (PEI)-complexed siRNA in vivo. *Gene Ther.* **12**, 461-466.
283. Bettinger, T., Remy, J.S., and Erbacher, P. (1999) Size reduction of galactosylated PEI/DNA complexes improves lectin-mediated gene transfer into hepatocytes. *Bioconjugate Chem.* **10**, 558-561.
284. Stryer, L. (1995) Biosynthesis of nucleotides. In Biochemistry. WH Freeman and Co, New York, p 739-762.
285. Parekh-Olmedo, H., Czymmek, K., and Kmiec, E.B. (2001) Targeted gene repair in mammalian cells using chimeric RNA/DNA oligonucleotides and modified single-stranded vectors. *Science's S.T.K.E.* **73**, 1-12.
286. Igoucheva, O., Alexeev, A., Pryce, M., and Yoon, K. (2003) Transcription affects formation and processing of intermediates in oligonucleotide-mediated gene alteration. *Nucl. Acids Res.* **31**, 2659-2670.
287. Clamme, J.P., Krishnamoorthy, G., and Mely, Y. (2003) Intracellular dynamics of the gene delivery vehicle polyethylenimine during transfection: investigation by two-photon fluorescence correlation spectroscopy. *Biochim. Biophys. Acta* **1617**, 52-61.
288. Erickson, S.K. and Fielding, P.E. (1986) Parameters of cholesterol metabolism in the human hepatoma cell line, HepG2. *J. Lipid Res.* **27**, 875-883.
289. Ferrara, L., Parekh-Olmedo, H., and Kmiec, E.B. (2004) Enhanced oligonucleotide-directed gene targeting in mammalian cells following treatment with DNA damaging agents. *Exper. Cell Res.* **300**, 170-179.
290. Rosengart, T.K., Lee, L.Y., Patel S.R., Sanborn, T.A., Parikh, M., Bergman, G.W., Hachamovitch, R., *et al.* (2000) Angiogenesis gene therapy, phase I assessment of an adenovirus vector expressing $VEGF_{121}$ cDNA to individuals with clinically significant severe coronary artery disease. *Circulation* **100**, 468-474.
291. Raper, S.E., Grossman, M., Rader, D.J., Thoene, J.G., Clark, B.J. 3rd, Kolansky, D.M., *et al.* (1996) Safety and feasibility of liver-directed ex vivo gene therapy for homozygous familial hypercholesterolemia. *Ann. Surg.* **223**, 116-126.
292. Mujynya-Ludurge, K., Viswambharan, H., Driscoll, R., Ming, X.F., von Segesser, L.K., Kappenberger, L., Yang, Z., and Vassali, G. (2005) Endothelial nitric oxide synthase gene transfer restores endothelium-dependent relaxations and attenuates lesion formation in carotid arteries in apolipoprotein E-deficient mice. *Basic Res. Cardiol.* **100**, 102-111.
293. Yoshioko, T., Okada, T., Maeda, Y., Ikeda, U., Shimpo, M., Nomoto, T., Takeuchi, *et al.* (2004) Adeno-associated virus vector-mediated interleukin-10 gene transfer inhibits atherosclerosis in apolipoprotein E-deficient mice. *Gene Ther.* **11**, 1772-1779.
294. Behr, J.P. (1997) The proton sponge: a trick to enter cells the viruses did not exploit. *Chimia* **51**, 34-36.
295. Klemm, A.R., Young, D., and Lloyd, J.B. (1998) Effects of polyethylenimine on endocytosis and lysosome stability. *Biochem. Pharmacol.* **56**, 41-46.
296. Diaz-Font, A., Cormand, B., Chabas, A., Vilageliu, L., and Grinberg, D. (2003) Unsuccessful chimeraplasty strategy for the correction of a mutation causing Gaucher disease. *Blood Cells Mol. Dis.* **31**, 183-186.

PUBLICATIONS

ORIGINAL WORKS

Sperber, G., Mohri, Z., Schepelmann, S., Dickson, G, and Owen, J.S. (2006) Editing of the LCAT gene to generate potentially atheroprotective variants using synthetic RNA-DNA oligonucleotides (chimeraplasts). *Work in progress.*

Mohri, Z., **Sperber, G.,** Manzano, A., Tagalakis, A.D., Dickson, G, and Owen, J.S. (2005) Gene editing of the wild-type *APOE3* gene to the dysfunctional variants *APOE2* and *APOE4* using synthetic RNA-DNA oligonucleotides (chimeraplasts). *Gene Therapy and Molecular Biology* **9**, 143-152.

Manzano, A., Mohri, Z., **Sperber, G.,** Ogris, M., Graham, I., Dickson, G., and Owen, J.S. (2003) Failure to generate atheroprotective apolipoprotein AI phenotypes using synthetic RNA/DNA oligonucleotides (chimeraplasts). *J. Gene Med.* **5**, 795-802.

Graham, I.R., Manzano, A., Tagalakis, A.D., Mohri, Z., **Sperber, G.,** Hill, V., Beattie, S., Schepelmann, S., Dickson, G., and Owen, J.S. (2001) Gene repair validation. *Nat. Biotechnol.* **19**, 307-508.

CONFERENCE PARTICIPATION

Sperber, G. Studies in chimeraplasty. Royal Holloway University of London, School of Biological Sciences Postgraduate Symposium, May 2002. *Poster presentation.*

Sperber, G., Ogris, M., Bettinger, T., Mohri, Z., Dickson, G., and Owen, J.S. Improving chimeraplast uptake and gene conversion using chemically-modified polyethylenimine (PEI). Ninth Annual Meeting of the European Society of Gene Therapy, November 2001. *Poster presentation.*

Manzano, A., **Sperber, G.,** Dickson, G., and Owen, J.S. Chimeraplasts as reagents to probe structure-function relationships in Apo-AI and LCAT. 24th European Lipoprotein Club Meeting, September 2001. *Oral presentation.* (Reviewed in Dallinga-Thie, G. et al. (2002) European Lipoprotein Club: Report of the 24th ELC Annual Conference. *Atherosclerosis* **162**, 439-447.)